



**HAL**  
open science

# Impact of chronic viral infection on the CD8 preimmune repertoire: when do we lose our naivety?

Cécile Alanio Bréchet

► **To cite this version:**

Cécile Alanio Bréchet. Impact of chronic viral infection on the CD8 preimmune repertoire: when do we lose our naivety?. Immunology. Université Pierre et Marie Curie - Paris VI, 2015. English. NNT : 2015PA066376 . tel-01272594

**HAL Id: tel-01272594**

**<https://theses.hal.science/tel-01272594>**

Submitted on 11 Feb 2016

**HAL** is a multi-disciplinary open access archive for the deposit and dissemination of scientific research documents, whether they are published or not. The documents may come from teaching and research institutions in France or abroad, or from public or private research centers.

L'archive ouverte pluridisciplinaire **HAL**, est destinée au dépôt et à la diffusion de documents scientifiques de niveau recherche, publiés ou non, émanant des établissements d'enseignement et de recherche français ou étrangers, des laboratoires publics ou privés.

# Université Pierre et Marie Curie

École doctorale Physiologie et Physiopathologie (ED 394)

*Immunobiologie des Cellules Dendritiques (Unité Mixte Pasteur/Inserm U818)*

## **Impact d'une infection virale chronique sur le répertoire T CD8 préimmun : A quel moment perd-on sa naïveté?**

Par Cécile BRECHOT épouse ALANIO

Thèse de doctorat de Immunologie

Dirigée par Matthew L. Albert

Présentée et soutenue publiquement le 02 Juillet 2015

Devant un jury composé de :

François LEMOINE, MD, PhD

Marion PEPPER, PhD

Marc BONNEVILLE, VetD, PhD

Andrès ALCOVER, PhD

Ludovic DERIANO, PhD

Matthew L. ALBERT, MD, PhD

Président

Rapporteur

Rapporteur

Examineur

Examineur

Directeur de thèse



# Université Pierre et Marie Curie

École doctorale Physiologie et Physiopathologie (ED 394)

*Laboratory of Dendritic Cell Biology (Mixed Pasteur/Inserm U818 unit)*

## **Impact of chronic viral infection on the CD8 preimmune repertoire: When do we lose our naiveté?**

By Cécile ALANIO, née BRECHOT

Doctoral thesis in Immunology

Directed by Matthew L. Albert

Defended publically on July 2<sup>nd</sup>, 2015

In front of a jury composed of:

François LEMOINE, MD, PhD  
Marion PEPPER, PhD  
Marc BONNEVILLE, VetD, PhD  
Andrès ALCOVER, PhD  
Ludovic DERIANO, PhD  
Matthew L. ALBERT, MD, PhD

Président  
Rapporteur  
Rapporteur  
Examineur  
Examineur  
Directeur de thèse



# Abstract

---

The CD8 preimmune repertoire is defined as the set of circulating antigen-specific T CD8 lymphocytes that have not been activated yet by their cognate antigen. Because those cells are very rare, they have not been evaluated in humans. We developed a tetramer-based enrichment protocol that allowed for the first time direct detection and enumeration of those rare naive antigen-specific CD8 T cells in healthys. We then used this tool to characterize the CD8 preimmune repertoire in patients with chronic hepatitis C viral infection. We found that their naive CD8 T cells are dysregulated, being hypersensitive to TCR signals, and with increased proportions of memory-phenotype (MP) cells in inexperienced populations. These perturbations are reversible after viral clearance, highlighting the added benefit of early antiviral treatment. Finally, using a transgenic model (OTI), we observed high proportions of MP inexperienced T cells in the blood of *cxcr3*-deficient unimmunized mice. This suggests that CXCR3-dependent lymphocyte trafficking could account for some preimmune repertoire alterations. Altogether, our work demonstrates that inexperienced T cells can lose their naiveté in several pathological situations. The impact of these findings will need to be considered when designing future immunotherapeutic strategies - especially when « inflammatory » patients are being targeted. Additionally, we highlight the challenge of interpreting T-cell immunophenotyping studies without getting knowledge into antigen-specific populations.

Key-words: preimmune repertoire; CD8 T cell dysfunction; TCR signaling; viral immunology; chronic inflammation; tissue immunity

# Résumé

---

Le répertoire T CD8 préimmun correspond aux lymphocytes T spécifiques d'antigène circulant en périphérie, et n'ayant pas encore été activés. Ces cellules sont très rares, et de ce fait, n'ont jusqu'ici pas pu être étudiées de façon approfondie. Nous avons dans un premier temps développé un protocole d'enrichissement basé sur la technologie des tétramères. Nous avons pu détecter et énumérer des lymphocytes T CD8 naïfs spécifiques d'antigènes dans le sang de sujets sains. Nous avons ensuite utilisé cet outil pour évaluer le répertoire T préimmun de patients chroniquement infectés par le virus de l'hépatite C (cHCV). Nous avons démontré que celui-ci est significativement perturbé, avec des cellules hypersensibles à l'activation TCR et une proportion importante de lymphocytes T de phénotype mémoire alors qu'ils n'ont pourtant pas rencontré leur antigène cible. Ces anomalies disparaissent après résolution de l'infection, soulignant l'intérêt d'instaurer précocément un traitement antiviral chez ces patients. Enfin, nous avons observé dans un modèle de souris transgéniques (OTI) une proportion importante de T inexpérimentés de phénotype mémoire chez les animaux non-immunisés déficients en *cxcr3*. Nos travaux démontrent que les lymphocytes T inexpérimentés peuvent perdre leur naïveté dans différentes situations pathologiques. Ces résultats devraient être pris en considération pour l'optimisation de futures stratégies d'immunothérapie, notamment lorsque des patients dits "inflammatoires" sont la cible de vaccinations. Enfin, nos résultats soulignent la difficulté d'interpréter les données d'immunophénotypage en l'absence d'information sur la spécificité antigénique.

Mots-clés : répertoire préimmun; lymphocyte T CD8; signal TCR; immunologie anti-virale; inflammation chronique; immunité tissulaire

# Table of contents

---

<b>ABSTRACT</b> .....	<b>5</b>
<b>RÉSUMÉ</b> .....	<b>6</b>
<b>TABLE OF CONTENTS</b> .....	<b>7</b>
<b>LIST OF FIGURES</b> .....	<b>11</b>
<b>LIST OF TABLES</b> .....	<b>13</b>
<b>REMERCIEMENTS</b> .....	<b>15</b>
<b>ABBREVIATIONS</b> .....	<b>17</b>
<b>FOREWORD</b> .....	<b>21</b>
<b>RESEARCH PLAN</b> .....	<b>23</b>
I.    DEVELOP TOOLS FOR SCREENING RARE ANTIGEN-SPECIFIC RESPONSES IN HUMANS ....	24
II.   EVALUATE THE IMPACT OF CHRONIC INFECTION ON THE PREIMMUNE REPERTOIRE ....	24
III.  STUDY THE IMPACT OF CXCR3 RECEPTOR ON INEXPERIENCED T CELLS .....	25
<b>CHAPTER 1. GENERAL INTRODUCTION</b> .....	<b>27</b>
I.    PREIMMUNE REPERTOIRE .....	31
A.   THYMIC DEVELOPMENT .....	31
1)  Thymus anatomy and function .....	31
2)  Early thymocyte development .....	34
3)  Thymic selection of the MHC-restricted preimmune repertoire .....	34
4)  Maturation and emigration of mature SP thymocytes .....	36
B.   PERIPHERAL NAIVE T CELLS .....	38
1)  Recent Thymic Emigrants .....	38
2)  Population size and TCR repertoire .....	39
3)  Homeostasis and homeostatic proliferation .....	43
4)  CD5 expression and dynamic tuning of lymphocytes .....	45
5)  Activation, differentiation and activation-induced cell death .....	47
6)  Phenotypic and functional diversity .....	50
7)  Impact of precursor frequency and diversity .....	51
II.   CHRONIC INFLAMMATION .....	54
1)  General introduction .....	54
2)  HCV as a model of chronic inflammation .....	56
(a)  Epidemiology .....	57
(b)  Virus genome .....	58
(c)  Tropism and entry receptors .....	59
(d)  From acute to chronic infection .....	61
(e)  Extrahepatic manifestations .....	64
(f)  Treatment and clearance benefits .....	65
(g)  Antiviral immune responses .....	67
3)  HBV as a comparative model of chronic hepatitis .....	72

4) Viro-induced chronic inflammation .....	73
5) T cells and inflammation .....	75
III. T CELL TRAFFICKING .....	77
1) Short introduction about chemokines .....	77
2) Naive T cell trafficking .....	78
3) Effector and resident memory T cells trafficking.....	79
4) Role of CXCR3 in T cell biology .....	81
5) Focus on CXCL10 .....	84
<b>CHAPTER 2. DEVELOP TOOLS FOR SCREENING RARE ANTIGEN-SPECIFIC RESPONSES .....</b>	<b>87</b>
I. INTRODUCTION .....	89
II. TETRAMER ASSOCIATED MAGNETIC ENRICHMENT (TAME).....	90
A. PREPARATION OF PMHCI TETRAMERS .....	90
B. PREPARATION OF PHOTOCLEAVABLE PMHCI TETRAMERS .....	91
C. DEVELOPMENT OF TAME FOR HUMAN SAMPLES.....	92
D. TAME INCREASES DETECTION OF AG-SPECIFIC T CELLS BY UP TO 100-FOLD .....	93
E. DETECTION OF NAIVE CD8 T CELLS SPECIFIC FOR HIV GAG P17 <sub>77-85</sub> .....	96
F. ENRICHMENT AND ENUMERATION OF MULTIPLE SPECIFICITIES .....	97
III. DISCUSSION .....	98
A. TAME PERMITS ENUMERATION AND CHARACTERIZATION OF RARE AG-SPECIFIC T CELLS FROM HUMAN PERIPHERAL BLOOD .....	98
B. EPITOPES HAVE CONSERVED PRECURSOR FREQUENCIES AMONG INDIVIDUALS.....	99
IV. PROSPECTIVES .....	101
<b>CHAPTER 3. DEFINE THE INFLUENCE OF CHRONIC HCV INFECTION ON THE PREIMMUNE REPERTOIRE. ....</b>	<b>117</b>
I. INTRODUCTION .....	119
II. EVALUATION OF THE PREIMMUNE REPERTOIRE DURING CHRONIC HCV .....	120
A. GATING STRATEGY .....	120
B. BULK LEVEL .....	121
C. ANTIGEN-SPECIFIC LEVEL.....	122
D. NAIVE T CELL HOMEOSTASIS DURING CHRONIC HCV .....	124
III. DISCUSSION .....	127
IV. PROSPECTIVES .....	129
<b>CHAPTER 4. STUDY THE IMPACT OF CXCR3 RECEPTOR ON INEXPERIENCED T CELLS .....</b>	<b>167</b>
I. INTRODUCTION .....	169
I. IN THE THYMUS.....	170
II. IN PERIPHERY .....	171
A. MP CELLS IN THE BLOOD OF NON-IMMUNIZED <i>CXCR3</i> <sup>-/-</sup> ANIMALS .....	171
B. DISTINCT TCR ACTIVATION PATTERN .....	171
C. MP OTI CELLS IN THE SKIN OF UNIMMUNIZED WT ANIMALS.....	172
D. MP OTI CELLS ARISE IN HOMEOSTATIC ENVIRONMENTS.....	173
III. DISCUSSION .....	174

IV. PROSPECTIVES.....	175
<b>CHAPTER 5. GENERAL DISCUSSION.....</b>	<b>189</b>
I. IMMUNOPHENOTYPING CHALLENGES .....	191
II. PREIMMUNE REPERTOIRE AND PERSONALIZED MEDICINE.....	192
III. PREIMMUNE REPERTOIRE AND PERSISTENT VIRUSES.....	193
<b>METHODS.....</b>	<b>195</b>
I. GENERATION OF PMHC CLASS I TETRAMERS THROUGH LIGAND EXCHANGE.....	197
II. TAME PROTOCOL.....	216
<b>MANUSCRIPTS.....</b>	<b>219</b>
<b>REFERENCES .....</b>	<b>223</b>



# List of figures

---

Figure 1: Location, morphological aspect and anatomic structure of the thymus.....	33
Figure 2: Chemokine-driven trafficking and maturation of T cells into the thymus.....	36
Figure 3: Emigration of SP thymocytes from thymus.....	37
Figure 4: Comparison of recent thymic emigrants and mature naïve T cell function.....	39
Figure 5: Antigen specificity and tetramer staining.....	42
Figure 6: Naïve T cell phenotype, homeostasis, and homeostatic proliferation.....	45
Figure 7: Dual role of CD5 in lymphocyte activation and survival.....	47
Figure 8: Sequence of critical events after TCR activation.....	49
Figure 9: Composition of the preimmune repertoire.....	53
Figure 10: Segregation of TLR agonists based on their induced protein signatures.....	55
Figure 11: Prevalence and distribution of HCV genotypes.....	58
Figure 12: HCV genome organization, and polyprotein processing.....	59
Figure 13: Life cycle of the Hepatitis C Virus (HCV) and targets of therapy.....	61
Figure 14: Clinical, virological, and immunological course of acute HCV infection.....	63
Figure 15: Extrahepatic manifestations related to HCV.....	65
Figure 16: Molecular processes that signal the host response to HCV infection.....	67
Figure 17: Weak CD8 T cell responses during cHCV.....	71
Figure 18: Natural course of HBV chronic infection.....	72
Figure 19: Bystander infection negatively impacts effector to memory transition.....	76
Figure 20: Human chemokines and their receptors.....	79
Figure 21: Memory T cell heterogeneity in the blood and in tissues.....	83
Figure 22: Schematic model of chemokine antagonism.....	86
Figure 23: Preparation of pMHC I tetramers.....	103
Figure 24: Peptide exchange technology.....	105
Figure 25: Development of Tetramer Associated Magnetic Enrichment (TAME).....	107
Figure 26: TAME increases detection of antigen-specific T cells by up to 100-fold.....	109
Figure 27: Comparison of CCR7 and CD27-based naïve gating strategies.....	111
Figure 28: Naïve CD8 T cells specific for HIV Gag p17 <sub>77-85</sub> can be detected on healthy donors.....	113
Figure 29: Enumeration of epitope-specific CD8 T cells reveals conserved precursor frequency among HD...	115
Figure 30: Schematic representation of critical steps in immune-mediated clearance of HCV infection.....	133
Figure 31: Validation of CD45RA/CD27 gating strategy for identifying naïve CD8 T cells in cHCV.....	135
Figure 32: Perturbed naïve CD8 T cell repertoire during chronic infection.....	137
Figure 33: Increased peripheral expansion of selected naïve population.....	139
Figure 34: Mart1-specific CD8 T cell MP during chronic infection may be reversed by viral clearance.....	141
Figure 35: Sensitivity of sjTRECs and Vb repertoire assays.....	143
Figure 36: MP cells are a common feature of self and non-self antigen-inexperienced populations.....	145
Figure 37: CD5 expression on T cells during homeostatic or pathologic conditions.....	147

Figure 38: Decreased cell surface expression of CD5 on naïve CD8 T cells from cHCV patients.....	149
Figure 39: Schematic representation of the impact of low levels of CD5 on T cell activation.....	151
Figure 40: Lower threshold for TCR activation in cHCV patients.....	153
Figure 41: Increased blastogenesis and CD25 expression after TCR activation in cHCV patients.....	155
Figure 42: Increased AICD after TCR activation in cHCV patients.....	157
Figure 43: Anti-CD5 blocking Abs recapitulate the hypersensitivity phenotype.....	159
Figure 44: Cytokines levels detected in plasma of cHCV, and SVR patients, as compared to HD.....	161
Figure 45: In vitro priming of Mart1-specific CD8 T cells.....	163
Figure 46: Proposed models for dysregulation of naïve CD8 T cells during HCV chronic infection.....	165
Figure 47: <i>cxc3<sup>-/-</sup></i> mice have lower numbers of CD8SP thymocytes.....	177
Figure 48: <i>cxc3<sup>-/-</sup></i> mice present increased numbers of circulating MP CD8 T cells.....	179
Figure 49: Activation profile of OTI-CXCR3KO cells after stimulation with the Ova peptide.....	181
Figure 50: MP cells are found into the skin of OTI-WT transgenic unimmunized animals.....	183
Figure 51: MP cells are present in OTI-CXCR3KO cells of mixed bone marrow chimeras .....	185
Figure 52: Proposed model of MP Ag-specific inexperienced T cells migration.....	187

# List of tables

---

Table 1: Naive and memory phenotype of CD8 T cells in humans and mice. ....	29
Table 2. Mouse and human adults preimmune repertoire numbers.....	40
Table 3. Diversity of the CD8 T cell preimmune repertoire.....	51
Table 4. Hepatotropic viruses. ....	56
Table 5. Calculation of epitope-specific T cell numbers, and validation. ....	94
Table 6. Description of the patients included in the Tetra cohort. ....	121



# Remerciements

---

*To my three naïve T cells, with all my love*

**I** would like to thank Marion Pepper and Marc Bonneville for their deep relecture of the manuscript, as well as François Lemoine, André Alcover and Ludovic Deriano for their participation to the Jury. I would like to thank also Lars Rogge, Fernando Arenzana-Seisdos, and Sébastien André, for nurturing excellent discussions about science, and for their support during the entire course of my PhD.

**C**lassical, but so obvious, I will start by thanking my mentor, Matthew. For such a great time in your lab. For being on my side since the very beginning. For your tender acceptance (and self control) after I announced my ~~first second~~ third pregnancy. For your active support for women in science – which includes an exceptional capacity to answer a mean of 5 emails during late evenings and weekends. For your permanent optimism, your laughs, and your contagious joie de vivre. For your amazing ability to sense (and teach) non-spoken things. For being so unpredictable... and so open to unpredicted projects or discoveries. And because you also are a daily challenge to work with... but in such a good way ☺!

**D**ifficult to list here all the family members implicated in this crazy project. My love thank goes to my grandmother, Marie-Rose: your generosity and intelligence are an infinite source of inspiration (I imagine your face when you will hear that I wrote that in English...!). The golden medal is then attributed to my husband, Alexandre. For being still there after three babies and four years of PhD – you should be awarded. For your (almost) infinite tolerance and love. For the paupiettes – I will never forget. For your amazing gestion of the home team, at the same time you build your own brilliant career. You should be proud. Thanks to my mother, Jeanne-Marie, for the Friday nursery and other concrete supports, and for being an example of working-mother; to my father, Christian, for your permanent and strong support, for relaxing Sunday evenings, and for actively preparing my progeny for Roland Garros tournament (soon?); to Patrizia, for offering an inspirative example of private life/work organization, and for your woman-to-woman support and advices; to my brother Nicolas, for being the first one (and unique one actually) proposing to build a CD5-agonist (or antagonist?) trial in his intensive care unit patients, for never revealing the incredible secret about the t..., and for being always behind me; to my brother Davide, for great help with the kids, for taking care of our lunches, and for simply being you; to my sister Carole, for her love and support – my only regret is that you did not initiate Nader (and me) to the pole-dance art; and to my brother Lucas, for incredible help with the kids over last spring. Thanks also to Florence, for very nice discussions – your turn now ☺, to Ariel, Marc, Marie-Laure, all the cousins and “related”: we are a great family team. Last but not least, I would like to thank my family-in-law, Elisabeth, Georges, and Edouard, as well as all the Alanio/Deaton members: you are my second and so warm and supportive family. A special thank to Emile and Martin who literally saved my life in the last month of my PhD.

- a big thank to my children Malo, Titouan and Ambre, for your patience. I will never have made all this work without you. You learned me that doing 100 things at the same time is completely possible, that sleeping is a detail, and that the important thing in life is to be equilibrated. You are an inexhaustible source of giggles and happiness. I love you. And yes, now we can go to Disneyland ☺.

**C**rucial thank to Aurélie. Not necessarily because of very productive discussions on the data themselves (hum), but more for all your support: this started with Radio Pipette and Radio Diva, and later evolved into more private conversations (in the middle of the corridor), where I think we shared almost all of the spicy details of our hectic mother/wife/worker life. Our trip in San Francisco was the “apothéose” of a strong friendship. And yes, I still think that the immunophenotyping is dead, and that you have so much to learn from reading carefully the protocols ☺.

**I** am very happy to count you, Milena, as a close friend. We shared very nice moment inside and outside the lab. I appreciate your honesty and integrity. I am very grateful that you never installed video cameras into the P2<sup>+</sup>-CIH to respect the privacy of (my) late evening musically inspired sorts... Well... I just discovered that you indeed installed a video camera... without advertising me? Since when? Do you keep the records?

**H**e is also my friend and brother (because you are born in 1989!!), and so smart and charming... Nader, thank you for your support over these past years (and for ordering the coffee!). This was an honor – and a challenge – to have you as co-PhD. Your maturity is impressive. You will do an amazing career. Looking forward to build Alanio-Yatim (or Yatim-Alanio!?) projects together in the near future.

- a special thought for the CIH members who never blamed me after my disrespectful move to the second floor... for all my P2<sup>+</sup> friends... and for Lars and Elisabetta, as well as all the members of their lab, that

welcomed me at the 5<sup>th</sup> floor quite a number of time... You were extremely supportive, inside and outside the lab, and I now count you as my friends. Viva Italia!!

**F**ew more lines to thank namely members of ICD and CIH (mostly 2007-2015) families (apologize for the very few recent additions, or those that I might have forgotten). Thanks to: Armanda, for your strong help to settle in the lab in the first year(s) of my PhD; Biljana - always a pleasure to spend time with you; Brieuc (or Pierre?), because each time I see you I feel happy and it makes me laugh. I wish you all the best for the years to come – you will be awesome; Caroline, I wish you all the best in life and science; Claire, your work during PhD was very inspirative: thanks for your support even after leaving the lab – and the template ;-); Clémence, for your cheerfulness and your spontaneity; Darragh, for your careful relectures of the thousands of versions of the HCV paper; Dilay, for your “joie de vivre”; Estelle, for you amazing work and your nice attentions with the home team; Gaby, for your support and nice words; Helen L., for your help in starting the project; Hélène S., for saving my life several times by removing the dead flies on my desk with a lot of courage, and also for your mature and helpful advices with the kids; Isabelle, for being a faithful member of the pulldown team, and for you strong support since I arrived in the lab; Jérémie - it is a real pleasure to have you as close neighbor, your “insatiable curiosité” is fantastic - thanks for your advices for the paper as well as the writing of this manuscript; Marie-Laure, for being international expert in orchidées’s breeding (what is your secret finally?) and for a communicative happiness; Marine, for your work while I was not there; Matt, I think I never laughed as much as during our few days in Amsterdam; Melissa, because each time I go to the FACS I imagine you knitting in front of your data and that is a very relaxing picture (how do you pass the tubes??); Molly, because I admire you, and feel proud and inspired to be by your side – even if you sometimes stress me by being more organized than me (is it possible?) – looking forward to build 25-combicolor panels with you ;-)!; Philippe, for sharing my excitement about phospho experiments – even when it was not at all exciting, and for all our fun discussions; Pierre-Emmanuel, for being devoted to eat all what I don’t like during official lunches and dinners, and for carrying the heavy secret of the “coquilles saint Jacques” with a lot of discretion; Rosa, for being such a positive person, for learning me everything about the mice - including how to speak to them “à la portugaise” and some breeding secrets, and because nobody else would have runned to exchange that spleen kidney...; Stéphanie, because you were extremely supportive from the very beginning (do you remember the “charges publiques/privées” ratio?) and all over the course of my career. It is always a great pleasure to discuss and work with you – a shot in the arm when facing difficulties on the regular project(s). You should be very proud of what you are accomplishing in the Labex project; Tracy, for taking care of my children almost as carefully as of my mice; Valentina, for your smile and life energy; Vincent B., for your deep commitment to work in general, and tetramer technology in particular - looking forward to celebrating the 10mg production!; Vincent R., for all your unbiased analysis and your help with R - always a great pleasure to interact with you (except for society games...!).

**O**utside of Pasteur, I would like to thank Stanislas Pol, and all the Cochin team: Vincent Mallet, Farhad Heshmati, Laurence Bousquet, Sylvie Lagaye, and Jesintha Gaston, as well as the different ARC that coordinated the C11-33 study, both in Pasteur and in Cochin. Thanks also to Victor Appay, for your listening and help at different stages of the project.

**R**espectful thanks to people who educated me to Medical Biology, and Immunology. I do appreciate a lot your advices and still very active support. This includes Loic Garçon – so nice memories of my research initiation (is the ekta still working with a pen?), Antoine Toubert, Emmanuel Clave, Nicolas Dulphy, Franck Pagès, Eric Tartour, Dominique Charron, François Delhommeau, Sébastien Maury, David Klatzman, Olivier Lascols, Cécile Badoual, Lucienne Chatenoud, Geneviève Plu-Bureau, Julie Dechanet, Eliane Piaggio, Antoine Garbarg-Chenon, Martine Raphaël, Michelle Rosenzweig, Stéphanie Huguot-Jacquot, Olivier Adotevi, Françoise Aucouturier, and all the members of related labs.

**E**-warm thanks to Ton Schumacher and his group - Mariit van Buuren, Pia Kvistborg, and Mireille Toebes, for enriching a lot my perspectives and for strong moral support; to Robert Thimme and Tobias Flecken (don’t decross your fingers!), Annick Lim, and Kerstin Johnsson for interesting discussions and collaborations. Thanks also to David Michonneau who initiated me to bone marrow transplantation for mice, and to Fabrice Lemaitre and Philippe Bousso for their help all around the project. Big thanks to members of the Pasteur CNR mycology unit, for occupying my husband while I was writing this manuscript, and to all members of the Immunology Department - especially François Huetz, Jim di Santo, and Gerard Eberl, for support and nice discussions.

**V**igorous thanks to my friends: Malik, Delphine B., Julie, Manu, (The Dream Team is back!!), Pierre-Marie, Charlotte, Elisabeth F, Delphine G., Sandrine, Laurent, Julia, Antoine, Karen, Hady, Sylvie, Thomas, Elise, Cédric, all the kids, all my doctor colleagues, and also the desperate mothers: thank you for your support and lots of fun (and less fun but intense) moments over these past years.

**E**normous thanks to Molly, Rosa, Vincent M. and Philippe for deep relecture of this manuscript.

**R**espectful thanks to Claudine and to all the “Maman de” (Elise, Théo, Garance, Mathis, Eloise, Fodé,...), for their amazing help with home team organization.

# Abbreviations

---

<b>Abb.</b>	<b>Full name</b>
aa	aminoacids
Ab	Antibody
Abs	Antibodies
Ag	Antigen
Ag-specific	Antigen-specific
Ags	Antigens
AICD	Activation-induced cell death
AIRE	AutoImmune Regulator
APC	AlloPhycoCyanin
APC	Antigen Presenting Cell
APECED	Autoimmune PolyEndocrinopathy Candidiasis Ectodermal Dystrophy
BMC	Bone marrow chimeras
BrdU	BromodéoxyUridine
CCR7	CC-motif chemokine receptor 7
CD	Cluster of Differentiation
cDCs	conventional Dendritic Cells
CDR3	Complementarity Determining Region 3
cHBV	chronically infected HBV patients
CHC	Hepatocellular Carcinoma
cHCV	HCV chronic infection
CLDN1	claudin 1
CLP	Common lymphoid progenitor
CMJ	CorticoMedullary Junction
CMV	Cytomegalovirus
COX-2	cyclooxygenase-2
CR	Cross-Reactivity
cTECs	cortical Thymic Epithelial Cells
CTLA-4	Cytotoxic T-Lymphocyte-Associated protein 4
CXCI	C-X-C motif Chemokine
CXCR3	C-X-C motif Chemokine Receptor
DAAs	Direct Acting Antiviral agents
DC	Dendritic Cell
DN	Double Negative
DNA	DeoxyriboNucleic Acid
DP	Double Positive
DPP4	Dipeptidyl peptidase-4
DUSP	DUAL Specificity protein Phosphatases
ELISA	Enzyme-Linked ImmunoSorbent Assay
ELISPOT	Enzyme Linked Immunospot
ELP	Early lymphoid progenitor (=LMPP)
ERK	Extracellular signal-Regulated Kinases
ETP	early thymocyte precursors
FasL	Fas ligand
FITC	Fluorescein IsoThioCyanate
Flu	Influenza virus
Flu M1	Influenza virus Matrix protein 1
FOX	Forkhead box protein
GFP	Green Fluorescent Protein
GMP	Good Manufacturing Practice
HBV	Hepatitis B virus
HCC	Hepatocellular carcinoma
HCV	Hepatitis C virus
HD	Healthy Donor

HIV	Human Immunodeficiency Virus
HLA	Human Leukocyte Antigen
HP	Homeostatic Proliferation
HSA	Heat-Stable Antigen (CD24)
HSCs	Hematopoietic Stem Cells
hTERT	human TElomerase Reverse Transcriptase
HVR	Highly Variable Region
ICS	Intracellular Cytokine Staining
IFN	Interferon
IFNg	Interferon gamma
Igs	immunoglobulins
IkB	inhibitor of NFkB
IL	InterLeukin
IL-1 $\beta$	interleukin-1 $\beta$
IL-R	InterLeukin Receptor
Iono	Ionomycin
IP10	Interferon gamma-induced protein 10kDa (=CXCL10)
ISGs	Interferon Stimulated Genes
ITIM	immunotyrosine-based inhibition motifs
iTreg	induced Treg
KCs	Kuppfer cells
KLF2	Krüppel-like Factor 2
KW	Kruskal-Wallis
LAT	linker for activation of T cells
LCMV	lymphocytic choriomeningitis virus
LDA	Limiting Dilution Assay
LDL	Low Density Lipoprotein
LIP	lymphopenia-induced proliferation
LM	Listeria monocytogenes
LMPP	Lymphoid-primed multipotent progenitor
LT $\beta$ R	lymphotoxin $\beta$ receptor
Ly6C	Lymphocyte antigen 6C
mAb	monoclonal Antibody
MACS	Magnetic-Activated Cell Sorting
MadCAM	Mucosal addressin Cell Adhesion Molecule
MAP	mitogen-activated protein
MART1	Melanoma-associated Antigen recognized by T cells 1 (= MelanA)
MC	Mixed cryoglobulinemia
MFI	Mean Fluorescence Intensity
MHC	Major Histocompatibility Complex
miRNA	micro RiboNucleic Acid
MMP	Multipotent Progenitors
MP	Memory Phenotype
mRNA	messenger ribonucleic acid
mTECs	medullary Thymic Epithelial Cells
MW	Mann-Whitney
NFAT	Nuclear factor of activated T-cells
NK	Natural Killer
NP	Naive Phenotype
NS	Non-Structural
NY-ESO-1	Cancer/testis antigen 1
OCLN	occludin
OTI	Ova-specific T cells
PAMP	Pathogen-Associated Molecular Pattern

PBMC	Peripheral Blood Mononuclear Cells
PD-1	Programmed cell Death-1
pDCs	plasmacytoid Dendritic Cells
PE	PhycoErythrin
peg-IFN	pegylated IFN
PFA	ParaFormAldehyde
PI3K	Phospholinositide 3-Kinase
PKR	protein kinase R
PMA	Phorbol 12-Myristate 13- Acetate
pMHC	peptide- Major Histocompatibility Complex
pMHCI	peptide- Major Histocompatibility Complex class I
PMSF	phénylméthylsulfonyle
PNAd	Peripheral lymph Node Addressin
pre-RTEs	thymus-leaving RTE precursors
Qa	MHC Antigen
Qdots	Quantum dots
RAG	Recombination-Activating Gene
RBV	RiBaVirine
RE	Endoplasmic Reticulum
RIGI	Retinoic-acid-Inducible Gene I
RNA	RiboNucleic Acid
RTE	Recent Thymic Emigrants
S1P	Sphingosine-1-Phosphate
S1P1	S1P receptor 1
SC	Subcutaneous
sIP10	short form of IP10
SIRPa	Inhibitory Receptor Signal regulatory Protein a
SIV	Simian Immunodeficiency Virus
sjTREC	signal-joint T cell Receptor Excision Circle
SLOs	Secondary Lymphoid Organs
SP	Single-positive
SRB1	scavenger receptor class B type 1
STAT	Signal Transducers and Activators of Transcription
SVR	Sustained Virologic Responder
TAME	Tetramer-Associated Magnetic Enrichment
T <sub>CM</sub>	Central Memory T cell
TCR	T cell Receptor
T <sub>EM</sub>	Effector Memory T cell
T <sub>EMRA</sub>	Late Effector Memory T cell
Tg	Transgenic
Th	T helper
TLR	Toll Like Receptor
T <sub>N</sub>	Naive T cell
TNF	Tumor Necrosis Factor
TRAF6	tumor necrosis factor (TNF) receptor-associated factor
Treg	regulatory T cell
T <sub>RM</sub>	Resident memory T cell
TSAs	Tissue Specific Antigens
UV	UltraViolet
VLDL	Very Low Density Lipoprotein
VM	Virtual Memory
YATEC	Young Adults Thymectomized during Early Childhood
β2m	beta-2-microglobulin



# Foreword

---

Life is about learning and growing. When I joined Matthew Albert's lab, I thought applying for a PhD would mean being part of a scientific project, focusing on a specific topic for years, hopefully making some interesting discoveries, and at the end, becoming an expert of the subject. What took me a while is to realize that PhD is far more than that. It is a life experience. What it learns you is far beyond science, but this requires to be well surrounded. And I could not dream of better mentor than Matthew. From the beginning, he offered me freedom, and trust. The first year, I was so free that I was surprised, stressed by the hurry to start getting results, and frustrated and angry. He accepted that, heard my complaints, but never changed his way of doing. I realized a bit later that this was the best gift he could offer me. This learned me curiosity, this learned me to talk to people in the lab as well as outside, to build a project from the very beginning – balancing my own interests with feasibility, and to realize that every scientific experience – even far from my initial interests, is extremely enriching. I am now convinced that there is no better learning than floating, touching to different subjects, testing different techniques, and acquiring a big picture before going deeper into one direction. Behind that, it was also essential to my own growth. I am proud to measure the progress made, and I really hope to be able one day to drive myself students in such a good way.

My interest to immunology started when I learned that we all have garbage cells, capable of purifying our body from the inside. I still have the poster that my SVT teacher offered me after realizing my fascination about them. My interest to naïve T cells came a bit later. Naïve T cells are like young PhD students: well educated, more or less mature, full of good intentions, but with no concrete idea of what is expected from them. Similar to young PhD students, everything is still possible for them, they have a lot of potential, but their maturation will depend on their environment and on the encounters they will have. Like our children, they are our future. And their diversity is an incredible richness and the basis of a harmonious and tolerant (homeostatic) society. We are responsible for preserving and encouraging that diversity.

By this late-evening digression, I hope to illustrate my profound commitment to my project, as well as how much fun I had during these four years of PhD and the writing of this manuscript



# Research Plan

---

The preimmune T cell repertoire is defined as the set of  $\alpha/\beta$  T cell-receptor (TCR) - expressing lymphocytes that have completed thymic development and entered the secondary lymphoid organs, but have not yet been activated by high-affinity TCR binding to a foreign peptide-major histocompatibility complex (pMHC) (Jenkins et al., 2010). These mature inexperienced T cells continuously circulate from bloodstream to lymphoid organs and back into the blood, and are maintained by low-affinity contacts with non-cognate ligands in the periphery, as well as survival cytokines. Antigen (Ag)-specific CD8<sup>+</sup> T cells get activated when their TCR bind to class I pMHC at the surface of an antigen-presenting cell (APC). They undergo robust proliferation, with up to 50 000 fold expansion possible within a week (Blattman et al., 2002), and differentiate into effector T cells that disseminate throughout the body to combat infection.

CD8<sup>+</sup> T cells are one of the major components of adaptive immunity. They play a critical role in both antiviral and antitumor immunity. To adequately function, the immune system has to be able to mount exquisitely specific responses to a vast repertoire of possible antigens. To establish the basis for such a diverse response to potential foreign antigens, the genes coding for the  $\alpha$  and  $\beta$  chains of the TCR undergo somatic recombination and nucleotide insertion, allowing for the potential generation of  $\sim 10^{15}$  different specificities. The loss of over 95% of thymocytes during thymic development reflects the stringent selection processes that shapes the T cell repertoire (Kyewski and Klein, 2006). Remarkably, only 1 to 3% of double positive thymocytes survive thymic selection. While this might suggest that the repertoire size is in the order of  $10^{13}$  unique clones, there is another limiting factor – the capacity of the human body. Estimates have suggested that the total  $\alpha\beta$  TCR diversity in the blood is  $2.5 \times 10^7$  (Arstila et al., 1999). Many questions remain about the  $\sim 10^6$  fold gap between the theoretical and observed numbers of different TCR in the peripheral blood of human. One thing is clear, even for identical twins possessing the same genetic information, their T cell repertoires are distinct and in some cases may account for discordance in the development of diseases such as type I diabetes or multiple sclerosis. Given the number of CD8<sup>+</sup> T cells present in an adult human ( $5 \times 10^9$ ), the estimated number of cells per specificity is in the range of 100 – 1000 cells, *i.e.* a precursor frequency of  $10^{-6}$ - $10^{-7}$  (= 1 cell in 1 to 10 millions of CD8). These very low numbers explain that thus far, the question of the frequency, natural diversity, and migration of naive CD8 T cells in normal or pathological situations, as well as their impact on primary and memory immune responses has not been evaluated in humans. Results for these questions hold important implications for understanding the dynamics of an immune response, in particular in relation to vaccine design. To address them, we aimed to:

## I. DEVELOP TOOLS FOR SCREENING RARE ANTIGEN-SPECIFIC RESPONSES IN HUMANS

Recent studies in the mouse model just reported an elegant method combining pMHC tetramer staining and magnetic bead enrichment, which allows the tracking *in vivo*, under physiological conditions, of Ag-specific CD4<sup>+</sup> and CD8<sup>+</sup> T cells from the naive preimmune repertoire through the entire stages of an immune response. Specifically, it permitted the first time detection and characterization of the CD4<sup>+</sup> and CD8<sup>+</sup> preimmune repertoire in these animals (Moon et al., 2007; 2009; Obar et al., 2008). Based on these technical improvements, as well as our own experience in the lab, we developed and standardized a similar tetramer-associated magnetic enrichment protocol (TAME) for detecting rare Ag-specific CD8<sup>+</sup> T cell responses in human samples (Alanio et al., 2013). We applied it to healthy donors, in order to explore the preimmune repertoire in physiological conditions. This allowed for the first time direct detection, enumeration and characterization of rare naive Ag-specific T cells in healthy humans (Alanio et al., 2010). Interestingly, we detected higher than 100-fold differences in precursor frequency across these epitopes (from  $0.6 \times 10^{-6}$  to  $1.3 \times 10^{-4}$ ), but conserved frequencies among individuals. These results were published in *Blood* in 2010 (**Manuscript 1**) (Alanio et al., 2010). The detailed method of enrichment in both mouse and human was separately published in *Methods in Molecular Biology* in 2013 (**Manuscript 2**) (Alanio et al., 2013).

## II. EVALUATE THE IMPACT OF CHRONIC INFECTION ON THE PREIMMUNE REPERTOIRE

Chronic inflammation is known to perturb immune homeostasis and negatively impact the T cell repertoire. Functional impairments of CD8<sup>+</sup> T cells have been characterized in several persistent viral infections, including HIV and hepatitis C virus (HCV) infection in humans, SIV infection in macaques, and lymphocytic choriomeningitis virus (LCMV) infection in mice (Ahmed and Rouse, 2006). Such impairments have been shown at the level of differentiated memory/effector viral-specific CD8<sup>+</sup> T cells (Stelekati and Wherry, 2012). Recently, chronic infections were shown to also impair the development of unrelated immune responses in mouse models, as well as in humans chronically infected with HCV (Stelekati and Wherry, 2012). We investigated whether this effect could be the reflect of a bystander effect of HCV chronic viral infection on the CD8<sup>+</sup> T cell preimmune repertoire. We performed a cross-sectional study of patients with chronic hepatitis C viral infection (cHCV), assessed during chronic phase or post-virologic clearance (**Manuscript 3**, Submitted). Using TAME and functional assays, we studied Ag-inexperienced CD8<sup>+</sup> T cells (tumor or viral antigen-specific populations in tumor-free and CMV<sup>neg</sup> patients). cHCV patients showed increased differentiation towards memory-phenotype (MP) cells, which correlated with lower surface expression of CD5, a

negative regulator of TCR signaling. Accordingly, we demonstrated increased TCR-induced ERK phosphorylation and high susceptibility to cell death. Our study provides the first evidence that naive CD8<sup>+</sup> T cells are dysregulated during the course of a chronic viral infection, and suggest that bystander alteration of the preimmune repertoire might participate to the negative impact of chronic infections on the development of CD8<sup>+</sup> T cell memory.

### **III. STUDY THE IMPACT OF CXCR3 RECEPTOR ON INEXPERIENCED T CELLS**

Our laboratory recently provided the first evidence for dipeptidylpeptidase 4 (DPP4) mediated chemokine antagonism in chronic HCV pathogenesis. DPP4 (also known as CD26) is a member of the family of X-prolyl dipeptidylpeptidases, and is capable of enzymatically removing the N-terminal two amino acids of proteins. Specifically, we detected N-terminal truncation of the chemokine interferon-induced protein 10 (IP-10 or CXCL10) in cHCV patients, which correlated with higher DPP4 plasma activity, reduced trafficking of CXCR3-expressing lymphocytes and poor response to treatment.

As both CXCL10 and its receptor CXCR3 have been occasionally reported as implicated in intrathymic retention of CD8<sup>SP</sup> T cells, we hypothesized that disruption of chemokine gradients might perturb the development of mature and fully functional naive T cells. Utilizing animal models, we investigated the impact of *Cxcr3* deletion on CD8<sup>+</sup> inexperienced T cells development and behavior in periphery. In the thymus, we observed a subset of CD8<sup>+</sup> T cells that is *Cxcr3*-dependent, and could correspond to rehoming memory T cells. In the periphery, we observed an increase in proportions of MP CD8<sup>+</sup> T cells. To be able to track naive Ag-specific populations in the context of chemokine gradient disruption, we crossed OTI transgenic (*i.e.* mice expressing only CD8<sup>+</sup> T cells specific for the ovalbumin antigen) with CXCR3KO mice. At steady state, we found that OTI T cell populations harvested from the spleen and blood of OTI CXCR3KO animals contain an increased proportion of MP cells as compared to WT animals. This correlated with a distinct pattern of activation of those cells after stimulation by the Ova peptide *in vitro*. In parallel, we found homeostatic MP CD69<sup>+</sup>CD103<sup>+</sup> OTI cells in the skin of WT but not CXCR3KO animals, resembling resident memory T cells (Ariotti et al., 2014). Whether it is tempting to speculate that high proportions of MP cells are circulating into the blood as a result of trafficking defect, additional results on mixed bone marrow chimeras favor the hypothesis of a direct effect of *Cxcr3*-deficiency.

Ultimately, our work aims at identify if shaping the preimmune repertoire towards higher or lower reactivity is possible, and could be used as a strategy for improving vaccine efficacy.



# Chapter 1.

## General Introduction

---



CD8<sup>+</sup> T cells are one of the major components of adaptive immunity (Rocha and Tanchot, 2004). They play a critical role in both antiviral and antitumor immunity. Mature circulating CD8<sup>+</sup> T cells that have not yet encountered their specific antigens are known as naive T cells. Naive T cells continuously circulate from bloodstream to lymphoid organs and back to the blood, making contact with thousands of antigen presenting cells (APCs) within the lymphoid tissue every day. They get activated when their TCR bind to peptide-MHC Class I complexes (pMHCI) at the surface of an APC. Activated antigen (Ag)-specific CD8<sup>+</sup> T cells undergo robust proliferation, with up to 50 000 fold expansion possible within one week, at the same time differentiating into effector T cells that can disseminate throughout the body to combat infection (Blattman et al., 2002). The expansion phase is followed by contraction, marked by high levels of cell death, resulting in a small population of memory CD8<sup>+</sup> T cells, generally 5-10% of the peak cell number. The memory pool is thought to persist throughout one's life, a level 100-fold higher than the initial frequency (Badovinac et al., 2007), and further subsets into "effector memory" (T<sub>EM</sub>) and "central memory" (T<sub>CM</sub>) depending on their ability to traffic to lymphoid tissues (Sallusto et al., 2004). Upon secondary encounter with antigen, memory cells undergo a faster expansion, thus providing a more rapid response to subsequent infection.

During all these steps, CD8<sup>+</sup> T cells undergo characteristic changes in surface expression of various molecules, as presented in **Table 1**. In humans, naive T cells are characterized by basal expression of CD45RA, homing surface molecules (CD62L), and lymph node chemokine receptors (CCR7), together with co-stimulation molecules (CD28, CD27). They do not display activation markers (CD25, CD69, CD44, HLA-DR) and typically express certain adhesion molecules (CD57) but not others (CD11a). In mouse, naive and memory T cell subsets are identified by their pattern of expression of the homing surface molecules CD62L and the activation marker CD44. In both mouse and humans, while none of these molecules alone may specify a naive T cell, their combination allows precise identification (De Rosa et al., 2001).

	Human							Mouse	
	CD45RA	CD45RO	CD27	CD11a	CCR7	CD28	CD62L	CD44	CD62L
Naive	+	-	+	-	+	+	+	-	+
Central Memory	-	+	+	+	+	+	+	+	+
Effector Memory	-	+	-	+	-	+	-	+	-
Late Effector Memory	+	+	-	+	-	-	+	+	-

**Table 1: Naive and memory phenotype of CD8 T cells in humans and mice.**

To adequately function, the immune system has to be able at any moment to mount exquisitely specific responses to a vast repertoire of possible antigens. To establish the basis for such a diverse response to potential foreign antigens, the genes coding for the  $\alpha$  and  $\beta$  chains of the TCR undergo somatic recombination and nucleotide insertion, allowing for the potential generation of  $\sim 10^{15}$  different specificities. This diversity is stringently regulated as evidenced by the loss of over 95% of thymocytes during thymic development, further shaping the T cell repertoire (Kyewski and Klein, 2006). First, positive selection provides survival signals for those double-positive thymocytes bearing a TCR capable of interacting with self-pMHC. Coincidentally, negative selection induces apoptosis in cells bearing a TCR that reacts with self-pMHC with a too high affinity. Remarkably only 1% of double positive thymocytes survive thymic selection. While this might suggest that the repertoire size is in the order of  $10^{13}$  unique clones, there is another limiting factor – the capacity of the human body. Only a small fraction of this potential repertoire is used during an individual's lifetime. Estimates have suggested that the total  $\alpha\beta$  TCR diversity in the human blood is  $2.5 \times 10^7$  (Arstila et al., 1999). Given the number of  $CD8^+$  T cells present in an adult human ( $5 \times 10^9$ ), the estimated number of cells per specific population is in the range of 100 – 1000 cells, giving a precursor frequency of  $10^{-6}$ - $10^{-7}$  (= 1 naive Ag-specific T cell into  $10^6$ - $10^7$   $CD8^+$  T cells). In fact, it is not only the diversity but also the high degree of cross-reactivity built in the T cell repertoire that ensures recognition of virtually any presentable peptide (Zippelius et al., 2002).

# I. PREIMMUNE REPERTOIRE

My work has focused on the preimmune repertoire in physiological and pathological conditions. In this section, I introduce thymus anatomy and function, in order to provide a context for understanding naive T cell homeostasis.

## A. Thymic development

### 1) Thymus anatomy and function

The thymus is a gland in the upper part of the chest, behind the sternum and the lungs (**Figure 1A**) (Chidgey et al., 2007). It starts developing before birth. In newborns and young children, it is large as compared to the size of the body (**Figure 1B**). It grows during childhood, reaching its largest size (about 40 grams) at puberty. Then, the thymus slowly involutes, and the proportion of fatty tissue increases during adulthood. The thymus is composed of 2 irregularly shaped lobes, each of which has 3 layers (**Figure 1C**):

- The capsule is the connective tissue covering the outside of the thymus;
- The cortex is the middle layer;
- The medulla is the inner layer.

The cortex of the thymus is supplied by extensive networks of capillaries that are connected to postcapillary venules and arterioles at the corticomedullary junction (CMJ).

The thymus plays a unique role in the adaptive immune system by supporting T cell development. Intrathymic cells can be divided into 4 categories depending on their origin:

- T lymphocytes in development (thymocytes);
- Cells derived from hematopoietic stem cells : dendritic cells (DCs) – including  $CD8\alpha^+SIRP\alpha^-$  cDCs and pDCs, as well as small populations of B cells, macrophages, and natural killer (NK) cells;
- Resident stromal cells that are derived from non-hematopoietic lineage : this includes epithelial cells that reside either in the medulla or the cortex, mesenchymal cells, and endothelial cells;
- $CD8\alpha^-SIRP\alpha^+$  cDCs migrating from the peripheral blood (Wu and Shortman, 2005), which promote central tolerance by bringing blood-borne antigens to single-positive (SP) thymocytes (Hadeiba et al., 2012);

- Mature CD4<sup>+</sup> and CD8<sup>+</sup> T lymphocytes that rehome into the thymus after having been released in the circulation (Hale and Fink, 2008) : this was first demonstrated in unmanipulated mice transgenic for green fluorescent protein (GFP) under the control of the *RAG2* promoter (Rag2p-GFP) (Yu et al., 1999). Comparative quantification of GFP<sup>+</sup> and GFP<sup>-</sup> mature T cells within the thymus of these mice evaluated the proportion of recirculating mature CD4<sup>+</sup> and CD8<sup>+</sup> T cells around 10-20%, with an interesting positive correlation with age (Hale and Fink, 2008). Most of these cells express high levels of CD44, and locate to the medulla. Based on their long term persistence, they are now identified as intra-thymic T resident memory (T<sub>RM</sub>) cells (Mackay and Gebhardt, 2013). As compared to T<sub>CM</sub> and T<sub>EM</sub> memory subsets, T<sub>RM</sub> have specific non-circulating properties (Shin and Iwasaki, 2013). They have been identified in parabiosis and transplant experiments as resting tissue memory CD8<sup>+</sup> T cells that are maintained independently of the circulating memory population (Clark, 2015). They are conserved across species (mouse, rat, pigs), and found in multiple tissues such as the gastrointestinal tract, lung, skin and reproductive tract. In the thymus, T<sub>RM</sub> have been shown to provide potent local immunity, preserving thymic integrity and normal T-cell development in the face of infection with thymus-invading pathogens (Hofmann et al., 2013). Whether they also play a role into thymic selection processes is a matter of debate (Hale and Fink, 2008).

The CD3 molecule is detectable (i) intracellularly in all thymocytes, and (ii) at the surface of positively selected double-positive (DP) thymocytes and in all later stages of T cell development (Brodeur et al., 2009). As such, it is a useful immunohistochemical marker for T-cells in paraffin-embedded tissue sections (**Figure 1D**). It permits distinction between (i) the cortex - composed of a network of cortical thymic epithelial cells (cTECs) and DCs surrounding densely packed immature thymocytes; and (ii) the medulla - containing relatively fewer mature thymocytes supported by medullary thymic epithelial cells (mTECs) and DCs.

Involution of the thymus happens with age (Boehm and Swann, 2013). It corresponds to changes in the macroscopic architecture as well as decreased function (Ahmed et al., 2009). It has been evidenced by the decrease of the number of signal-joint T cell receptor delta excision circles (sjTRECs) detected by RT-PCR in T lymphocytes isolated from age-stratified healthy donors (Douek et al., 1998). sjTRECs are episomal DNA circles generated by the excision of the TCR $\delta$  locus during the recombination of the  $\alpha$  chain of the TCR. Importantly, they localize to the cytoplasm of T cells and are not replicated. As deletion of the TCR $\delta$  locus usually occurs in both alleles, it is assumed that cells that have successfully rearranged their  $\alpha$  chain contain 2 copies of sjTREC. sjTREC copy numbers are usually normalized (i) to albumin gene copy number - two copies are also present per cell, and (ii) per 150 000 cells. Two biological parameters complicate the interpretation of sjTREC as a measure of thymic function: longevity of naive T cells, and sjTREC dilution by cell division. Naive T cells are long lived (up to 7 years in humans), and data from thymectomized individuals have reported that

sjTREC-containing cells do not necessarily reflect recently-produced cells (Sauce et al., 2012). Additionally, naive T cell division – even without phenotypic changes, can occur (Martin and Surh, 2014; Tough and Sprent, 1994), and as sjTRECs do not replicate, any T cell division dilutes sjTREC content by 2 (Hazenberg et al., 2000b). Estimating thymic function by the amount of sjTREC in the periphery therefore is a powerful but indirect method that needs to be interpreted with caution (Hazenberg et al., 2003). Recent studies on thymic tissue from age-stratified humans have confirmed involution of the thymus with aging, with the CD8<sup>+</sup> T cell compartment being more affected than its CD4<sup>+</sup> counterpart, but there is considerable variation among individuals. Importantly, although macroscopically rearranged, the thymus was demonstrated to be functional in individuals over the age of 70 (Ferrando-Martínez et al., 2009), and higher thymic function correlated with reduction of all-cause mortality in the elderly (Ferrando-Martínez et al., 2011).

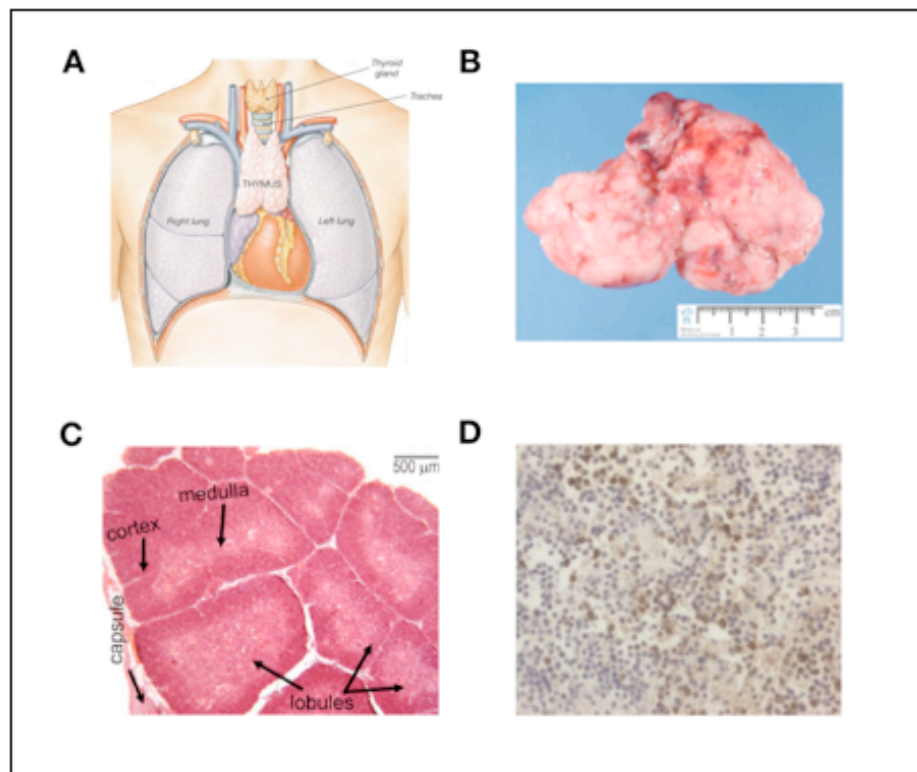


**Figure 1: Location, morphological aspect and anatomic structure of the thymus.**

A. Location of the thymus in the thoracic cavity. B. Morphological aspect of the thymus. C. The thymus consists of 3 anatomic structures: (i) the capsule; (ii) the cortex; and (iii) the medulla. D. Immunohistochemistry of the thymus (Formalin/PFA-fixed paraffin-embedded sections) with anti-CD3 antibody, staining the intracytoplasmic portion of the CD3 antigen. From Abcam commercial website.

## 2) Early thymocyte development

Within the bone marrow, haematopoietic stem cells differentiate into multipotent progenitors (**Figure 2**). A subset of them expressing high levels of FLT3 initiates transcription of recombination activating gene 1 (*RAG1*) and *RAG2*. These cells are termed lymphoid-primed multipotent progenitors (LMPPs) or early lymphoid progenitors, and develop into common lymphoid progenitors (CLPs). T lymphocytes are the unique hematopoietic cells that mature outside of the bone marrow. Their generation requires CLPs to be released from the bone marrow into the blood, and to enter the thymus through blood vessels located at the corticomedullary junction (CMJ) (Ciofani and Zúñiga-Pflücker, 2006). These thymus-settling progenitors undergo massive proliferation, and their progeny of early thymocyte precursors seed into the cortex region of the thymus, where they constitute the more immature subset of the CD4<sup>-</sup>CD8<sup>-</sup> double negative (DN1) compartment. ETPs are phenotypically identified as CD117<sup>+</sup>CD44<sup>+</sup>CD25<sup>-</sup>. They further divide into three sequential subsets: DN2 (CD117<sup>+</sup>CD44<sup>+</sup>CD25<sup>+</sup>), DN3 (CD117<sup>lo/-</sup>CD44<sup>-</sup>CD25<sup>+</sup>), and DN4 (CD117<sup>-</sup>CD44<sup>-</sup>CD25<sup>-</sup>) (Godfrey et al., 1993). DN subsets are all restricted to the cortex, and support critical events in T cell maturation: rearrangement of the TCR $\beta$  chain in DN2 cells, expression of pre-TCR ( $\beta$  chain and invariant  $\alpha$  chain) and  $\beta$ -selection in DN3 cells, and rearrangement of the TCR $\alpha$  chain in DN4 cells (Starr et al., 2003). These processes are critically regulated by the activity of RAG1 and 2, as illustrated by mice deficient in *RAG1*, *RAG2*, or any component of the pre-TCR complex, presenting a blockage in  $\alpha\beta$  T cell development at the DN3 stage. Of note, at this stage, DN precursors can also rearrange TCR $\gamma$  and TCR $\delta$  loci, and give rise to TCR $\gamma\delta$  T cells.

## 3) Thymic selection of the MHC-restricted preimmune repertoire

Still in the cortex, DN4 cells differentiate into double positive (DP: CD4<sup>+</sup>CD8<sup>+</sup>) thymocytes, and undergo positive and negative selection. Only 1% of them survive these processes (Bouneaud et al., 2000). Briefly, the latest event of cortical maturation is the positive selection process, mediated by cTECs (cortical TECs), where early DP cells with TCR conformations that are non-responsive to self-pMHC ligands die by neglect, and those that are overly reactive to self-pMHC undergo programmed cell death (Klein et al., 2014). It ensures that the preimmune repertoire is MHC-restricted and composed of low affinity thymocytes. Positive selection is also the step where (i) a thymocyte becomes a CD4<sup>+</sup> (if recognizing self-pMHCI complexes) or a CD8<sup>+</sup> (if recognizing self-pMHCI complexes) T cell (Tubo and Jenkins, 2014), and (ii) T cells undergo a process of TCR desensitization (Grossman and Paul, 2015). Positively selected late DP cells and SP CD8<sup>+</sup> or CD4<sup>+</sup> spend about 4-5 days in the medulla. There, TCR engagement by autoreactive immature thymocytes induces their apoptosis. This is negative selection, which is mediated by mTECs that have the unique ability to express the transcription factor Aire, and promote the intrathymic expression of tissue-specific antigens (TSAs). It ensures that the post-selection repertoire exported from the thymus comprises T

cells that are largely non-responsive to self, yet capable of responding with remarkable specificity to foreign peptides.

Interestingly, there is a concerted regulation of thymocyte migration at several critical steps of their maturation (Dzhagalov and Phee, 2011). This is mediated by (i) tonic TCR signals in the cortex, and (ii) differential expression of chemokines (Figure 2) (Halkias et al., 2013). Chemokines are a group of low-molecular-weight, structurally related molecules that provide attractive or repulsive signals to target cells through interactions with seven-transmembrane, G protein-coupled receptors (Thelen and Stein, 2008). They induce leukocyte movement (chemokinesis) and support directed migration (chemotaxis), either as soluble gradients or as anchored forms on the extracellular matrix (Sarris et al., 2012).

Schematically, intrathymic chemokines regulate:

- The seeding of LMPP and CLP progenitors into the thymus, which involves CC-chemokine receptor 9 (CCR9; which is expressed by subsets of LMPPs and CLPs), CCR7 (which is expressed by some LMPPs and highly expressed by CLPs), and PSGL1 (P-selectin glycoprotein ligand-1);
- The retention of DN4 and early DP thymocytes into the cortex, which involves interaction between CXCL12 (or SDF-1) and its receptor CXCR4 (Halkias et al., 2013);
- The attraction of late DP and mature SP thymocytes into the medulla, involving interaction between the chemokines CCL19 and CCL21 and their receptor CCR7.

Switch of expression from one receptor to another, for example from CXCR4 to CCR7 as a consequence of successful positive selection, is part of the maturation process. Only thymocytes with sufficient maturity are able to migrate towards a new subpart of the thymus – and thus the next step of maturation (Dzhagalov and Phee, 2011; Halkias et al., 2013).

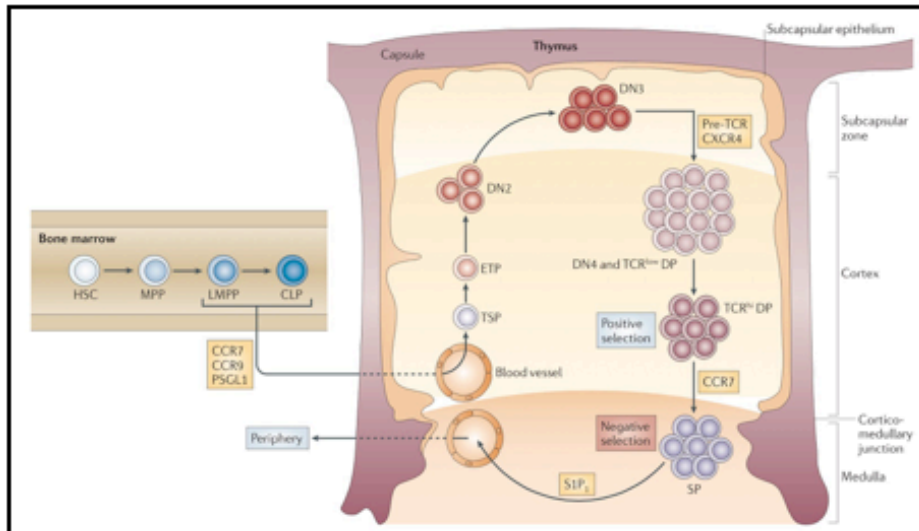


**Figure 2. Chemokine-driven trafficking and maturation of T cells into the thymus.** Haematopoietic stem cells (HSCs) differentiate into multipotent progenitors (MPPs), and subsequently give rise to lymphoid-primed multipotent progenitors (LMPPs; also known as ELPs) and common lymphoid progenitors (CLPs). CLPs migration to the CMJ of the thymus is regulated via CCR9 and CCR7 expression. There, progenitors differentiate into thymus-settling progenitors (TSPs), ETPs (or DN1), DN2 and DN3 cells that rearrange their TCR beta chains while migrating to the subcapsular zone. Expression of the pre-TCR and CXCR4 on DN3 thymocytes permits beta selection, cell proliferation, differentiation to the DN4, TCR $\alpha$  rearrangement and finally the generation of DP cells. Positively-selected DP thymocytes upregulate CCR7, and mature into single positive (SP) cells that migrate into the thymic medulla, where they are negatively selected. Finally, mature self-tolerant T cells emigrate from the thymus by a SIP1-dependent mechanism. From Love *et al.*, Nat Rev Immunol 2011.

#### 4) Maturation and emigration of mature SP thymocytes

During their estimated 4-5 days into the medulla, in parallel with negative selection, SP thymocytes undergo an ordered terminal differentiation program, transitioning from a semi-mature CD69<sup>hi</sup>CD62L<sup>lo</sup>CD24<sup>hi</sup> phenotype to a mature CD69<sup>lo</sup>CD62L<sup>hi</sup>CD24<sup>lo</sup> phenotype. They also progressively acquire resistance to apoptosis. Most of the medullary SP thymocytes express high levels of CCR7, and restricted subsets also express CCR8, CCR9 and CXCR4. However, these data arise from studies on mouse CD4SP maturation, and very little is known about the relevance of this finding for the CD8SP compartment. Recent studies focusing on human CD8SP documented that 20-40% of the CD8SP subset expresses CXCR3 - and not CCR7 (Annunziato, 2006). These cells, as well as TCR $\gamma\delta$  and NK cells that also express CXCR3 in the thymus, were successfully attracted by CXCR3 ligands in transwell experiments, although CXCL11 (I-TAC) appeared to be less active than CXCL10 (IP-10) and CXCL9 (MIG). All three chemokines are actively produced in the thymic medulla (Annunziato *et al.*, 2001), and thus likely play a role in retention of these specific subsets of cells in the medulla.

After completing their developmental program, mature SP thymocytes leave the thymus and join the population of peripheral circulating lymphocytes. The majority of thymocytes emigrate via perivascular spaces at the CMJ (Zachariah and Cyster, 2010). Similar to intrathymic migration, thymic

export is not a passive, but rather an active process, where sphingosine-1-phosphate (S1P) receptor 1 (S1P<sub>1</sub>) has to be selectively turned on. Schematically, when semi-mature SP thymocytes are receiving signals through engagement of TCR with self-ligands in the context of negative selection screens, FOXO1 is phosphorylated by AKT, and moves away from its transcriptional activity (**Figure 3**). This leads to the downregulation of Krüppel-like factor 2 (Klf2) expression, which is required for the transcription of *CCR7*, *Sell* (which encodes CD62L) and *S1PR1* (which encodes S1P<sub>1</sub>). In addition, TCR signaling induces CD69 expression, which downregulates surface expression of S1P<sub>1</sub>. When the cell is mature, negative selection and TCR signaling cease. This releases FOXO1, which translocates to the nucleus, and promotes the transcription of several genes, including *S1PR1*. Additionally, downregulation of CD69 increases S1P<sub>1</sub> surface expression. These events render SP thymocytes responsive to S1P present in high concentrations into the blood, and induce their export from the thymus (Garris et al., 2014).

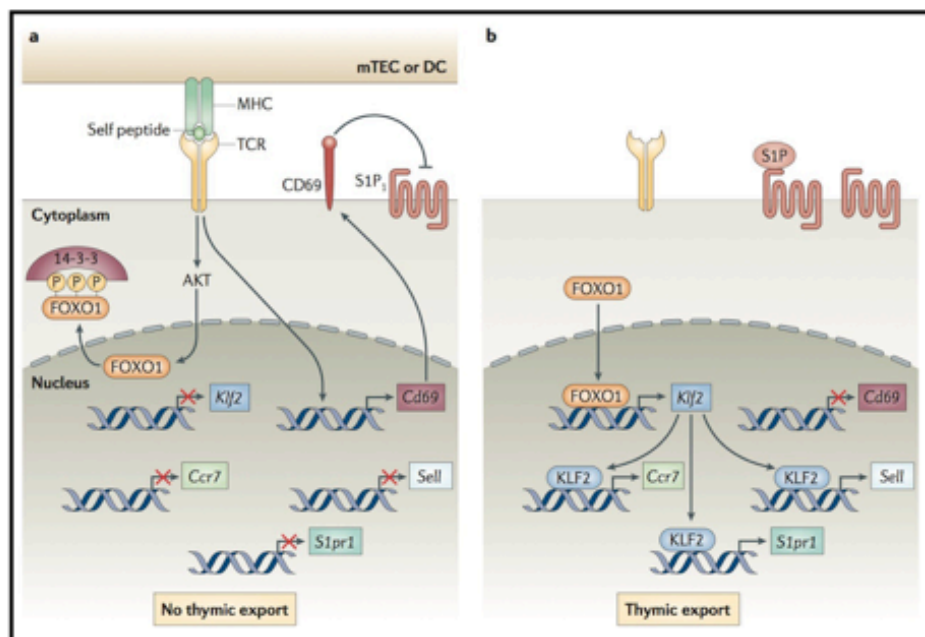


**Figure 3. Emigration of SP thymocytes from thymus.**

"Semi-mature" SP thymocytes receive activating signals through their TCRs by interaction with pMHC complexes expressed by mTECs and DCs. TCR signaling results in the phosphorylation and inactivation of FOXO1. This leads to the downregulation of *S1PR1*, which encodes S1P<sub>1</sub>. In addition, TCR signaling induces the expression of CD69, which downregulates the surface expression of S1P<sub>1</sub>. When SP thymocytes are mature, TCR signaling stops, and this results in the nuclear translocation of transcriptionally active FOXO1, and expression of *CCR7*, *CD62L* and *S1P<sub>1</sub>* via *KLF2*. It also results in the downregulation of CD69, alleviating CD69-directed downregulation of S1P<sub>1</sub> surface expression. Increased surface expression of S1P<sub>1</sub> renders SP thymocytes responsive to S1P chemotactic signals and promotes their export from the thymus. From Love *et al.*, Nat Rev Immunol 2011.

## B. Peripheral naive T cells

### 1) Recent Thymic Emigrants

Recent thymic emigrants (RTEs) constitute the population of T cells that just exited the thymus (Fink, 2013). RTE numbers decrease in parallel to global thymic function (Appay and Sauce, 2014). They are phenotypically and functionally immature, and it takes about 3 weeks before they acquire the features of standard « mature naive T-cells » (Dong et al., 2013; Fink, 2013). RTEs were identified in the mouse by direct injection of fluorescein isothiocyanate (FITC) into the thymus - and retrieval of FITC<sup>+</sup> peripheral T cells later on, or analysis of mice surgically implanted with thymic lobes from congenic donors. More recently, they were tracked using *RAG1-GFP* (recombination activating gene – green fluorescent protein) knockin and *RAG2p-GFP* transgenic (Tg) mice in which the *RAG1* or *RAG2* promoters drive GFP expression. In the *RAG2p-GFP*, the GFP signal remains detectable even after *RAG* gene expression is over, and GFP<sup>+</sup> peripheral T cells are considered as RTEs. In all of these models, RTEs were found to account for a large fraction of the peripheral naive T cells in neonates, but less than 10% in adults. Most but not all RTEs are Qa2<sup>lo</sup>CD24<sup>hi</sup>. Post-thymic maturation includes:

- downregulation of CD24 and CD3/TCR and upregulation of Qa2, CD28, CD45RB, IL-7R $\alpha$ , and Ly6C for CD4<sup>+</sup> RTEs;
- downregulation of  $\alpha 4\beta 7$ ,  $\alpha E$  integrins (LPAM-1 and CD103 respectively), and CCR9 for CD8<sup>+</sup> RTEs (Staton et al., 2006).

If stimulated by foreign pMHC during this short maturation period, RTEs proliferate poorly, and produce fewer cytokines and fewer effector and memory cells as compared to « mature » naive T cells (Boursalian et al., 2004). Their progeny typically display decreased levels of Ly6C at their cell surface. This might contribute to the relative immunodeficiency observed in newborns. TCRs expressed by RTEs contain longer complementarity determining region 3 (CDR3) regions, suggesting the existence of more autoreactive cells (Kyewski and Klein, 2006; Matsutani et al., 2007). The expression of inhibitory receptors such as CTLA-4 and PD-1 may also help prevent autoreactive RTEs from harmful tissue damage (Fink and Hendricks, 2011). Additionally, a subset of RTEs highly express  $\alpha 4\beta 7$ ,  $\alpha E$  integrin, and CCR9, facilitating their homing to gut-associated lymphoid tissues where they likely play a role in the tolerance to self- and harmless food- antigens (Staton et al., 2006).

How much these findings translate to humans is largely unknown, as there are no clear markers of RTEs in humans. sjTRECs have long been used as markers of recent thymic emigrants, but sjTREC data must be interpreted cautiously, as discussed above (Hazenberget al., 2003). While some human CD4<sup>+</sup> RTEs have been shown to express CD31 and PTK7, no markers are available to track CD8<sup>+</sup> RTEs, although they are likely enriched in the CD103<sup>+</sup> subset of naive peripheral CD8<sup>+</sup> T cells (McFarland et al., 2000). As such, very little is known in humans about their existence, their

functionality, their repertoire, as well as variations in numbers during physiological or pathological situations, which could significantly impact the adaptive immune responses.

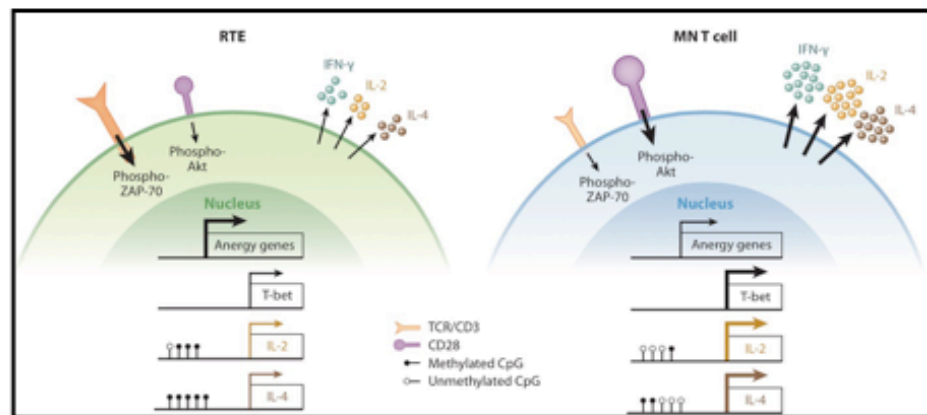


**Figure 4. Comparison of recent thymic emigrants and mature naive T cell function.** RTEs express more TCR and less CD28 than MN T cells. As compared to MN cells, when stimulated by anti-CD3/CD28 antibodies, CD4 RTEs generate more phospho-ZAP-70 and less phospho-Akt. This leads to specific patterns of gene expression, and ultimately less proliferation, and low secretion of IFN- $\gamma$ , IL-2, and IL-4 cytokines. From Fink, *Ann Rev* 2012.

## 2) Population size and TCR repertoire

How many T cells do we have in our body? This question is seemingly a simple one, but is still unresolved (Ganusov and De Boer, 2007). Mice have about  $9 \times 10^7$   $\alpha\beta$ T cells (60% are CD4<sup>+</sup> T cells and 40% are CD8<sup>+</sup>), and at steady-state, 70% of them have a naive phenotype (**Table 2**) (Jenkins et al., 2010). 95% of those naive T cells are located into secondary lymphoid organs (SLOs) through interactions of their surface receptors (CD62L, CCR7,  $\alpha 4\beta 7$  integrin) to specific ligands (PNAd, CCL21, MadCAM) (Andrian and Mackay, 2000). In humans, these numbers are extrapolated from animal studies, and normalized by the body surface area. Thus, it is estimated that we have  $10^{10}$  T cells in the blood,  $40 \times 10^{10}$  cells in lymphoid tissues,  $3 \times 10^{10}$  cells in the gut,  $3 \times 10^{10}$  cells in the lungs, and  $10^{10}$  cells in other organs. This is a total of about  $5 \times 10^{11}$   $\alpha\beta$ T cells in our body (Ganusov and De Boer, 2007; Thome et al., 2014). 70% of them are CD4<sup>+</sup> T cells and 30% are CD8<sup>+</sup> T cells. Within both circulating subsets, 30% display a naive phenotype. Both naive CD4<sup>+</sup> and CD8<sup>+</sup> T cell numbers decrease with age, but less dramatically than thymocyte numbers. This reflects peripheral compensation of T cell loss by increased proliferation of naive T cells (Braber et al., 2012; Ferrando-Martínez et al., 2010) – which does not necessarily translate into loss of their naive phenotype (Tough and Sprent, 1994). However, if this phenomenon partially compensates for the number of circulating naive T cells, it does not prevent the loss of diversity of the peripheral TCR repertoire, and ultimately leads to naive T cell oligoclonality, likely influencing immune responses in the elderly (Qi et al., 2014).

	Mouse (adult)	Human (adult)
<b>Number of <math>\alpha/\beta</math> T cells</b>	$8 \times 10^7$ (SLOs) $+ 0.5 \times 10^7$ (blood) $+ ?$ (non-lymphoid organs) $= 9 \times 10^7$	$40 \times 10^{10}$ (SLOs) $+ 1 \times 10^{10}$ (blood) $+ 7 \times 10^{10}$ (non-lymphoid organs) $= 5 \times 10^{11}$
<b>CD4/CD8 percentages</b>	60/40	70/30
<b>Naive percentages</b>	70% (CD44 <sup>lo</sup> CD62L <sup>hi</sup> )	30% (CD45RA <sup>+</sup> CD27 <sup>+</sup> )
<b>Number of naive T cells (CD4/CD8)</b>	$60 \times 10^6$ $(36 \times 10^6 / 24 \times 10^6)$	$3 \times 10^{11}$ $(2 \times 10^{11} / 1 \times 10^{11})$
<b>Lifespan of naive T cells (CD4/CD8)</b>	7 weeks / 11 weeks	4 years / 7 years
<b>Theoretical number of different specificities before/after thymic selection</b>	$10^{15} / 10^{13}$	$10^{15} / 10^{13}$
<b>Estimate number of different specificities after thymic selection (TCR sequencing approach)</b>	$2 \times 10^6$	$3 \times 10^7$
<b>Average number T cell clone</b>	30	10,000
<b>Average number of T cells responding to a given pMHC</b>	500	500
<b>Average number of T cells specific for individual foreign pMHC populations</b>	150,000	5,000,000
<b>Measured average precursor frequency (CD4/CD8)</b>	$10^{-4} / 10^{-6}$	$10^{-4} / 10^{-6}$

**Table 2. Mouse and human adults preimmune repertoire numbers.**

Grey area indicates results from estimations, whereas white areas indicate experimental measurements.

T cell specificity relies on the somatic TCR gene rearrangements during T cell development, and relates to the capacity of a given T cell to specifically recognize its cognate epitope when presented in the context of a pMHC complex. Given that the number of potential TCR amino acid sequences potentially produced by V(D)J recombination ( $> 10^{15}$ ) is greater than the total number of naive cells, it is theoretically possible that each cell carries a unique TCR and responds to a different foreign pMHC. However, estimates of T cell repertoire composition have revealed that the average T cell clone exists in 30 copies in mice and 10 000 copies in humans. This must arise by cell division after TCR $\alpha$  locus rearrangement, either in the thymus or during homeostatic proliferation in periphery. Many questions remain about the  $\sim 10^6$  fold gap between the theoretical and observed numbers of different TCRs in the peripheral blood of humans.

In generating a « useful » repertoire, there are some major constraints (Mason, 1998):

- The repertoire must be able to react to a very large number of individual peptides presented by the MHC class I and II antigens, to ensure that pathogenic peptides do not go unrecognized. It

is estimated that 1 peptide is generated every 30 aminoacids (aa), and « only »  $10^{10}$  different peptides can be presented by one given MHC molecule;

- it must be highly specific to allow responses to foreign but not to self-peptides;
- the frequency of inexperienced T cells that can recognize a given foreign peptide must be sufficiently large to ensure a rapid response to a foreign antigen containing that peptide, but at the same time sufficiently low to fit into a size-limited animal.

As there are far more potential foreign peptides in the environment than the organism has T cells, a very high level of crossreactivity – *i.e.*, the ability for an individual T cell to recognize multiple peptides - is now recognized as an essential feature of the T-cell receptor (Nelson et al., 2015; Su and Davis, 2013; Su et al., 2013). One given naive T cell is estimated to have the capacity to bind  $10^6$  different peptides. Inversely, one given pMHC complex can be recognized by at least 500 different clones (Kedzierska et al., 2006). Those clones can be restricted by the same or different haplotypes, and it is not excluded that  $CD4^+$  T cells participate in the complexity (Legoux et al., 2010). With the number of foreign nonamer peptides estimated to be  $\sim 10^{10}$  for a given MHC molecule, there is theoretically less than one chance in  $10^4$  that a T cell reacts with one chosen at random. This makes the T cell repertoire appear artificially highly antigen specific. As such, the composition of the foreign peptide-specific T cell repertoire is shaped by the degree of TCR cross-reactivity between similar self and foreign peptides (Nelson et al., 2015). However, since a T cell must see at least 100 immunogenic pMHC complexes to get activated, a self-antigen that is under this level of expression in the periphery will be ignored by the immune system - the majority of those that exceed this threshold being deleted into the thymus. Importantly, when a T cell is primed, this leads to a reduction in the heterogeneity of TCR gene usage, with a degree of affinity selection that ensures that only T cells that respond to low concentrations of peptide give rise to memory cells (McHeyzer-Williams and Davis, 1995). As a consequence, the repertoire of memory cells is less diverse, and as a consequence less crossreactive than naive cells.

The generation of MHC class I tetrameric or tetrameric complexes (commonly referred as MHC tetramers) represents a major technical advance for the study of T cell repertoires (Altman et al., 1996; Altman and Davis, 2003) (**Figure 5**). MHC class I tetramers are reagents that carry multiple pMHC complexes, and thus have the ability to interact with multiple TCRs on a single  $CD8^+$  T cell. Fluorescent-labeling of MHC tetramers permits identification of Ag-specific T lymphocytes based on the avidity of their TCR, independent of their functional or differentiation state (Davis et al., 2011). Using MHC tetramers, it is possible to directly track and quantitate Ag-specific T cells (*i.e.* all T cell clones that are able to recognize a given pMHC complex) during the course of immunization (Klenerman et al., 2002). And by co-staining with antibodies directed against phenotypic cell surface proteins, one can define subsets of cells of interest based on their activation or differentiation state, or chemokine receptor expression (Romero et al., 2002). MHC tetramer technology has been successfully coupled to conventional functional assays (*e.g.*, CFSE dilution, intracellular cytokine staining - ICS),

and specific T cells can be sorted for elispot, cytotoxicity assays, gene expression studies, or for generating long-term cultures (Baitsch et al., 2011). Tetramers are now widely used in the immune monitoring of T cell responses following therapeutic or prophylactic vaccination. Finally, the availability of good manufacturing practice (GMP)-grade tetramers is enabling the *ex vivo* expansion of T cells for immunotherapy (Kanodia et al., 2010).

However, the limit of detection of multimers, of  $10^{-5}$ , does not allow exploration of the preimmune repertoire prior to peptide-induced expansion. To solve that issue, in 2007, MHC tetramers were coupled to magnetic bead enrichment in mice (Moon et al., 2007; Obar et al., 2008). This permitted for the first time, a direct evaluation of Ag-specific  $CD4^+$  - and later  $CD8^+$  - T cell precursor frequencies (*i.e.*, frequencies of T cells specific for peptides that have never been seen by the immune system). They were found in the range of  $10^{-6}$  to  $10^{-4}$  (*i.e.* 1 cell in 10,000 to 1,000,000 T cells). Following from these studies, we and others developed a similar enrichment protocol for human  $CD8^+$  T cells (see **Chapter 2**) (Alanio et al., 2010; Legoux et al., 2010). With that tool, we found precursor frequencies also ranging from  $10^{-6}$  to  $10^{-4}$ . Similar ranges were later observed for the human  $CD4^+$  T cell preimmune repertoire (Kwok et al., 2012; Su et al., 2013).

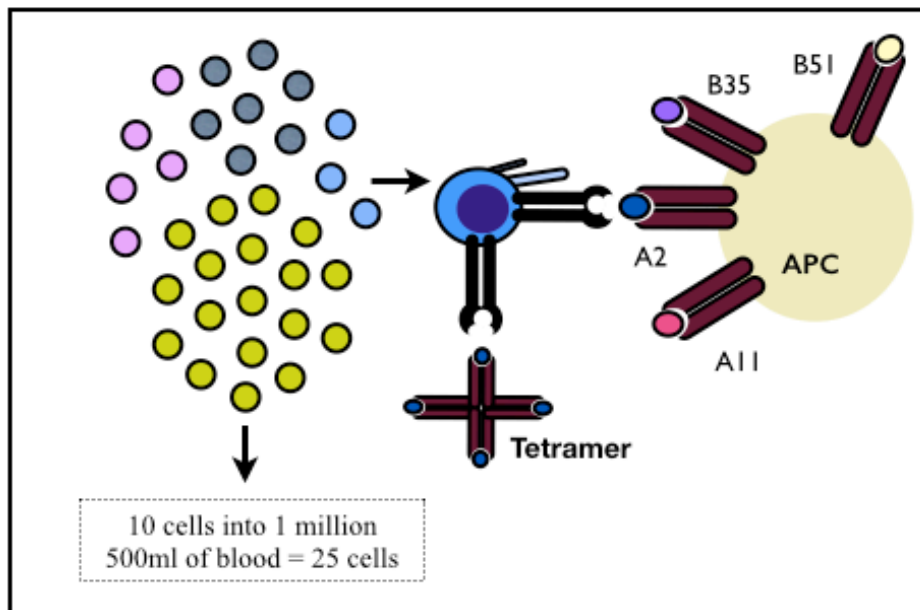


**Figure 5. Antigen specificity and tetramer staining.**

The naive T cell compartment is a pool of T cells with different antigenic specificities defined by the ability of their TCR to bind to a specific pMHC complex at the surface of an APC. To track antigen-specific T cells, we use fluorescent tetrameric molecules with a known peptide loaded on four streptavidin-linked engineered MHC molecules. This provides very limited information, screening only one epitope from the pathogen, in the context of one of the six potential MHC molecules present at the surface of presenting cells.

### 3) Homeostasis and homeostatic proliferation

Mature naive phenotype T cells are relatively long-lived, with a half-life of 7–11 weeks in mice and 4–7 years in humans (Braber et al., 2012; Jenkins et al., 2010; Sprent and Surh, 2011). They have low basal metabolic activity, and actively maintain quiescence while sustaining their naive differentiation state (Hamilton and Jameson, 2012; Tough and Sprent, 1994). Quiescence is a complex process requiring the interplay of a number of different regulatory mechanisms that prevent T cell activation, including:

- repression of NFκB activity via the continuous synthesis of IκB (inhibitor of NFκB) induced by two members of the forkhead family of transcription factors, FOXO3 and FOXJ1;
- continuous inactivation of NFAT by inhibition of its dephosphorylation that avoid its translocation to the nucleus;
- KLF2-, ELF4-, and KLF4- dependent downregulation of the expression of genes essential for cell cycle progression such as *Cdk2*.

Two homeostatic signals are crucial to maintain naive T cells alive (**Figure 6**) (Hamilton and Jameson, 2012; Jameson and Fulton, 2011):

- IL-7. This cytokine is synthesized by CD45-negative stromal cells, and is primarily produced in the thymus, lymph nodes and bone marrow. In IL-7<sup>-/-</sup> and IL-7R(CD127)<sup>-/-</sup> mice, both CD4<sup>+</sup> and CD8<sup>+</sup> naive cells die within 1-2 weeks after their transfer. IL-7 binding to IL-7R, via JAK1-3/Stat5 signaling, promotes survival by tilting the balanced expression of anti/pro apoptotic molecules such as Bcl-2 and Bim towards the former (Schluns and Lefrançois, 2003). IL-7 responsiveness is controlled by modulation of expression of IL-7R via (i) an autocrine loop, and (ii) the transcription factor Foxo1;
- TCR-self-pMHC interactions. Both tonic TCR signaling of T cells, and MHC contacts maintain cell viability (Sprent and Surh, 2011). In their absence, T cells die within several weeks. This interaction is subtly controlled by TCR tuning during T cell development. Indeed, although intrathymic DP and SP T cells are more sensitive to activation by antigen than mature T cells, they undergo a process of TCR desensitization (or tuning) in the late step of maturation (Grossman and Paul, 2015). This sets the threshold for TCR activation just above the level required for T cell maintenance in the periphery, thereby keeping the cells in a self-tolerant state.

Contact with these survival factors occurs in secondary lymphoid organs, such as lymph nodes (LNs), where professional APCs and local stromal cells provide a key source of MHC molecules and IL-7 respectively. In line with this model, the numbers of naive T cells are significantly reduced under

conditions where homing to lymph nodes is hampered (Boyman et al., 2012). This is further supported by the common transcriptional regulation of key elements of homing and survival such as CD62L (L-selectin), CCR7, and IL-7R of naive T cells (Kerdiles et al., 2009).

Homeostatic proliferation (HP) occurs naturally in the neonatal period, but is most prominent in hosts with acute lymphopenia. In the latter case, it is driven by sudden high concentrations of cytokines, such as IL-7, IL-15 and IL-2. This is a result of low consumption by dramatically decreased numbers of lymphocytes. HP corresponds to the expansion, but also in some cases differentiation and conversion to memory-phenotype (MP) cells, of inexperienced T cells occurring independently of antigenic stimulation. CD8<sup>+</sup> T cells are more sensitive to HP than CD4<sup>+</sup> T cells (Sprent and Surh, 2011). In humans, HP-derived T cells are chronically activated (CD28<sup>+</sup>CD57<sup>+</sup>), highly proliferative (Ki67<sup>+</sup>), oligoclonal, memory-like (usually CCR7<sup>+</sup>), and capable of producing proinflammatory cytokines. In mice, HP cells typically have a central-memory phenotype, and are functionally indistinguishable from Ag-driven memory cells (Sallusto et al., 2004). However, they display low levels of  $\alpha$ 4-integrin (CD49d) (Cheung et al., 2009). The reasons why half of CD8<sup>+</sup> naive T cells express this marker in non-lymphopenic adult animals are unclear, but could reflect under-estimated homeostatic proliferation rates. Importantly, HP-derived cells have been identified as a driving force for lymphopenia-associated autoimmunity in both mice (King et al., 2004; Le Saout et al., 2008) and humans (Jones et al., 2013).

Recent studies using tetramer-enrichment tools demonstrated that MP cells represent up to 30% of inexperienced Ag-specific T cells in both mice and humans (Haluszczak et al., 2009; Legoux et al., 2010; Su and Davis, 2013). These cells may reflect cross-reactivity, and/or more likely, derive from HP, as: (i) large numbers of specificities are concerned, (ii) they are found in germ-free animals (Haluszczak et al., 2009), and (iii) they increase in numbers in the context of acute lymphopenia (Goldrath et al., 2000). Notably, in the latter case in mice, Ag-specific inexperienced T cell populations were found to reverse to a naive phenotype within about a month after homeostatic conditions were restored. This parallels the observation of restoration of bulk naive T cell polyclonality within two years in humans (Jones et al., 2013). The mechanisms underlying these observations are unclear.

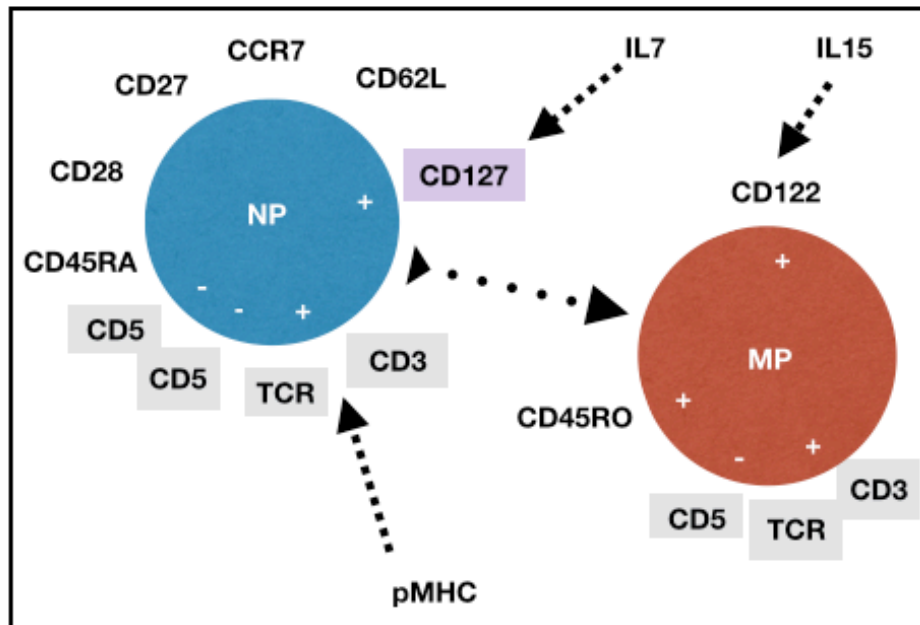


**Figure 6. Naive T cell phenotype, homeostasis, and homeostatic proliferation.** Schematic overview of critical factors involved into naive T cell homeostasis. CCR7 and CD62L are homing molecules. CD45RA, CD28 and CD27, contribute to maintaining cells in a quiescent state. Naive T cells are maintained in the periphery through interactions of (i) CD3/TCR complexes with pMHC molecules, and (ii) CD127 (IL-7R) with IL-7. CD5 is a key molecule acting as a negative regulator of T cell activation, and activation-induced cell death. Dysregulation of at least one of these balancing signals leads to abnormal activation of NP cells, and generation of MP cells.

#### 4) CD5 expression and dynamic tuning of lymphocytes

One of the key molecules in TCR tuning is CD5 (**Figure 7**) (Grossman and Paul, 2015; Soldevila et al., 2011). CD5 is a type I glycoprotein of 67-kDa, constitutively expressed at the cell surface of all thymocytes and mature T cells, as well as a subset of B cells. It belongs to the type B superfamily of scavenger receptor cysteine-rich, and also exists in a soluble form, which acts as a decoy receptor. It is composed of three extracellular regions and a highly conserved cytoplasmic domain containing multiple Ser/Thr and Tyr phosphorylation sites, including two potential immunotyrosine-based inhibition motifs (Raman, 2002).

Both soluble and membrane-bound human CD5 molecules bind and sense pathogen-associated molecular patterns (PAMPS) of fungal origin ( $\beta$ -glucans) via the extracellular portion of the molecule (Fenutria et al., 2014). CD5 has also been reported to interact with several surface molecules present on APCs including CD5L, CD72, gp40-80, gp150, and IgV(H) framework region sequences, but whether these are true ligands remains unclear (Soldevila et al., 2011).

Via its intracytoplasmic portion, CD5 negatively regulates TCR signaling. This effect was first

observed in CD5<sup>-/-</sup> mice, where T cells are hyperresponsive to TCR stimulation, with increased proliferation, and enhanced phosphorylation of TCR signaling effectors such as LAT, phospholipase C $\gamma$ 1, or Vav (Tarakhovsky et al., 1995). The mechanism of action has now been clarified (Grossman and Paul, 2015). Upon TCR ligation, CD5 is rapidly engaged in the immunological synapse, where it physically associates with the CD3 molecule, and recruits inhibitory molecules of TCR signal such as SHP-1, RasGFP and Cbl.

The level of CD5 expressed at the cell surface of antigen-specific naive T cells is set on thymocytes at the time of positive selection, and positively correlates with the strength of encounter with self-pMHC ligands. CD5<sup>hi</sup> cells are thymocytes with the highest affinity for self-ligands – just under the level triggering intrathymic deletion - and thus those for which the threshold for TCR activation needs to be significantly lowered in the periphery. CD5 and IL-7R expression are positively associated, providing a mechanistic basis for crosstalk between TCR and cytokine signals during homeostasis. In the context of inflammation, CD5<sup>hi</sup> naive CD8<sup>+</sup> T cells show superior use of inflammatory cytokines *in vitro* and *in vivo*, as well as improved clonal recruitment and expansion in response to foreign pMHC. This highlights that (i) predetermined heterogeneity dictates the capacity of naive T cells to respond to foreign antigens, and that (ii) T cells with the strongest reactivity to intrathymic self-peptides dominate the response to foreign pMHC.

However, in more complex systems, peripheral modulation of CD5 level does exist. It decreases when cells are deprived in pMHC contact (Smith et al., 2001), or IL-7 and IL-21 cytokines (Soldevila et al., 2011). Inversely, it increases when cells are chronically exposed to self-antigen in the periphery (Hawiger et al., 2004). Levels of CD5 are negatively regulated at the transcriptional level by E47 and GATA-3 (Arman et al., 2004; Ling et al., 2007), and positively by ETS1 (Tung et al., 2001). Peripheral down- and up-regulation of CD5 levels translates into increased and decreased responsiveness of CD8<sup>+</sup> T cells to antigenic stimulation respectively. It is a way to tune (i) tumor-infiltrating lymphocytes to promote increased antitumor activity (Tabbekh et al., 2013), or (ii) auto-reactive cells to diminish responsiveness to chronically exposed self-antigens (Hawiger et al., 2004; Stamou et al., 2003).

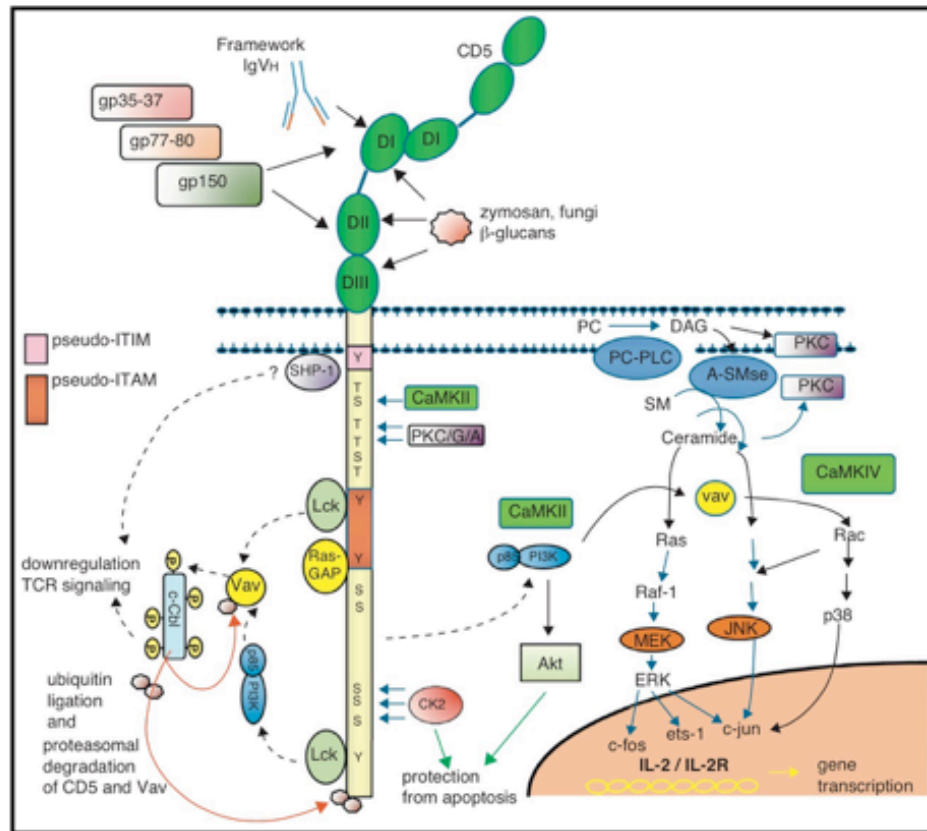


**Figure 7. Dual role of CD5 in lymphocyte activation and survival.**

Extracellular domains of CD5 can bind to gp35–37, gp77–80, gp150, Framework IgV<sub>H</sub>, CD5 itself, zymosan, beta glucans, and fungi. Intracellular signaling molecules that associate with CD5 cytoplasmic tail are: Lck, PI3K, CaMKII, PKC (activation); C-Cbl, RAS-GAP, SHP-1 (negative regulators); CK2 (prosurvival molecule). The downstream effectors activated by CD5 are shown. The association of SHP-1 to membrane proximal tyrosine of CD5 is controversial. From Soldevila *et al*, *Curr Opin Immunol* 2011.

### 5) Activation, differentiation and activation-induced cell death

Engagement of the TCR occurs when it binds to its agonist pMHC complex with sufficient avidity to overcome the threshold for activation established during T cell development (Poltorak *et al.*, 2013). It results in the sequential recruitment and phosphorylation of the src-family kinase Lck, the TCR-associated  $\gamma$ ,  $\delta$ , and  $\zeta$  chains, the kinase ZAP-70, the coreceptor-associated linker for activation of T cells (LAT), and the mitogen-activated protein (MAP) kinase ERK. At the single cell level, the ERK response is digital: 70-80% of maximum signal reached within few minutes after activation with different agonists concentrations, *versus* no significant response with antagonists (Grossman and Paul, 2015). At the population level, increase in ligand concentration results in an increased number of activated cells with a maximal ERK response, likely reflecting the pre-existing variations among individual cells. These proximal events translate into transcriptional promotion of the expression of

genes involved in T cell differentiation and proliferation. Schematically, important events of T cell activation include (**Figure 8**):

- At hour (H)6, upregulation of the T cell activation marker CD69, a calcium-dependent type II transmembrane receptor of the lectin superfamily. Its expression peaks at 24 hours, and is down-regulated after 48 hours;
- At H12, upregulation of CD25, the  $\alpha$ -chain of the IL-2 receptor. Its expression peaks at 48 hours, and diminishes after 72-96 hours;
- From day (D)2 to D4, modification of the surface phenotype, with acquisition of memory markers. Of note, CD45RA and CD45RO are two different isoforms, and the transition in mRNA expression is detectable as soon as 24 hours after activation. Late persistence of the CD45RA molecule result from slow turnover of the molecule at the cell surface;
- At D2, blastogenesis with limited division. It is transient, lasting only one day;
- At D3, proliferation and rapid expansion (up to 50 000 fold expansion within one week) as illustrated by high levels of 3H-thymidin incorporation (Blattman et al., 2002).

Ultimately, the activated T cells differentiate into effector cells that disseminate throughout the body to combat infection.

A properly functioning immune system is dependent on programmed cell death at every stage of lymphocyte development. Following T-cell activation and proliferation, activation-induced cell death (AICD) controls the expansion of activated T lymphocytes and ensures tolerance and homeostasis. It is an apoptotic pathway triggered by (i) the death receptor CD95 (APO-1, Fas) - a subset of the tumor necrosis factor receptor (TNFR) family, and its natural ligand (CD95L, FasL), engagement of which leads to caspase activation (Green et al., 2003); and (ii) TNF, TRAIL, and Bim molecules. AICD regulation happens predominantly at the transcriptional level, with regulation of *FasL*, *TRAF1* and *TRAF2*, *c-IAPs*, and *c-FLIP* gene expression – the latter being a negative regulator of Fas and TRAIL receptor signaling.

Besides its action on regulating T cell activation, CD5 has emerged as an important regulator of T-cell survival – low levels of CD5 correlate with increased susceptibility to cell death (**Figure 7**). This is the mechanism accounting for the paradoxical observation of delayed onset and decreased severity of EAE in CD5<sup>-/-</sup> mice (Axtell et al., 2006). Ag-reactive T cells from those mice are hypersensitive to activation, but unable to persist after the proliferation phase. Similarly, low levels of CD5 on human TILs increases their susceptibility to AICD (Tabbekh et al., 2011). CD5-mediated T-cell survival involves different pathways than those implicated in the regulation of TCR activation. This is evidenced by bone marrow chimera (BMC) experiments, where reconstitution of CD5<sup>-/-</sup> mice with

CK2-binding deficient mutant CD5 restores resistance to AICD, but not sensitivity to activation (Axtell et al., 2006). CD5 expression promotes lymphocyte survival through activation of CK2, which induces the expression of pro-survival molecules such as Bcl-2 and Bcl-x1, and inhibits proteins associated with apoptotic pathways, such as FasL, caspases and Bid.

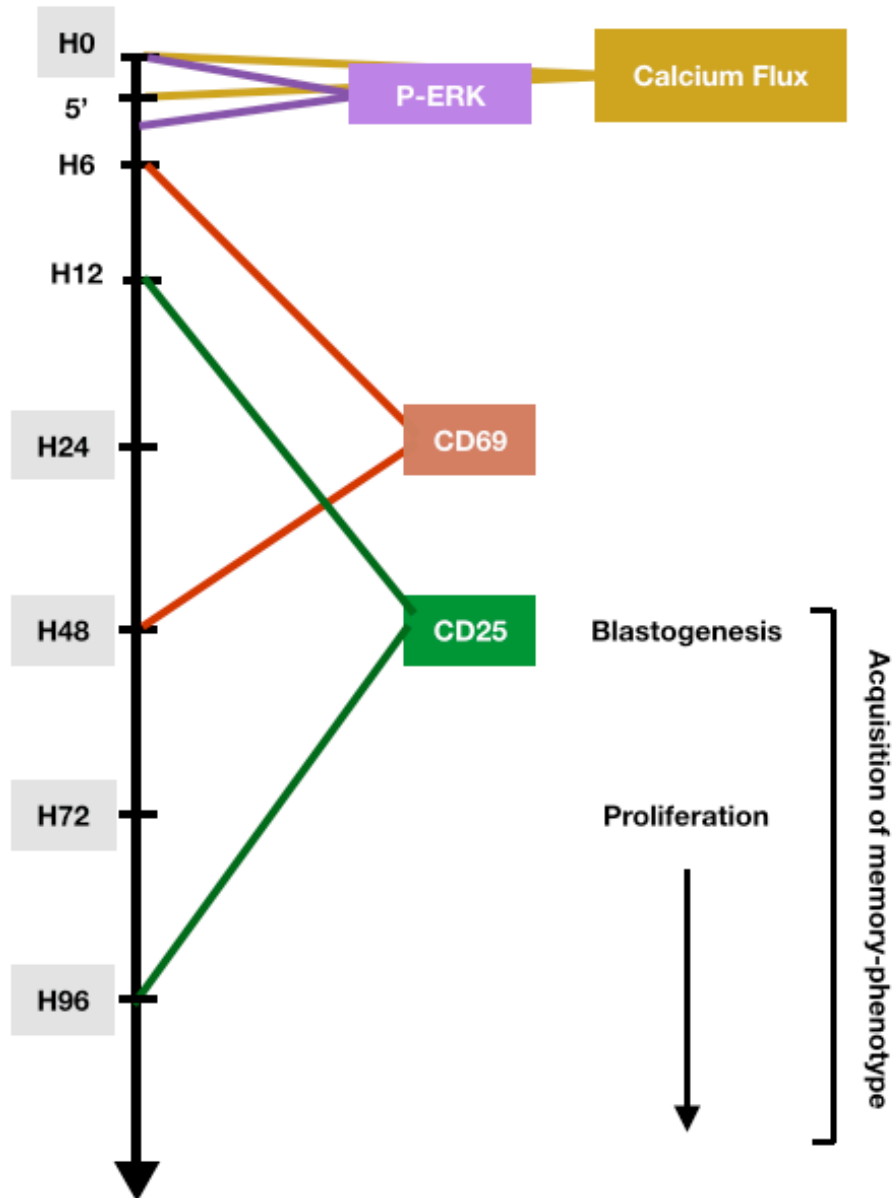


**Figure 8. Sequence of critical events after TCR activation.**

After TCR stimulation at H0, calcium flux (peak 1 minute) and ERK phosphorylation occur within a few minutes (peak 5 minutes) as a reflection of signal transduction. At H6 and H12, CD69 and CD25 expression are detectable at the surface of activated cells. Proliferation starts at H72 after a one-day period of blastogenesis. Acquisition of memory-phenotype happens from H48 to H96.

## 6) Phenotypic and functional diversity

Naive T cells have long been seen as a homogeneous population (Stemberger et al., 2009). However, over the last decade, it became evident that the preimmune repertoire contains a considerable degree of phenotypic and functional heterogeneity.

Schematically, in homeostatic conditions, the preimmune repertoire is a mixture of:

- 10% RTEs (cf Chapter IB1);
- 70% mature naive-phenotype cells, further subdivided into:
  - CD49d<sup>hi</sup> or CD49d<sup>lo</sup> cells – in the mouse CD8<sup>+</sup> compartment (cf Chapter IB3);
  - CD5<sup>hi</sup> and CD5<sup>lo</sup> populations (cf Chapter IB4);
- and 20% memory-phenotype cells, which is a mixture of:
  - cells arising from HP (cf Chapter IB3);
  - crossreactive cells (cf Chapter IB2);
  - innate memory cells, or virtual memory (VM). These cells appear soon after birth, and increase in frequency during aging (Jameson et al., 2015). They are present in germ-free mice. They are phenotypically similar to cells arising from homeostatic proliferation (CD49d<sup>lo</sup>). However, they have unique functional properties: poor TCR-induced IFN $\gamma$  synthesis, and preferential differentiation into central memory cells (Lee et al., 2013). VM cells lead to enhanced pathogen control in mouse models, and might be involved in preimmune resistance to infection (Rudd et al., 2011).

Obviously, any change in the proportion of one or multiple of these subpopulations will tune the preimmune repertoire from poor to high reactivity. **Table 3** shows the characteristics of each of these subsets, and their expected contribution to the global response of the Ag-specific population.

Cell Type	Fraction	Subset / Abbreviation	Specific markers (mice)	Specific markers (humans)	Repertoire / Specificity	Activation Threshold	Additional diversity within the subset	Symbol
Recent Thymic Emigrant	10 %	RTE	$\alpha 4\beta 7^{\text{hi}}$ CD103 <sup>hi</sup> CCR9 <sup>+</sup>	Unknown (sjTRECs <sup>hi</sup> CD103 <sup>+</sup> )	Unknown	High	Unknown (probably high)	
Naive-phenotype	70 %	NP	CD62L <sup>h</sup> CD44 <sup>lo</sup>	CD45RA <sup>+</sup> CD27 <sup>+</sup>	Diverse; self and non-self	Normal	High (CD5, CD49d)	
		Homeostatic Proliferation (HP)	CD44 <sup>hi</sup> CD49d <sup>lo</sup>	Unknown (CD45RO <sup>+</sup> )	Restricted; self and non-self	Low	Low	
Memory-phenotype	20 %	Cross-reactive cells (CR)	CD44 <sup>hi</sup>	Unknown (CD45RO <sup>+</sup> )	Restricted; non-self	Low	Low	
		Virtual Memory (VM)	CD44 <sup>hi</sup> CD49d <sup>lo</sup> IFN $\gamma$ <sup>lo</sup>	Unknown (CD45RO <sup>+</sup> )	Unknown	Very low	High	

**Table 3. Diversity of the CD8 T cell preimmune repertoire.**

### 7) Impact of precursor frequency and diversity

Direct measurements of Ag-specific populations in mice have shown that the size of Ag-specific inexperienced populations vary in a predictable fashion, with significant differences among distinct epitopes, but highly conserved frequencies among individuals that express at least one similar MHC allele. The impact of such variations on later immune responses is key, and has been investigated in mice. Early (<1 week) after peptide immunization, whatever the dose of peptide utilized, there is a positive correlation between pre- and post- immunization CD4<sup>+</sup> T cell frequencies (**Figure 9A**). Similar observations were reported for CD8<sup>+</sup> T cells, but when precursor frequencies are significantly different (>5-fold) (Kotturi et al., 2008; Obar et al., 2008). Besides magnitude, T cell precursor frequency was also demonstrated in mice as a key factor for early kinetics (an increased precursor frequency resulting in a more rapid response), and immunodominance hierarchy (Kotturi et al., 2008; Lo et al., 2014; Obar et al., 2008). It also predicts qualitative aspects of the memory T cell response, with increased precursor frequencies translating into rapid acquisition of a CD62L<sup>hi</sup> central-memory phenotype (Obar et al., 2008). Finally, precursor frequencies is a mode of virus escape in LCMV model of infection (Kotturi et al., 2008). In humans, the same impact of precursor frequency on the magnitude and immunodominance patterns of responses were found in studies of influenza-infected humanized HLA-transgenic mice (Tan et al., 2011), HCV-specific peripheral T cells (Schmidt et al., 2011), and B.anthraxis-vaccinated individuals (Kwok et al., 2012).

It is important to consider that some studies on mice infected with influenza (Cukalac et al., 2014; La Gruta et al., 2010), or Respiratory Syncytial Virus (RSV) (Ruckwardt et al., 2011) did not confirm the

« precursor frequency to magnitude » correlation. One possible explanation for this discrepancy is that the impact of precursor frequency will only manifest in situations where the other parameters that influence immunodominance are controlled and comparable. This includes efficiency of antigen processing and presentation, MHC binding properties, epitope abundance at the surface of presenting APCs, viral load and kinetics of viral protein expressions. Alternatively, qualitative properties of the initial Ag-specific population, such as the proportion of high-affinity T cells, might influence its behavior after immunization (Cukalac et al., 2014). In other words, the work presented above has now established precursor frequency as a crucial factor in shaping adaptive immune responses, but qualitative parameters must also be taken into account when trying to predict the effective epitope-specific response after antigenic challenge (Jenkins and Moon, 2012). In particular, each of the subsets identified as part of the T cell inexperienced populations (as reported in **Table 3**) has a specific threshold for TCR activation and sensitivity to cytokine signals, and a specific pattern of function. RTEs and CD5<sup>hi</sup> NP cells have increased threshold for TCR activation (Berkley et al., 2013; Dalloul, 2009). Inversely, MP cells are hyperresponsive when encountering their cognate antigen (Haanen et al., 1999; Lee et al., 2013; Younes et al., 2011). However, how much the proportion of each of these subsets inside a given Ag-specific population influences the global behavior of that population during homeostasis and after immunization is unknown (**Figure 9B**).

Interestingly, in both CD4<sup>+</sup> and CD8<sup>+</sup> naive T cells in mice, early in the course of a primary response (*i.e.* 4-6 days after peptide immunization), TCR diversity of the expanded population is similar to the one present before immunization (Moon et al., 2007) (Obar et al., 2008). This apparently conflicts with the idea that priming of cells results in a drastic reduction in the heterogeneity of TCR usage as early as day 6 after immunization (McHeyzer-Williams and Davis, 1995). However, clonal selection of high-affinity clones happens predominantly after day 4 (Malherbe et al., 2004). Additionally, whereas the two conflicting studies examine the repertoire at the level of V $\alpha$  and/or V $\beta$  expression profile, the latter explore the diversity at the level of CDR3 sequences. More recent studies indicate that the diversity of the naive population is more at the level of the CDR3 diversity than at the level of V $\beta$  chain selection (Neller et al., 2015). This means that individual V $\alpha$  and V $\beta$  families are likely to have the same ability to be recruited during the course of an infection, but that does not exclude the fact that within each of those families, there are predominant CDR3-divergent clones that are selected.

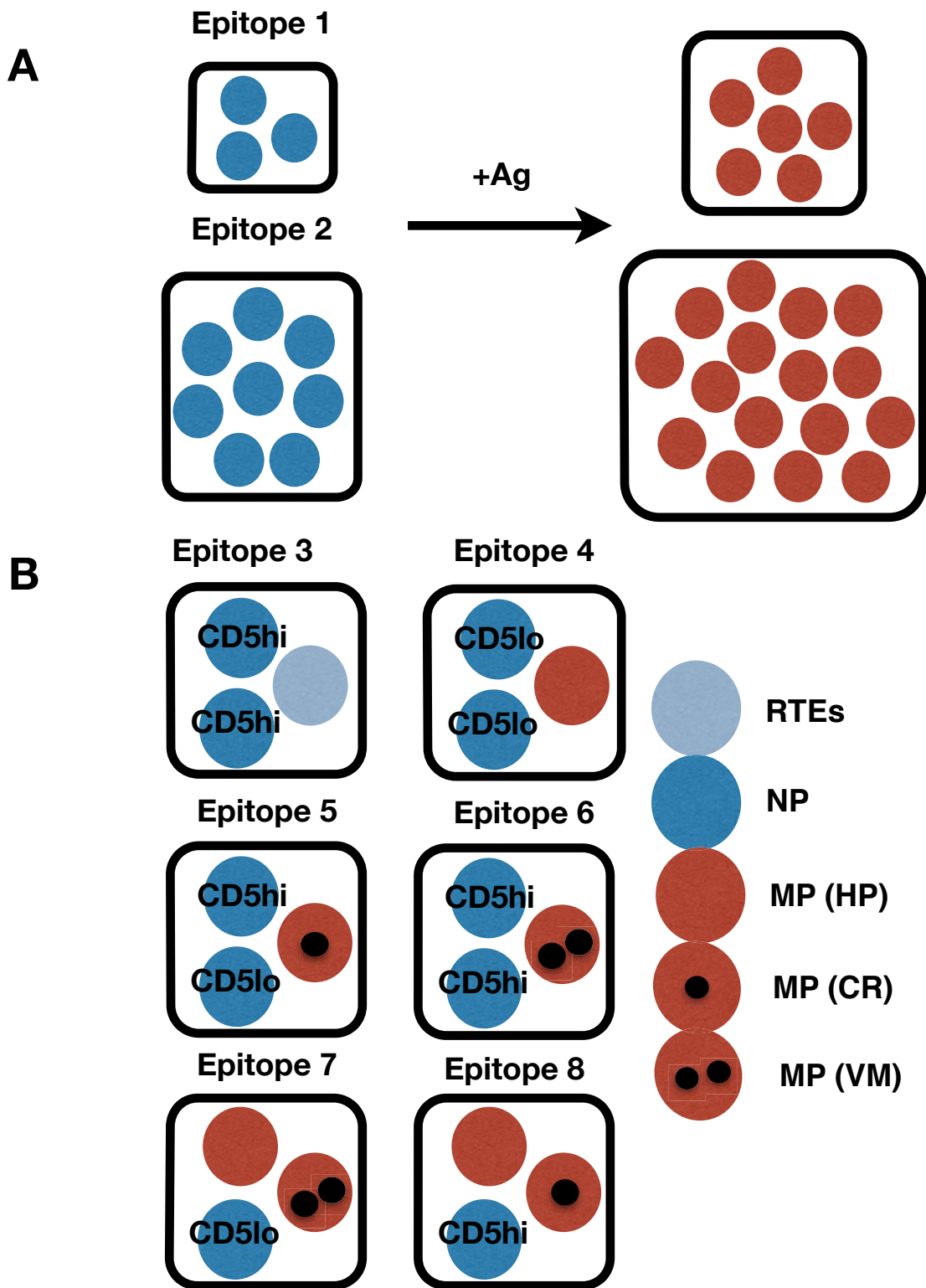


**Figure 9. Composition of the preimmune repertoire.**

The preimmune repertoire is composed of mature naive-phenotype cells (NP, dark blue), recent thymic emigrants (RTEs, light blue), and memory-phenotype cells (MP, red) that can arise by homeostatic proliferation (HP), cross-reactivity (CR, one black point), or be virtual memory cells (VM, two black points). A. Precursor frequency positively correlates with the magnitude of subsequent responses. In this simple situation, considering other parameters influencing immunodominance are controlled, epitope 2 will drive bigger expansion than epitope 1. B. However, the composition of a given antigen-specific population is likely to be more complex, and based on specific functional features of each of these subsets, likely influence the behavior of the population during and after expansion.

## II. CHRONIC INFLAMMATION

In this section, I introduce general notions about inflammation. I present the hepatitis C virus (HCV) and characteristics of related chronic infection, and detail the reasons why we chose HCV as a model of chronic inflammation.

### 1) General introduction

Inflammation is the immune response of tissues to injury. Classical signs of acute inflammation include pain, heat, and redness. It is usually acute and localized, in response to trauma or infection. However, if the causal agent persists, inflammation can become chronic and/or systemic. Circulating monocytes are first attracted to the site of inflammation, where they differentiate into long-lived tissue-homing macrophages. Locally, they get activated by macrophage activating factors such as IFN- $\gamma$  and MCP-1, while they are actively retained by migration inhibition factors, such as GM-CSF and IFN- $\gamma$  (Feghali and Wright, 1997). Activated macrophages contribute to the inflammatory process by chronically elaborating low levels of IL-1 and TNF. This induces a cascade of recruitment/activation of immune cells that secrete a complicated network of multiple cytokines. Schematically, we can differentiate:

- cytokines participating in humoral inflammation: IL-3, IL-4, IL-5, IL-6, IL-7, IL-9, IL-10, IL-13, and transforming growth factor- $\beta$  (TGF- $\beta$ );
- cytokines contributing to cellular inflammation: IL-1, IL-2, IL-3, IL-4, IL-7, IL-9, IL-10, IL-12, interferons (IFNs), IFN- $\gamma$  inducing factor, TGF- $\beta$ , and tumor necrosis factor (TNF)- $\alpha$  and - $\beta$ .

The Labex Milieu Interieur (Thomas et al., 2015) is a large-scale study ongoing in the lab, with the aim to assess the determinants underlying human immunological variance within the healthy population. On 1,000 healthy donor samples, it illustrated that the global pattern of secretion rather than the level of each individual cytokine defines a very specific and conserved proteomic signature to a given stimulus (**Figure 10**) (Duffy et al., 2014). Deconvoluting pathogen complex responses into a sum of specific signatures now appears as a reasonable strategy, and will hopefully result in identification of critical pathways that could be targeted with therapies.

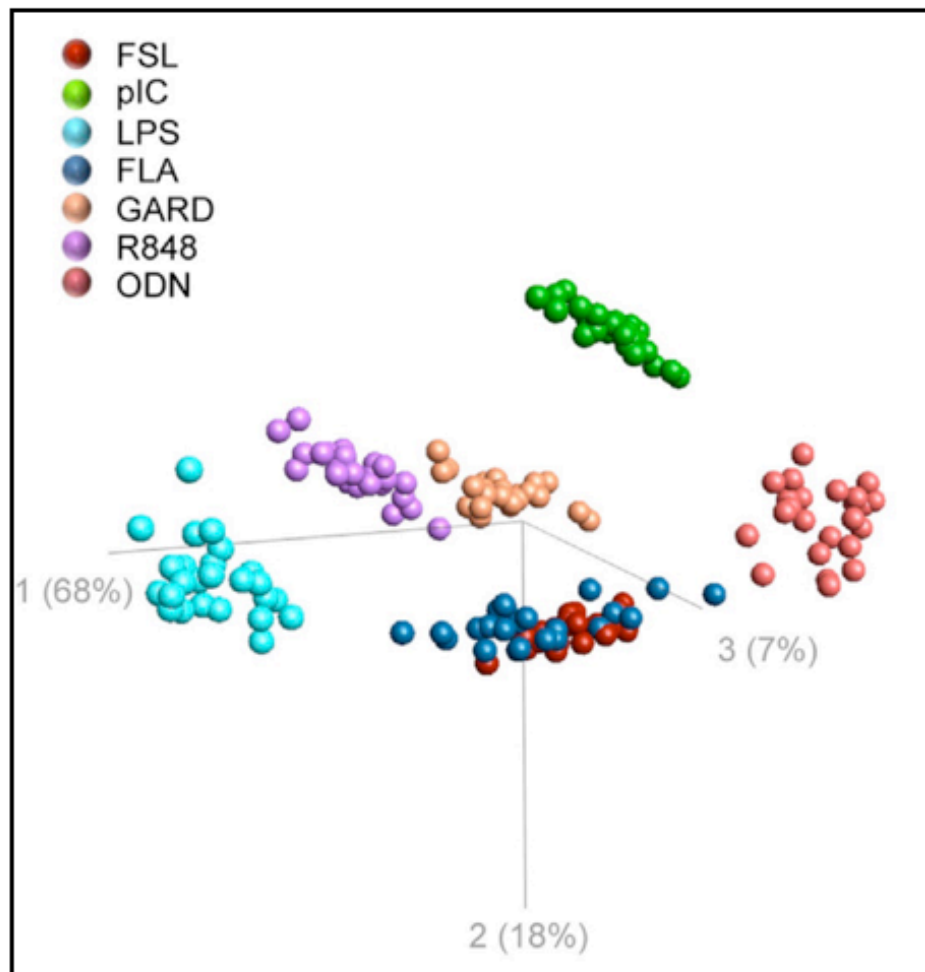


**Figure 10. Segregation of TLR Agonists Based on Their Induced Protein Signatures.** Principal component analysis (PCA) was performed on the data set obtained from 25 healthy donors. Analysis was here restricted to the 7 whole-blood stimulations that contained TLR agonists (FSL, pIC, LPS, FLA, GARD, R848, ODN). Each colored circle represents a different whole-blood stimulation condition, and the PCA was run with the 11 most differentially induced proteins (cutoff value was determined by ANOVA,  $q$  value  $< 10^{-60}$ ). The PCA plot shown captures 85% of the total variance within the selected data set. From Duffy *et al.*, *Immunity* 2014.

Macrophages also release ROS and proteases, leading to important tissue damages - a hallmark of chronic inflammation. Some tissues have only little ability to regenerate (e.g. skin, neurons, cardiac cells), and are more affected than others. Aberrant repairing is frequent, and triggers fibrosis and neo-angiogenesis, leading to restructured and often less functional tissues.

Chronic inflammation is a feature of many human diseases including:

- allergy or food intolerance: asthma, celiac disease;
- inflammatory bowel diseases: Crohn's disease;
- rheumatologic disorders: rheumatoid arthritis, spondyloarthritis;
- persistent infection with mycobacteria, parasites, or fungi;
- autoimmune disorders: systemic lupus erythematosus, multiple sclerosis, psoriasis;
- atherosclerosis, obesity, diabetes, cancer, and Alzheimer's disease;

- and chronic viral infections: HIV, HCV, HBV, CMV, as well as other latent viruses such as EBV, HSV1/2, or HTLV1.

## 2) HCV as a model of chronic inflammation

Hepatitis literally means inflammation of the liver. It can be acute or chronic, symptomatic or not, and relate to many different causes. Viral hepatitis is the leading cause worldwide, and refers to infection with one of the five hepatotropic viruses A, B, C, D and E. Major characteristics are summarized in **Table 4**.

	HAV	HBV	HCV	HDV	HEV
Discovery (year)	1973	1965 (HBsAg) 1970 (HBV particle)	1989	1977 (Delta antigen) 1986 (HDV cloned)	1983 (virus particle) 1990 (HEV cloned)
Genome	+ssRNA	partially dsDNA	+ssRNA	-ssRNA	+ssRNA
Virus structure	28 nm; nonenveloped nucleocapsid	42 nm; enveloped nucleocapsid	50 nm; enveloped nucleocapsid	40 nm; enveloped nucleocapsid	27–34 nm; nonenveloped nucleocapsid
Classification	Hepadnavirus genus; Picornaviridae family	Orthohepadnavirus genus; Hepadnaviridae family	Hepacivirus genus; Flaviviridae family	Deltavirus genus	Hepevirus genus; Hepeviridae family
Genotype	3 major genotypes; 6 subtypes	8 genotypes (8% intergroup divergence)	6 major genotypes; more than 50 subtypes; quasispecies in each infected patient	8 genotypes	4 genotypes; 24 subtypes
Mutation rate	high (1/1,000–1/6,000 bases/year)	low (1/100,000 bases/year)	high (1/1,000 bases/year)	high (1/300–1/3,000 bases/year)	high (1/700 bases/year)
Viral half-life time	unknown	2–3 days	3 hr	unknown	unknown
Virion production	unknown	10 <sup>10</sup> –10 <sup>12</sup> virions/day	10 <sup>12</sup> virions/day	unknown	unknown
Worldwide prevalence	1.5 million people	350 million people	170 million people	20 million people	14 million people
Transmission	enteral, fecal-oral	parenteral	parenteral	parenteral	enteral, fecal-oral; infrequent: parenteral
Disease outcome	acute, self-limited	mostly acute, self-limited if infection occurs during adulthood; mostly chronic after neonatal infection	acute, 60%–80% develop chronic infection	depends on HBV infection; 2% of HBV/HDV coinfections and 90% of HDV superinfections persist	acute, self-limited; chronic infection mainly in immunocompromised patients
		15%–25% of patients with chronic hepatitis B die from liver failure or liver carcinoma	1%–5% of patients with chronic hepatitis C die from liver failure or liver carcinoma	70%–80% of patients with chronic hepatitis D develop cirrhosis; 60% of these die within 10 years	57,000 death/year in worldwide
Vaccine	yes (inactivated or live attenuated); vaccination prevents infection for more than 25 years	yes (recombinant HBsAg); vaccination of neonates prevents persistent infection	no (not available)	vaccine against HBV protects against HDV infection	yes (approved in China)
Treatment of persistent infection	not applicable	IFN- $\alpha$ -based therapy achieves seroconversion in a minority of patients; nucleos(t)ide analogs suppress but do not eradication of HBV	pegylated IFN- $\alpha$ , ribavirin, direct acting antivirals; HCV clearance in 45%–80% of individuals depending on HCV genotype	high doses of IFN- $\alpha$ -based therapy effective in only about 20% of patients; HDV relapses in most cases after cessation of treatment	not applicable

**Table 4. Hepatotropic viruses.**

Virological and clinical characteristics of HAV, HBV, HCV, HDV and HEV infections. From Park *et al*, Immunity 2014.

Our laboratory focuses on chronic infection with the hepatitis C virus (HCV), because it is a major public health problem, and a leading cause of primary liver cancer. HCV naturally trigger an immune-mediated inflammatory response (hepatitis) that is either:

- acute, self-limited, and beneficial – leading to clearance of the infection in about one-third of the patients;
- chronic, systemic and deleterious - slowly destroying the liver and possibly leading to extrahepatic manifestations, including extra-hepatic carcinogenesis.

### (a) Epidemiology

Hepatitis C virus (HCV) was identified in 1988, and cloned in 1997. Chronic infection by the HCV virus concerns 2-3% of population worldwide, *i.e.* 130-170 million people (Mohd Hanafiah et al., 2013). Prevalence vary from one country to another, from <1% to >10%. Higher attack rate concerns Africa and Middle East, with a maximum of 14% in Egypt. The latter is a unique situation, where high prevalence of HCV infection is related to the usage of collective material for massively treating schistosomiasis in the 70's (Frank et al., 2000). In France, prevalence of positive serology - defined as the detection in blood of anti-HCV IgG antibodies, is estimated 1%, *i.e.* ~350 000 individuals. Two-third are chronically infected, *i.e.* with detectable viral RNA in their blood. It is important to note that humans are the only known natural host for this virus; however, it can be transmitted to chimpanzees – and recently to genetically humanized mice - for experimental purposes (Dorner et al., 2014).

HCV virus circulates as 7 different genotypes, classified from 1 to 7, and further subdivided in subtypes identified by an alphabetical letter (1a, 1b,...). These subtypes correspond to nucleotidic variations from 20 to 30% (Simmonds et al., 2005). Different genotypes and subtypes of HCV virus comes from its high nucleosidic mutation rate of  $1.5 \times 10^{-3}$ /protein/year, which result from error prone replication by the RNA-dependent RNA viral polymerase. As such, different isolates – or quasispecies, also coexist within subtypes, and their evolution is largely dependent on the selective pressure of targeting CD8<sup>+</sup> T cells (Bailey et al., 2012). In France, genotype 1 is predominant (60%) - with 30% of subtypes 1b and 25% of genotype 1a, then genotype 3 (20%), genotype 2 (9%), genotype 4 (9%), genotype 5 (2%) and genotype 6 (<1%) (Hajarizadeh et al., 2013) (**Figure 11**).

HCV virus is mainly parenterally transmitted, by transfusion or transplantation of infected samples, or usage of drugs intravenously (IV). The latest is now the main contamination mode in France (4,000 new cases, mainly in the two first years of usage), whereas transfusion of infected blood samples account for 40% of infection worldwide. Short exposure, trauma with infected needle, or mucosal exposure are less infectious. Percutaneous transmission is unlikely, which is very different from the hepatitis B virus (HBV) (Park and Rehermann, 2014). Of note, reinfection after treatment and clearance of the virus is possible if risk factors are not controlled.

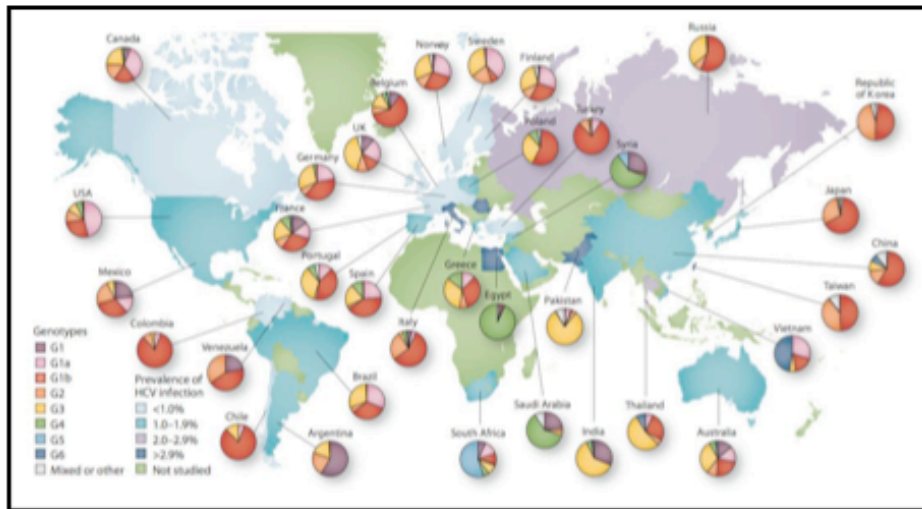


**Figure 11. Prevalence and distribution of HCV genotypes.** World map of the prevalence of HCV (color-coded) and distribution of HCV genotype (pies). From Hajarizadeh *et al.*, 2013.

### (b) Virus genome

HCV is a small enveloped virus belonging to the flaviviridae family, hepacivirus gender. Its genomic structure is composed of a 9.6 kb single-strand RNA of positive polarity (**Halliday et al., 2011**). It contains a single open-frame reading encoding for a 3000 amino-acid (aa) polyprotein (**Penin et al., 2004**). Non-coding areas contains highly conserved regions which are important for replication and translation of the virus genome. The polyprotein is cleaved by both host and virus proteases into the endoplasmic reticulum (RE) membrane, leading to the generation of 10 mature proteins (**Figure 12**):

- the N-terminal region encodes structural proteins: the core, and the envelop glycoproteins E1 and E2, which are essential for ligation of the virus to membrane receptors at the surface of host target cells;
- the C-terminal region encodes for non-structural proteins (NS): p7, NS2, NS3, NS4A, NS5A and NS5B. These proteins are not incorporated into viral particles. They participate to intracellular replication of the virus. In particular, NS5B is a RNA-dependent RNA-polymerase, which permits synthesis of a negative strand from the positive strand of the transmitted virus. Importantly, detection of negative strand of the RNA then sign active replication of the virus.

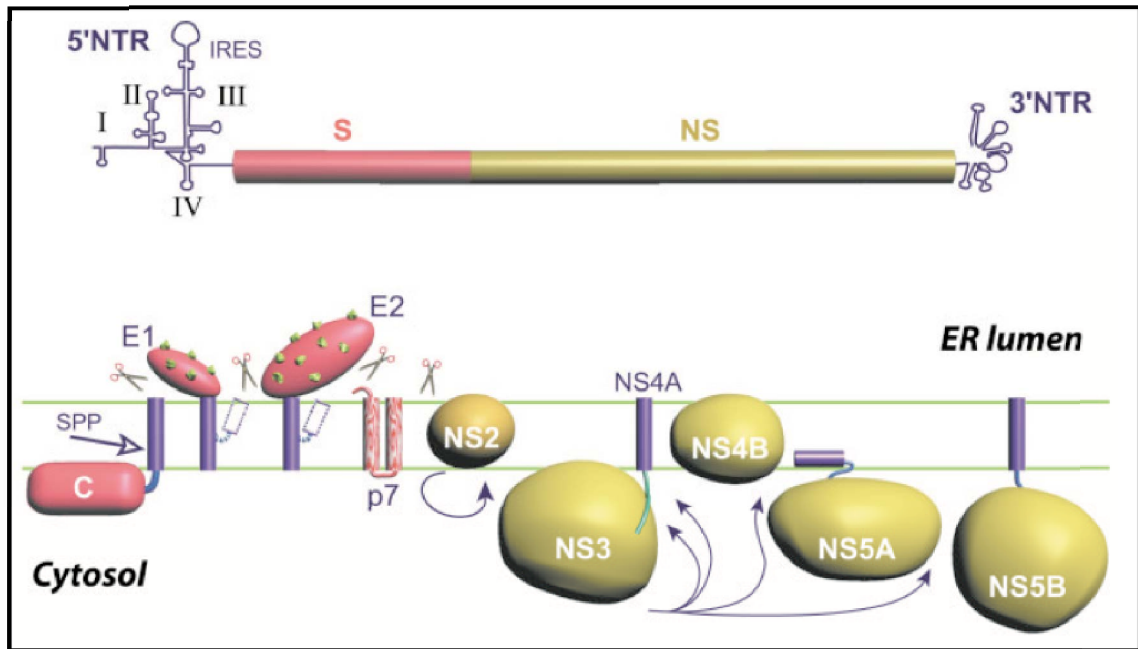


**Figure 12. HCV genome organisation, and polyprotein processing.**

HCV genome organization (top) and polyprotein processing (bottom). The central 9.6-kb ORF codes for a polyprotein of about 3000 aa. S and NS correspond to regions coding for structural and nonstructural proteins, respectively. The polyprotein processing leads to generation of the 10 proteins that are part of the virus machinery. From Penin *et al.*, *Hepatology* 2004.

After viral replication, viral particles, composed of viral genome, core protein, and E1 and E2 glycoproteins, are assembled by budding of the RE, and transported to the membrane by the host secretion system before exocytosis. In the blood, circulating HCV particles show heterogeneous and lower density than expected from its putative viral structure. This is likely related to binding of the virion to very-low- (VLDL) or low- (LDL) density lipoproteins (Shimizu *et al.*, 2011). These lipoviro-particles (LVP) have a diameter >100 nm, and contain the apolipoprotein B (ApoB). It has been proposed that LVP protect the virus from the host immune surveillance and/or increase interaction with lipoprotein receptors, which could act as a HCV receptor.

### (c) Tropism and entry receptors

HCV liver tropism is mediated by expression of entry receptors at the cell surface of hepatocytes (Penin *et al.*, 2004; Sattentau, 2008) (**Figure 13**). By circulating within blood, HCV is in direct contact with the basolateral surface of hepatocytes where it ligates surface receptors allowing its entry within the cells. Early step of viral attachment is a low-affinity interaction between the LPV and the LDL receptor and/or glycosaminoglycans, both largely expressed on the target cell membrane. Then, HCV can use numerous higher affinity receptors to enter hepatocytes in a coordinated multistep process. This includes the scavenger receptor class B type I, the tetraspanin CD81, the tight junction proteins claudin 1 and occludin (OCLN), the receptor tyrosine kinases epidermal growth factor receptor and ephrin receptor A2, and the cholesterol uptake receptor Niemann–Pick C1 like 1. Of these, CD81 and

OCLN comprise the minimal human factors needed for HCV uptake into rodent cells (Dorner et al., 2014).

Other sites of replication have been reported, including biliary cells, salivary glands, epithelial cells, pancreas, thyroidis, bone marrow, spleen, lymph nodes and brain (Zignego and Bréchet, 2001). The more debated concerns the ability of HCV to infect lymphocytes. Whereas some studies were biased by identifying the virus within cells possibly contaminated by viral particles (viremic patients at the time of collection), others clearly demonstrate replication in the absence of detection of the virus into the blood (Kondo and Shimosegawa, 2013). In a recent study, despite comparable expression levels of CD81, only T cell lines displaying moderate to high levels of CD5 protein were found to be susceptible to HCV infection (Sarhan et al., 2012). Both anti-CD5 and anti-CD81 MAbs inhibited infection of permissive T cells, indicating that both are required for HCV entry into T cells. Considering the pan-T cell expression of CD5, it suggests that while CD81 may contribute to broad recognition of cells by HCV, CD5 facilitates HCV tropism specifically toward lymphocytes. As degree of infection usually correlates with levels of expression of entry receptors, it is possible that naive T cells, which express the highest levels of CD5, are the main target lymphocyte population for HCV, and a previously ignored reservoir for the virus.

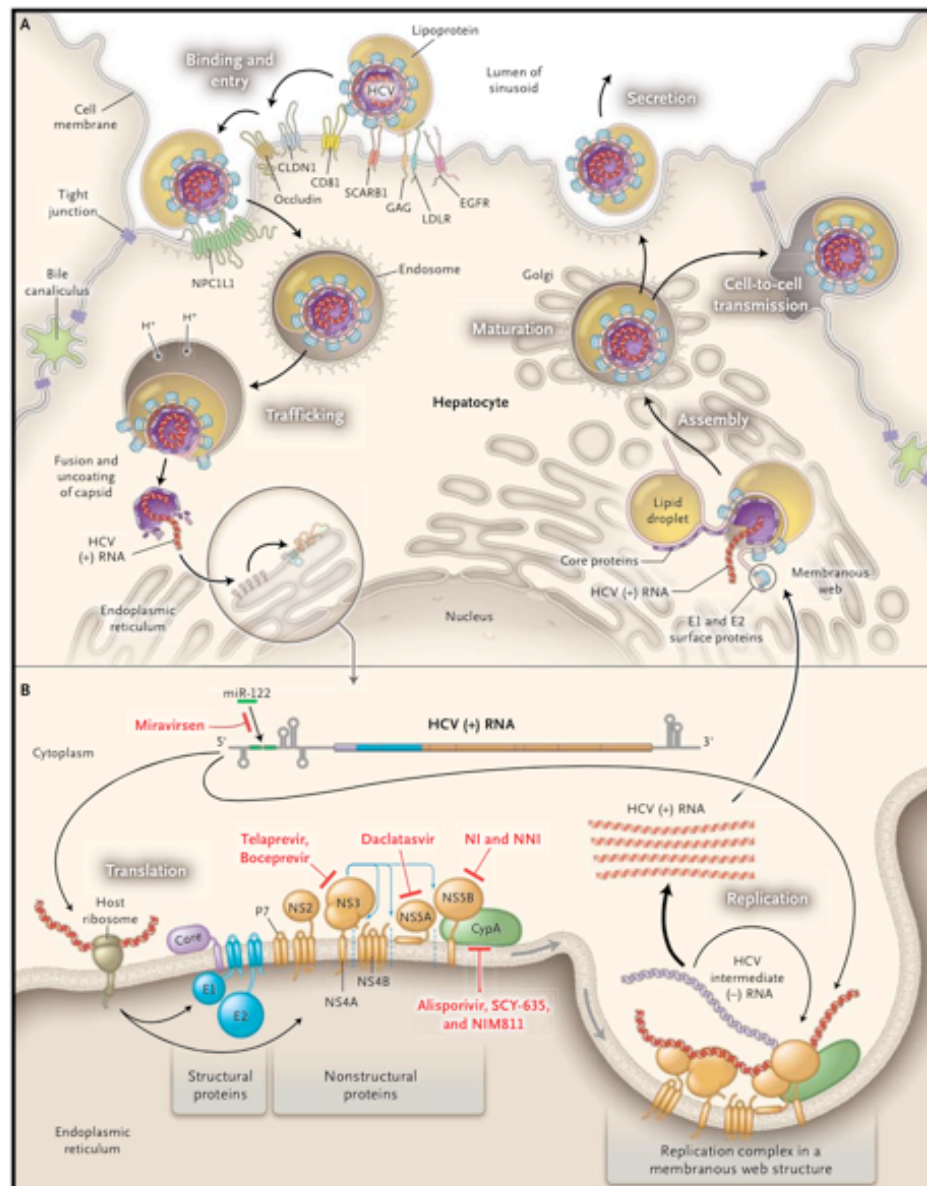


**Figure 13. Life Cycle of the Hepatitis C Virus (HCV) and Targets of Therapy.**

A. Sequential steps of HCV life cycle into an hepatocyte. The virus forms complexes with lipoproteins and circulates in the blood. HCV entry factors include scavenger receptor B1 (SCARB1), CD81, claudin 1 (CLDN1), occludin, epidermal growth factor receptor (EGFR), and Niemann-Pick C1-like protein 1 (NPC1L1). B. Organisation of virus-encoded proteins on the endoplasmic reticulum membrane, and targets of actual therapies. The symbols (+) and (-) refer to the positive and negative strand, respectively, of the viral genome. CypA cyclophilin A, E envelope glycoprotein, GAG glycosaminoglycan, LDLR low-density lipoprotein receptor, NI nucleoside analogue inhibitor, NNI non-nucleoside analogue inhibitor, and NS nonstructural protein. From Liang *et al*, NEJM 2013.

*(d) From acute to chronic infection*

Acute infection by HCV leads to acute hepatitis – *i.e.* that started less than 6 months ago. The incubation period averages 6 to 10 weeks. 80% of HCV-induced hepatitis are asymptomatic, with cases being detected by serology. Others present clinical symptoms such as asthenia, fever, jaundice, acholic stools, and dark urines. After exposure, it takes (**Figure 14**):

- 2-14 days for the virus to be detectable in the blood, in parallel with an increase in transaminases;
- 8–12 weeks to cellular immunity to take place, and thus to anti-HCV antibodies to develop and be detectable by serology (Halliday et al., 2011) ;
- 20 weeks to the virus to be either spontaneously cleared (30%), or persistent (70%).

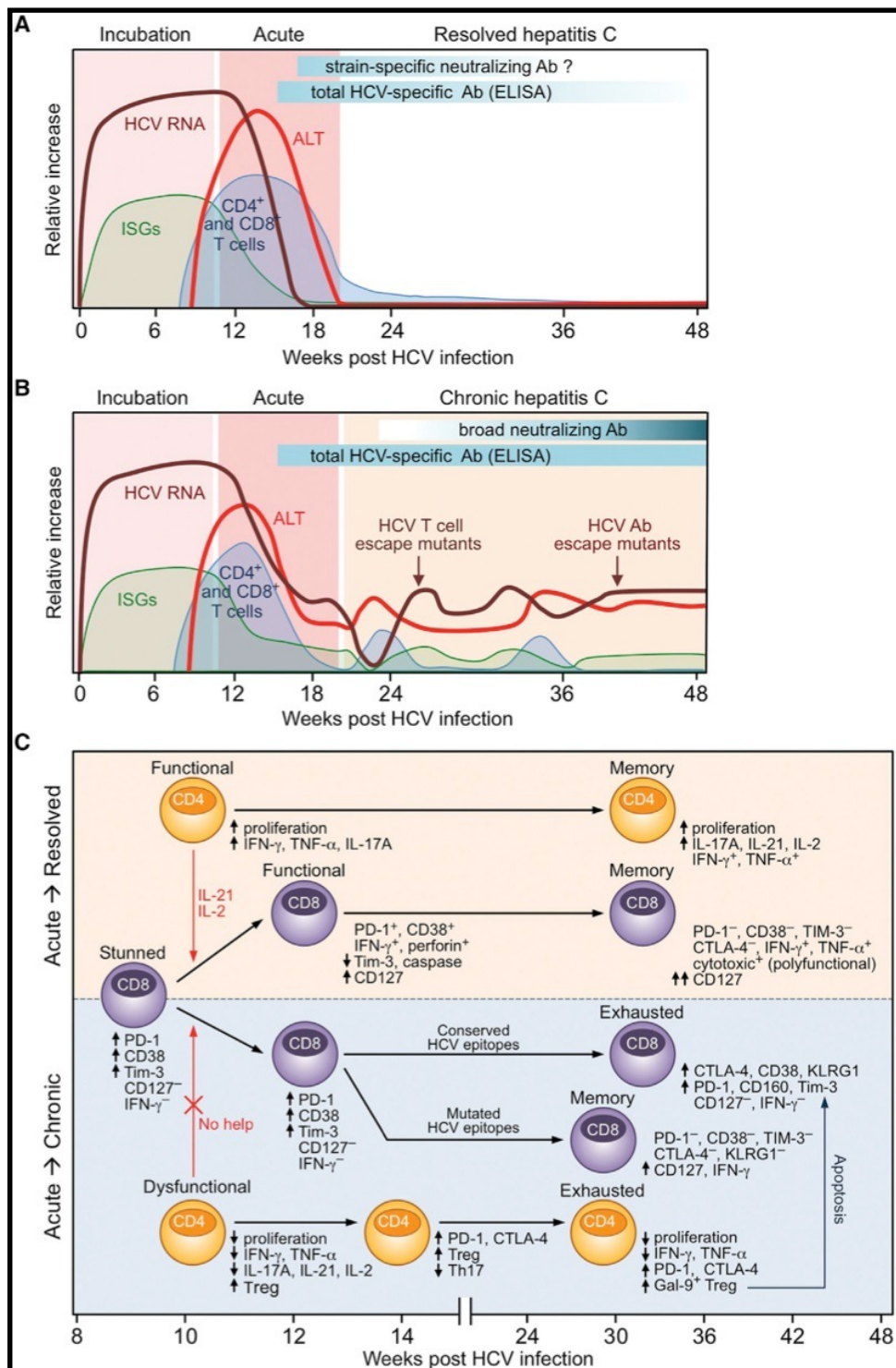


**Figure 14. Clinical, Virological, and Immunological Course of Acute HCV Infection.**

A. Acute hepatitis C followed by clinical recovery. The acute phase is marked by elevated alanine aminotransferase (ALT) levels and the onset of HCV-specific CD4<sup>+</sup> and CD8<sup>+</sup> T cell responses around weeks 8 to 12. HCV-specific antibodies are detectable by enzyme immunoassay (ELISA) a few weeks later, but the impact of low titers of strain-specific neutralizing antibodies is still controversial. After spontaneous resolution of acute HCV infection, HCV-specific memory T cell responses remained detectable for decades whereas antibodies disappear from the circulation. B. Acute hepatitis C followed by chronic infection. HCV RNA titers decrease 2–3 log<sub>10</sub> after the acute phase and remain relative stable in the chronic phase. Selection of HCV escape mutants is mostly driven by T cells in the acute and early chronic phases of infection and by increasing titers of broadly targeted neutralizing antibodies in the chronic phase. The intensity of the shaded background indicates the degree of intrahepatic inflammation in the different phases of hepatitis. From Park *et al*, *Immunity* 2014.

Chronic infection by HCV is defined as persistence of the virus for more than 6 months. It associates with hepatic injury such as necrosis, inflammation and fibrosis. HCV is not cytopathic, except in rare immunocompromised situations. It rather leads to immune-mediated liver injury. Histology testing distinguishes persisting chronic hepatitis - considered as benign, and active chronic hepatitis. Chronic HCV infection may evolve to cirrhosis in 10-20% of patients, depending on the presence or absence of cofactors (Wiese et al., 2013). Cirrhosis can complicate with liver-related complications (ascites, hepatic encephalopathy, icterus, variceal bleeding, spontaneous bacterial peritonitis), or lead to hepatocellular carcinoma (HCC). Incidence for disease progression is 2-4%/year (Kew, 2012), and risk factors are gender (male), ethnicity (african origin), age (> 40yrs at the time of infection), co-infection with HBV, immunosuppression (including HIV co-infection), metabolic syndrome, including diabetes, obesity, insulino-resistance and steatosis, and alcohol consumption. Main risk factor for evolution of HCV patients toward HCC is alcohol consumption. Of note, HIV co-infected patients have also an increased progression towards cirrhosis, an increased liver-related mortality, and earlier and more aggressive HCC. Mortality related to HCV account for 86 000 deaths per year in Europe in 2002, within 35% related to cirrhosis, and 32% to HCC. After diagnosis of HCC, 33% of patients die within one year. When cirrhosis and its complications are established, the only curative treatment is the liver transplantation.

#### *(e) Extrahepatic manifestations*

Clinical manifestations of chronic HCV are not restricted to the liver (Zampino et al., 2013). Several extra-hepatic manifestations are occasionally observed in those patients (**Figure 15**):

- 50% present with mixed cryoglobulinemia (MC), a benign B-cell lymphoproliferative disease. Its definition is biological, and corresponds to the detection into the serum of immunoglobulins (Igs) capable to reversibly precipitate at low temperatures. HCV-related MC are typically type II (the precipitate is composed of both monoclonal and polyclonal Igs), or type III (the precipitate is only formed by polyclonal Igs). Viral antigens and HCV-RNA are consistently isolated from the precipitate, suggesting a direct role of the virus in MC pathogenesis. Only 15% of patients with MC are symptomatic, associating with a poor prognosis related to development of B-cell malignancies in 10% of them. Clinical symptoms of MC are those of vasculitis due to precipitation of Igs complexes in small- and medium-sized blood vessels. Livedo, purpura, ulcers, arthralgia, and arthritis are related to thrombosis of small vessels and systemic inflammation. Vasculitis can also affect the kidneys, the gastrointestinal tract, the peripheral nervous system, and/or other body compartments;
- 50% present neurological symptoms including cognitive disorders, depression, and asthenia, with perturbed quality of life;
- 30-50% present steatosis, insulinoresistance, and/or metabolic syndrome;

- some develop cardiovascular diseases, including atherosclerosis and coronaropathy, independently of the precited metabolic loss of balance, which translates into increased mortality (Lee et al., 2012) ;
- some develop extra-hepatic cancers, which are not restricted to a particular site, suggesting disruption of a common mechanism for carcinogenesis. Esophagus, prostate, and thyroid cancers, as well as non-Hodgkin B cell lymphomas are more frequently reported (Lee et al., 2012).

Non-cryoglobulinemic extrahepatic manifestations are thought to reflect the activation of pro-inflammatory immune responses rather than to be related to the virus itself.

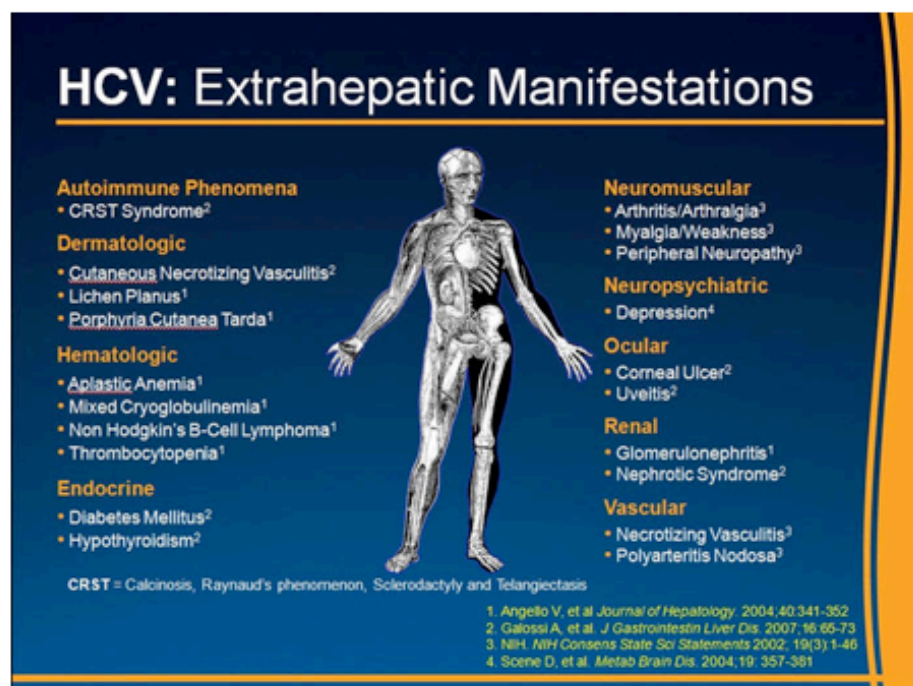


**Figure 15. Extra-hepatics manifestations related to HCV.**  
List of extra hepatic manifestations related to chronic HCV. From [http://hcvets.com/data/hcv\\_liver/2012HCVCComorbidityBurden.htm](http://hcvets.com/data/hcv_liver/2012HCVCComorbidityBurden.htm)

### (f) Treatment and clearance benefits

HCV is to date the only chronic viral infection that can be cured. Curing is achieved by induction of a Sustained Virologic Response (SVR) by appropriate treatment. Sustained virologic responders (SVRs) - *i.e.* patients achieving SVR, are individuals with no detectable virus in the serum 3-6 months after the end of the treatment. It probably correspond to complete eradication of the virus from the blood, the liver, and any potential other reservoir. Indeed, after SVR, reappearance of the virus never happens, even when patients later undergo severe immunosuppression (e.g. chemotherapy or organ transplantation).

In the 80's, patients were initially treated with subcutaneous injections (SC) of alpha-interferon (IFN  $\alpha$ ). It acts both directly on the virus, and indirectly by immuno-modulating the cellular immune response, reinforcing the endogenous interferon naturally present in response to HCV. It cured only 6-12% of patients after 6 months. Extension to 12 months increased prolonged response to 16-20%. In the 90's, a nucleosidic analogue - ribavirine (RBV), was proposed in association with IFN $\alpha$ . Also it had no effect in monotherapy, it permitted to double virological efficacy when associated to IFN $\alpha$  administration. Its mechanism of action is uncertain, but is likely multiple, with (i) immunomodulation in favor of Th1 lymphocytes; (ii) incorporation into the viral genome - thus limiting its replication; (iii) direct inhibition of viral polymerase NS5B; (iv) mutagenesis during viral replication; and (v) modulation of IFN-induced gene expression (Feld and Hoofnagle, 2005). Development of pegylated interferon (peg-IFN $\alpha$ ) permitted to reduce the number of SC to 1 per week. Combination of peg-IFN $\alpha$  and RBV (800 mg/day for genotypes 2 or 3, or adapted to the weight [13-15 mg/kg/day] for genotypes 1 or 4) was for long the reference treatment. It permits clearance of the virus in 45% of genotype 1, 85 % of genotype 2, 70 % of genotype 3, 65 % of genotype 4, and 75% of rare genotypes 5 and 6. Factors influencing duration and modality of treatment are viral genotype, initial viremia, presence of extensive fibrosis or cirrhosis, IL28B genotype, response to a previous treatment, and viral kinetic at 4 and 12 weeks of treatment. Typically, patients are treated 24 (genotype 2 and 3) to 48-72 weeks (genotype 1, 4, 5).

With improved knowledge on the cell cycle of HCV, direct acting antiviral agents (DAA) have been recently developed (Pol et al., 2013) (**Figure 12**). First molecules in 2011 were inhibitors of NS3/NS4A protease (telaprevir and boceprevir). Association of these molecules to peg-IFN $\alpha$  and RBV permitted to increased SVR to 75 % in genotype 1 naive patients, and is the recommended treatment for genotype 1 patients, especially those at risk of non responding to classical bitherapy. However, protease inhibitors can lead to serious secondary events such as cutaneous eruptions, or severe anemia in 49% of treated patients. Also, these treatments are expensive – 35 000 euros for one tritherapy, and thus not affordable worldwide. Since then, other direct molecules have been developed: second generation of proteases inhibitors, nucleos(t)idic or non nucleos(t)idic polymerase NS5B inhibitors, and inhibitors of the NS5A replication complex. The current interferon-free oral combinations allow more than 90% of cure for all patients. The main limitation remains their cost, estimated between 40 000 to 75 000 euros per individual.

On the liver, viral clearance leads to fibrosis – and even cirrhosis - regression, and significantly reduces liver-related morbi-mortality. The estimated 10-years mortality rate is 1.9% on SVR patients, in comparison with 27.4% on non-responders (van der Meer et al., 2014). Sustained virologic response also leads to normalisation of transaminases, and improvement of extrahepatic manifestations, both MC-related or not (Lee et al., 2012).

(g) Antiviral immune responses

Viral infection leads to several intracellular events that permit to initiate the host immune response, both inside the infected cells and within the micro environment (Gale and Foy, 2005). HCV viral RNA is sensed inside the hepatocytes by pathogen-associated molecular pattern molecules (**Figure 15**). Several HCV RNA structures are recognized by cytosolic pattern recognition receptors. The HCV internal ribosomal entry site is recognized by RNA-dependent protein kinase R (PKR), whereas double-strand RNA is recognized by cytosolic retinoic-acid-inducible gene I (RIG-I) and TLR3. This leads to phosphorylation, dimerization and nuclear translocation of IRF3, which induces IFN $\beta$  synthesis. IFN- $\beta$  binds to the IFN- $\alpha/\beta$  receptor and signals through activation of the associated Tyk2 and Jak1 protein kinases to direct the phosphorylation and assembly of a STAT1–STAT2 heterodimer and trimeric ISGF3 complex containing IRF-9. The ISGF3 complex locates to the cell nucleus, where it binds to the ISRE on target genes and drives the expression of numerous Interferon Stimulated Genes (ISGs). This includes: (i) synthesis of IRF-7, that lead to production of IFN- $\alpha$  subtypes and amplifies ISG expression, (ii) IFN $\alpha$  and  $\beta$  themselves, and (iii) pro-inflammatory cytokines such as TNF $\alpha$  or CXCL10 (IP-10). However, viral proteins largely interfere with these pathways, and reduce dramatically IFN $\alpha/\beta$  production to levels that are undetectable in HCV-infected patients. As such, type I interferons are usually barely detectable at the RNA level in the liver, and usually undetectable at the protein level in the blood of acutely infected patients. In contrast, type III interferons are robustly detected in the two organs, and their expression parallel viremia and ISGs levels (Park et al., 2012).

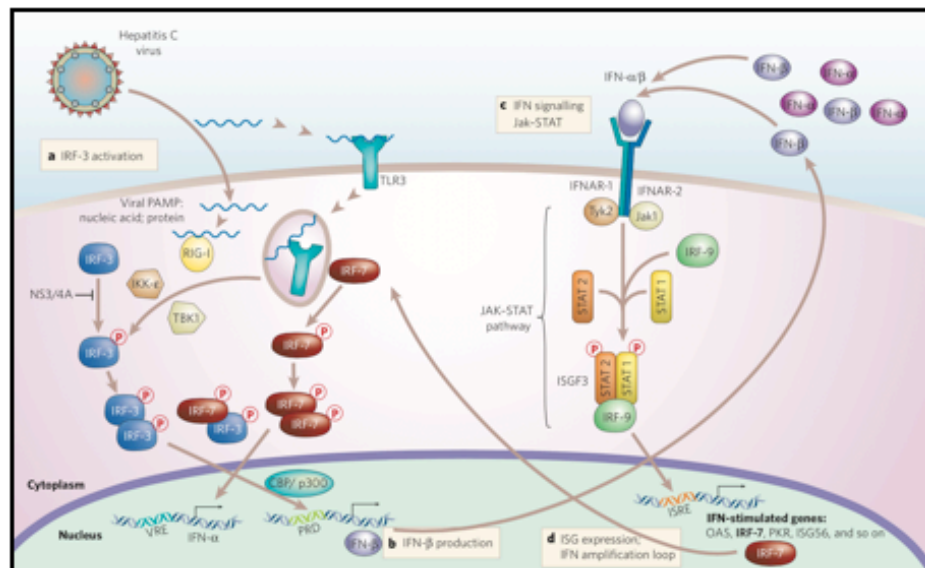


**Figure 16. Molecular processes that signal the host response to HCV infection.**

A. HCV RNA binds to RIG-I or TLR3, leading to phosphorylation, activation and translocation of IRF-3 to the cell nucleus, where it binds to promoters of target genes, including IFN- $\beta$ . B. IFN- $\beta$  production and secretion from the infected cell. C. IFN- $\beta$  binds to the IFN- $\alpha/\beta$  receptor and signals through Tyk2 and Jak1 protein kinases to direct the phosphorylation and assembly of a STAT1–STAT2 heterodimer and trimeric ISGF3 complex containing IRF-9. The ISGF3 complex locates to the cell nucleus, where it binds to the ISRE on target genes and drives ISG expression. D. ISGs expression, leading to production of IFN- $\alpha$  subtypes that further signal ISG expression (amplification loop). From Gale *et al*, Nature 2005.

Beside hepatocytes, HCV virus can also be sensed by:

- Macrophages after phagocytosis;
- Plasmacytoid dendritic cells (pDCs) after take up HCV RNA via exosomes (demonstrated *in vitro*, but not yet *in vivo*).

Inside those cells, the virus triggers TLR7, and initiates an inflammatory IL-1 $\beta$  response, as well as IFN $\alpha$  production (Park and Rehermann, 2014). With no inhibition by viral particles, they could thus be the source of ISG-inducing type I IFNs.

High levels of IFN $\alpha$  in the early steps of infection contribute to NK cells activation. After recognition and elimination of infected cells, they produce proinflammatory cytokines (IFN $\gamma$ ) and participate to polarization of T cell responses toward cytotoxicity. NK cells with the greater capacity to produce IFN $\gamma$  translates into more efficient clearance of HCV (Albert et al., 2008).

Inflammatory chemokines such as RANTES, MIP-1 $\alpha$ , and MIP-1 $\beta$  quickly recruit circulating immature DC (imDC) to the site of inflammation (e.g. the HCV-infected liver), where they can take up viral antigens. This is mediated by their binding to their corresponding chemokine receptors (CCR1, CCR2, and CCR5 respectively) at the surface of imDC. This is followed by functional maturation of DC, in parallel with modifications of the pattern of expression of chemokine receptors. Mature DC typically express high levels of CCR7, which leads them to quit the tissue, and home into CCL19 and CCL21-expressing T cell areas of lymphoid tissues. This migration step is required for appropriate priming of HCV-specific T cells. As HCV-specific T cell responses play a key role in viral clearance, and are often found as defective in the context of chronic infection, the functionality of cDCs in the context of cHCV has been regularly questioned, and led to controversial conclusions. Initial reports have shown impaired maturation and allostimulation of monocyte-*in vitro*-derived DCs from patients with chronic HCV infection. However, more recent analysis using direct strategies to identify and characterize circulating DCs reported no phenotypic or functional differences between cHCV patients and healthy donors (Longman et al., 2005).

Despite rapid innate responses, HCV-specific adaptive immune responses are not detectable before 8–12 weeks after infection (Park and Rehermann, 2014). This is observed irrespectively of clinical outcome. Importantly, the appearance of HCV-specific CD8 T cells in the blood precisely coincides with the CD8 T-cell infiltration to the liver, as assessed by CD8 $\beta$  mRNA levels. This delay is very unique to HCV. It has been proposed that secretion of high levels of chemokines by the HCV-infected liver at early time points could sequester unprimed CD8 T cells expressing the corresponding receptors. After this delay, one can observe:

- HCV-specific humoral responses: they are mainly targeting the highly variable region 1 (HVR1) of the E2 glycoprotein (Halliday et al., 2011). Their appearance is variable between individuals, and always significantly delayed after the infection. They are restricted in their isotype profile, found at low levels only, and not maintained for life. In sum, HCV-specific antibodies happening during the course of chronic infection do not confer protection: reinfection can occur after clearance, and clearance can occur without detection of specific antibodies.
- HCV-specific cellular immune responses (Klenerman and Thimme, 2012) : HCV-specific T cells likely play a key role in the elimination of the virus as (i) there is a temporal correlation between increased expression of CD8 $\beta$  and IFN $\gamma$  mRNA into the liver, viral clearance and the appearance of HCV-specific CD8<sup>+</sup> T cell responses in both blood and the liver of acutely infected humans and chimpanzees (Thimme et al., 2002) ; (ii) depletion of either CD4<sup>+</sup> or CD8<sup>+</sup> T cells prevents HCV clearance in the chimpanzee model (Shoukry et al., 2003) ; and (iii) there is a strong correlation between protective class I HLA alleles such as HLA-B27, HLA-B57, and HLA-A3 and spontaneous viral clearance (Fitzmaurice et al., 2011). Specifically:
  - ❖ patients who later clear the virus typically mount broad CD4<sup>+</sup> T cell responses, with high proliferation and cytokine production capacities (Missale et al., 2012; Shoukry et al., 2003). In contrast, HCV-specific CD4<sup>+</sup> T cell responses are absent or weak in those who subsequently develop chronic infection. *In vivo* depletion of CD4<sup>+</sup> T cells from HCV-recovered chimpanzees abrogates protective CD8<sup>+</sup> T cell-mediated immunity upon rechallenge. This highlights that CD4<sup>+</sup> T cell help is required for the generation and maintenance of protective CD8<sup>+</sup> T cells, but do not seem to mediate direct antiviral effects (Shoukry et al., 2003) ;
  - ❖ in contrast, whatever the clinical outcome, all patients typically present “stunned” HCV-specific CD8<sup>+</sup> T cells, with impaired proliferation, IFN $\gamma$  production, and cytotoxicity, as well as transient surface expression of PD-1 and CD38. Antiviral therapy in this phase of the infection results in a rapid decay of CD8 T cell responses, suggesting that most of these HCV-specific CD8<sup>+</sup> T cells are short-lived, antigen-dependent effector cells. If HCV infection is self-limited, dysfunction progressively resolves, HCV-specific CD8<sup>+</sup> T cell responses are stronger, broader, higher-affinity, and express high levels of Bcl2 and CD127 (Neveu et al., 2008). If not, they remain weak, restricted, and low-affinity, and the infection evolves toward chronicity (**Figure 17**).

Schematically, perturbations of CD8 T cell responses in cHCV patients concern:

- their number: HCV-specific responses are weak and hardly detectable even by cell-based (tetramer) assays (Klenerman and Thimme, 2012);
- their affinity: cell lines derived from cHCV patients are typically low-avidity, and express low levels of CD3. Importantly, this phenomenon is reversible as emergence of high-avidity clones correlates with the control of the infection (Neveu et al., 2008);
- their phenotype: HCV-specific responses are classically blocked into an early central-memory phenotype (Appay et al., 2002).

Several mechanisms have been identified that participate to this failure:

- a lack of CD4 help. As mentioned above, CD4<sup>+</sup> T-cell help is required for the induction and maintenance of sustained CD8<sup>+</sup> effector T-cell functions (Shoukry et al., 2003);
- chronic antigenic stimulation: this has been demonstrated in mice with lymphocytic choriomeningitis virus (LCMV) infection. High levels of persisting viral antigen result in sequential loss of T cell function: the capacity to produce IL-2 is lost first, followed by cytotoxicity, TNF- $\alpha$ , and ultimately IFN- $\gamma$  production (Park and Rehermann, 2014) ;
- T-cell dysfunction: antiviral T cells typically express high levels of pro-apoptotic and activation molecules such as Bim and PD-1 respectively (Larrubia et al., 2011), and low levels of Tbet (Kurktschiev et al., 2014). They have reduced effector functions, with a poor capacity of proliferating and secreting IFN- $\gamma$  after *in vitro* stimulation. Restoration of HCV-specific CD8<sup>+</sup> T cells can be achieved *in vitro* by blocking both CTLA4 and PD-1/PD-L1 interactions (Fuller et al., 2013);
- increased numbers of Treg cells and inhibitory cytokines (e.g., IL-10 and TGF- $\beta$ ) (Larrubia et al., 2011) : the liver is a naturally tolerogenic environment. One of the mechanisms is that Kupffer cells, as well as intrahepatic regulatory T cells, constitutively express IL-10 and TGF- $\beta$  cytokines that induces tolerance in liver-infiltrating lymphocytes. As such, high levels of IL-10 during acute infection are associated with progression of chronic infection. Also, increased numbers of regulatory T cells are found in the blood and liver of chronic HCV patients. probably attenuate liver inflammation, but are deleterious for generation of efficient immune responses;
- viral escape: HCV is a RNA virus with a very high replication rate. Due to its error-prone polymerase, many different viral variants (quasi-species) co-evolve in a single person. CD8<sup>+</sup> T-cell responses are the driving force for viral sequence variations. Eventually, this results in viral persistence by affecting (i) the epitope processing and presentation, (ii) binding to MHC molecules, or (iii) TCR recognition.

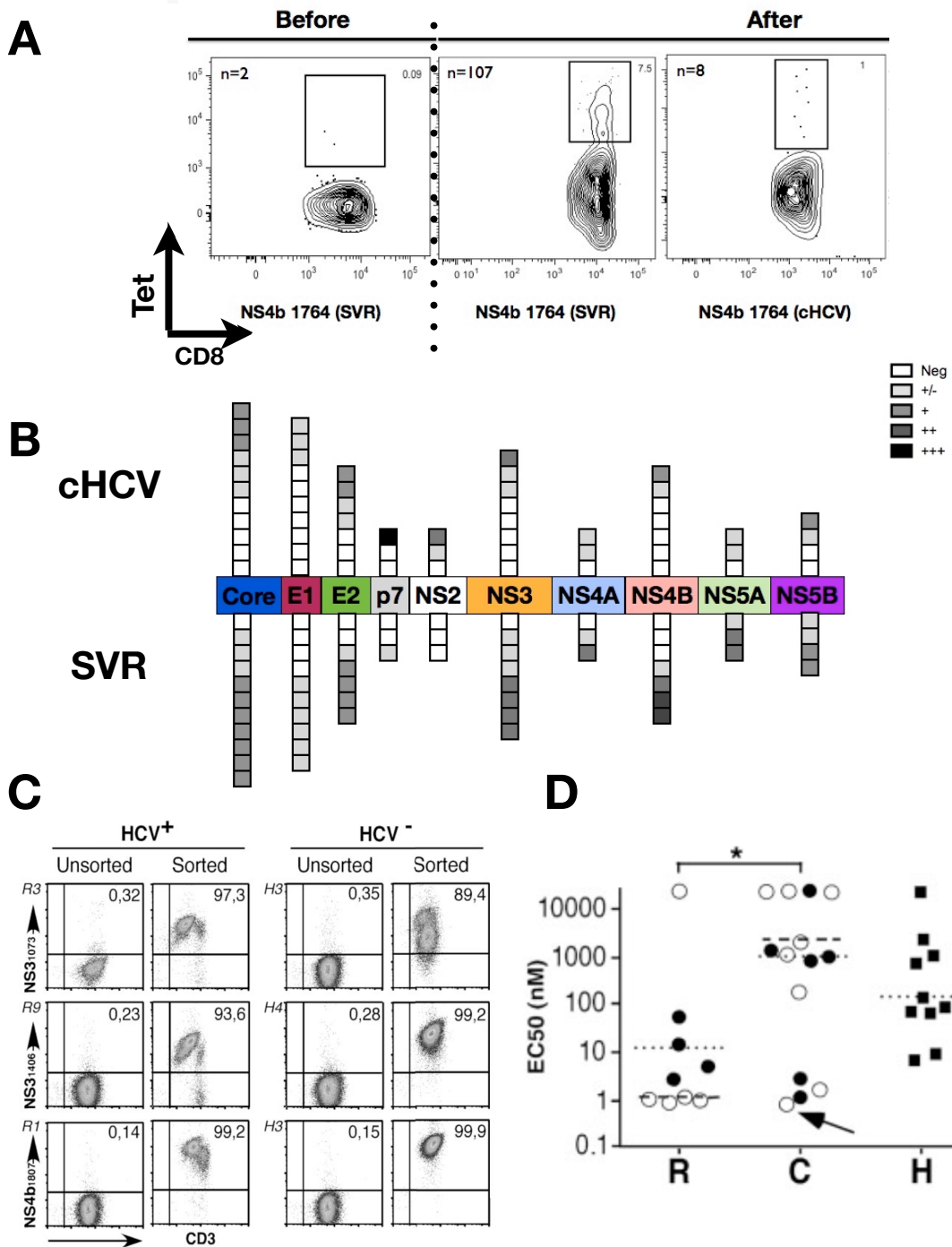


**Figure 17. Weak CD8 T cell responses during cHCV.**

A. Example of tetramer-based detection of HCV-specific T cells before enrichment (left) and after enrichment (right) in one cHCV and one SVR patient. B. Schematic representation of results obtained from a large screen of *in silico* predicted epitopes from the entire sequence of the HCV virus for one cHCV (up) and one SVR (bottom) patients. Responses detected after enrichment are represented by a black and white gradient as indicated in the legend: negative responses ( $\leq 0.1\%$  of CD8<sup>+</sup> T cells), very low (0.1-1%), low (1-5%), medium (5-10%) or high ( $\geq 10\%$ ) frequencies. C. Immunophenotyping of cell lines of HCV-specific T cells from HCV-seropositive and seronegative donors. Of interest is the apparent heterogeneity of the cell lines obtained from the cHCV patients, with dual aspect of expression of CD3 – and thus likely dual level of affinity. From Neveu *et al*, Hepatology 2008 (Neveu *et al.* 2008). D. Analysis of functional and TCR avidity of NS3<sub>1073</sub>-specific T cells from resolved (R), chronic HCV (C), or healthy donors (H), as expressed as peptide concentration (nM) necessary to achieve 50% of maximal target-cell lysis. From Neveu *et al*, Hepatology 2008.

### 3) HBV as a comparative model of chronic hepatitis

The hepatitis B virus is a DNA virus composed of a nucleocapsid core (HBc Ag) surrounded by an outer lipoprotein coat (envelope) containing the hepatitis B surface antigen (HBs Ag) (**Table 4**). It replicates via reverse transcription of a pregenomic RNA (pgRNA). Similar to HCV, HBV virus is hepatotropic, non cytopathogenic, and a major public health problem. Indeed, 350 millions persons are currently infected with HBV worldwide, with high risk of developing severe liver disease – chronicity, cirrhosis, liver failure and hepatocellular carcinoma (HCC), like in chronic HCV infection.

After acute infection, 95% of infected adults clear spontaneously the HBV virus – but only 1% in the case of vertical transmission from mother to neonate. This is a major difference with HCV infection, where spontaneous clearance happens in 1/3 of patients whatever their age. Schematically, chronic HBV infection evolves through three immune phases (**Figure 18**):

- immune tolerant (IT): HBe Ag<sup>+</sup>, HBV DNA<sup>high</sup>, ALT normal ;
- immune clearance, or immunoactive (IA): HBe Ag<sup>+</sup>, HBV DNA<sup>high</sup>, ALT elevated, clinical symptoms ;
- inactive chronic carrier (ICC): HBe Ag<sup>-</sup>, HBV DNA<sup>low</sup>, ALT normal.

HBe Ag is a viral protein that is secreted by the HBV-infected cells. It is associated with chronic HBV infections. HBe Ag positivity is a marker of active viral disease and infectiousness. However, rare cases of e-Ag negative virus mutations can lead to false negativity of HBe Ag, and to misinterpretations.

## Natural History of Chronic HBV Infection

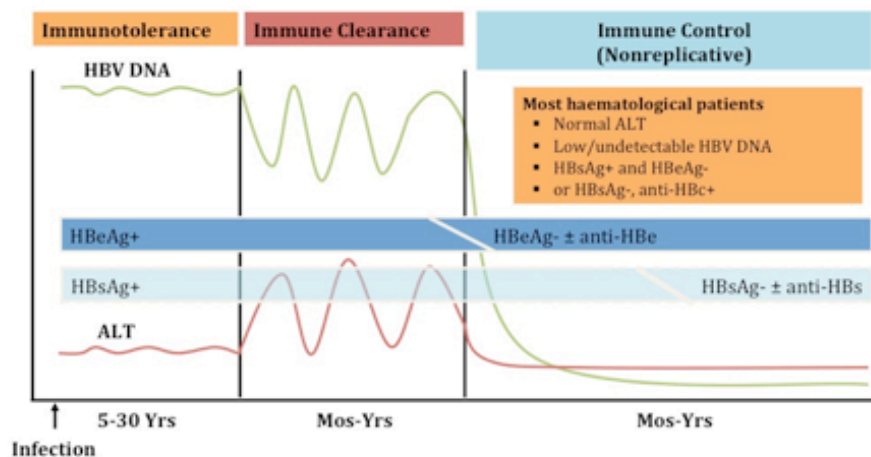


**Figure 18. Natural history of chronic HBV infection.**

After acute infection, 95% of infected adults clear spontaneously the HBV virus – but only 1% in the case of vertical transmission from mother to neonate. Schematically, chronic HBV infection evolves through three immune phases - immunotolerance; immune clearance (or immunoactive); and immune control. Those phases are defined by the evolution of three biological parameters (HBV DNA, HBeAg, ALT). Yrs: years. Most: months.

The phases of chronic HBV infection are not considered static and patients who initially develop the IT phase usually progress to the IA phase, and later on to the ICC state. Progression in the reverse direction can also happen, either spontaneously, or after withdrawal of antiviral or immunosuppressive therapies (corticosteroids, TNF $\alpha$  blockers, cancer chemotherapy). The HBV genome form a covalently closed circular DNA (cccDNA) microchromosome that persists in the nucleus of virus-infected hepatocytes, serving as a template for viral mRNA synthesis (Zhang et al., 2013). It also integrate into the host genome (Jiang et al., 2012b). As such, in contrast to HCV, current antiviral agents control but do not eliminate HBV. Integrative events and very low levels of cccDNA persist indefinitely into hepatocytes, and are key events of hepatocarcinogenesis. This explains lifelong (i) risk of HCC emergence, and (ii) maintenance of anti-HBV responses, despite clinical resolution of the infection.

Like HCV, acute HBV is cleared by a strong adaptive immune response that confers lifelong protective immunity. However, due to its special replication strategy, HBV behaves as a stealth virus, and do not induce ISG expression, even if infecting almost 100% of hepatocytes. This is a major difference between the two viruses. HBV rather induces a type III interferon response, that leads to increased expression of CXCL10, OAS2, and RSAD2 in the human liver (Sato et al., 2015). This does not impair the induction of a vigorous HBV-specific CD4<sup>+</sup> T cell response, that appear much earlier than in HCV infection. Similar to HCV, vigorous multi-epitope-specific CD4<sup>+</sup> and CD8<sup>+</sup> T-cell responses are essential for viral clearance, and as illustrated by the negative effect of depletion of either CD8<sup>+</sup> or CD4<sup>+</sup> T cells. When evolving towards chronicity, there is an inverse correlation between virus levels, and detection of HBV-specific T cells in the blood. CD8<sup>+</sup> T cell failure is mainly due to T cell dysfunction, with similar characteristics as during HCV infection (high sensitivity to cell death, high expression of PD-1, low levels of Tbet, and poor effector functions). This exhaustion phenotype is efficiently reversed by PD1/PDL1 blockade.

Comparison between HBV and HCV physiopathogenesis raise the hypothesis that the absence rather than presence of a strong type I IFN response is critical for the induction of successful CD4<sup>+</sup> and CD8<sup>+</sup> T cell responses. Mechanisms accounting for this observation are unknown.

#### 4) Viro-induced chronic inflammation

Inflammation is a physiological pathway in response to exogenous stimuli. However, a chronic inflammatory state or an excessive inflammatory response can produce deleterious effects. Liver cells, including hepatocytes, hepatic stellate cells (HSCs), Kupffer cells (KCs), bile duct epithelial cells and sinusoidal endothelial cells, are implicated in the synthesis and secretion of a large number of pro-inflammatory stimuli (proinflammatory cytokines, chemokines, growth factors and inflammatory enzymes), and thus plays a central role in the initiation and the regulating this process (Zampino et al., 2013).

HCV causes major liver inflammation by:

- Direct pathways:
  - ❖ NS5A promotes inappropriate upregulation of cyclooxygenase-2 (COX-2), which is an inducible COX isozyme able to contribute to chronic inflammation and fibrosis through production of various prostaglandins (Nunez, 2004);
  - ❖ Non-structural proteins (NS3, NS4, NS5) lead to TNF- $\alpha$  and IL-1 $\beta$  production by KCs;
- Indirect pathways: after its recognition by hepatocyte and innate cells, it triggers recruitment and activation of inflammatory cells into the liver. Interleukin-1 $\beta$  (IL-1 $\beta$ ) and related inflammasome play a central role in orchestration of this inflammatory response (Petrilli et al., 2007), inducing local production of several pro-inflammatory cytokines and chemokines, such as IL-6, IL-8, and macrophage inflammatory proteins (MIP-1 $\alpha$  and MIP-1 $\beta$ ), by hepatocytes ;
- Mediating the recruitment of both virus- and non-virus- specific T cells into the liver (Maini et al., 2000), leading to overreaction with liver antigens, and liver damages.

Outside of the liver, cHCV also triggers systemic inflammation, as illustrated by increased levels of pro-inflammatory cytokines in their serum, activated blood monocytes, and increased local and systemic oxidative stress (Mencin et al., 2009). Recent studies highlighting the frequency of extrahepatic HCV-related diseases brought new interests into systemic inflammation (Lee et al., 2012). In particular, increased ratios of proinflammatory/anti-inflammatory cytokines (TNF- $\alpha$ /IL10 and IL-6/IL-10) correlates with an increased risk of cardiac failure and death in cHCV patients (Oliveira et al., 2013). Additionally, increased oxidative stress has been proposed as a strong inducer of damaged DNA, potentially promoting the development and progression of hepatocellular carcinoma (HCC) as well as extrahepatic cancers (Maki et al., 2006). Several groups are now dissecting HCV-related systemic inflammation with the aim to identify targets for anti-inflammatory therapies that could help prevent or treat related complications, as well as pathological pathways involved into carcinogenesis or diabetes development.

HBV also induces strong liver inflammation in parallel of viral replication. However, the exact mechanisms are unknown. It was recently demonstrated that RIG-I can sense some pregenomic RNAs within the infected cells, triggering a specific type III/not type I interferon response (Sato et al., 2015). Clinically, it is less frequently associated with extrahepatic manifestations, and those are different from those induced by HCV in both their localization and pathogenesis (vessels in polyarteritis nodosa, kidney in glomerulonephritis).

## 5) T cells and inflammation

Naive CD8<sup>+</sup> T cells need three concomitant signals: (i) TCR, (ii) CD28 ligation, and (iii) inflammatory cytokines (Richer et al., 2013; Wilson and Brooks, 2013) to get activated, and differentiate into a spectrum of effector populations possessing unique capacities for survival, proliferation, cytokine expression, cytotoxicity, and memory formation. Currently, there is great interest in understanding how distinct inflammatory cytokines direct and tune CD8<sup>+</sup> T cell responses. Indeed, while there is a detailed literature on CD8<sup>+</sup> memory T cells generation and function in response to specific pathogens, it is less clear how these response behave in the context of concurrent infection. This becomes an important distinction since approximately one third of the world's population harbors a persistent infection – mostly HIV, malaria, and tuberculosis (Krishnamurty and Pepper, 2014). If non-pathogenic microbes are considered (such as herpes viruses), this rate is clearly 100% (Virgin, 2014), and we currently know very few about how they shape the immune system.

To date, only two bystander effect of chronic infection on unrelated T cell responses have been extensively documented:

- inflammatory cytokines tune the affinity of unrelated memory T cells for a faster and more efficient effector response to cognate antigens (Richer et al., 2013). This has been well demonstrated in the model of listeria monocytogenes (LM) and lymphocytic choriomeningitis virus (LCMV) infections. This is mediated by IL-12 and IFN-I cytokines (Raué et al., 2013), that enhance the downstream TCR signaling ;
- the inflammatory environment associated with a persistent infection divert memory cells from a long-lived fate to a more terminally differentiated effector phenotype, with a conserved inflammation-driven gene expression program (**Figure 19**).

Importantly, those two effects are reversible when infection is resolved, meaning that they are not hard-wired, but rather an active phenomenon. The possibility that similar effects affect the other T cell compartments has not been explored yet.

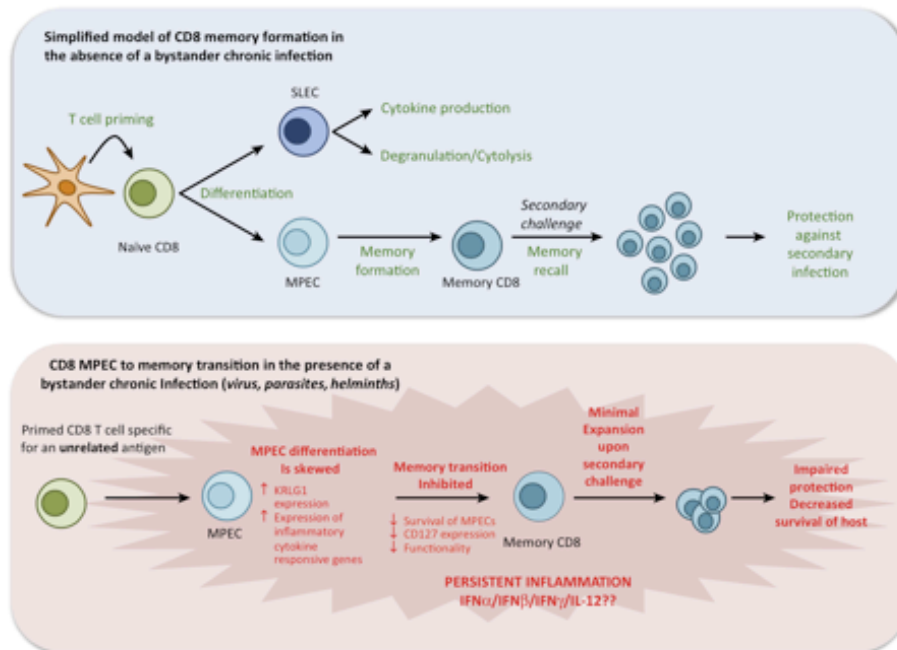


**Figure 19. Bystander infection negatively impacts effector to memory transition.**

Naive CD8<sup>+</sup> T cells that are primed by antigen presenting cells proliferate and differentiate to form effector cells. In some infections, such as LCMV, short-lived effector cells (SLECs) driven by inflammatory cues express high levels of cytokine and cytolytic activity. Memory precursor effector cells (MPECs) can survive the contraction to form long-lived memory CD8<sup>+</sup> T cells in the lymphoid organs. Recently, it was demonstrated that bystander chronic infection negatively impacts the MPEC to memory cell transition. Inflammation from bystander infection skews MPEC differentiation such that survival, cytokine production, and protective capacity of the CD8<sup>+</sup> memory cells is diminished and gene expression programs associated with chronic inflammation develop. Additionally, inflammation tunes the threshold for TCR activation of unrelated memory cells. From Krishnamurty and Marion Pepper, Trends Immunol 2014.

### III. T CELL TRAFFICKING

#### 1) Short introduction about chemokines

Chemokines are 8- to 12-kDa heparin-binding molecules with the ability to drive leukocyte trafficking and positioning within tissues. Chemokine-mediated trafficking of leukocytes allows these immune players to be directed to the places where they are needed. Therefore these processes play a critical role in regulating not only immune responses and inflammation but also homeostatic cell positioning. To allow cell migration, multiple chemokines and chemokine receptors can be involved, ensuring flexibility and specificity of leukocyte recruitment (Oo et al., 2010).

In the human system, there are more than 50 chemokines and 20 chemokine receptors that can be divided into structural subsets based on the presence of NH<sub>2</sub>-terminal cysteine motifs (**Figure 20 and Table 5**). The large CC chemokine family consists of chemokines in which the first two cysteine residues are adjacent, whereas in CXC chemokines, they are separated by a single amino acid residue. Fractalkine (CX<sub>3</sub>CL1) is the only member of the CX<sub>3</sub>C chemokine family in which three amino acid residues separate the first two cysteines. Finally, two related chemokines, XCL1 and XCL2, both of which bind the XCR1 receptor, lack two adjacent cysteine residues. Chemokines exert their chemotactic functions by binding to cell-surface G protein-coupled receptors (GPCRs), resulting in mobilization of intracellular Ca<sup>2+</sup>, which results in receptor internalization and the initiation of signaling pathways that facilitate chemotaxis. Consistent with G<sub>i</sub> association, the majority of chemokine responses are inhibited by treatment with pertussis toxin, which blocks the global G protein receptor. Chemokines are generally classified into two functional groups, 'inflammatory' and 'homeostatic/constitutive', based on whether they are induced by inflammation or constitutively expressed and involved in homeostatic immune regulation. However, this distinction is somehow erroneous, as classical homeostatic chemokines such as CCL19 and CCL21 (CCR7 ligands) and CXCL13 (CXCR5 ligand) are also induced at sites of chronic inflammation.

Lymphocyte chemotaxis is a complex process by which cells move within tissues and across barriers (Wei et al., 2003). It consists ligand recognition, cell polarization, and directed cell migration, and requires integration by the cell of numerous signals that will help it decide in which direction to move. Chemotaxis starts occurring at relatively low concentrations of chemokines, and is dose-dependent. However, at high concentrations, cells are paralyzed and no longer migrate.

Lymphocytes chemokinesis is the cell mobilization through cytoskeletal rearrangements (Wei et al., 2003). T cell progress by a series of repetitive lunges, repeatedly balling-up and then extending. This cycle appears to be driven by an intrinsic rhythmicity, with a period of about 2 minutes. During each cycle, the cell progresses an average distance of about 20 micrometers, *i.e.* T cells have a mean velocity of 10 micrometers per minute. However, following each pause, there is a high probability that

the cell will take off in another direction. Thus, tracks of T cells display a random walk pattern when followed over long times, although motions at short time are more linear.

## 2) Naive T cell trafficking

To be able to engage an immune response, naive T cells permanently patrol SLOs, therefore optimizing the chance to encounter an APC harboring a cognate antigen. This process is largely aided by CCR7-mediated migration, induced by CCL19 and CCL21 – expressed at high levels in high endothelial venules in SLOs. Similar as thymic export, egress from the lymph node is an active process, and requires both gradual desensitization to CCR7 signals, and re-expression of S1P<sub>1</sub>. The balance between « stay » and « go » signals through CCR7 and S1P<sub>1</sub> is a point of regulation of duration of naive T cells stay into the lymph nodes (Takada and Jameson, 2009). Naïve T cells also express CXCR4. CXCR4 on naive T cells also promotes lymph node entry by binding to CXCL12, which is produced by the follicular reticular cells and presented on the high endothelial venules lumen. This is a minor signal compared with CCR7, as mice deficient in CXCR4 exhibit defects in naive T cell homing only in the absence of CCR7 signaling (Okada et al., 2002).

In the context of infection, CCR7 and its ligands CCL19 and CCL21 recruit naive T cells and mature APCs to the lymph nodes, and promote their mobility to optimize rare antigen-specific naive CD8<sup>+</sup> T cell and cognate antigen-loaded DC encounters. During these early transient encounters, unknown signals upregulate the expression of various chemokine receptors, including CCR5, CCR4, and CXCR3, and downregulate CCR7 on the CD8<sup>+</sup> T cells. CCR5 and CCR4 ligands are then produced by DCs that have come into contact with antigen-specific or activated CD4<sup>+</sup> T cells, CD8<sup>+</sup> T cells, and/or NKT cells, resulting in additional recruitment of naive CD8<sup>+</sup> T cells (Griffith et al., 2014).

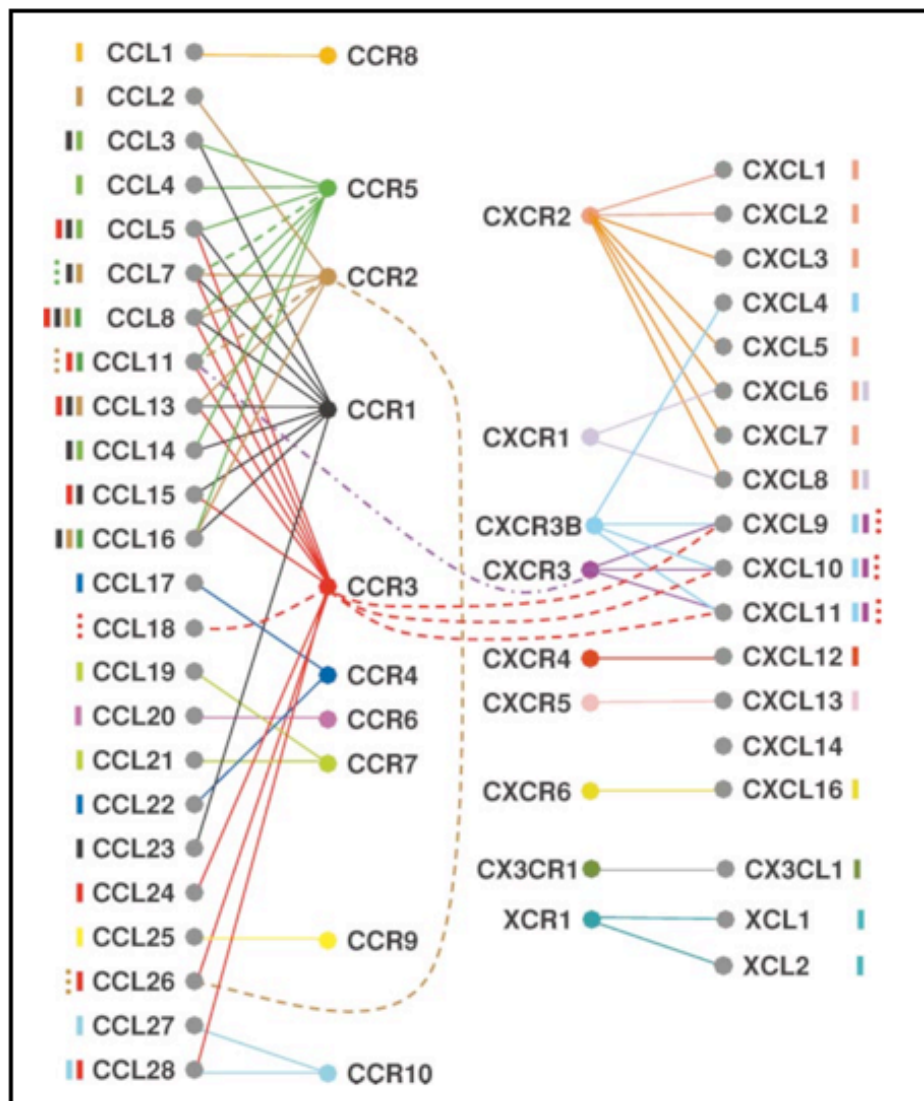


**Figure 20. Human chemokines and their receptors.**

Solid and dashed lines connect receptors with their agonists and antagonists, respectively, and are color coded to correspond with the colors of individual receptor hubs. The dashed-dotted line that connects CXCR3 with CCL11 represents a nonagonist-nonantagonist binding interaction. The bars next to individual chemokine numbers reflect the colors assigned to their apposite receptors. From Rot *et al*, Annual Rev Immunol 2004.

### 3) Effector and resident memory T cells trafficking

After activation, effector CD8<sup>+</sup> T cells downregulate LN-homing CD62L and CCR7 and start expressing chemokine receptors such as CXCR3, CCR5, CXCR6, CCR6, CXCR1, and CX3CR1. These induced chemokine receptors mediate effector CD8<sup>+</sup> T cell migration to sites of inflammation. Importantly, the site of priming appears to imprint effector T cells with the ability to traffic to particular organs (Agace, 2006). In the gut, CD103<sup>+</sup> DCs and stromal cells from Peyer's patches and mesenteric LNs produce retinoic acid that triggers expression of  $\alpha 4\beta 7$  and CCR9 on T cells. Interactions with their cognate ligands - endothelial-derived MAdCAM and epithelial-derived CCL25

- directs activated T cells to the small intestine. Similarly, T cells primed within the skin-draining inguinal LN preferentially migrate to the skin. This is mediated by cutaneous lymphocyte antigen (CLA), the mouse E/P-selectins, and the chemokine receptors CCR4, CCR8, and CCR10. CCR10 expression is induced by the active form of vitamin D<sub>3</sub>, locally synthesized by skin DCs (Sigmundsdottir et al., 2007).

T<sub>CM</sub> cells are defined by the coexpression of LN-homing CD62L and CCR7, and their recirculation through the blood and SLOs. Unlike naive cells, however, they express inflammatory chemokine receptors such as CXCR3 and CXCR4 that may serve as a CCR7-independent LN entry (Scimone, 2004). Recently, the expression of CXCR3 on T<sub>CM</sub> has been found to have a critical role for their function (Sung et al., 2012). The CD8<sup>+</sup> T<sub>CM</sub> response was directly compared with naive CD8<sup>+</sup> T cells after injection of antigen-pulsed DCs or infection with LCMV. Surprisingly, the response to antigen-pulsed DCs was similar in naive T and T<sub>CM</sub> cells except for an enhanced IFN- $\gamma$  response by the T<sub>CM</sub>. However, when the same comparisons were made during LCMV infection, T<sub>CM</sub> had higher CD69 expression, proliferation, and IFN- $\gamma$  production compared with the naive cells. This was related to the specific recruitment of CXCR3<sup>+</sup> T<sub>CM</sub> into specific T cell zones of the LN with a predominance of LCMV-infected macrophages. CXCR3 ligands chemokines then recruit additional CXCR3<sup>+</sup> T<sub>CM</sub> to the periphery of the LN and sites of active LCMV infection in a feed-forward mechanism that resulted in their quick activation and expansion in response to infection. Thus, CCR7-mediated LN homing coupled with CXCR3 expression on T<sub>CM</sub> positions these cells to quickly control the spread of virus within the lymphatic system upon rechallenge.

Resident-memory T cells (T<sub>RM</sub>) have been defined by their preferential tissue residence. These cells have been definitively identified in the skin, vaginal mucosa, central nervous system, salivary gland, lung, and intestine and are characterized by the increased expression of CD103 and CD69 and a lack of CD62L and CCR7 (Mueller et al., 2013). Chemokines are important in both the development and maintenance of CD8<sup>+</sup> T<sub>RM</sub>. Into the skin, during HSV infection, CD8<sup>+</sup> T<sub>RM</sub> development is dependent upon localization of CD8<sup>+</sup> effector precursor cells to the epidermis by CXCR3-CXCL10 interactions, strong enough to counteract a CCR7-dependent tissue exit signal (Mackay et al., 2013). CD8<sup>+</sup> T<sub>RM</sub> are further maintained in the tissue by downregulation of S1P<sub>1</sub> (Skon et al., 2013). T<sub>RM</sub> trigger a state of tissue-wide pathogen alert, and provide protection from reinfection or reactivation of latent skin viruses (Ariotti et al., 2014; Gebhardt et al., 2009; Jiang et al., 2012a). CD8<sup>+</sup> T<sub>RM</sub> quickly produce IFN- $\gamma$  in response to cognate antigen. This results in robust local production of chemokines, such as CXCL9, which recruits circulating memory CD8<sup>+</sup> T cells independent of their antigen specificity (Ariotti et al., 2014).

Finally, mucosal-associated invariant T (MAIT) cells are a conserved sub-population of T cells, characterized by their expression of the semi-invariant V $\alpha$ 7.2-J $\alpha$ 33 chain of the TCR, and restricted to the non-polymorphic MHC class I-related protein 1, MR1 (Kurioka et al., 2014). Those cells are

broadly reactive to microbes, and in particular critical in the control of *Bacillus Calmette-Guérin* (BCG), *Klebsiella pneumoniae*, and *Francisella tularensis* infections in mice. MAIT cells are enriched in the intestine and the liver, and represent up to 20% of CD8<sup>+</sup> T cells in the periphery in humans. They have been described to be CD8ab, CD8aa, or double-negative (DN), although a differential role for these subsets has not been explored (Walker et al., 2012). In adult blood, MAIT cells are the dominant population among CD8<sup>+</sup> T cells expressing the C-type lectin-like receptor CD161 at high levels. These CD161hi CD8<sup>+</sup> T cells are polyclonal, and functionally and transcriptionally distinct from other CD8<sup>+</sup> T cell populations, with the ability to be activated by IL-12 and IL-18 in a TCR-independent manner. Different from NKT, those cells are naive and low numbers in the newborn thymus and cord blood, and later evolve to abundant and effector-memory phenotype cells in adults. They share similarities with Th17 cells, and are activated and enriched non-specifically at inflammatory sites such as liver and joints, where they have the ability to kill target cells via important cytotoxicity.

#### 4) Role of CXCR3 in T cell biology

CXCR3 is a seven-transmembrane domain receptor (G protein-coupled receptor) that has the ability to bind three chemokines: CXCL9 (also known as MIG, monokine induced by gamma-interferon), CXCL10 (or IP-10, interferon-induced protein of 10kDa), and CXCL11 (or I-TAC, interferon inducible T cell alpha chemoattractant) (Groom and Luster, 2011). In human T cells, three isoforms of CXCR3 exist as a result of alternative splicing: CXCR3-A – the classical and more abundant form of the receptor, CXCR3-B – which not only binds CXCL9, CXCL10 and CXCL11, but also PF4/CXCL4, and CXCR3-alt – which binds only CXCL11 (Ehlert et al., 2004). Of the three CXCR3 ligands, CXCL11 has the highest receptor affinity and is the most potent agonist in chemotaxis and calcium-mobilization assays. The binding of chemokines causes a conformational change of the receptor, activating an associated G protein that initiates cAMP and phosphatidylinositol signal transduction pathways. In parallel, the binding leads to a rapid concentration-dependent internalization of the chemokine receptor, which is not observed after the binding of antagonists. By preventing association of G proteins with the seven-transmembrane domain of the receptor, pertussis toxin is a natural inhibitor of G protein-coupled receptor.

Naive T cells do not express CXCR3. The expression of this chemokine receptor on T cells is quickly upregulated after T cell priming, and later present on up to 40% of CD4<sup>+</sup> - preferentially on T helper type 1, and 60% of CD8 memory T cells. It is also expressed by natural killer cells, B lymphocytes, endothelial cells, mast cells, and thymocytes. In T lymphocytes, the stimulation of CXCR3 by its agonists leads to elevation of intracellular calcium as well as activation of phosphoinositide 3-kinase (PI3K)/Akt-dependent signaling and p44/42 extracellular signal-regulated kinase (ERK) pathways. CXCR3 activation has also been shown to induce rapid tyrosine phosphorylation of several proteins including zeta-associated protein of 70 000 MW (ZAP-70), linker

for the activation of T cells (LAT), and phospholipase-C-g1 (Smit, 2003). Interestingly, recent data suggest that chemokine receptors are recruited to the immunological synapse, and that there is a cross-talk between T-cell receptor and CXCR3-signalling pathways and that this participates in the fine tuning of immune responses (Dar and Knechtle, 2007).

The expression of CXCR3 is regulated at the transcription level by the transcription factor Tbet (T-box expressed in T cells), and permits the circulation of memory cells towards tissues that do express its specific ligands during the process of inflammation. CXCR3 and its ligands were shown to be implicated in the recruitment of:

- activated CD4<sup>+</sup> and CD8<sup>+</sup> T cells, and innate lymphocytes such as NK and NKT, into inflamed tissues;
- pDCs and subsets of B cells in the peripheral lymph nodes;
- and tissue-resident memory (T<sub>RM</sub>) T cells into nonlymphoid tissues (Clark, 2015) (**Figure 21**). Of note, T<sub>RM</sub> T cells have been identified in several organs such as small intestine, vaginal mucosa, brain, lung, salivary glands, and thymus (Mackay and Gebhardt, 2013; Mueller et al., 2014), and are characterized by high expression levels of the  $\alpha$ E integrin (CD103) and the marker CD69 (Mueller et al., 2014). These T cells are fully functional, quickly producing interferon- $\gamma$  upon local peptide stimulation, and triggering a state of tissue-wide pathogen alert (Ariotti et al., 2014).

CXCR3-binding chemokines are often expressed in inflamed tissues, and mediate local recruitment of primed CD4<sup>+</sup> and CD8<sup>+</sup> effector T cells that do express CXCR3 after having been primed into the draining lymph node. These chemokines have different temporal and spatial patterns of expression, relating to (i) their production by distinct cell types during the course of an immune response, and (ii) intracellular transcriptional regulation. Whereas CXCL9 is strongly induced by IFN- $\gamma$  but not type I interferons (IFN-  $\alpha/\beta$ ), CXCL11 is induced by both IFN- $\gamma$  and  $\beta$ , but not  $\alpha$ , and CXCL10 is strongly induced by all three, as well as by TNF- $\alpha$ . Through activation of IRF3 and the release of IFN- $\alpha$ , IP10 is the only ligand also induced by innate sensors, such as the TLRs and the RNA helicases (RIG-I and MDA-5).

Locally, effector cells secrete IFN $\gamma$ , and trigger an inflammatory amplification loop that further increases the recruitment of other lymphocytes into the site of inflammation.

Besides playing a crucial role in lymphocyte trafficking to inflamed peripheral tissues, recent studies indicate that CXCR3-ligands are also expressed in SLOs during T cell activation. Here, engagement of CXCR3 on T cells promotes their intranodal migration into areas where Ag-loaded DCs accumulate (e.g. medullary region of lymph nodes), permitting an efficient initiation of adaptive immune

responses (Groom et al., 2012). In addition, CXCR3-engagement in SLOs also results in T cell costimulation and activation, as evidenced by spatial association between CXCR3 and CD3 intracellular signaling (Friedman et al., 2006; Newton et al., 2009); and T cell differentiation choice towards short-lived effector rather than memory cells (Kurachi et al., 2011).

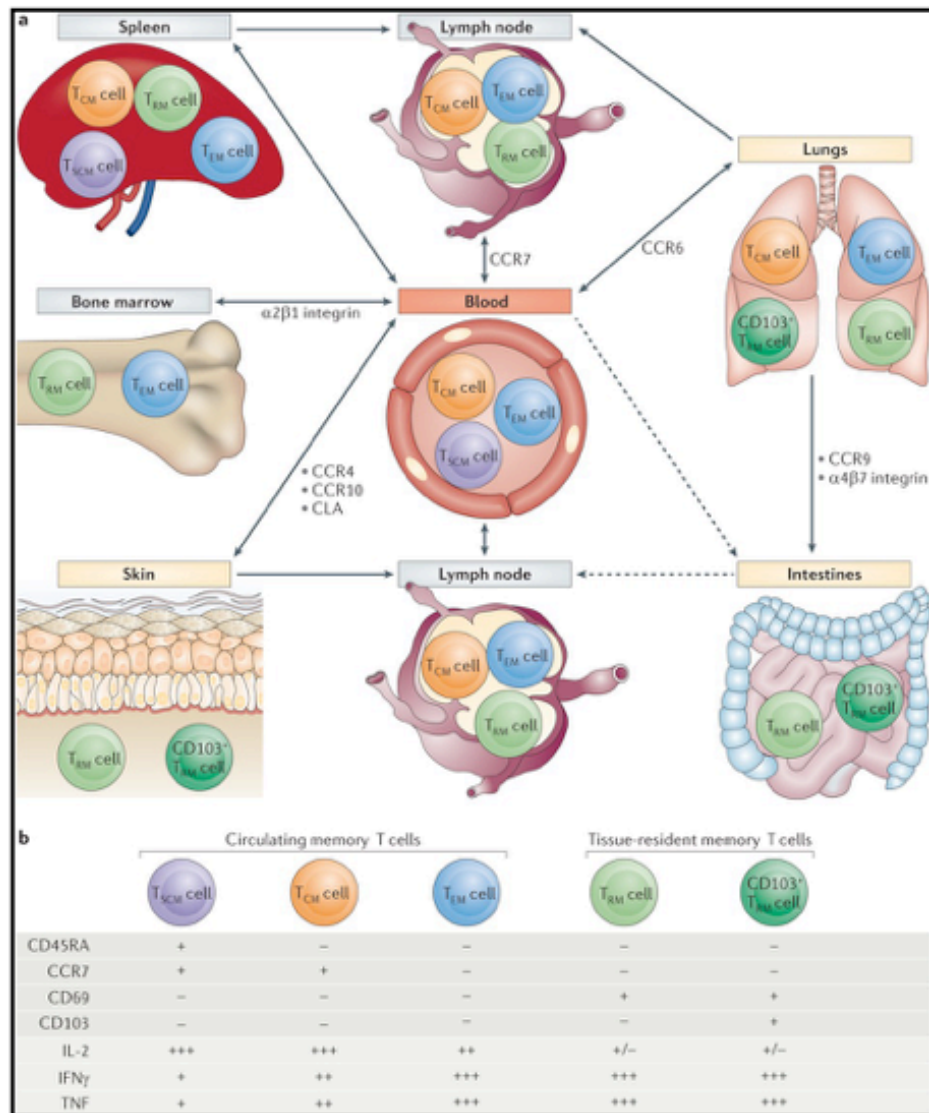


**Figure 21. Memory T cell heterogeneity in the blood and in tissues.**

A. The tissue distribution and the migration patterns of the major human memory T cell subsets are shown. Tissue-resident memory T (T<sub>RM</sub>) cell populations are defined by high expression of CD103 and are predominantly present in the skin, lungs, bone marrow and intestines, but they can also be found within the CD69<sup>+</sup> T cell subsets in the spleen, lymph nodes, and thymus organ. B. Key phenotypic and functional properties of circulating and resident subsets are shown. From Farber et al, Nat Rev Immunol 2013.

## 5) Focus on CXCL10

CXCL10 influences effector cells behavior into nonlymphoid tissues. This has been evidenced in mice chronically infected with *Toxoplasma gondii* in the brain, where treatment with anti-CXCL10 antibodies result in decreased numbers of local CD8<sup>+</sup> T cells, and a subsequent increase in parasite burden (Khan et al., 2000). This effect relates to a significant decrease in the average cell velocity within the tissue, and is reproducible by pertussis toxin (PTX) injection.

CXCL10 can be expressed by many different types of cells, including non-hematopoietic (endothelial, keratinocytes, fibroblasts, mesangial cells, astrocytes, hepatocytes), and hematopoietic (monocytes, neutrophils, DCs) cells. It is highly expressed in many Th1-type inflammatory diseases, often correlating with infiltration of T cells in the inflamed tissue. As many other molecules, CXCL10 can undergo post-translational modifications which might alter its function (**Figure 22**). It is believed that these modifications constitute a general mechanism to control leukocyte trafficking and inflammation (Rot and Andrian, 2004). Post-translational modifications of CXCL10 include:

- C-terminal cleavage by matrix metalloproteinase 9 (MMP9);
- Citrullination by peptidylarginine deiminase (PAD);
- and N-terminal cleavage of 2 amino acids by members of the X-prolyl dipeptidyl peptidase (DPP) family - the most characterized being dipeptidyl peptidase IV (DPP4 or CD26).

Whereas the two first modifications do not abrogate the chemotactic activity of CXCL10, DPP4-mediated NH<sub>2</sub> truncation seems to generate a dominant negative form of the protein, capable of binding CXCR3 but not inducing signaling. DPP4-truncated CXCL10 acts, therefore, as an antagonist of the bioactive chemokine. Our lab provided *in vivo* evidence of a role for CXCL10 antagonism in chronic HCV disease pathogenesis (Casrouge et al., 2011b). Indeed, patients chronically infected by HCV have high levels of the antagonist form of IP10 in their blood, explaining the paradoxical observation that this correlates with poor control of the disease. It is currently unknown if similar perturbations can induce impairments of trafficking in other infection such as HIV and malaria.

Besides CXCL10, many other chemokines were shown to be altered by post-translational modifications, resulting in the formation of antagonist molecules. Pertinent *in-vivo* examples include the degradation of monocyte chemoattractant protein-3 (MCP3) by MMP2, reported to be relevant to the pathogenesis of spondyloarthritis; and the cleavage of stromal cell-derived factor-1 (SDF1 or CXCL12) in HIV-associated neurodegeneration, also mediated by MMP2 (Moelants et al., 2013). Nevertheless, these studies are particularly challenging due to (i) the inability to discriminate the different forms of the analytes using sensitive immune-based assays, and (ii) the necessity to inhibit the activity of proteolytic plasma enzymes that may continue to act even after collection of the biological samples. Regarding the first challenge, specific assays that permit discrimination of the

truncated (short, 3-77) from the untruncated (long, 1-77) form of CXCL10 have now been successfully developed, and permit to monitor these two molecules in biological samples (Casrouge et al., 2011a).

DPP4 is a transmembrane glycoprotein expressed by hepatocytes, kidney epithelium and various tissue endothelium (Gorrell, 2005). DPP4 (CD26) is also expressed at the cell surface of B, T and NK lymphocytes. Its expression can be increased on T cells after TCR engagement (Dang et al., 1990). Its enzymatic activity is directed toward luminal or extracellular spaces, and its substrates include soluble and stromal factors (e.g., hormones and chemokines). DPP4 functions as a homodimer (Chiravuri et al., 2000), and in addition to its dipeptidylpeptidase activity, it may have endopeptidase activity (Bermppohl et al., 1998). Under steady state conditions, DPP4 may be shed (or possibly secreted), and enzymatically active soluble DPP4 (sDPP4) can be found in plasma, urine and semen (Durinx et al., 2000; Wilson et al., 2005). This phenomenon can be modulated during inflammation – for example during HCV chronic infection (Casrouge et al., 2011b). In addition to its enzymatic activity, DPP4 possess other biological functions that may be dictated by heterodimeric interactions with FAP $\alpha$ , plasminogen 2, ADA, CD45 or extracellular matrix proteins (Gorrell et al., 2001). Oral DPP4 inhibitors such as sitagliptin (FDA approved 2006, Merck *and co*, as Januvia) exist, and are clinically approved alone or in combination with other oral antihyperglycemic agents in the context of type II diabetes treatment. They have been developed based on their capacity to prevent GLP1 (Glucagon-like-peptide-1) and GIP (Glucose-dependent insulintropic polypeptide) inactivation, leading to an increased insulin secretion. To date, the effect of DPP4 inhibitors on chemokine and lymphocyte trafficking has not been studied. Using *in vivo* models, our group has recently demonstrated DPP4 inhibition as a way to protect the biologically active form of CXCL10 – leading to an increased local recruitment of lymphocytes and improvement of adjuvant-based immunotherapy, adoptive T cell transfer and checkpoint blockade (Barreira Da Silva, Nat Immunol 2015, In press). These findings support the use of DPP4 inhibitors as a strategy to enhance tumor immunotherapy.

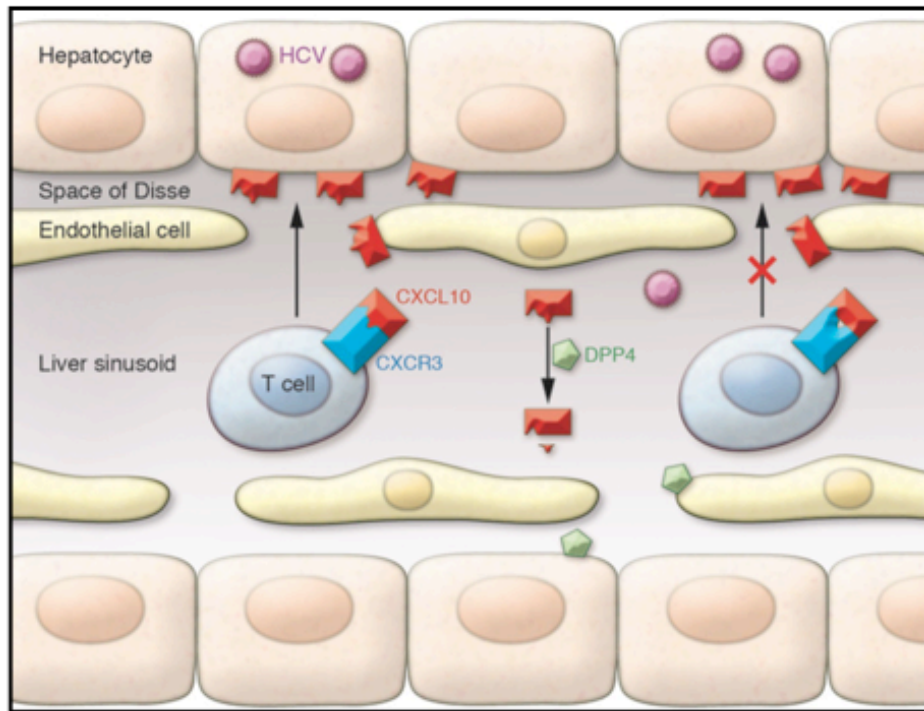


**Figure 22. Schematic model of chemokine antagonism.**  
 IP-10 (or CXCL10) produced in the infected or tumor cell recruits CXCR3-expressing T cells from the blood (left). When processed by DPP4, sIP-10 antagonizes T cell recruitment (right). From Charles *et al*, JCI 2011.

## **Chapter 2.**

# **Develop tools for screening rare antigen-specific responses**

---



# I. INTRODUCTION

Standard quantitative assays for measuring specific CD8<sup>+</sup> T cell responses, such as pMHC tetramers, Intracellular Cytokine Staining (ICS) and Enzyme Linked Immunospot (Elispot), with a limit of detection of  $\sim 10^{-4}$  (=1 cell in  $10^4$  CD8) and  $5 \times 10^{-5}$  respectively, do not allow to study naive Ag-specific CD8<sup>+</sup> T cells (Jenkins et al., 2010). Thus, most of our current knowledge about precursor frequencies prior to immunization and during first steps of activation relies on:

- Limiting Dilution Assays (LDA). In humans, it has long been the only way to evaluate precursor frequency. LDA are *in-vitro* assays in which 24-replicates cultures are set up at multiple dilutions of cells and stimulated in an Ag-specific manner (e.g. irradiated APCs, peptide and growth factors) (Taswell, 1981). After one to two weeks, cultures are combined with functional detection of specific cells via Elispot or ICS, and negative wells are scored for each dilution. According to Poisson statistics, when 37% of the tested wells are negative, there is a 95% confidence that specific cells in the positive wells derived from a single precursor. Even with recent improvements and standardization (Geiger et al., 2009), limits of this assay persist: (i) this requires exogenous stimulation, introducing potential bias and significant inter-assay variability; and (ii) it relies on one of many possible T-cell functions, and thus fail to detect epitope-specific T cells that lack that function.
- *In vivo* experimental models in mouse, utilizing adoptive transfer of monoclonal TCR transgenic (Tg) T cells into histocompatible mice secondarily exposed to their relevant antigen (Moon et al., 2009). Their main advantage is to identify epitope-specific T cells purely on the basis of TCR expression. However, only a limited number of antigenic specificities are available, these cells are monoclonal, and transfer efficiencies for each are unknown (ranging from 1 – 20%), making it difficult to estimate a broad panel of precursor frequencies. Also, these studies present some technical challenges. Indeed, high frequency transfer (1 to  $5 \times 10^6$  cells) generate populations 1,000 times larger than the endogenous naive epitope-specific populations, creating unphysiological situations where Ag-induced activation is inefficient due to increased competition. In contrast, transferring low number ( $1 \times 10^4$  cells) of TCR transgenic cells that approximates the endogenous naive repertoire is possible, but the detection of transferred T cells then necessitates a cell enrichment step, and more sophisticated flow cytometry techniques.

These limitations indicated the need to directly study polyclonal naive T cells (Badovinac et al., 2007; Ford et al., 2007; Marzo et al., 2005). To this end, an elegant method combining pMHC tetramer staining and magnetic bead enrichment was recently developed (Moon et al., 2007; Obar et al., 2008). It allowed for the first time direct detection, enumeration and characterization of rare naive Ag-specific T cells in mice. With this tool, it was further demonstrated that precursor frequency is as a critical factor for the magnitude of primary and memory responses after immunization,

immunodominance hierarchy, kinetic of responses, and differentiation patterns of memory. In humans, tetramers and magnetic beads enrichment have already been coupled to purify memory CMV-specific CD8<sup>+</sup> T cells for clinical purposes (Luxembourg et al., 1998), but never optimized for naive T cell detection. Thus, the question of the frequency of naive CD8<sup>+</sup> T cells specific for a given Ag in humans, their repertoire, and their impact on primary and memory immune responses in physiological or pathological situations have not been yet evaluated.

In this context, we developed and validated a new assay for tracking rare epitope-specific naive CD8<sup>+</sup> T cell from human peripheral blood. This assay, based on pMHCI tetramer staining and magnetic beads enrichment, permitted detection, enumeration and phenotyping of previously undetectable naive populations specific for HIV-1 Gag p17<sub>77-85</sub>, HCV NS3<sub>1073-1081</sub>, HCV Core<sub>132-140</sub>, NY-ESO-1<sub>157-165</sub>, and CMV pp65<sub>495-503</sub> in peripheral blood of seronegative healthy donors (HDs). Interestingly, we detected higher than 100-fold differences in precursor frequency across these epitopes (from 0.6x10<sup>6</sup> to 1.3x10<sup>4</sup>), but conserved frequencies among humans. These results were published in Blood journal in 2010 (**Manuscript 1**). The detailed experimental procedure was published in Methods in Molecular Biology in 2013 (**Manuscript 2**).

## II. TETRAMER ASSOCIATED MAGNETIC ENRICHMENT (TAME)

### A. Preparation of pMHCI tetramers

MHC tetramers are reagents that carry multiple peptide-MHC Class I (pMHCI) complexes, and thus have the ability to interact with multiple TCRs on a single CD8<sup>+</sup> T cell (Altman and Davis, 2003). Using MHC tetramers, it is possible to directly track and quantitate Ag-specific T cells during the course of immunization, independently of their function or differentiation state (Klenerman et al., 2002). In our studies, we use manually prepared tetramers. Global scheme of their preparation is presented in **Figure 23A** (from (Bousso, 2000)). Detailed protocol is available in the Protocols section. Briefly, inclusion bodies of heavy chain of HLA molecules - with BirA substrate peptide fused to the extracellular portion - and  $\beta$ 2-microglobuline protein ( $\beta$ 2m) are prepared in *E. Coli*, purified and stored at -80°C (**Figure 23B**). At Day 0, we achieve the HLA-peptide refolding by diluting each inclusion bodies subunit in a large volume of buffer containing the antigenic peptide, and we maintain the reaction for 4 days at 4°C. To improve the yield, we perform two supplementary heavy chain injections at Day 1 and 2. At Day 4, we concentrate the folding reaction using a stirred cell with a 30kDa cutoff membrane, then perform biotinylation by incubation with recombinant BirA enzyme (Avidity, Denver, CO) overnight. At Day 5, we purify the trimolecular complexes MHC/ $\beta$ 2m/peptide on a size exclusion chromatography column (**Figure 23C**). We collect fractions containing the biotinylated MHC peptide complexes (pMHC), pool them, and concentrate on a 30kDa

cutoff membrane. The extent of biotinylation reaction is visualized by SDS-Page electrophoresis by incubating samples with an excess of avidin (**Figure 23D**). Biotinylated monomers are stored at -80°C. When needed, we add fluorescently labelled streptavidin (e.g., PE, APC, Qdots) to the biotinylated pMHCI complexes to generate fluorescent tetramers that can be stored for several weeks in the dark at 4°C (**Figure 23E**). PE streptavidin is often the first choice because of its brightness and stability. We regularly validate the quality of our production by comparing stainings obtained with commercially *versus* manually prepared tetramers.

## B. Preparation of photocleavable pMHCI tetramers

The production of a single pMHC-complex as presented above is time-consuming and labor-intensive, and thus has limited application for high-throughput screening formats, or when low amounts of a large number of different specificities is needed. To address this issue, the group of Ton Schumacher developed conditional HLA ligands that authorize the generation of monomers in a highly adaptable manner (Bakker et al., 2008; Hadrup et al., 2009b; Toebes et al., 2006). During the first months of my PhD, I had the great opportunity to be trained by Ton Schumacher's group on this technology. In brief, the generation of pMHCI photocleavable monomers follows the same steps as in the above section (Bousso, 2000) (**Figure 24A**). The UV peptide permits stabilization of the monomer, and thus production of large numbers of photocleavable stocks. Then, when needed, UV-mediated cleavage is performed, and the complex is disintegrated except if there is an efficient binding peptide in the medium that rescues it from degradation. Main advantages of this technology is (i) to permit generation of tetramers with up to 200 different specificities at the same time - thus authorizing extensive analysis of the repertoire, and (ii) to produce small amounts of each – which dramatically reduces costs and time when tetramers with different specificities are needed, or for testing on small numbers of samples. We now routinely produce and use in our lab the HLA-A<sub>0201</sub>, HLA-A<sub>0101</sub>, HLA-A<sub>0301</sub>, HLA-B<sub>0801</sub>, HLA-A<sub>1101</sub>, H2-D<sup>b</sup> and K<sup>b</sup> photocleavable tetramers, as well as CD8<sup>null</sup> HLA-A<sub>0201</sub>, which allows avidity studies.

In addition to the use of UV-induced peptide exchange for the generation of pMHC reagents for T cell staining, this technology is also used to test *in vitro* the affinity of *in silico* predicted MHC-ligands (Hadrup et al., 2009b). This application relies on the demonstration that stabilization of the MHC molecule after peptide exchange is correlated to the binding capacities of a peptide (**Figure 24B**). We evaluate ligands affinity by a semi-quantitative ELISA standardized with known low, middle, and high-affinity binders. This assay can be performed in 96- and 384- well formats, allowing the screening of hundreds or thousands of candidate peptides (**Figure 24C**).

### C. Development of TAME for human samples

Conventional pMHC tetramer stainings are of insufficient sensitivity to study rare naive antigen-specific CD8<sup>+</sup> T cells. Based on recent technological improvements in mouse models, we worked on the development of a pMHCI tetramer-based enrichment protocol for human studies. We used unqualified buffy coats collected on healthy donors in blood banks. Buffy coat represents the thin layer between the upper clear fluid (plasma) and the bottom red fluid (red blood cells) that is obtained after centrifugation of an anticoagulated blood sample, and contains most of the white blood cells and platelets (**Figure 25A**). We isolated PBMCs using standard procedures, and performed HLA-A2 immunophenotyping (**Figure 25B**). As expected based on frequencies in the general population, we found about half of these samples to be HLA-A2 positive. Importantly, FACS-based HLA-A2 typing identifies the serotype allele, but does not inform on the 8 possible A2 subtypes. In Caucasian populations, the assumption that HLA-A2 positive individuals are of HLA\*A<sub>0201</sub> subtype is acceptable, and correct in a large majority of cases (100% in a pilot study of 20 samples collected in our laboratory). However, this is not true for non-caucasian populations, where HLA subtypes vary greatly, and where high-resolution molecular HLA definition is thus clearly needed. Indeed, inappropriate matching between the HLA alleles of the biological sample and the pMHC reagents used for monitoring can lead to dramatic changes in our ability to detect T cells and/or predict immunogenic peptides (van Buuren et al., 2014). In future clinical studies, this issue will need to be addressed by (i) the use of high-resolution PCR-based haplotyping (Erlich, 2012), and (ii) the engineering and use of HLA subtype tools (van Buuren et al., 2014).

Our enrichment protocol starts with the staining of PBMCs with PE-labeled pMHCI tetramers, where we typically put aside a small aliquot for flow cytometry analysis, corresponding to the «Before» fraction (**Figure 25C**). We incubate stained samples with anti-PE antibodies linked to magnetic particles, allowing enrichment of bound-cells by magnetic-activated cell sorting (MACS) column. We then recover, count and phenotype bound (« Enriched ») and unbound (« Depleted ») fractions with multicolor flow cytometry. Detailed protocol is available in the Methods section (Alanio et al., 2013). In order to optimize detection and enumeration of rare tetramer positive events, our protocol includes multiple levels of inclusion and exclusion gating strategies (**Figure 25D**). This permits to minimize background and focus on genuine T cell-events. First, a side-scatter area versus width plot is used to identify cell aggregates, which are excluded from the analysis. The remaining single-cell events are then analyzed on a plot of non-T cell lineage (dump) markers versus CD3. Non-T cell antibodies all being conjugated with the same fluorochrome, dump-positive events correspond to all mononuclear blood cells we are not interested in, comprising monocytes (CD14<sup>+</sup> and CD16<sup>+</sup>), B lymphocytes (CD19<sup>+</sup>), NK cells (CD56<sup>+</sup>), and dead cells because of inclusion of a viability dye with similar fluorescence characteristics. Of note, CD56 has to be removed when considering enrichment of activated T cells. Gating on CD3<sup>+</sup>Dump<sup>-</sup> events thus allows for putative T-cell events to be gated away from most other cell type, including dead cells and highly autofluorescent cells that potentially reside

along the center diagonal of the plot. These CD3<sup>+</sup> T-cell events are then plotted for CD8 versus tetramer stainings, which allows for the selection of CD8<sup>+</sup> Tetramer<sup>+</sup> subpopulation. Of note, in some experiments, CD3 staining is not included in order to free a channel on the cytometer, and Dump<sup>-</sup> CD8<sup>+</sup> T cells are directly gated, both strategies being demonstrated as equivalent (Hadrup et al., 2009a).

## **D. TAME increases detection of Ag-specific T cells by up to 100-fold**

In order to validate our protocol, and to define the output of the assay, we first focused on three HLA-A<sub>0201</sub>-restricted epitopes targeted by specific T cell populations that can be routinely detected by conventional pMHCI tetramer staining in healthy donors:

- Matrix-1 (M1<sub>58-66</sub>), which is an immunodominant epitope from the Influenza A virus (Flu) sequence. Most if not all of the adults will have encounter this antigen in their life, with a frequency of memory tetramer-positive cells in blood expected to be around  $1.2 \times 10^{-3}$  of CD8<sup>+</sup> T cells;
- CMVpp65<sub>495-503</sub>, which is an immunodominant peptide from the Cytomegalovirus (CMV) sequence. About half of the French population is expected to be seropositive for the virus, with extremely high frequencies of memory tetramer-positive cells in blood (estimated to be  $2 \times 10^{-2}$ ). The other half will be naive for this antigen, permitting eventual detection of inexperienced T cell populations in these individuals;
- Melanoma-associated Antigen recognized by T cells, MART1<sub>26-35</sub> (also known as MelanA), which is a skin self-restricted epitope targeted by very high numbers of naive CD8<sup>+</sup> T cells in peripheral blood of healthy individuals,  $\sim 6 \times 10^{-4}$  of CD8<sup>+</sup> T cells (Pittet et al., 1999).

We enriched cells for each of these specificities, and analysed «Before», «Enriched» and «Depleted» subsets by flow cytometry (**Figure 26A and B**). After enrichment, Ag-specific populations were clearly defined with few cells lost (usually 10-30%) in the depleted fraction. In other words, capture on the column is quite efficient and given that the majority of populations of interest are less abundant than CMV, we extrapolate that there is less than 10% loss in the depleted fraction. As limit of detection of conventional tetramer staining is only  $10^{-4}$ , we confirmed that there are no or few remaining specific cells in the « Depleted » fraction by a more sensitive assay, the IFN $\gamma$ -ELISPOT (**Figure 26C**). We observed reactivity for Flu-M1<sub>58-66</sub> peptide from « Before » fraction, as well as from the fraction depleted with another pMHCI tetramer (MART1<sub>26-35</sub>), but not from the fraction depleted with Flu-M1<sub>58-66</sub> tetramer, confirming that reactive cells were specifically retained within the magnetic

column. Concerning MART1<sub>26-35</sub>, we did not detect any reactivity both before and after depletion, which is in accordance with specific cells reactive for this epitope being of naive phenotype, and not able to be activated by a short period of activation. By comparing frequencies before and after enrichment, we evaluated TAME's yield being 550x, 35x, and 260x for Flu, CMV, and MART1 populations, respectively – and classically up to 100-fold in multiple experiments. This is in agreement with mouse studies, where the enrichment procedure typically achieves 100-fold enrichment. The starting number of cells utilized in the assay determines both precursor frequency calculation, and in most instances the limit of sensitivity for the assay. For example, a population around  $10^{-6}$  (*i.e.* 1 cell in  $10^6$  CD8) will only be detectable with a minimum of  $10^7$  starting cells.

To quantify the size of the epitope-specific populations within each sample, we use a calculation described in following blue box adapted from (Moon et al., 2009). The number of epitope-specific T cell-numbers is based on the absolute number of tetramer-positive cells within the « Enriched » fraction. We systematically analyze in each experiment the « Depleted » fraction, and if necessary, we add the number of remaining tetramer-positive cells to the number calculated in the « Enriched » to give the total number of specific cells for the entire sample. To validate the accuracy of our enumeration strategy, we compared enumeration of MART1<sub>26-35</sub>-specific CD8<sup>+</sup> T cell before and after enrichment in 6 healthy donors. Mean precursor frequencies were  $4 \times 10^{-4}$  ( $1.2$  to  $6.6 \times 10^{-4}$ ), and  $1.5 \times 10^{-4}$  ( $9 \times 10^{-5}$  to  $2.1 \times 10^{-4}$ ) respectively. We find the observed 2.8-fold difference acceptable with the benefits far outweighing the loss: better definition of specific population with decrease in non-specific background, and the possibility of enumerating cells with precursor frequencies under  $10^{-4}$ . As an external validation, a recent study on library method – a recently developed high-throughput limiting dilution assay, reports a strong positive correlation between precursor frequencies determined by the two methods (Campion et al., 2014).

**CALCULATION OF EPITOPE-SPECIFIC T-CELL NUMBERS**

The number of total CD8+ T cells within any sample is :

**CD8+ T cell number = (total cell number)x(number of CD8 in the acquired « Before » sample)/(single cell acquired in the same « Before »sample)**

The absolute number of endogeneous epitope-specific T cells (« Enriched » fraction only) is :

**Epitope-specific T-cell number = (total cell number before enrichment)x(proportion of single cells)x(proportion of non-dump CD3 T cells)**

**x(proportion of CD8 T cells)x(proportion of tetramer-positive cells within CD8 T cells)**

The endogeneous frequency is then:

**Precursor frequency = Epitope-specific T-cell number / CD8+ T cell number**

**Table 5. Calculation of epitope-specific T cell numbers, and validation.**

Box indicates the strategy for calculating epitope-specific T cell numbers (adapted from Moon *et al.*, Nat Protocols 2009).

With potential clinical application in mind, we evaluated the impact of freezing cell procedures on our protocol (**Figure 26D**). From one single donor, fresh versus frozen cells were enriched using Flu-M1<sub>58-66</sub>, CMVpp65<sub>495-503</sub> and MART1<sub>26-35</sub> PE-labeled HLA-A0201 tetramers. Cell phenotypes and precursor frequencies were found to be similar in both conditions:  $4.7 \times 10^{-3}$  versus  $3.9 \times 10^{-3}$  for Flu-M1<sub>58-66</sub>,  $3.5 \times 10^{-2}$  versus  $3 \times 10^{-2}$  for CMVpp65<sub>495-503</sub>,  $1.7 \times 10^{-4}$  versus  $1.5 \times 10^{-4}$  for MART1<sub>26-35</sub>, on frozen and fresh samples, respectively.

Finally, we used remaining free FACS channels for naive/memory phenotypic T-cell markers. There is no way to functionally assert that a cell is naive - only that a cell lacks memory functions. However, the lack of effector function can also mean that it does not respond to the cognate antigen, and we cannot easily distinguish these two options. Naiveness of a T cell is thus a phenotypic definition. Based on literature, we first identified naive T cells using antibodies targeting CD45RA, CD27, CD11a, and CCR7. CD45RO was excluded as it is the exact inverse picture of CD45RA, and thus redundant. CD62L was excluded because it is known to be lost during freeze/thaw procedures, and thus not suitable for clinical studies. To test the efficiency of our panel to discriminate naive versus experienced populations, we stained the three pre-cited enriched specific populations (**Figure 26B**). Consistent with a memory phenotype, 99% of the cells specific for Flu-M1<sub>58-66</sub> were found CD45RA<sup>-</sup>, CD11a<sup>+</sup>, CD27<sup>-</sup>. 99% of cells specific for CMVpp65<sub>495-503</sub> were also found CD11a<sup>+</sup> and CD27<sup>-</sup>, but CD45RA<sup>-/+</sup>, consistent with a predominantly late memory phenotype, as expected from literature [26]. This differed from MART1<sub>26-35</sub>-specific populations, where 98% of the cells were CD45RA<sup>+</sup>, CD11a<sup>dim/lo</sup> and CD27<sup>+</sup>, consistent with their naive status. The Labex Milieu Interieur, driven by Matthew Albert and Luis Quitana-Murci, is a large-scale study ongoing in the lab, which aim at assessing the determinants underlying human immunological variance within the healthy population. Eight-color antibody panels and procedures for staining and lysis of whole blood samples were standardized and automated, and permitted extensive and reproducible immunophenotyping of 1 000 healthy individuals (Hasan et al., 2015). As such, it represents solid foundations for defining reference values in healthy donors. In the T cell panel, naive and memory T cell subsets were defined by their expression of CD45RA and CD27 (Bretschneider et al., 2013; Hamann et al., 1997), and the expression of CCR7 and HLA-DR were also evaluated (**Figure 27A**). A strong correlation between percentages of naive cells defined by both CD45RA/CCR7, and CD45RA/CD27 combinations confirmed the redundancy of those markers for naive T cell identification – which does not rule out the need of CCR7 in defining specific memory T cell subsets (**Figure 27B**). In order to provide additional validation, we:

- sorted from a healthy donor naive, central memory, effector memory and late effector memory CD8<sup>+</sup> T cell subsets based on their CD45RA/CD27 expression patterns, and quantified sjTRECs as a measure of « naiveness » of the T cell population (Clave et al., 2009) (**Figure**

27C). As expected, we found the highest levels of sjTRECs in CD45RA<sup>+</sup>CD27<sup>+</sup> T cell population;

- tested intracellular release of calcium after ionomycin stimulation, and found distinct kinetics in naive T cells as compared to memory (Roederer et al., 2004) (**Figure 27D**);
- performed transcriptomic analysis on some selected autophagy and cell death related genes, and found lower Bcl2 and cIAP gene expression in naive T cells as compared to memory (Ahmed and Rouse, 2006) (**Figure 27E**).

We now routinely define naive T cells as co-expressing high levels of CD45RA and CD27.

### **E. Detection of naive CD8 T cells specific for HIV Gag p17<sub>77-85</sub>**

To address the issue of naive Ag-specific T cells, we further applied our tetramer enrichment protocol to the detection of cells specific for an epitope unknown from the healthy immune system. We decided to focus on the HIV Gag p17<sub>77-85</sub> HLA-A0201 epitope, as our HLA-typed healthy individuals receive serologic testing from the blood bank to confirm the absence of HIV infection. Clinical relevance and tetramer availability were also important criteria in our choice.

Using TAME, we were able to detect naive CD8<sup>+</sup> T cells for HIV Gag p17<sub>77-85</sub> epitope in a HIV-negative individual, with a measured physiological precursor frequency being  $0.3 \times 10^{-6}$  (**Figure 28A**). These cells were not detectable before the enrichment step, but defined a relevant population after enrichment. Further phenotyping found 95% of specific T cells sharing a naive phenotype (CD45RA<sup>+</sup>, CD27<sup>+</sup>, CD11a<sup>dim/lo</sup>) (**Figure 28B**). As internal control from the same donor, 99% of MART1<sub>26-35</sub> specific cells were of naive phenotype, and precursor frequency was  $1.8 \times 10^{-4}$ , which is comparable to other experiments. To confirm specificity of our HIV Gag p17<sub>77-85</sub> tetramer staining, we stained a LYMPHOCYTE clone specific for this epitope, and found 100% of these CD8<sup>+</sup> specific T cells correctly labeled. Further phenotyping confirmed an antigen-experienced status of these cells (CD45RA<sup>-</sup>, CD11a<sup>+</sup>, CCR7<sup>+</sup>), which were derived from a HIV1-positive patient.

The lymphocyte clone specific for HIV Gag p17<sub>77-85</sub> also allowed us to better define the limit of detection of our assay (**Figure 28C**). We spiked titrated amounts of the clonal CD8<sup>+</sup> T cells within known amounts of healthy PBMCs to achieve a precursor frequency of the T-cell clone of 0,  $10^{-7}$ ,  $10^{-6}$ ,  $10^{-5}$ , and  $10^{-4}$ , and tested our ability to detect these cells before and after enrichment. For example, to achieve a precursor frequency of  $10^{-5}$ , we spiked 200 clonal lymphocytes within 100 million PBMCs (of which 20 millions were CD8<sup>+</sup> T cells). TAME was performed and pre-enriched vs. enriched tetramer-positive cells were compared. In the absence of tetramer enrichment, the limit of detection was between  $10^{-4}$  and  $10^{-5}$ , consistent with prior evaluation of the tetramer technology. Using TAME, we were able to detect as few as 2 cells spiked into 100 million PBMCs, corresponding to a limit of

detection of  $10^{-7}$ . Given the ability to control for nonspecific staining with this protocol, the true limit is the number of PBMCs used in the protocol. As such, the theoretic limit may be less than  $10^{-7}$ , but for routine clinical monitoring we calculate a working limit of detection to be approximately  $10^{-6}$ , corresponding to observation of 10 to 20 cells in approximately  $10 \times 10^6$  of  $CD8^+$  T cells contained in 50 mL of blood.

To confirm the specificity of tetramer-reactive cells, we enriched  $CD8^+$  T cells from PBMCs, and stimulated them for 7 days with autologous mature dendritic cells (DCs) pulsed with MART1<sub>26-35</sub> peptide (**Figure 28D**). As described, the MART1<sub>26-35</sub>-enriched population was naive before stimulation. After the 7-days coculture, the entire population down-regulated CD45RA and expressed CD11a, whereas the HIV Gag p17<sub>77-85</sub>-specific cells in the same culture well remained naive. These data suggest that the naive T cells measured in our assays are indeed capable of responding to Ag-specific stimulation.

Finally, in order to maximize the number of informations obtained from a single tube, and reduce the amount of blood needed for several precursor frequency determinations, we developed multitetramer enrichment strategies. For this, we prepare HLA-A0201 tetramers with streptavidin-PE, plus same tetramers labeled with one specific color (**Figure 28E**). Enrichment is performed with anti-PE microbeads to simultaneously enrich all specific populations. We discriminate each specific T cell population by reading the second color on  $CD8^+PE^+$  events. This strategy leads to comparable percentages, output, and precursor frequencies of epitope-specific T cells as compared to single labeled populations. As simultaneous anti-PE/anti-APC enrichment with anti-APC microbeads works fine, we can with this technique multiplex up to 12 simultaneous tests within a single enrichment assay. We did not had the chance to test it, but we are confident in its possible achievement.

## F. Enrichment and enumeration of multiple specificities

After these steps of development, we applied our tool to the evaluation of precursor frequencies for multiple epitopes on 5 to 17 HDs (**Figure 29A**). We could detect T cells for all specificities. The calculated precursor frequency for MART1<sub>26-35</sub> was consistent with prior reports, with a median of  $1.3 \times 10^{-4}$  (n=13) (Pittet et al., 1999). Undetectable by conventional assays, it was also possible to establish a range for the frequency of NY-ESO-1, HIV-, HCV-, and CMV-specific T cells in cancer-free and seronegative persons. Median frequencies were  $3.6 \times 10^{-6}$  for the NY-ESO1<sub>157-165</sub> self-antigen (n=5);  $1.9 \times 10^{-6}$  for HIV Gag p17<sub>77-85</sub> (n=13);  $0.6 \times 10^{-6}$  for HCV Core<sub>132-140</sub> antigen (n=5);  $5.3 \times 10^{-6}$  for HCV NS3<sub>1406-1415</sub> antigen (n=5); and  $0.6 \times 10^{-6}$  specific T cells for CMVpp65 in seronegative patients (CMVpp65(sn); n=6). Although we found significant variations when comparing one epitope to another, quite surprisingly, precursor frequency for a single epitope persons was conserved on different individuals. These results were obtained by staining  $100 \times 10^6$  of PBMC, and correspond to absolute cell numbers ranging from 6 to 202 (Median 50). Of note, although most of the cells

belonging to these detected populations were of naive phenotype, a subset of of memory-phenotype cells – usually less than 30%, was often detected (**Figure 29B**).

### III. DISCUSSION

#### A. TAME permits enumeration and characterization of rare Ag-specific T cells from human peripheral blood

Two recent studies in mice reported a method for the direct detection of naive antigen-specific CD4<sup>+</sup> or CD8<sup>+</sup> T cells (Moon et al., 2007; Obar et al., 2008). We have now successfully modified this protocol and our study represents the first direct detection of naive antigen-specific CD8<sup>+</sup> T cells, prior to immunization, on human peripheral blood. Of the 6 specificities tested in mice, observed frequencies of specific CD8<sup>+</sup> T cells ranged from  $6 \times 10^5$  to  $3 \times 10^4$ , corresponding to 80 to 200 cells per animal. Here, excluding MART1<sub>26-35</sub>, which is known to be an exception (Pittet et al., 1999), we determined CD8<sup>+</sup> T-cell precursor frequencies that ranged from  $6.0 \times 10^7$  to  $5.3 \times 10^6$ . With an estimated total number of CD8<sup>+</sup> cells of approximately  $10^{11}$  (Arstila et al., 1999), measured frequencies correspond to 1 700 to 20 000 cells, a value that is in fact quite close to the estimations made by indirect methods (Coulie et al., 2002). However, our technique offers 2 important advantages:

- it permits direct detection of T cells by mean of their TCR and not by their functional capacity;
- it allows to track polyclonal specific T cell under physiological conditions;
- it does not require *in vitro* culture, thus removing the intrinsic biases and variations inherent to limiting dilution assays. Indeed, those assays require to stimulate T cells with cytokines, and thus assume that their sensitivity to these stimuli is identical, *i.e.* that no cell will be favored by this artificial environment. Recent papers demonstrate that this usually holds true under homeostatic conditions, with a good correlation between frequencies obtained with libraries generation and tetramer enrichments (Geiger et al., 2009). However, heterogeneity of the T cell preimmune repertoire – especially under pathogenic conditions, makes it less clear that this can be a general assumption.

Although TAME is a promising tool for fundamental and clinical studies, it is important to recognize the limitations of this approach:

- There may not be an exact correlation between the capacity of a T cell to bind a pMHCI tetramer, and its capacity to become activated when confronted with the respective pMHCI on an APC. Specifically, T cells detected by tetramer staining may not be capable of responding

to the specific stimulus because of unproductive cross-reactivity. Such T cells would not per se be anergic, but more likely responsive to an alternative (possibly related) peptide;

- Tetramer-based assays are restricted to a given HLA, and even to a certain subtype of HLA. They thus require extensive HLA-phenotyping of the patients, as well as development of tools for every possible HLA subunit. Important efforts are actually made by the community to permit these achievements and already, our collection of five photocleavable HLA Class I tetramers (A0201, A0101, A0301, A1101, B801) permits a coverage of >90% of individuals of Western European populations;
- In comparison with mouse studies – where spleen and/or lymph nodes are usually examined, starting material in human studies is often peripheral blood. Our expectation that our assay accurately reflect naive precursor frequency is based on the assumption that naive T cells continuously circulate, and do not stop into specific tissues (Andrian and Mackay, 2000).

## **B. Epitopes have conserved precursor frequencies among Individuals**

We applied tetramer enrichment for detection of populations for which, except for MART1<sub>26-35</sub>, precursor frequencies were unknown. For all of them, we were able to detect naive Ag-specific T cells from the peripheral blood of HDs. Perhaps the most surprising result is that precursor frequencies for Ag-specific inexperienced populations are very conserved among individuals. While similar observations were made in mice, the use of inbred strains resulted in the different animals sharing 6 of 6 histocompatibility molecules, as compared to the use of non-haploidentical human donors in our study. These results suggest that some extrinsic factor determines the number of cells per pMHC specificity. This has not been previously considered and may indicate that (i) positive selection is a highly conserved process in between individuals, or that (ii) peripheral self-pMHC complexes are involved in the determination of the diversity and pool size for the repertoire (Bouneaud et al., 2000; Ziegler et al., 2009). The latter assumption is in line with recent observations that crossreactivity between self and foreign peptides influences naive T cell population size and autoimmunity (Nelson et al., 2015).

Our data also indicate significant differences in precursor frequencies from one epitope to another:

- MART1, also called MelanA, is a self-protein of unknown function that is expressed by melanocytes and the majority of malignant melanoma cells. Previous studies have found a large thymic output of naive CD8 T lymphocyte specific for this antigen in the peripheral blood of HDs (Pittet et al., 1999). Here we confirm that precursor frequency is exceptionally high, and that targeting lymphocytes are for the most part of naive phenotype;
- HCV NS3<sub>1073-1081</sub> epitope is one of the most frequently targeted epitopes during chronic infection with the hepatitis C virus (HCV). NS3<sub>1073-1081</sub>-specific T cell responses being

associated with clearance of acute HCV, this epitope is an interesting candidate for a peptide vaccine. We found a relatively high precursor frequency for this population. This is in agreement with the observation that HCV NS3<sub>1073-1081</sub> - but not CMVpp65 or HIV Gag p17<sub>77-85</sub> - specific T cell lines can be readily generated by *in vitro* priming from HDs (Neveu et al., 2008) ;

- T cells specific for HIV Gag p17<sub>77-85</sub> are 16-fold less frequent than those targeting NS3<sub>1073-1081</sub>. Gag p17<sub>77-85</sub> was one of the first identified epitope of HIV. Despite its dominance in patients with chronic infection, this epitope is paradoxically considered as a poor immunogen because of its rare reactivity in acute infection (Kan-Mitchell et al., 2006). Future studies will be needed to determine if the poor precursor frequency can account for these observations;
- CMV is a ubiquitous herpes virus, which persists lifelong after primary infection and be pathogenic in immunocompromised individuals. About half of healthy donors are seropositive for this virus. Precursor frequency on seronegative individuals is 20-fold lower than for NS3<sub>1073-1081</sub>. Considering mouse studies which have shown correlation between precursor frequency and magnitude of the response, it may be surprising that this epitope, for which we confirm very abundant specific populations after immunization, has such a low precursor frequency. We interpret these data as a result of CMV being a chronic infection with continuous restimulation of CMV-specific CD8<sup>+</sup> T cells.

With the exception of MART1, we observed up to 30% of memory-phenotype (MP) cells into Ag-specific inexperienced populations. In the CD4 preimmune repertoire, those cells were found more abundant, with 20-90% of memory-phenotype cells in Ag-specific anti-viral T cells of unexposed individuals (Su and Davis, 2013; Su et al., 2013). Interestingly, same populations were found naïve-phenotype when harvested from cord blood samples. In this study, crossreactivity with environmental antigens is identified as having a critical role in shaping the adult healthy CD4 preimmune repertoire. Examples of CD8<sup>+</sup> T cell crossreactivity have been occasionally reported, for example in between HCV NS3<sub>1073-1081</sub> or HIV Gag p17<sub>77-85</sub> and influenza A virus determinants (Acierno et al., 2003; Kennedy et al., 2006). Lower levels of memory-phenotype cells in the CD8 preimmune repertoire as compared to CD4 can be explained by the later being restricted to extracellular antigens, and thus intrinsically more sensitive to changes in their environment. Inversely, CD8 T cells are more sensitive to homeostatic signals, and the contribution of HP in that population is expected to be high (Sprenth and Surh, 2011).

Overall, our data indicates the potential for up to 30-fold differences in precursor frequencies across different specificities. Using these tools, recent studies demonstrated that precursor frequency account for related immunogenicity in humanized mouse (Tan et al., 2011) and humans (Schmidt et

al., 2011). Identifying epitopes with the highest precursor frequency is of great interest for the design of future vaccine strategies, as it will hopefully correlate with stronger CD8<sup>+</sup> T cell responses, and a better clinical outcome of vaccination in healthy, or in viral and tumoral diseases.

## IV. PROSPECTIVES

Tetramer-based enrichment assays are now standardized for both mouse and humans. However, some technical improvements can still be hoped in order to increase their use by the scientific community – and thus our knowledge about Ag-specific populations. Our experience in tetramer production makes us believe that there is only few space for optimization in the generation of the tetramer molecules itself. However, improvement of the enrichment technology is more feasible. First, the screening of a larger number of specificities on a minimal amount of sample can be achieved by more complex combicolor coding strategies, where each Ag-specific T cell is concomitantly labeled with a defined combination of two fluorochrome-labeled tetramers (Hadrup et al., 2009a). Although we developed these assays in our lab, we had difficulties in getting clean-enough datas to screen rare T cell populations. We are optimistic that the use of last-generation spectral analyzers such as the SP6800 from Sony – by removing the need of compensation, will permit to improve its sensitivity. Second, we would ultimately like to build sort of Luminex-beads tetramer enrichment assays, permitting high-throughput exploration of the Ag-specific repertoire – including cells with rare frequencies. This would require the use of a component that would at the same time label the cell for specificity, and have a specific physicochemical property that can be exploited for enrichment. This could be magnetism, like in the StrepTag technology, but others might also be possible. Alternatively, we plan to work with companies to standardize enrichment procedures and adapt them to constraints of clinical laboratories. Finally, an important point is also to improve detection of Ag-specific T cells within tissues slides. At the moment, coupling tetramer staining to classical immunohistochemical protocols is impossible. Here again, exploiting components with original physico-chemical properties would be of great help.

Beside technical aspects, we believe our enrichment protocol will permit to address a number of unresolved questions:

- Are precursor frequencies stable over time and/or over decades of life? Measuring precursor frequencies in a cohort of healthy donors several times sequentially will inform us on the distribution of inexperienced T cells in the body and the stability of the T cell preimmune repertoire;
- Are MP cells proportions in inexperienced populations stable over time and/or over decades of life? Are MP proportions fixed for a given specificity similarly as precursor frequency? Are

there detectable ranges of physiological variations? What is the participation of HP to MP generation? Same analysis as mentioned before, coupled to naive/memory phenotyping, will help answering these questions. Comparing the middle-age adult preimmune repertoire to Ag-specific T cells isolated from cord blood, infants, or elderly will also be of great interest. Cord blood samples being supposedly germ-free (though arguably, not totally free of stimulation by specific pathogens), this will offer precious information on the origin of MP cells;

- Are recent thymic emigrants (RTEs) part of inexperienced Ag-specific populations, and what is their impact on T cell responses? It is known that RTEs are part of the naive repertoire, but still unclear whether they have a specific antigenic repertoire. Using single-cell technologies and sjTRECs analysis on neonate thymi and age-stratified infants cohorts, we hope it is possible to identify phenotypic markers for those cells, and track them in different situations, for example during childhood vaccinations;
- Are circulating naive T cells representative of the global naive population, or are they a specific subset that inform us only little about the entire body situation?
- Is the preimmune repertoire similarly shaped in other (non-A2) haplotype?
- Finally, do quality matters? The impact of precursor frequency is established in both mice and humans (Moon et al., 2007; Schmidt et al., 2011). We know from mice studies that each subpopulation found into the preimmune repertoire has a particular behavior after immunization. But it is unclear how much these parameters impact the Ag-specific response when considered all together.

Answers to these questions will require large application of TAME to clinical trials. This tool is sensitive enough to monitor Ag-specific specific CD8<sup>+</sup> T cell with a precursor frequency above  $0.5 \times 10^{-6}$  from 50-100mL of blood, an acceptable amount to obtain from patients during routine analysis. Some clinical settings would be of particular interest:

- Viral clearance, as described in **Chapter 3** in the context of chronic HCV;
- Preventive and therapeutic vaccination - childhood vaccination, HBV-vaccine non-responders, and cancer vaccines;
- Susceptibility to autoimmunity;
- Organ and stem cell transplantation, with the hypothesis that immunosuppression could (i) lead to extinction of the smallest inexperienced populations when T cell number decreases, and (ii) favor the proliferation of MP cells, which may account for some specific clinical features.

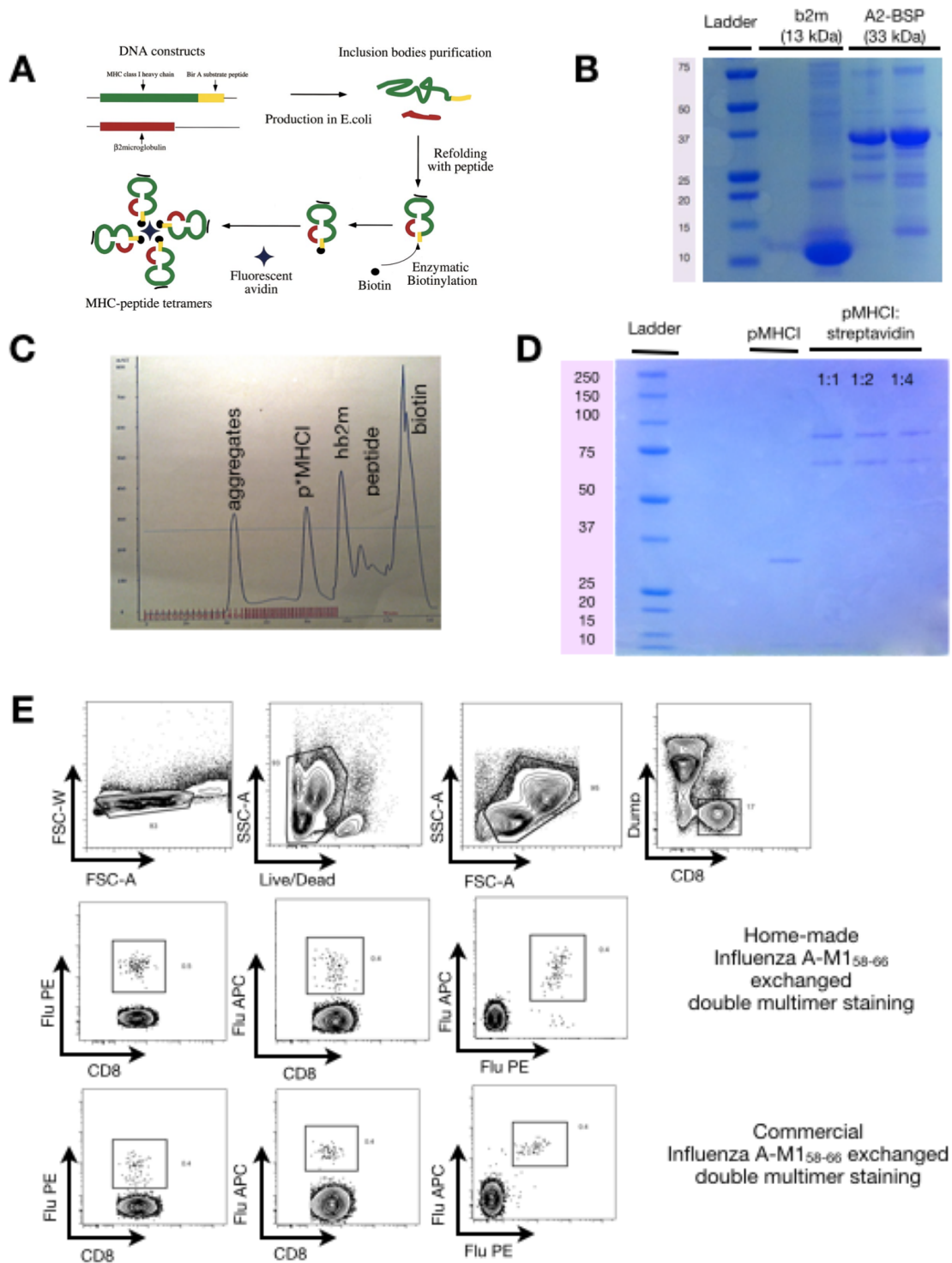


**Figure 23. Preparation of pMHC I tetramers.**

A. Schematic description of the generation of MHC-peptide tetramers (from Bousso, 2000). B. Control of the production of HLA-A<sub>0201</sub> heavy chains and  $\beta$ 2-microglobulin molecules by SDS/PAGE electrophoresis (NuPage 4-12% gel). C. Representative chromatogram from size-exclusion chromatography after HIV Gag p17<sub>77-85</sub> HLA-A<sub>0201</sub> monomer refolding. D. Control of monomers biotinylation by SDS/PAGE electrophoresis (NuPage 4-12% gel). In presence of an excess of avidin, biotinylated pMHC I monomers associate and form complexes of molecules. Disappearance of pMHC I band is proportional to the extent of monomer biotinylation. E. After UV-exchange, monomers are incubated with fluorochrome-labeled streptavidin, then used for staining cells together with monoclonal antibodies. Dump channel includes CD4, CD14, CD16, and CD19. Tetramer positive cells are defined as FSC-W<sup>lo</sup>Live/Dead<sup>neg</sup>LymphocytesDump<sup>-</sup>CD8<sup>+</sup>Tetramer<sup>+</sup> events.



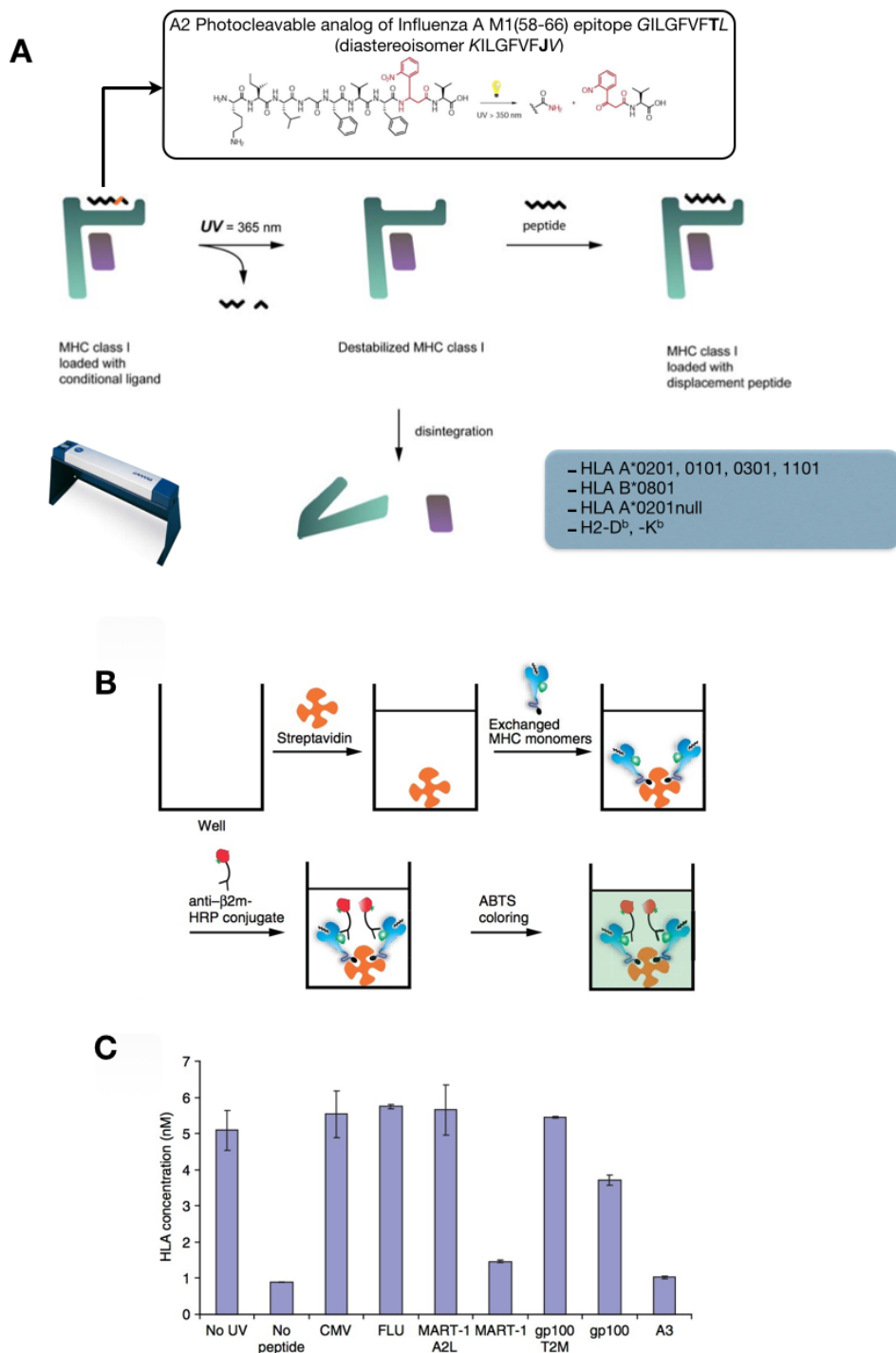


**Figure 24. Peptide exchange technology.**

A. UV-exchange facilitates tetramer production. Influenza A M1 epitope has been engineered to be able to disintegrate upon UV exposure. As such, in its entire form, it permits stabilization, thus large production, of class I monomers. And when needed, it can be cleaved and exchanged upon short UV exposure. Similar technology are in place in the lab for the alleles indicated in the blue box. (Adapted from Hadrup *et al*, Meth Mol Biol 2009). B. UV-exchange permits *in vitro* evaluation of peptide MHC binding properties by streptavidin-based sandwich ELISA. Exchanged biotinylated monomers to be tested are added to the streptavidin-coated wells. HRP-conjugated anti-β2-microglobulin antibody recognizes pMHC complexes bound to the well. ABTS is added as a substrate for HRP and gives a yellow-colored oxidation product. C. Example of an ELISA read-out. No UV, non-irradiated conditional MHC complex; no peptide, irradiation without rescue peptide; CMV, cytomegalovirus pp65(495–503); flu, influenza A Matrix 1(58–66); Mart-1 A2L, melanocyte lineage-specific protein A (26–35 A2L); Mart-1, melanocyte lineage-specific protein A (26–35); gp100 T2M, human melanoma associated antigen gp100(209–217 T2M); gp100, gp100(209–217); A3, HLA-A3 restricted gp100(17–25). (Adapted from Rodenko *et al*, Nat Protocol 2010).



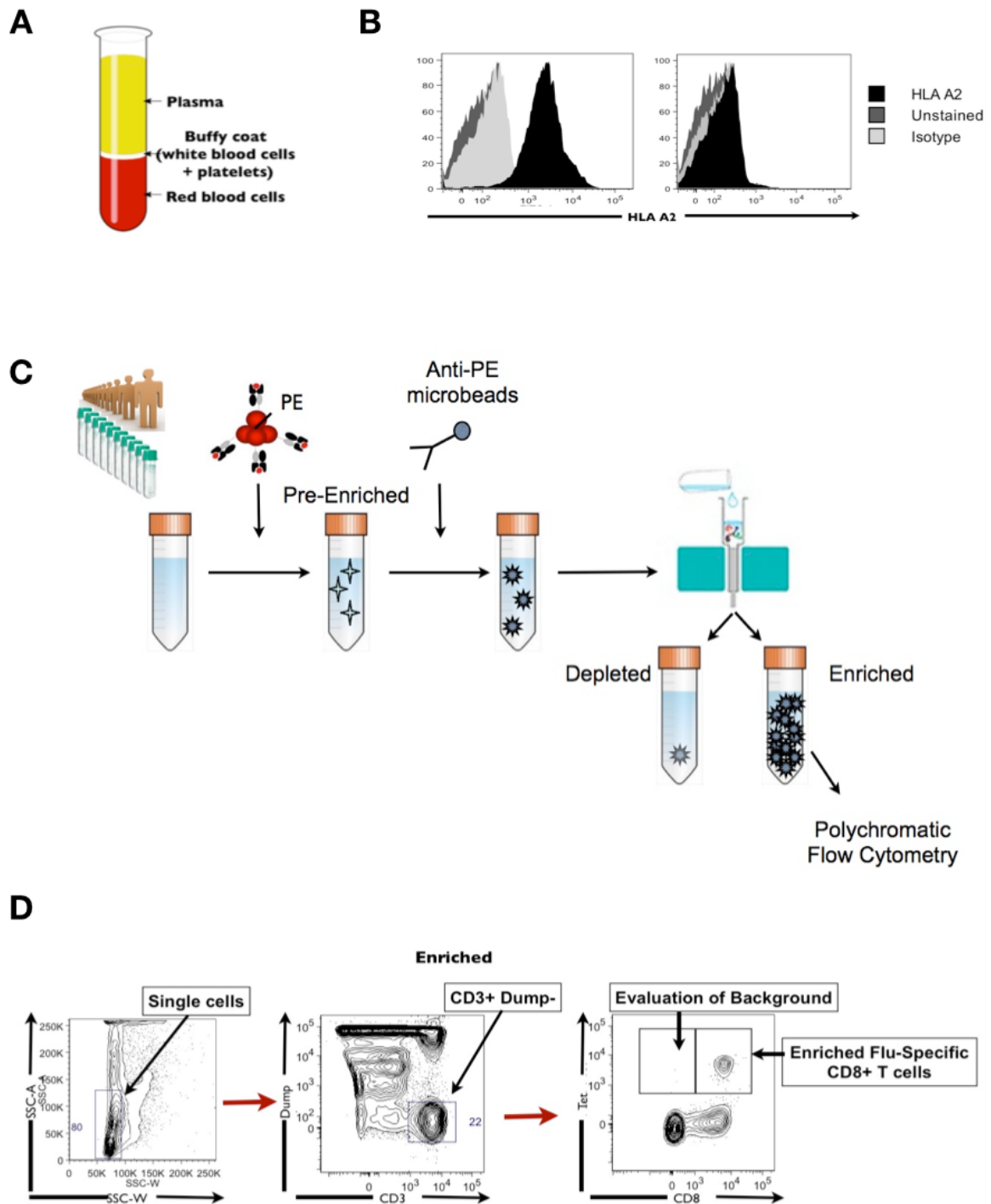


**Figure 25. Development of Tetramer Associated Magnetic Enrichment (TAME).**

A. Buffy coat is defined as a thin central layer after centrifugation of heparinized human plasma. B. HLA-A2 typing was performed on whole blood on each buffy coat. Histograms present representative A2-positive (left) and A2-negative (right) results gated on lymphocytes. C. Schematic representation of TAME. D. Gating strategy to reduce background.  $100 \times 10^6$  PBMC from healthy individuals were analyzed by eight-color flow cytometry following staining and TAME with a Flu-Matrix1 HLA-A0201 tetramer labelled with PE. Flu-specific  $CD8^+$  T cells from the enriched (bound) fraction were identified as side-scatter<sup>low</sup> dump<sup>-</sup>  $CD3^+$   $CD8^+$  Tet<sup>+</sup> events. The tetramer-positive gate was set using the  $CD8^-$  gated events as a negative control. Represented results show  $10^6$  collected events.



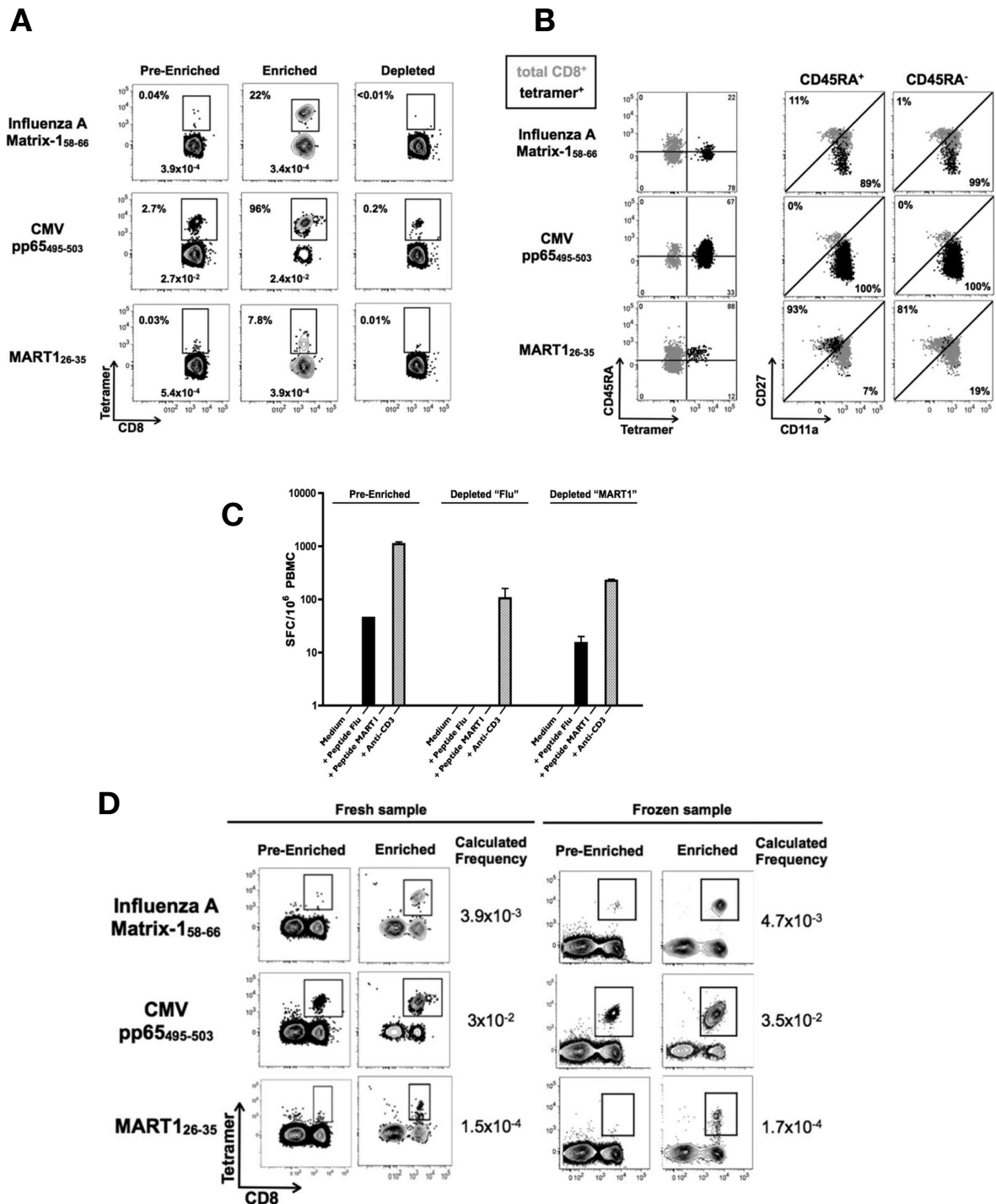


**Figure 26. TAME Increases Detection of Antigen-specific T cells by up to 100-fold.**

A.  $100 \times 10^6$  PBMC from HD were stained with Flu-M1<sub>58-66</sub>, CMVpp65<sub>495-503</sub> and MART1<sub>26-35</sub> HLA-A2.1 tetramers labelled with PE. Enrichment was performed by addition of anti-PE microbeads and MS magnetic column. « Pre-enriched », « Enriched », and « Depleted » fractions were analyzed on a LSRII cytometer. Represented results show  $2 \times 10^6$  collected events for « Before » and « Depleted » fraction, and acquisition of all sample for « Enriched » fraction. Plots are gated in total CD3<sup>+</sup> T cells.

B. Eight color flow cytometry on « Enriched » specific populations accurately discriminate naive (MART1<sub>26-35</sub>) and memory (Flu-M1<sub>58-66</sub>, CMVpp65<sub>495-503</sub>) situations.

C.  $2 \times 10^5$  PBMC were plated from « Before » and « Depleted » fraction for Flu-M1<sub>58-66</sub> or MART1<sub>26-35</sub> MHCII tetramer pulldown for IFN $\gamma$ -Elispot, and cells were stimulated by each corresponding peptide. Absence of Flu reactive cells in Flu-depleted fraction as compared with Before confirms efficient depletion of antigen-specific cells. Absence of IFN $\gamma$  producing cells in the Before fraction for MART1<sub>26-35</sub> is consistent with their naive phenotype.

D. Comparison of phenotype and precursor frequencies on fresh versus frozen samples. Frequencies represent the number of epitope-specific T cell within CD8<sup>+</sup>.



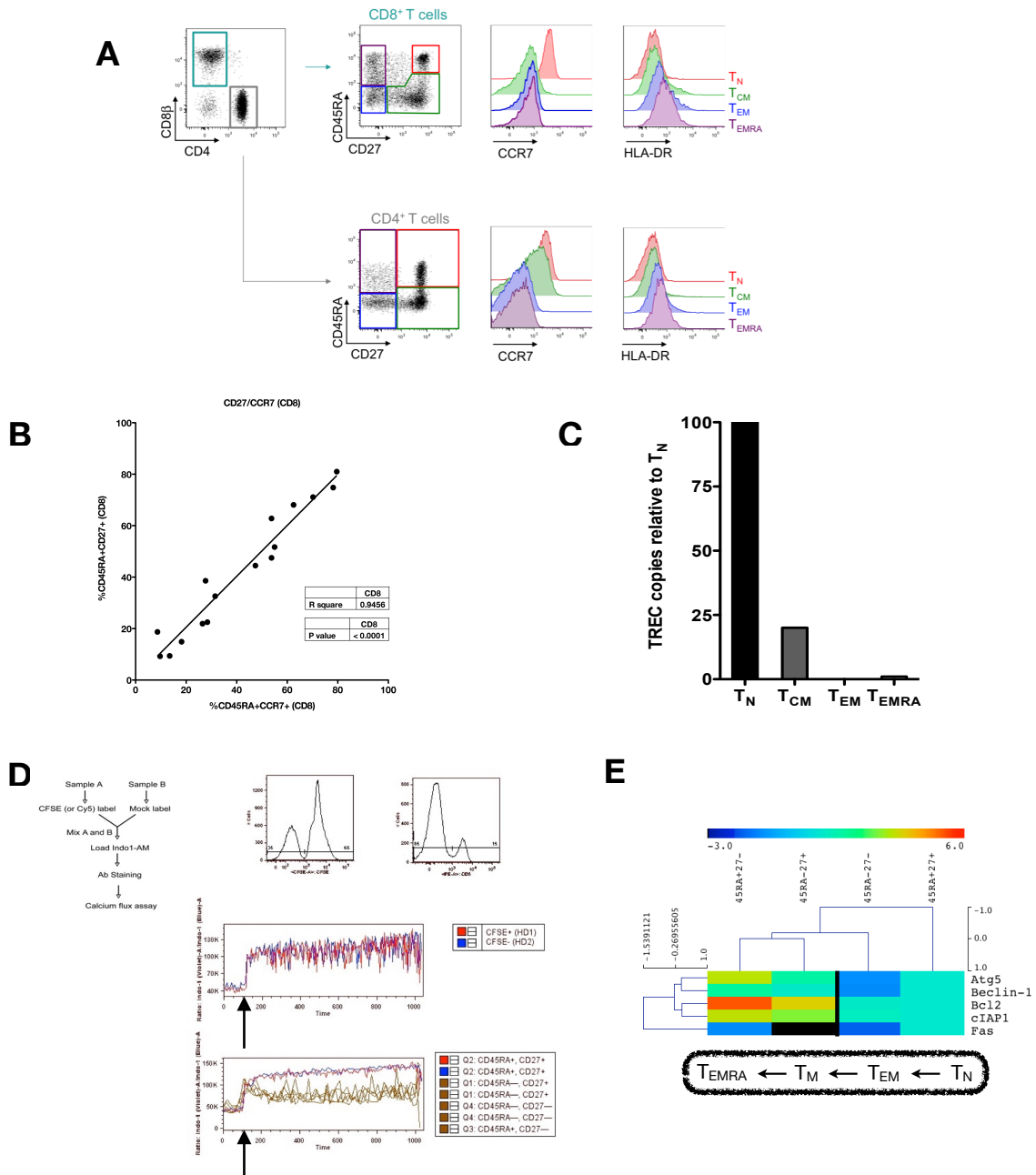


**Figure 27. Comparison of CCR7 and CD27-based naive gating strategies.**

A.  $1 \times 10^6$  PBMC were stained with the T cell panel developed in the context of the Labex Milieu Intérieur, including the following naive/memory markers: CD45RA, CCR7, and CD27. CD45RA/CD27 dot plots allow identification of CD45RA<sup>+</sup>CD27<sup>+</sup> naive, CD45RA<sup>-</sup>CD27<sup>+</sup> central memory, CD45RA<sup>-</sup>CD27<sup>-</sup> effector memory, and CD45RA<sup>+</sup>CD27<sup>-</sup> late effector memory CD4<sup>+</sup> and CD8<sup>+</sup> subsets. Expression of CCR7 and HLA-DR by each of these compartments is represented on histograms. B. Percentages of CD8<sup>+</sup> naive T cells as obtained by either CD45RA/CD27 or CD45RA/CCR7 gating strategies on 15 healthy donors were plotted. Linear regression Spearman R correlation coefficient and corresponding p-values are indicated. Of note, similar results are obtained on the CD4 T cell population. C. Percentage of sjTREC content in sorted naive/memory CD8 T cell subsets as defined by CD45RA/CD27 antibodies (HD). The percentage is normalized as compared to the amount found in the naive population. D. Development of calcium flux assay on primary cells. Pre-staining of the cells with CFSE allows simultaneous detection of calcium responses from two different donors. The arrow indicates the addition of Ionomycin to the cells. Ratio of Indo-1 Bound/Unbound is followed over time. The above histogram represents detection of calcium flux inside all CD8<sup>+</sup> T cells. The bottom histogram represents the same assay in gated naive/memory CD8<sup>+</sup> populations. E. Gene expression of Atg5, Beclin1, Bcl2, cIAP1, and Fas assessed by RT-PCR on the four naive/memory sorted subsets. Color gradient represents the fold changes as compared to the actin gene, and naive is set as the reference population.



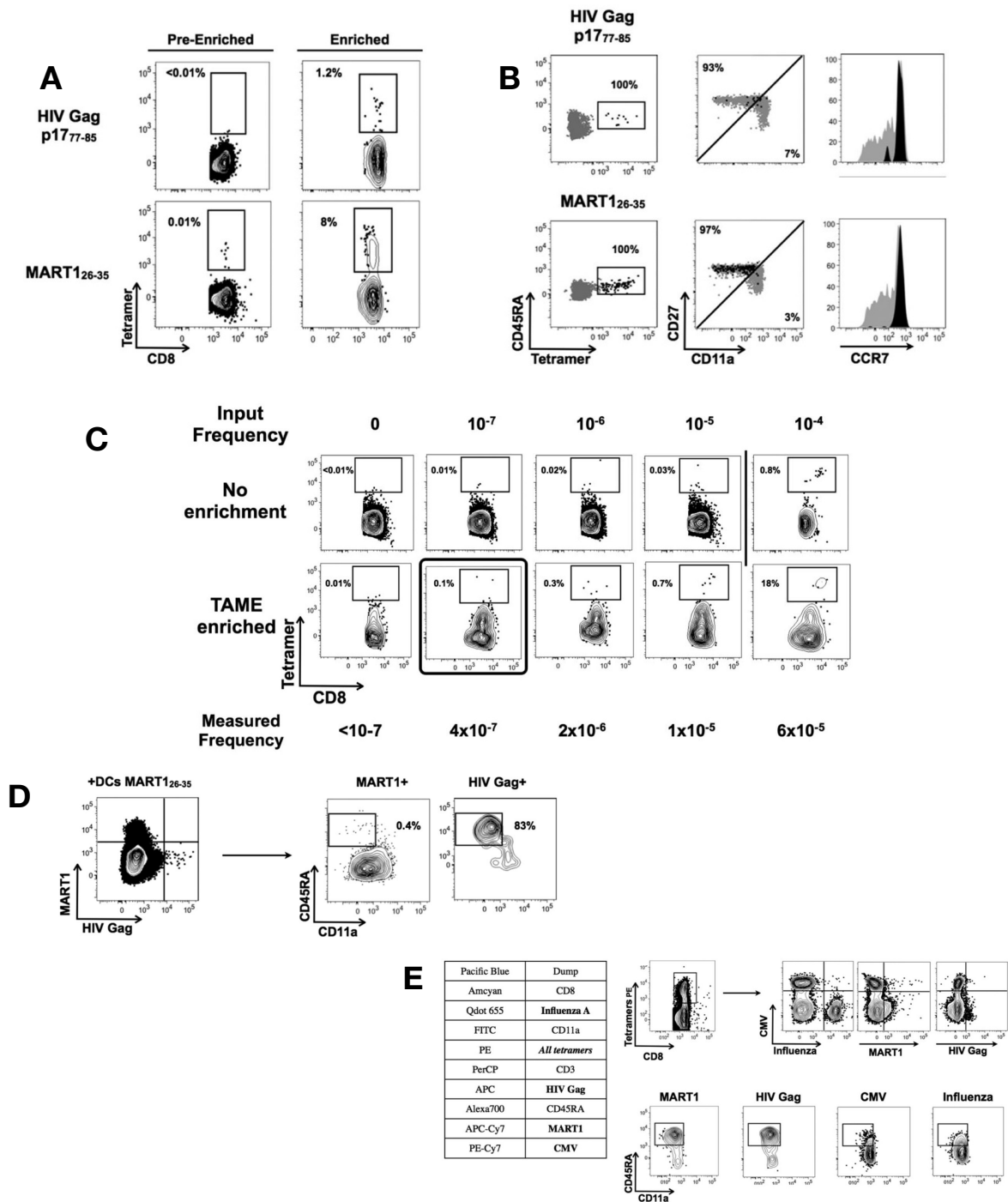


**Figure 28. Naive CD8<sup>+</sup> T cells Specific for HIV Gag p177-85 can be Detected on Healthy donors.**

A. TAME enrichment on 400 millions healthy PBMCs with HIV Gag p177-85 and MART1<sub>26-35</sub> HLA-A0201 tetramers labelled with PE. B. Phenotype of HIV Gag and Mart1-specific populations enriched in A (black) as compared to bulk CD8 T cells (grey). C. 2 000, 200, 20, and 2 lymphocytes specific for HIV Gag p177-85 epitope were spiked into  $100 \times 10^6$  PBMC of one single healthy donor. Samples were stained with HIV Gag p177-85 HLA-A0201 tetramer labelled with PE, and analyzed before or after tetramer enrichment. D. PBMCs were enriched in CD8 using magnetic microbeads, and enriched cells were cocultured for 7 days with DCs loaded with MART1<sub>26-35</sub> peptide. T cells were then harvested and stained with MART1<sub>26-35</sub> and HIV Gag p177-85 tetramers. E. A panel including MART1<sub>26-35</sub>, HIV Gag p177-85, CMVpp65<sub>495-503</sub>, and Flu-M1<sub>58-66</sub> HLA-A0201 tetramers was developed. All tetramers were labeled with PE, and a second tetramer labeled by a unique fluorochrome was used, as indicated. Simultaneous enrichment was performed using anti-PE microbeads. Within the global PE-enriched tetramer-positive population, each specificity was identified using the second tetramer label, and cell phenotype was analyzed using anti-CD45RA and anti-CD11a antibodies.



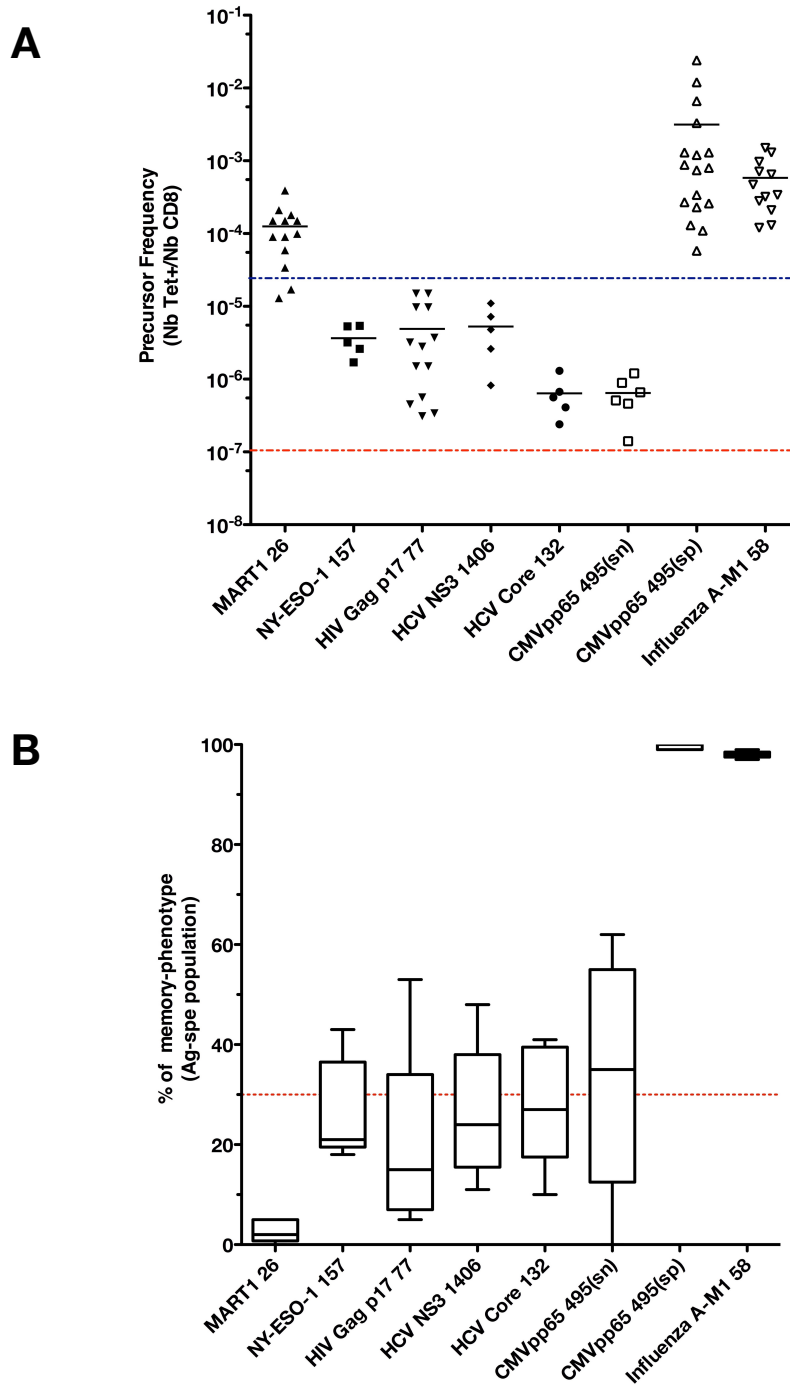


**Figure 29. Enumeration of epitope-specific CD8<sup>+</sup> T cells reveals conserved precursor frequency among HD.**

A. After performing TAME with MART1<sub>26-35</sub>, NY-ESO1<sub>157-165</sub>, HIV Gag p17<sub>77-85</sub>, HCV NS3<sub>1406-1415</sub>, HCV Core<sub>132-140</sub>, or CMVpp65<sub>495-503</sub> HLA-A0201 tetramers, CD8<sup>+</sup> T cells specific for each of these epitopes were enumerated. CMVpp65<sub>495-503</sub> in seropositive persons and Flu-M1<sub>58-66</sub> tetramer staining were used as positive controls. Each point represents a single healthy person. CMVpp65(sn) and CMVpp65(sp) indicate seronegative and seropositive donors, respectively, as confirmed by serologic testing. B. Proportions of memory-phenotype cells in each antigen-specific populations are represented.



**Chapter 3.**  
**Define the influence of chronic HCV  
infection on the preimmune repertoire.**

---



# I. INTRODUCTION

Functional impairments of CD8<sup>+</sup> T cells have been characterized in several persistent viral infections, including human immunodeficiency virus (HIV) and hepatitis C virus (HCV) infections in humans, simian immunodeficiency virus (SIV) infection in macaques, and lymphocytic choriomeningitis virus (LCMV) infection in mice (Ahmed and Rouse, 2006). In particular, it has been shown that chronic infection skews memory/effector CD8<sup>+</sup> T cells differentiation (Stelekati and Wherry, 2012), and drives virus-specific CD8<sup>+</sup> T cells towards an « exhausted » phenotypic state, as marked by high expression of the programmed cell death-1 (PD-1) molecule (Kim and Ahmed, 2010). Chronic infections have also been reported to impair immune responses to unrelated infectious microbes in mouse models (Richer et al., 2013; Stelekati and Wherry, 2012), as well as in humans infected with HCV (Park and Rehermann, 2014). This phenomenon correlates with a interferon (IFN) stimulated gene (ISG) transcriptional signature, suggesting an indirect effect of systemic type I IFN secondary to innate immune activation (Stelekati et al., 2014). Following from these observations, we hypothesized that chronic infection may alter the T cell preimmune repertoire, and by this way significantly impair our ability to mount appropriate responses after vaccination. Employing TAME, we evaluated this prediction in patients with chronic HCV viral infection of the liver. These findings will be relevant for the optimization of future vaccination strategies, where therapeutic vaccines are delivered to patients usually suffering from disease-related chronic inflammation.

We studied these questions on patients infected with the hepatitis C virus, for the following reasons:

- it is a model of chronic infection that is currently studied in our laboratory;
- it can be cured, allowing comparison of chronic and resolved patients. Outcome of infection is strongly determined by the host immune response, and in part explained by genetic polymorphisms (Klenerman and Thimme, 2012; Park and Rehermann, 2014; Thimme et al., 2002) ;
- T cells have a strong impact on the clinical outcome, with clearance of HCV during the acute phase of infection being dependent on efficient induction of sustained specific CD4<sup>+</sup> and CD8<sup>+</sup> T-cell responses (Park and Rehermann, 2014) ;
- therapeutic vaccination is actively tested in this pathology, and the ability to mount strong CD8<sup>+</sup> T cell responses is a biomarker of clinical efficacy. Alteration of the preimmune compartment could then lead to defective antigen-specific responses, and would need to be taken into account for improving responses to the vaccine;
- HCV patients typically have a poor response to unrelated vaccinations (Buxton and Kim,

2008; Moorman et al., 2011);

- HCV infection often associates with systemic manifestations – also referred as “extra-hepatic manifestations” (Ko et al., 2012; Lee et al., 2012);
- It is a clinical situation where it is ethically acceptable to propose leukapheresis collection from the patients for the benefit of research – permitting the access to high numbers of cells for the development of the project.

Schematically, the actual model for T-cell mediated clearance of the virus is represented in **Figure 30**. It requires (1) local antigen uptake and DC maturation and migration to draining lymph nodes; (2) immunodominant epitopes to be presented; (3) activated cells to traffic back to the liver and (4) lyse target cells into the tissue. However, this model does not address the question of the availability and quality of precursor T cells – that needs to be in place and fully functional to be efficiently activated.

We hypothesized that the study of naive T cells in patients chronically infected by HCV may provide new insights into dysregulated effector responses, and could account for both failure to control viral infection, and inflammation-related extrahepatic manifestations (Zampino et al., 2013). We also tested this hypothesis in the context of chronic infection with the hepatitis B virus (cHBV). Although HBV and HCV differ in their genomic structures, replication strategies and life cycles, both viruses are hepatotropic and can lead to development of liver cirrhosis and hepatocellular carcinoma (Rehermann, 2013; Schmidt et al., 2013). However, HBV classically induces less inflammation, and is less associated with extra-hepatic manifestations.

## **II. EVALUATION OF THE PREIMMUNE REPERTOIRE DURING CHRONIC HCV**

### **A. Gating strategy**

We mentioned in previous chapters the challenge of finding phenotypic markers for the accurate identification of naive/memory CD8<sup>+</sup> T cell compartments. An additional complexity concerns the applicability of those markers identified on healthy donors to pathological conditions. It is important to realize that the antibodies we use in immunomonitoring studies are not only markers, but do target molecules that are associated to one or multiple functions. Briefly, CD45RA is implicated in the TCR signal downregulation; CD62L (L-selectin), CD11a ( $\beta$ 2 integrin) and CCR7 (chemokine receptor) in the trafficking of T cells; CD28 and CD27 (member of the TNF superfamily) in the costimulation of T cells during priming (Kern et al., 2008). All of these molecules can eventually be modulated directly or indirectly by the pathology, and this can lead to major biases in the evaluation of naive/memory compartments. When starting the project, using 5 phenotypic markers for naive or memory T cells, we

confirmed that co-expression of high levels of CD45RA and CD27 identified naive T cells as efficiently in cHCV patients as in HD (**Figure 31**). Of note, although lower surface expression of CD27 after TCR stimulation have been reported on CD4<sup>+</sup> T cells in the context of chronic HCV (Yonkers et al., 2011), similar observations have not been reported for naive CD8<sup>+</sup> T cells, and we did not see evidence for this in our studies. However, we believe that this would not impact our ability to detect naive T cells with the CD45RA/CD27 gating strategy as we use a sufficiently large gate to include both CD27<sup>hi</sup> and CD27<sup>lo</sup> subpopulations.

## B. Bulk level

To test the hypothesis that chronic viral infection perturbs immune homeostasis, we evaluated the impact of cHCV and cHBV infections on the phenotype of circulating CD8<sup>+</sup> T cells. 28 cHCV, 35 patients achieving SVR after treatment for cHCV, and 18 cHBV patients were included in the study (**Table 6**).

	cHCV n=28	SVR n=35	cHBV n=18	p-value
Male, n (%)	16 (57)	20 (57)	14 (78)	0.33*
Age, years, median (IQR1-3)	53 (46-58)	44 (48-58)	46 (26-50)	0.06 <sup>§</sup>
HLA*A0201 positive, n (%)	11 (39)	18 (51)	18 (100)	0.0001*
Genotype 1/2/3/4, n (%)	18(64) / 7 (25) / 2 (7) / 1(4)	9 (24) / 17 (45) / 11 (29) / 1(2)	na	0.03*
Antibodies anti-HBe positive, n (%)	na	na	13 (72)	na
HBV DNA < 2000 IU/ml, n (%)	na	na	9 (50)	na
HCV RNA viral load, IU/ml, median (IQR1-3)	2 456 913 (1 561 888 - 5 614 850)	na	na	na
Cirrhosis, n (%)	6 (21)	11 (31)	3 (17)	0.71*
Treatment experienced, n (%)	18 (64)	34 (97)	5 (28)	<0.0001*
IgG anti-CMV positive, n (%)	12 (43)	11 (31)	16 (89)	0.002*
Leucocytes count, G/mm3, median (IQR1-3)	6.9 (5.1-8.8)	6.3 (5.2-7.6)	4.8 (3.8-6.5)	0.004 <sup>§</sup>
Lymphocytes count, G/mm3, median (IQR1-3)	2.2 (1.6-2.8)	2.0 (1.9-2.2)	na	0.14 <sup>§</sup>
Platelets count, G/mm3, median (IQR1-3)	212 (168-241)	232 (185-271)	212 (171-238)	0.50 <sup>§</sup>
Prothrombin time, %, median (IQR1-3)	99 (93-104)	98 (91-103)	92 (84-103)	0.23 <sup>§</sup>
ASAT level, IU/ml, median (IQR1-3)	42 (35-52)	25 (21-32)	34.5 (26.7-50.5)	0.0001 <sup>§</sup>
ALAT level, IU/ml, median (IQR1-3)	59 (42-75)	18 (15-28)	31.5 (27.7-49.5)	<0.0001 <sup>§</sup>
Total bilirubin level, µmol/l, median (IQR1-3)	8 (6-11)	8 (6-10)	6 (4-7)	0.03 <sup>§</sup>
Albumin level, g/l, median (IQR1-3)	41 (37-43)	43 (41-47)	45 (44-47)	<0.0001 <sup>§</sup>

ALAT: alanine aminotransferase; ASAT: aspartate aminotransferase; cHCV: chronic hepatitis C infection; CMV: cytomegalovirus; HBV: hepatitis B virus; HLA: human leucocytes antigen  
IQR1-3: interquartile range 1-3; na: not available; SVR: : sustained virological responders to anti-HCV treatment

\*: computed with Fisher exact Test

§: computed with Kruskal wallis Test (3 groups) or Mann Whitney Test (2 groups)

**Table 6. Description of the patients included in the Tetra cohort.**

### *Perturbed naive CD8<sup>+</sup> T cell repertoire during chronic infection*

Total lymphocyte numbers were within normal range for all tested patients (median 2.2+/-0.6G/l). Within the CD3<sup>+</sup> lymphocyte population, we observed similar percentages of circulating CD8<sup>+</sup> T cells (**Figure 32A, B**) and CD4<sup>+</sup> T cells (*data not shown*). However, absolute numbers of CD3<sup>+</sup> were significantly increased in our cohort of cHCV (KW  $p<0.0001$ ), translating into increased absolute numbers of CD8<sup>+</sup> and CD4<sup>+</sup> T cells in cHCV patients (KW  $p<0.0001$ ) (**Figure 32C**). We further

subsetted the CD8<sup>+</sup> T cells according to their surface expression of CD45RA and CD27. Decreased percentages of naive CD8<sup>+</sup> T cells have previously been reported in cHCV (Shen et al., 2010). Here, we confirmed these findings in age- and CMV- matched chronically infected patients, and extend this observation to HBV-infected individuals (KW  $p=0.0006$ , **Figure 32D, E**). Interestingly, due to the higher CD8<sup>+</sup> T cell numbers in cHCV patients, we found a the absolute numbers of naive CD8<sup>+</sup> and CD4<sup>+</sup> T cells to be in the normal range as compared to healthy donors (**Figure 32F**). We therefore interpreted the lower proportion of naive T cells to simply be a result of an expansion of the memory cell compartment.

To directly test this prediction, we isolated CD8<sup>+</sup> T cells and measured the frequency of signal joint TCR excision circles (sjTREC), by-products of TCR rearrangement, and previously validated as a measure of thymic production (Clave et al., 2009; Rehermann and Nascimbeni, 2005). Confirming previous studies, we found a significant decrease in sjTREC content of cHCV CD8<sup>+</sup> and CD4<sup>+</sup> T cells (MW  $p=0.009$ , **Figure 33A, B**). To address the bias due to differential naive T cell number, we isolated CD45RA<sup>+</sup>/CD27<sup>+</sup> naive CD8<sup>+</sup> T cells and assessed sjTREC frequencies. Surprisingly, we also observed within the naive compartment a significantly lower sjTREC content in cHCV patients as compared to HD (MW  $p=0.02$ , **Figure 33C**). To further characterize this phenotype, we assessed the V $\beta$  distribution within the naive repertoire of cHCV patients. cHCV patients showed a biased repertoire with increased representation of selected V $\beta$  families. A representative example of V $\beta$  usage plotted as % over the 24 tested families, and ordered by increasing size from one cHCV patient and one HD is shown (**Figure 33D**). To compare distributions, Lorenz curves and Gini coefficients were calculated for cHCV and HD ( $n=7$  per group), and compared by Mann Whitney (MW) test ( $p=0.03$ ) (**Figure 33E, F**). These data support an overall perturbed naive CD8<sup>+</sup> T cell repertoire in cHCV patients, with increased peripheral expansion of selected populations.

Altogether, these data support a perturbed naive CD8<sup>+</sup> T cell repertoire in cHCV patients that results from peripheral expansion of selected populations.

## C. Antigen-specific level

### *Mart1-specific CD8<sup>+</sup> T cell MP during chronic infection may be reversed by viral clearance*

To evaluate the impact of these perturbations on Ag-specific populations, we utilized TAME to evaluate Mart1-specific T cell populations. While similar absolute numbers of Mart1-specific CD8<sup>+</sup> T cells were observed in our respective study groups (**Figure 34A, B**), SVR and cHCV patients showed a more differentiated phenotype (**Figure 34C**), defined by fewer CD45RA<sup>+</sup>/CD27<sup>+</sup> (KW  $p<0.0001$ , **Figure 34D**) and increased proportions of memory-phenotype (MP) cells. Of note, when considering only naive-phenotype Mart1-specific cells, precursor frequencies were still comparable across the different study groups (data not shown).

We next compared cHCV patients to those who achieved viral clearance. Strikingly, sequential samples (available from a single patient who achieved cure) suggested that immune restoration of the naive compartment is possible (**Figure 34E**). Testing this observation in our cross-sectional cohort, we validated our findings and show a statistically significant increase in the frequency of naive-phenotype antigen-specific CD8<sup>+</sup> T cells that return as a function of time (KW  $p=0.04$ ; **Figure 34F**). In more detail in a single SVR patient, we clearly distinguish two distinct co-circulating Mart1-specific populations (**Figure 34G**). One expresses high levels of CD5, a negative regulator of TCR signaling, and is of naive-phenotype. The other express lower levels of CD5, and present an activated phenotype. Although we only have one time point available for analysis from this patient, based on the results presented before, we believe this is reflecting progressive reversion to a healthy phenotype after clearance of the HCV infection. Altogether, these results indicate that the MP cells within the preimmune repertoire of cHCV patients are a reflection of active infection, and unlikely to result from cross-reactivity or true memory T cell differentiation.

In preliminary experiments, we evaluated our capacity to enumerate sjTRECs and study repertoire of small quantities of sorted naive cells. Also sjTRECs and V $\beta$  usage were accurately estimated from as low as 10<sup>5</sup> naive CD8<sup>+</sup> T cells (**Figure 35A, B**), CDR3 profiles were no longer polyclonal when cell numbers were below 10<sup>6</sup>, reflecting biased analysis (**Figure 35C**). From leukapheresis, we were able to purify sufficient numbers of Mart1-specific naive- and memory- phenotype CD8<sup>+</sup> T cells from one HCV patient to compare immunoscope analysis on the V $\beta$  chain usage of these two populations (**Figure 35D**). In line with our data in bulk T cells, we observed a restricted repertoire of Mart1 naive T cells, with evidence of an expanded V $\beta$  clonotype in memory cells. These data argue in favor of MP cells being the expanded progeny of a perturbed naive T cell repertoire.

We next extended our observations to other antigen specificities by using two additional tetramers (hTERT<sub>1572-580</sub>, and human CMV pp65<sub>495-503</sub>) that are expected to detect inexperienced self- and virus-specific CD8<sup>+</sup> T cell populations in tumor-free, CMV-seronegative individuals. Here again, we found lower percentages of CD45RA<sup>+</sup>/CD27<sup>+</sup> cells and increased MP cells in the antigen-inexperienced populations of cHCV patients (representative plots are shown in **Figure 36A and B**; and combined results from 2-4 individuals per group in **Figure 36C**; 2-way Anova  $p=0.003$ ). In accordance with their MP, after 7h of peptide stimulation, the Mart1-, hTERT- and CMV- specific CD8<sup>+</sup> T cells present in cHCV patients were able to secrete higher amounts of IFN $\gamma$  (2-way Anova  $p=0.01$ ; **Figure 36D**). It is interesting to note that experienced populations – as specific for EBV BMLF1 in immunized patient, that typically contains a small proportion of naive-phenotype cells, are here again found more differentiated in cHCV patients (**Figure 36E**).

Altogether, our data highlights an overall perturbation of antigen-specific responses within the preimmune CD8<sup>+</sup> T cell compartment.

## D. Naive T cell homeostasis during chronic HCV

### *Decreased expression of CD5 on naive CD8<sup>+</sup> T cells associates with TCR hypersensitivity in cHCV patients*

To establish a mechanistic understanding of our findings we considered the key homeostatic factors for maintenance of naive CD8<sup>+</sup> T cells (Hazenbergh et al., 2000a; Ho and Hsue, 2009; Jenkins et al., 2010). We hypothesized that perturbations of the TCR activation threshold of naive T cells could explain increased differentiation of inexperienced populations. Among them, cell surface expression of CD5 expression has been shown to correlate with the threshold of activation in mice (Grossman and Paul, 2015). CD5 expression increases during thymic differentiation (**Figure 37A**) and is the highest on SP T cells. In periphery, it diminishes as a function of T cell differentiation (**Figure 37B**). Interestingly, inside bulk naive cells, Ag-specific populations display different levels of CD5 (Mart1 > HCV NS3<sub>1073</sub>) (**Figure 37C**). When evaluating CD5 expression under inflammatory conditions, we observed abnormal profiles in cHCV patients, with a single narrowed peak in both CD8<sup>+</sup> and CD4<sup>+</sup> T cells (**Figure 37D and E**). This was not observed in spondylarthritis patients (SPA), tested here as another inflammatory condition (**Figure 37D**). When MFI of CD5 was plotted for 3 different patients, we noticed that the main difference was a lower expression on naive CD8<sup>+</sup> T cells (**Figure 37E and F**). When studied across the entire cohort, we confirmed decreased abnormal CD5 levels that were highly significant for CD45RA<sup>+</sup>/CD27<sup>+</sup> naive CD8<sup>+</sup> T cells (KW  $p < 0.0001$ , **Figure 38A and B**) but not CD4<sup>+</sup> T cells - although there could be a trend also in this population (**Figure 38C**). Importantly, these phenotypic changes were also observed when focusing on Mart1-specific naive-phenotype cells (MW  $p = 0.04$ , **Figure 38D, E**).

Based on its role in regulating TCR signaling, we predicted that lower CD5 expression on naive T cells would result in their being hyperactivated upon stimulation. Indeed, under homeostatic conditions, CD5 negative regulation ensures TCR signaling cascade happens only in the case of high-affinity TCR/pMHC interactions (**Figure 39A**). If the CD5-induced brake is released, TCR signaling will happen for low affinity interactions (**Figure 39B**). This was tested functionally by evaluating TCR signaling in naive CD8<sup>+</sup> T cells, stimulating cells with low doses of plate-bound anti-CD3 and anti-CD28 Abs. In preliminary experiments, we (i) compared stimulation with soluble antibodies, beads-coated antibodies, and plate-bound antibodies, (ii) compared different doses of CD3 and CD28 antibodies, and (iii) evaluated induced kinetics of activation. Although not detailed here, these experiments lead us to define optimal conditions as (i) plate-bound stimulation (soluble is too weak, beads are too strong), (ii) 1ug/ml OKT3 + 0.5ug/ml CD28 (low as compared to the 10ug/ml usually

used in literature), and (iii)  $t=5$ mins to give the optimal p-ERK and p-P38 signals in both HD and cHCV. Indeed, while only weak induction of phosphorylated ERK (p-ERK) could be observed in HD during the first hour of stimulation, TCR stimulation induced a strong p-ERK and pP38 signals in both naive and memory cells from cHCV patients (**Figure 40A**). Differences were more apparent for naive and EMRA subsets, and concerned both percentages and MFI (**Figure 40B**). A typical profile for naive T cell activation is shown in **Figure 40C**. When studied on the entire cohort, seven of twelve cHCV patients tested showed significantly higher fold change at 5 minutes (MW  $p=0.02$ , **Figure 40D**).

Using the same stimulation protocol, we investigated the activation of the cells at later time points (24-120 hours). From FSC/SSC plots, we observed some differences, with presence of blastics cells at baseline – and further blasting after 24 and 48 hours of activation (**Figure 41A**). Blasting cells were mostly  $CD8^+$  T cells, and part of the  $CD25^+$  subset after stimulation (**Figure 41B**). When studying the kinetic of CD25 expression on naive  $CD8^+$  T cells over a 24h period of activation, we noticed significantly higher levels at 24 hours for most of the cHCV patients (**Figure 41C**). Same effect was not apparent in the context of cHBV (**Figure 41D**). When studied on the entire cohort, we found significantly higher levels of CD25 after TCR stimulation in cHCV patients (KW  $p=0.006$ , **Figure 41E**).

Using similar experimental designs, we evaluated if the blastic cells were in the process of dying (**Figure 42A**). Those cells were both  $CD4^+$  and  $CD8^+$  T cells, but mostly of the  $CD45RA^+/CD27^+$  phenotype (blue), and were expressing high levels of the activation marker CD25, as well as high levels of CD95 and proapoptotic Bcl2. This evaluation was done at H10 in order to precede activation-induced cell death (AICD) events. Activated caspase 3 was detectable at 24 hours, and significantly increased in naive T cell subsets from cHCV patients (**Figure 42B**), as well as total numbers of cells at 48 hours (**Figure 42C**). All of these findings highlighted an increased sensitivity to cell death after TCR activation in the context of cHCV.

### ***CD5 blockade in HD recapitulates the hypersensitivity phenotype***

In preliminary experiments, we observed that activation and AICD events at 24 hours were increased when T cells were receiving stronger TCR signals (**Figure 43A**). To establish a mechanistic link between CD5 expression and hyperactivation of naive T cells, we evaluated the effect of blocking CD5 signaling. HD PBMCs were exposed to blocking anti-CD5 Abs ( $\alpha$ CD5), followed by TCR stimulation. We observed increased levels of p-ERK after 5 minutes of TCR stimulation when HD cells were pre-incubated with  $\alpha$ CD5 (representative donor shown in **Figure 43B**; MW  $p=0.04$ , **Figure 43C**). Similarly, CD25 expression at 24 hours was higher when  $\alpha$ CD5 was used prior to TCR stimulation (representative donor shown in **Figure 43D**; MW  $p=0.04$ , **Figure 43E**), as well as the percentage of dying naive CD8 T cells as assessed by active caspase 3 staining (2-way Anova  $p=0.04$ ).

(**Figure 43F**). These data support a model where low expression of CD5 on naive T cells in cHCV patients results in dysregulation of the homeostatic TCR threshold. Low-affinity contacts may in turn result in T cell differentiation, providing an explaining for the increased frequency of memory-phenotype Ag-inexperienced cells.

As hypersensitivity to TCR activation can be induced by cytokine microenvironment (especially mediated by high levels of IL-7 and IL-15), we investigated the pattern of cytokine expression evaluated in a comparable cohort of HD, SVR and cHCV patients (**Figure 44**). We found no significant differences in IL-7 levels in the plasma of patients, but a trend for more IL-15. Notable differences were higher levels of IP10 and TNF $\alpha$ , and lower levels of Eotaxin and MCP1.

Finally, we used *in vitro* priming assays to evaluate the impact of naive dysregulation on the ability of those cells to be primed, recruited and expanded in a given Ag-specific response. We evaluated if we could grow Mart1-specific cells from either naïve or memory CD8<sup>+</sup> T cell subsets. We separated both using magnetic-enrichment kits targeting CD45RO cells. An example of the naive/memory phenotype of cells obtained in the enriched (CD45RO<sup>+</sup>) and in the depleted (CD45RO<sup>-</sup>) fractions of one HD and one cHCV is provided in **Figure 45A**. We primed enriched T cells with autologous mature DCs pulsed with Mart1 peptide. A cocktail of cytokines (TNF $\alpha$ , IL-1 $\beta$ , PGE2, and IL-7) was added at the time of the priming. Cultures were harvested at Day 10, and stained with Mart1- and unrelated PGT-tetramers. From the HD, after tetramer enrichment, we observed an expansion of Mart1- but not PGT-specific cells predominantly from the RO<sup>-</sup> fraction. In comparison, we did not detect any Mart1-specific T cells expanded from the cHCV patient (**Figure 45B**). This is to be interpreted in the context of lower numbers of total cells recovered from the cHCV patients. In a second independent assay, we tested on 3 cHCV patients two doses of peptides (low 10<sup>-8</sup>, and high 10<sup>-6</sup>), and two concomitant staining with either conventional or CD8<sup>null</sup> Mart1-specific tetramers (**Figure 45C**). The latter is a modified construct that was shared by P.Romero and M.Bonneville, and stains only high-affinity CD8<sup>+</sup> T cells (Neveu, 2006). With the low dose of peptide, we could detect a population of expanded Mart1 cells at Day 7 that further increased at Day 11. About half of the Day 7 population also stained with the CD8<sup>null</sup> tetramer – thus representing high affinity cells. As compared to Day 7, Day 11 cells showed fewer CD25 and CD5 expression, indicating their evolution towards a resting MP (**Figure 45D**). With the high dose of peptide, we detected a more abundant Mart1-specific population at Day 7, but similar proportions of high affinity cells. Interestingly, those cells were not detectable at Day 11, in the context of notable cell death in the well. Those datas were similar in the 3 tested cHCV individuals. However, for unclear reasons, expansions were highly variable from the HD, and our difficulties in getting robust controls lead us to consider alternative protocols that will be detailed in Prospectives.

### III. DISCUSSION

Our study offers the first evidence for chronic viral infection as a cause of CD8<sup>+</sup> T cell preimmune repertoire dysregulation. Specifically, we demonstrated that naive CD8<sup>+</sup> T cells are dysregulated in the context of cHCV, marked by (i) decreased sjTRECs levels, (ii) a restricted V $\beta$  repertoire, and (iii) a lower threshold for TCR engagement that correlates with lower surface expression of CD5.

Prior examples suggestive of preimmune repertoire perturbations have been documented in humans. Increased threshold for TCR activation in naive CD4<sup>+</sup> T cells in elderly persons has been proposed as participating in the diminished response to vaccination that occurs with increasing age (Li et al., 2012). Conversely, a decreased threshold for TCR activation, secondary to sustained cytokine production, leads to diverse autoimmune manifestations in rheumatoid arthritis patients (Deshpande et al., 2013; Singh et al., 2009). With respect to chronic infection, functional defects in the naive T cell compartment have also been documented in HIV-infected individuals, with non-cognate activation of T cells correlating with disease progression (Favre et al., 2011). These studies have all addressed global dysregulation of the naive T cell repertoire.

Due to their low frequency, little is known about the perturbations of antigen-specific populations in the context of chronic infection or inflammation. Due to the possibility of studying viremic vs. cured patients, we chose to investigate this question in cHCV patients. Analyzing rare (*i.e.*, frequency =  $10^{-7}$  -  $10^{-5}$ ) Ag-specific inexperienced CD8<sup>+</sup> T cells populations, we demonstrate increased proportions of memory-phenotype cells in cHCV patients. This is in line with previous data showing that 34% of cHCV patients without detectable tumor secrete IFN $\gamma$  when their harvested T cells are stimulated *in vitro* with tumor-specific peptides, as compared to 0% in comparable healthy donors (Mizukoshi et al., 2011). Additionally, we showed the naive T cells to be hyperreactive to TCR signaling. Despite these altered phenotypes, the absolute number of Ag-specific cells was comparable to healthy donors. This may be explained by the higher sensitivity to cell death, as indicated by *ex vivo* functional studies. Of note, cHCV patients are not thought to experience altered thymic output. As such, our findings provide the direct evidence that MP antigen-specific T cells can arise in non-lymphopenic humans.

It has been suggested that a high degree of cross-reactivity with environmental antigens is the trigger for differentiation and MP conversion (Sprent and Surh, 2011). This finding has been reported for human viral pMHC restricted CD4<sup>+</sup> T cells, in unexposed donors. While cross-reactivity is a possible explanation for our findings, we demonstrate in cured patients that the Ag-specific inexperienced cells are restored to a naive phenotype. This result favors an alternative model, where homeostatic proliferation accounts for the perturbed naive T cell repertoire in cHCV patients. Indeed, (i) several unrelated self- and non-self- populations are concerned – which goes against the hypothesis of cross-reactivity (Welsh et al., 2010), and (ii) Mart1-specific MP T cells are being clonally

expanded. These findings parallel rapid reversibility of a healthy preimmune repertoire after transient anti-CD52 (also known by alemtuzumab)-induced lymphopenia in multiple sclerosis patients (Jones et al., 2013). Consistent with our findings, it has been indeed shown a narrowing of the V $\beta$  repertoire and a dilution of sjTREC after this treatment, with a complete restoration of normal levels two years after therapy.

Infection and inflammation are known to lower the threshold of TCR signaling in memory T cell, making them more sensitive to activation (Richer et al., 2013). This effect is mediated by inflammatory cytokines (Raué et al., 2013). Our results extend this concept to naive T cells and introduce CD5 downregulation as a mechanism for hyperreactivity. CD5 tunes the TCR signaling threshold in peripheral T cells, with naive cells expressing higher levels than central memory or effector T cells (Tabbekh et al., 2013). In mice, Hawiger *et al.* demonstrated that anti-CD5 blocking antibodies or use of CD5<sup>-/-</sup> transgenic MOG-specific T cells resulted in higher sensitivity to experimental autoimmune encephalitis (Hawiger et al., 2004). In B cells, CD5 has also been shown to regulate activation and lower expression correlates with higher sensitivity to activation induced cell death (Tabbekh et al., 2013). In line with these findings, we demonstrate an increased sensitivity of CD5<sup>lo</sup> naive CD8<sup>+</sup> T cells to TCR ligation in cHCV patients. We further provide direct evidence that this hypersensitivity phenotype can be reproduced in HD by blocking CD5. While not evaluated in our patient cohort, we suggest that elevated levels of inflammatory cytokines may be responsible for the altered CD5 expression on naive cells. Interestingly HCV and HBV induce different cytokine and chemokine signatures (Park and Rehermann, 2014), possibly explaining the differential results in these two forms of viral hepatitis. However, one caveat is that our cHBV cohort was heterogeneous in viral loads and current clinical status (immune tolerance, immune clearance or inactive carriage phase). Further evaluation will thus be needed to confirm these initial observations in HBV chronic infection.

In mouse models, self-specific populations express higher levels of CD5 than foreign-specific ones, as a mechanism to maintain peripheral tolerance (Grossman and Paul, 2015). It would be interesting to confirm these findings in humans by measuring CD5 levels on different self- and non-self- Ag-specific naive populations. As cHCV globally decreases the level of CD5 on naive cells, our results suggest a model where it will have different impacts based on the starting level of CD5 (**Figure 46A**):

- self-specific populations, which have the highest initial levels, will come into the range of being « easily authorized to proliferate » - which explain why they are found unspecifically expanded and which may be linked to some clinical features such as extrahepatic systemic manifestations and lymphoproliferation during the course of cHCV infection;
- non-self-specific populations, which have the lowest initial levels, will come into the range of being deleted after TCR stimulation – which could explain (i) that HCV-specific populations are detected at low frequencies in HCV

patients, and (ii) that cHCV patients have poor responses to some vaccinations involving cellular immunity.

Additionally, at the level of a given naive antigenic specificity, a range of TCR avidity – and thus a range of CD5 expression, also exists and has recently been linked to some features of T cell activation *in vitro* (Fulton et al., 2014). With the assumption that the CD5 decreased levels observed in the context of HCV globally are homogeneously affecting cells in Ag-specific populations, this would favor the expansion of cells with the lowest affinity (highest CD5), and deletion of the highest ones (lowest CD5). This model would be in adequation with previous finding that the selection of high-avidity CD8 T Cells correlates with control of hepatitis C virus infection (Neveu et al., 2008).

Combination of low levels of CD5 and increased proportions of MP on both self and non-self specific populations may synergize, resulting in a highly reactive CD8<sup>+</sup> T cell compartment. As such, our data fits with the concept that autoimmunity may be triggered by infection (Jones et al., 2013; Welsh et al., 2010). This is indeed the case for cHCV patients, where disease pathogenesis includes systemic manifestations – many of which are believed to be immune-mediated (Lee et al., 2012). Further investigation in longitudinal cohorts is thus warranted, with the aim to establish a dysregulated preimmune repertoire as the cause of bystander manifestations of disease. Moreover, our data highlight the value of early cHCV treatment, as immune restoration may prevent long-term sequella.

In summary, our study indicates that naive CD8<sup>+</sup> T cells are dysregulated during cHCV, with marked perturbations of the preimmune repertoire. Specifically, low levels of CD5 at the surface of naive T cells, and high proportions of memory-phenotype cells represent two mechanisms by which antigen-inexperienced CD8<sup>+</sup> T cells are likely to be susceptible to stimulation and cell death. These findings should be considered when designing future immunotherapeutic strategies.

## IV. PROSPECTIVES

In the next months, we plan to better investigate the impact of our observations on the behavior of CD8<sup>+</sup> T cell responses after T cell priming. For this purpose, we plan to compare the outcome of two different *in vitro* assays.

First, we will generate T cell libraries using the protocol developed by the group of Frederica Sallusto (Geiger et al., 2009). In brief, from three cHCV and three HD tumor-free and CMV-seronegative patients, we will sort bulk naive CD8<sup>+</sup> T cells (2 000 cells per well). The cultures will then be stimulated by PHA in the presence of irradiated allogeneic feeder cells and Il-2, and expanded for 2 weeks. This will lead to a 1 000 - 5 000 – fold expansion. Aliquots from each culture will then be tested for their capacity to proliferate in response to Mart1, hTERT, gp100, HIV and CMV antigens

processed and presented by autologous monocyte-derived DCs. By comparing precursor frequency calculated at Day 0 by TAME to its estimation after library generation, we believe that this will inform us on the sensitivity of the preimmune T cells to cytokine-related expansion.

Second, we will evaluate Ag-specific T cell priming by cognate peptide. We will use an optimized 10-days protocol called ACE-CD8 (Greenberg and Ifl, 2014), that was designed to allow conclusions about the initial priming conditions. In brief, monocyte-derived DCs are matured with LPS/IFN $\gamma$  (to favor IL-12 production), loaded with the peptide, and cocultured with CD57/CD45RO depleted CD8<sup>+</sup> T cells. For the initial stage of the priming, IL-21 is the only cytokine to be added to the culture. All other cytokines required are produced by DCs or the T cells themselves. In the absence of IL-7 and IL-15, a proliferative advantage is thus provided to cells receiving a TCR stimulus, whereas non-specific T cells may be “starved” during this period. Starting at Day 3, cultures are supplemented by low amounts of IL-7 and IL-15 to favor expansion of the primed cells. No IL-2 is needed before 15 days of culture, and rather pushes the cells towards terminal differentiation. We will use this protocol on the same three cHCV and three HD patients as above, and follow both Ag-specific and non-specific T cell expansion and differentiation. This will permit to evaluate the ability of the preimmune cells to be primed, expanded, recruited into the response, and to survive after T cell activation.

Using these two assays on the same patients, plus our knowledge on their preimmune repertoire at baseline will permit to have a better idea of the consequences of naive dysregulation in cytokine and Ag-driven expansion.

As mid-term objectives, we propose to:

- Better characterize the tuning of human lymphocytes by CD5. Indeed, there are still many open questions. Is there a common pattern of CD5 expression among (i) different self- and non-self Ag-specific populations, and (ii) different donors? Is there a specific signature of CD5<sup>hi</sup> and CD5<sup>lo</sup> antigen-specific populations at baseline when engaged into an immune response (calcium flux, CD62L downregulation, ERK and p-38 phosphorylation, effector/memory differentiation, expansion, cell death)? Are CD5<sup>lo</sup> antigen-specific populations more prompt to divide towards MP cells as a result of aspecific peripheral pMHC/TCR interactions? For addressing these questions, we will enrich inexperienced Ag-specific populations from a cohort of 20 healthy donors, evaluate CD5 expression, sort CD5<sup>hi</sup> and CD5<sup>lo</sup> Mart1-specific populations, and evaluate their behavior using short, mid and long term functional assays as described previously. Cell lines derived from these assays will be later used for silencing experiments where we could specifically modulate CD5 expression and test its impact on activation and cell death following TCR stimulation;

- Test the reversibility of naive T cells alterations in cHCV patients *in vitro* after incubation with soluble human CD95-Fc. Recent papers indicate the rescue of T cells from TCR-mediated apoptosis with soluble CD95-Fc molecules both *in-vitro* and *in-vivo*, resulting in dramatic reduction of tumor growth in CD5-deficient mice (Tabbekh et al., 2011) ;
- Evaluate same questions in the CD4<sup>+</sup> T cell preimmune repertoire.

Finally, as long-term perspectives, we believe that our findings should be evaluated in the context of three aspects of cHCV pathogenesis:

- First, we believe that naive T cell hyperactivation is a systemic effect of cHCV, and as such could explain some of the extrahepatic manifestations observed in this disease;
- Second, patients with chronic HCV infection are at risk of developing hepatocellular carcinoma, mainly as an effect of tissue reorganization and inflammation. Our findings of MP cells in self- specific populations is intriguing, as those cells (*i.e.* gp100- or hTERT- specific T cells) are targeting antigens that will potentially later be over-expressed on the tumor site. One possible consequence is that those MP cells – being more reactive - will be an advantage for fighting the tumor when it will arise. Alternatively, those cells that will have experienced multiple rounds of aspecific proliferation for twenty years will possibly be exhausted before any story of cancer – and favor “easy” (*i.e.* unpressurized) tumor growth in those patients;
- Finally, cHCV patients typically have poor responses to adult vaccinations such as those against HAV and HBV (Buxton and Kim, 2008). We believe that this could be related to a failure of inducing adequate CD8<sup>+</sup> T cell responses in those patients because of an altered preimmune T cell repertoire targeting vaccine epitopes.

These three points will have to be addressed in the context of prospective cohorts.



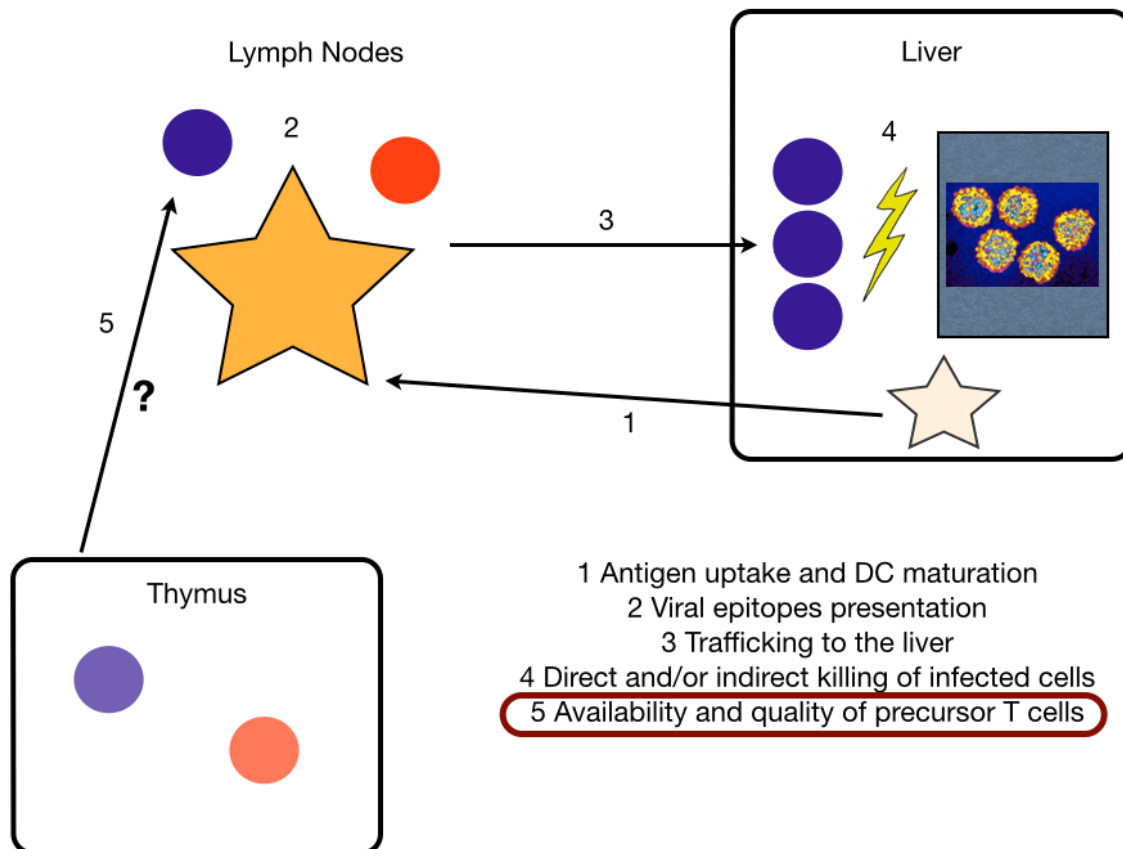


**Figure 30. Schematic representation of critical steps in immune-mediated clearance of HCV infection.**

1. Viral antigens uptake by local DCs leads to their maturation while migrating to the draining lymph node. 2. Presentation of viral epitopes to corresponding T cell precursors. 3. Trafficking of activated T cells back to the infected tissue. 4. Direct and/or indirect killing of infected cells by T cells. All of these four step are well recognized as critical for successful clearance of the infection. We propose to explore the step 5, about the availability and quality of precursor T cells, that we think are also critical points.



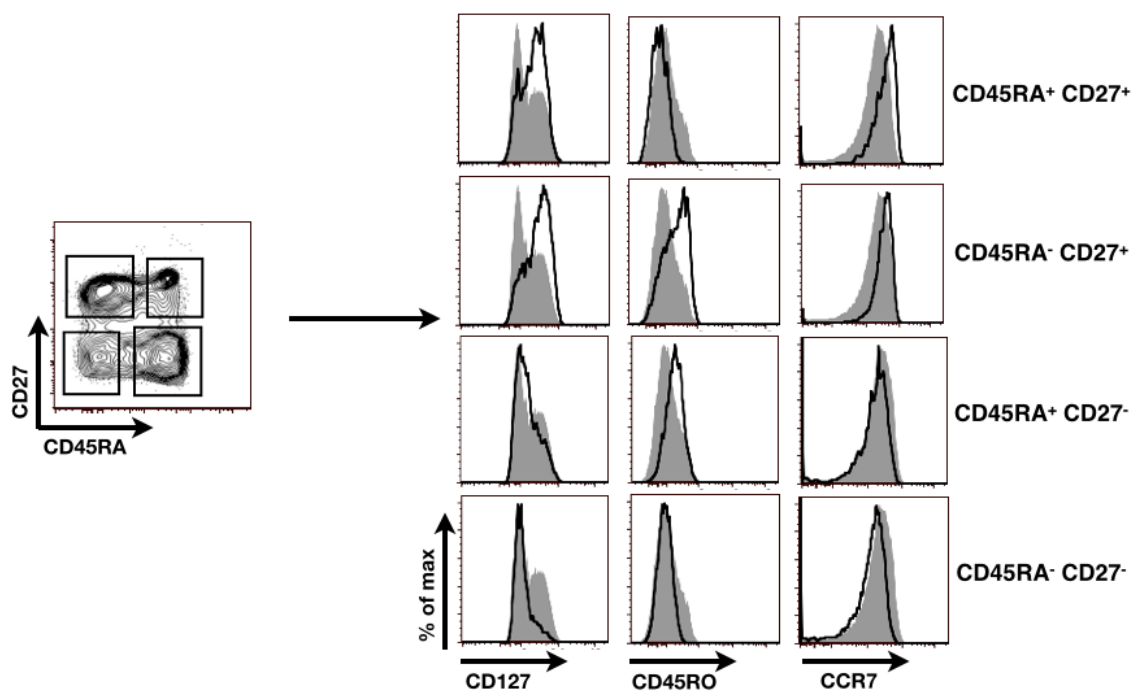


**Figure 31. Validation of CD45RA/CD27 gating strategy for identifying naive CD8<sup>+</sup> T cells in cHCV.**

Example of CD45RA/CD27 gating strategy in one cHCV patient. CD8<sup>+</sup> naive T cells are identified as CD45RA<sup>+</sup>CD27<sup>+</sup>. Pattern of CD127, CD45RO and CCR7 expression of each identified population is displayed on histogram overlays (black line represents the subpopulation of interest; grey ones the total CD8<sup>+</sup> population).



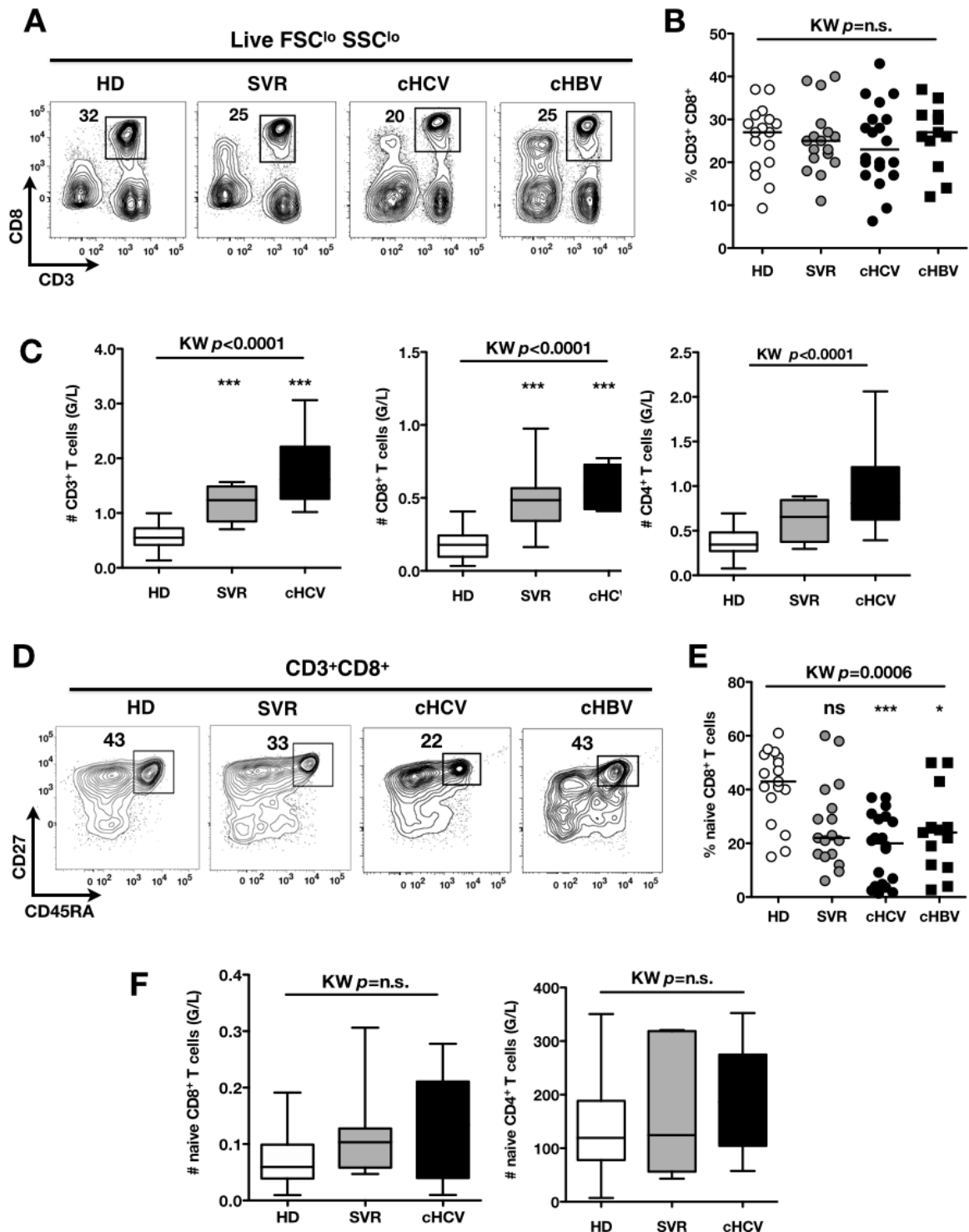


**Figure 32. Perturbed naive CD8<sup>+</sup> T cell repertoire during chronic infection.**

A. Representative examples of CD3<sup>+</sup>CD8<sup>+</sup> compartment in Healthy Donor (HD), Sustained Virologic Responder (SVR), chronic HCV (cHCV), and chronic HBV (cHBV) patients. FACS plots are gated into Live FSC<sup>lo</sup>SSC<sup>lo</sup> Peripheral Blood Mononuclear Cells (PBMCs). B. Combined data from the patient cohort is shown. C. Absolute numbers (G/L) of CD3<sup>+</sup> (left), CD8<sup>+</sup> (middle), and CD4<sup>+</sup> (right) T cells in the cHCV, SVR, and HD patients subsets. D. Representative examples of CD45RA<sup>+</sup>CD27<sup>+</sup> naive compartments in HD, SVR, cHCV, and cHBV patients. E. Percentages of naive CD8<sup>+</sup> T cells in the four donor subsets. F. Absolute numbers (G/L) of naive CD8<sup>+</sup> and CD4<sup>+</sup> T cells in the cHCV, SVR, and HD patients subsets. ns (not significant,  $p>0.05$ ), \* ( $p\leq 0.05$ ), \*\* ( $p\leq 0.01$ ), and \*\*\* ( $p\leq 0.001$ ) refer to Dunn's multiple comparison test of each subset toward healthy donors.



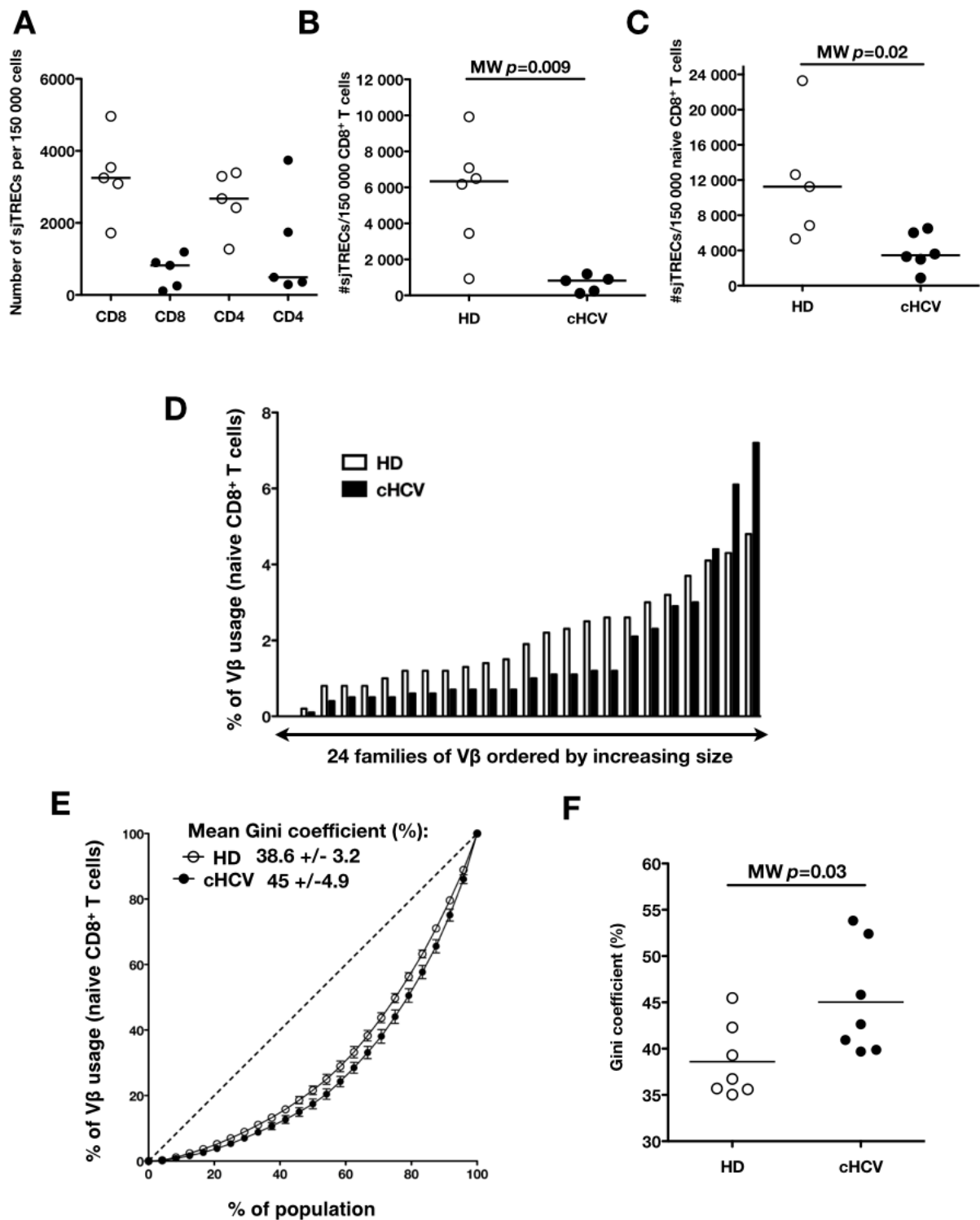


**Figure 33. Increased peripheral expansion of selected naive populations.**

A. Normalized numbers of signal-joint T cell receptor excision circle (sjTREC) per 150 000 CD3<sup>+</sup>CD8<sup>+</sup> cells in HD and cHCV samples. \*,  $p \leq 0.05$ . B. Normalized numbers of sjTREC per 150 000 naive CD8<sup>+</sup> in HD and cHCV samples. \*,  $p \leq 0.05$ . C. Representative example of the distribution of 24 FACS-screened V $\beta$  families in naive CD8<sup>+</sup> T cells from one cHCV and one HD sample. Families are ordered by increasing size in both individuals. D. Lorenz curves representing the mean distribution of % of usage of 24 FACS-screened V $\beta$  families from 7 cHCV and 7 HD patients. Mean corresponding Gini coefficients and standard deviations are indicated. E/ Individual Gini coefficients of all tested samples are represented for cHCV and HD subgroups.



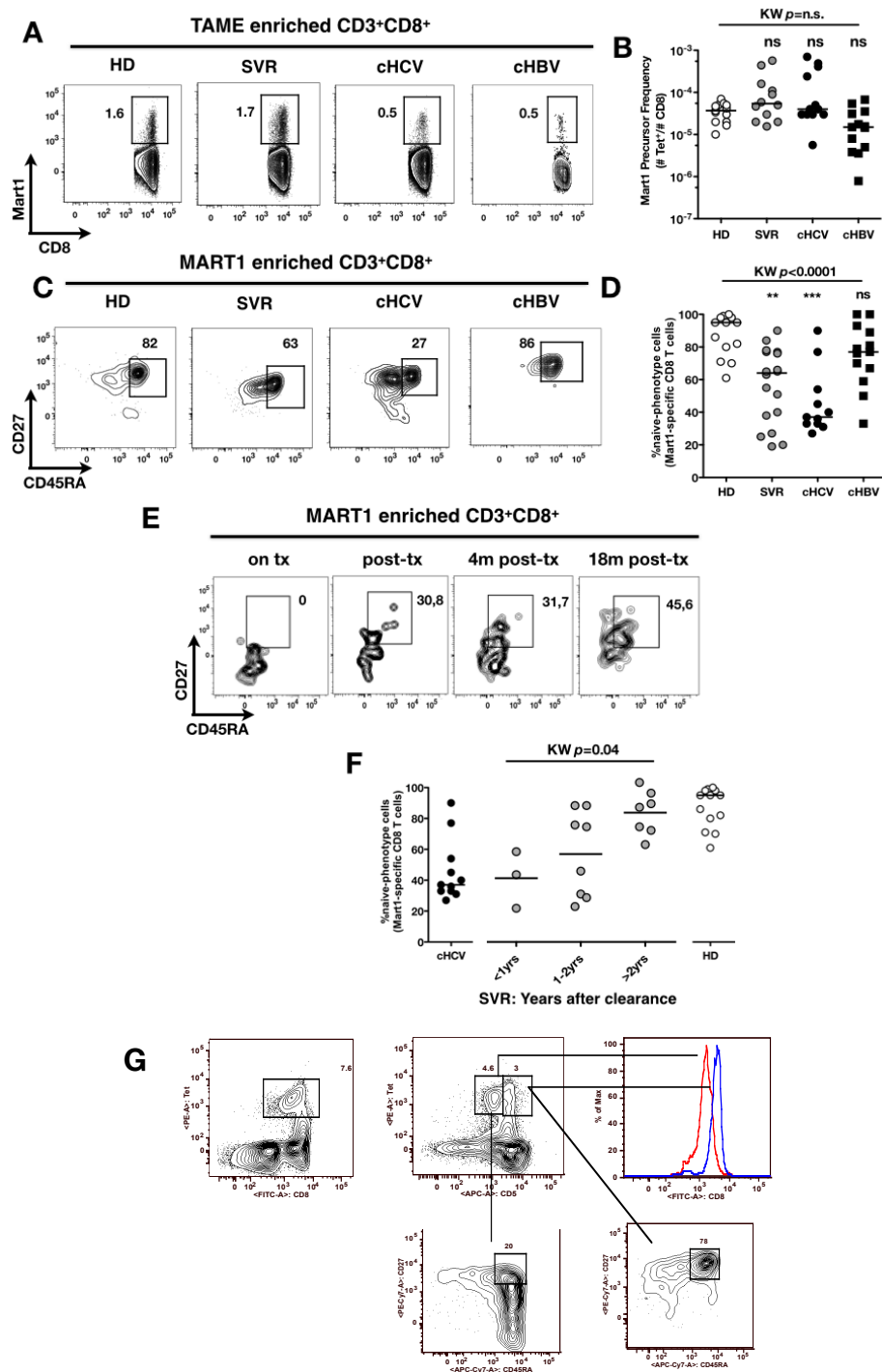


**Figure 34. Mart1-specific CD8<sup>+</sup> T cell MP during chronic infection may be reversed by viral clearance.**

A. Representative examples of Mart1-specific populations in HD, SVR, cHCV, and cHBV patients..  
 B. Mart1 precursor frequency in the four donor subsets. ns, \*\*\*, \*\* and \* refer to Dunn's multiple comparison test of each subset toward healthy donors. C. Representative examples of the CD45RA/CD27 phenotype of Mart1-specific populations in patients subsets as in A. FACS plots are gated on TAME-enriched Mart1-specific populations. D. Percentages of naive-phenotype cells in Mart1-specific populations in the four donor subsets. ns (not significant,  $p > 0.05$ ), \* ( $p \leq 0.05$ ), \*\* ( $p \leq 0.01$ ), and \*\*\* ( $p \leq 0.001$ ) refer to Dunn's multiple comparison test of each subset toward healthy donors. E. Follow up of one patient successfully treated for cHCV. On treatment (on tx), immediately post-treatment (post-tx), 4 months (m) and 18m post-tx data are shown. At each time point, an overlay of TAME-enriched Mart1-specific T cells (black) projected onto total CD8<sup>+</sup> T cells from the same patient (grey), and the CD45RA/CD27 phenotype of the above antigen-specific population are displayed. F. Percentages of naive-phenotype cells in the Mart1-specific populations vs. time elapsed since clearance of the virus in SVR patients (time-stratified, in years). G. Detection of two Mart1-specific populations in one single SVR patient.



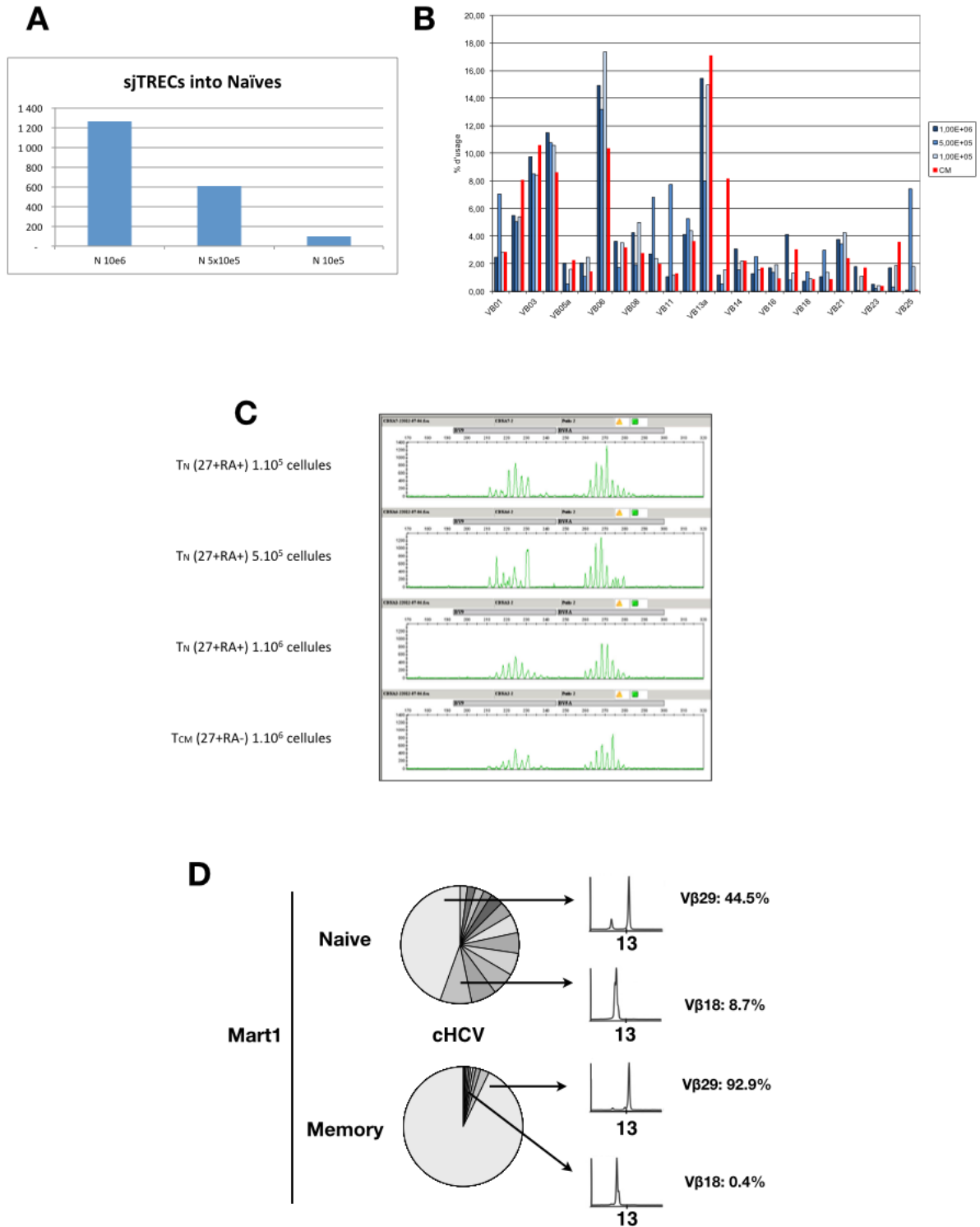


**Figure 35. Sensitivity of sjTRECs and Vβ repertoire assays.**

sjTRECs detection (A), Vβ repertoire (B) and CDR3 profiles (C) in titrated amounts of naïve T cells. D. Immunoscope of Mart1 naïve and memory phenotype cells.



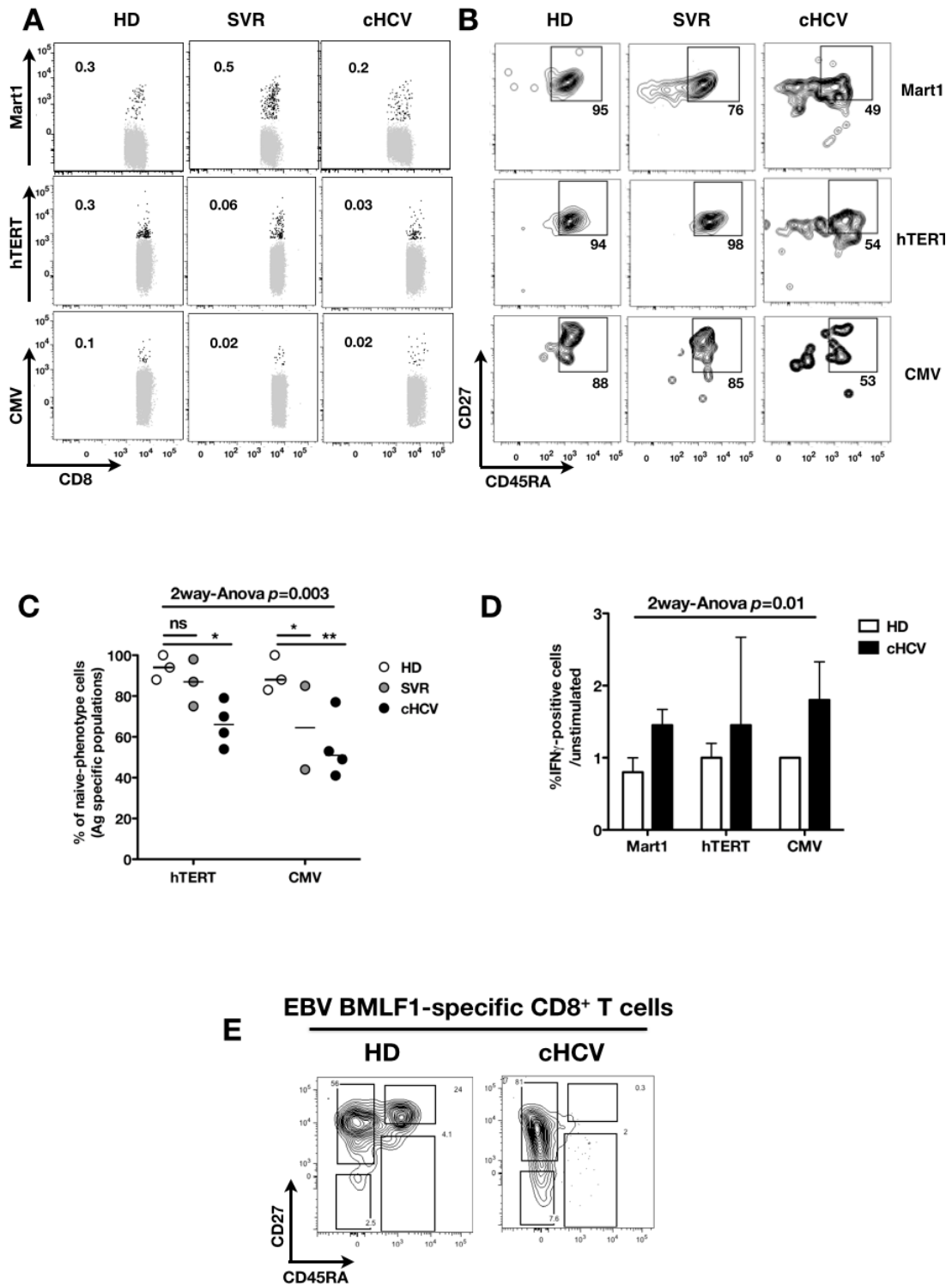


**Figure 36. MP cells are a common feature of self and non-self antigen-inexperienced populations.**

A. Representative examples of Mart1-, hTERT-, and CMV- specific populations are shown for HD, SVR, and cHCV patients. Enriched tetramer-specific populations are overlaid on total live FSC<sup>lo</sup>SSC<sup>lo</sup> CD3<sup>+</sup>CD8<sup>+</sup> PBMCs. B. Representative examples of CD45RA/CD27 phenotype of Mart1-, hTERT-, and CMV- specific populations in HD, SVR, and cHCV patients. FACS plots are gated into TAME-enriched antigen-specific populations. C. Cumulative representation of percentages of naive-phenotype cells into hTERT- and CMV- specific populations in the three pre-cited subsets of donors. D. Ratio of percentages of cells with IFN $\gamma$ -positive staining after Mart1-, hTERT-, and CMV- *in vitro* restimulation over unstimulated condition. E. Naive/memory phenotype of EBV BMLF1- specific CD8<sup>+</sup> T cells.



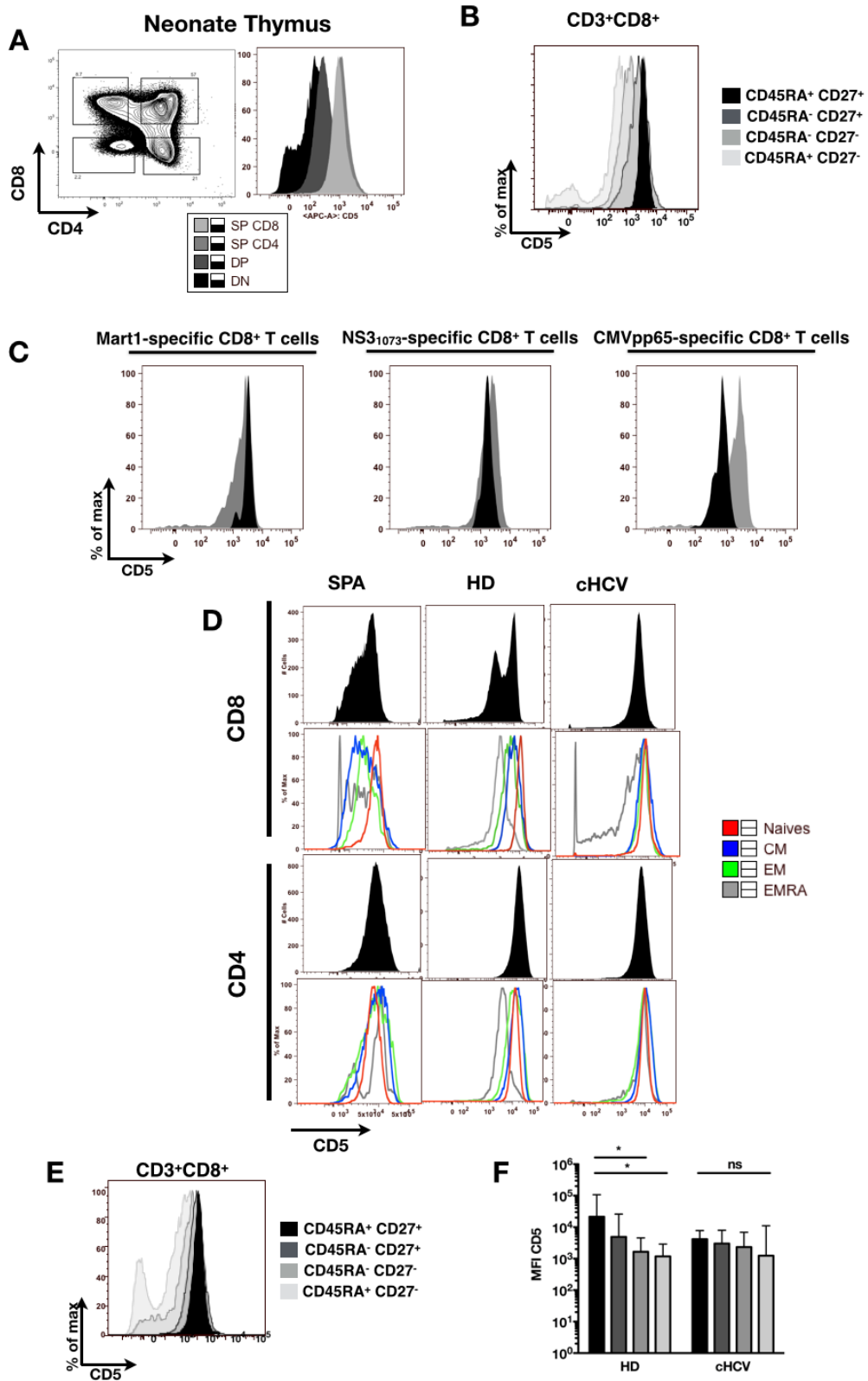


**Figure 37. CD5 expression on T cells during homeostatic or pathologic conditions.**

A. CD5 gradually increases during T cell development. B. Representative overlay of histograms of CD5 in T cell differentiation subsets (HD). C. Example of CD5 levels of Mart1-, NS3<sub>1073</sub>- and CMVpp65- specific T cell populations (black) as compared to those of bulk CD8<sup>+</sup> T cells (grey) in one CMV-seropositive healthy donor. D. CD5 profiles in bulk CD8 and CD4 populations (black histograms), and related subsets of differentiation (colored histograms) in spondylarthritis (SPA), and cHCV patients, or healthy donors (HD). E. Representative histograms of CD5 levels in CD8<sup>+</sup> T cells subsets in HD and cHCV patients. F. MFI of CD5 on CD8<sup>+</sup> T cell differentiation subsets of 3 HD and 3 cHCV donors (color code as in E).



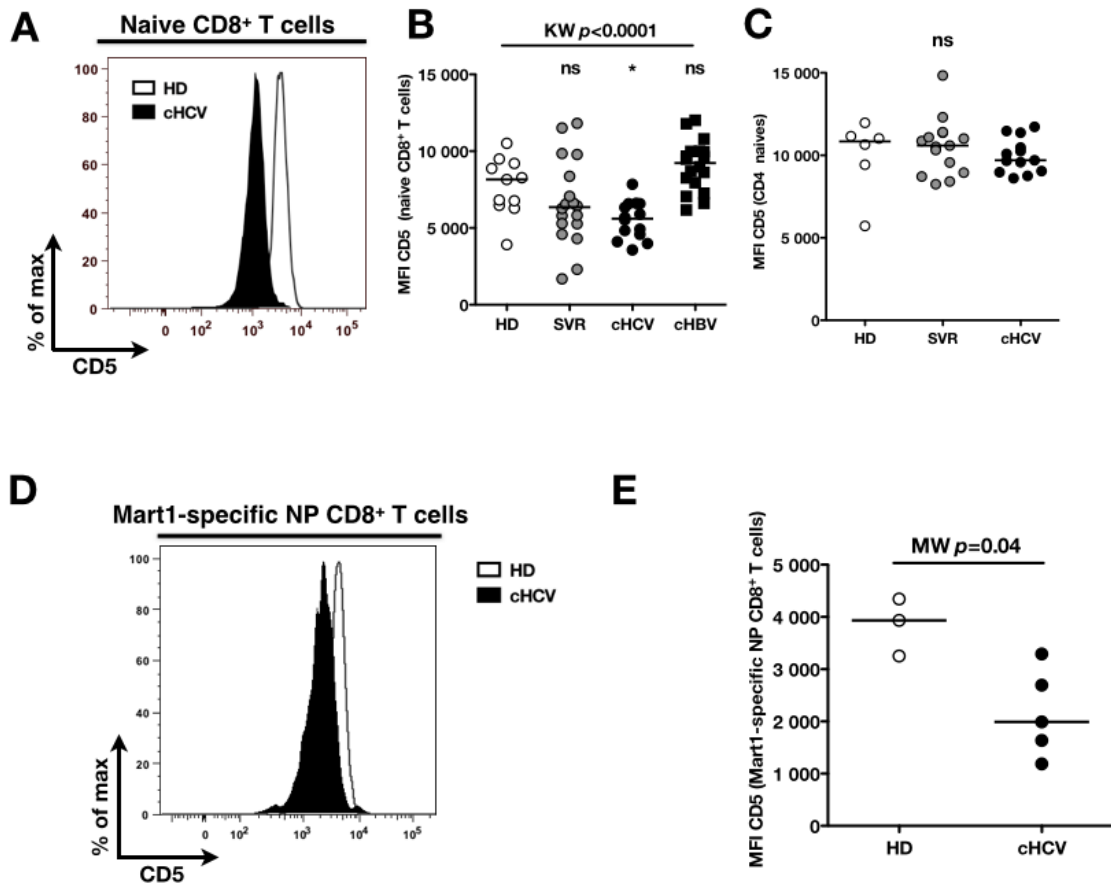


**Figure 38. Decreased cell surface expression of CD5 on naive CD8<sup>+</sup> T cells from cHCV patients.**

A. Representative histograms of CD5 levels on naive CD8<sup>+</sup> T cells from one HD and one cHCV patient. MFI of CD5 on the surface of naive CD8<sup>+</sup> T cells (B) or CD4<sup>+</sup> T cells (C) from HD, SVR, cHCV, and cHBV patients. ns, \*\*\*, \*\* and \* refer to Dunn's multiple comparison test of each subset toward healthy donors. D. Representative histograms of CD5 levels on naive-phenotype Mart1-specific CD8<sup>+</sup> T cells from one HD and one cHCV patient. E. MFI of CD5 on the surface of naive-phenotype Mart1-specific CD8<sup>+</sup> T cells from HD, SVR, cHCV, and cHBV patients. ns, \*\*\*, \*\* and \* refer to Dunn's multiple comparison test of each subset toward healthy donors.



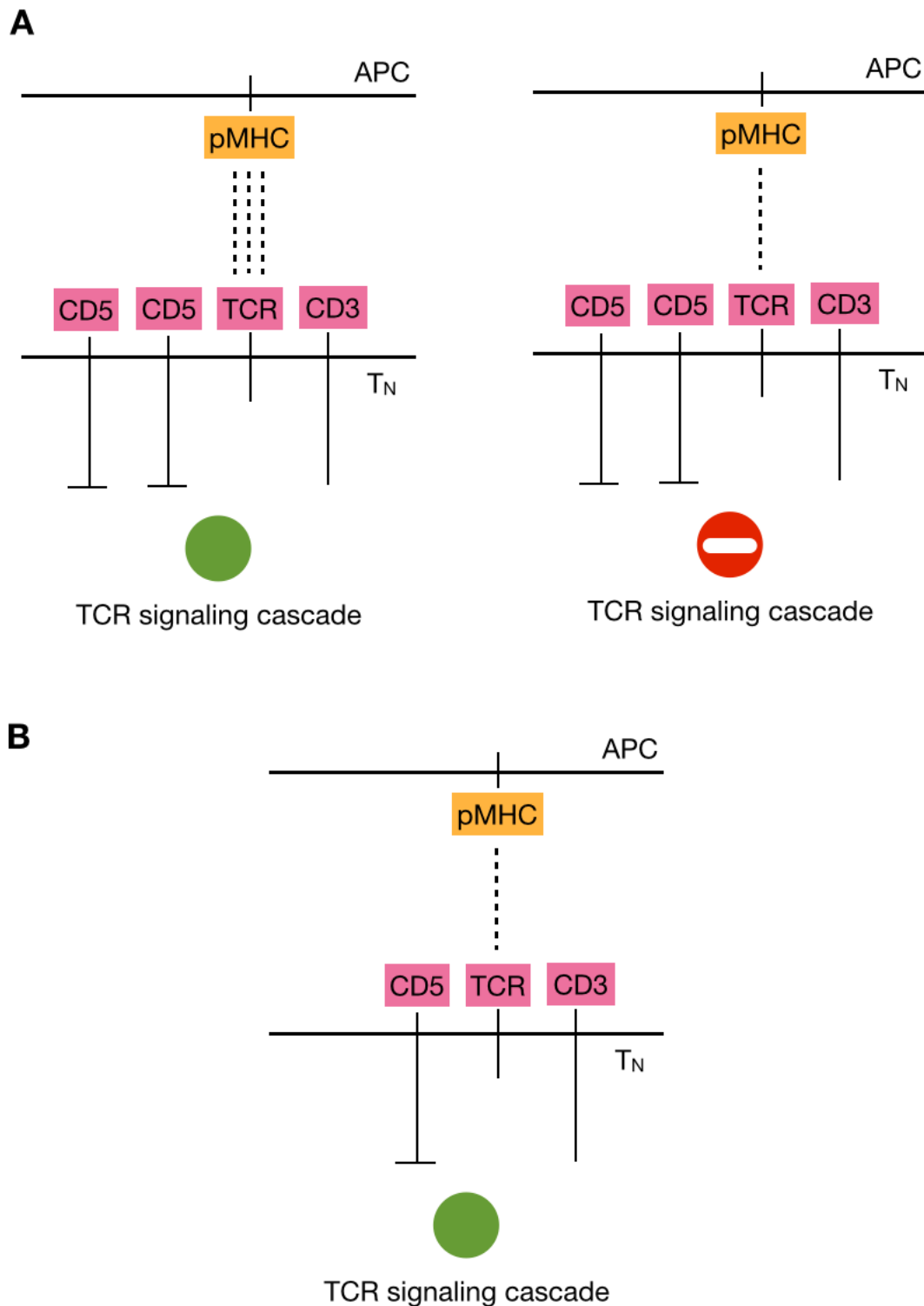


**Figure 39. Schematic representation of the impact of low levels of CD5 on T cell activation.**

A. CD5 is a negative regulator of TCR signaling. As such, it permits TCR signaling cascade to occur only in the context of a high-affinity interaction between TCR and pMCH complexes. B. Low levels of CD5 at the cell surface likely favor the expansion and differentiation of the cell even for low-affinity (non-cognate) peripheral interactions.



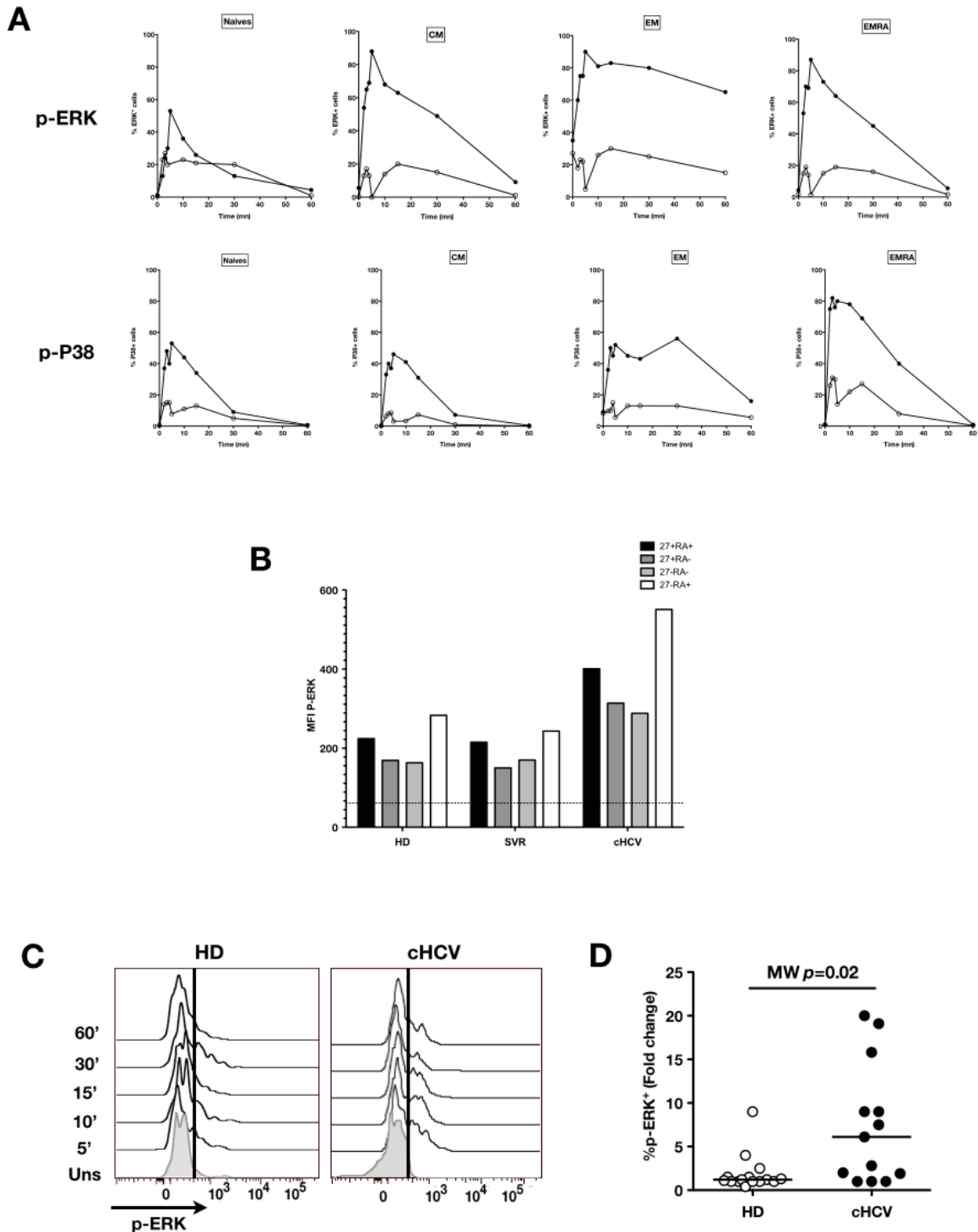


**Figure 40. Lower threshold for TCR activation in cHCV patients.**

A. Percentages of naive, CM, EM, and EMRA CD8<sup>+</sup> T cells with detectable intracellular phosphorylation of ERK (P-ERK, upper) and p38 (P-p38, lower), over time after CD3/CD28 plate-bound stimulation. B. MFI of P-ERK signals in same subsets from one HD, one SVR and one cHCV after CD3/CD28 stimulation. C. Representative overlay of histograms of phospho-ERK (p-ERK) signal at different time points following TCR stimulation from one HD and one cHCV patient. Plots are gated on naive CD8<sup>+</sup> T cell populations. D. Representation of fold-changes in percentages of p-ERK positive cells (t=5 mins) as compared to unstimulated condition in naive CD8<sup>+</sup> populations in HD and cHCV samples.



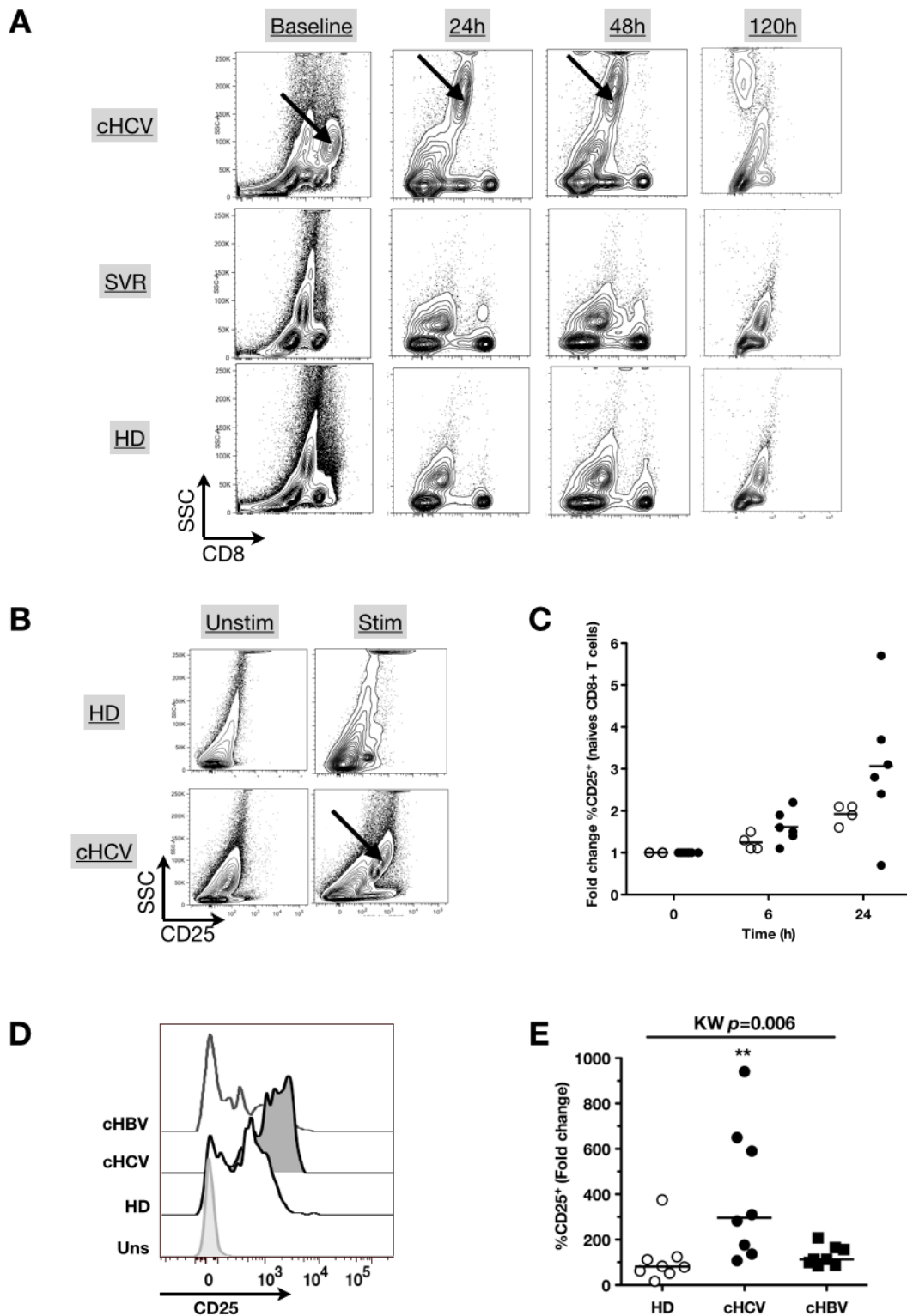


**Figure 41. Increased blastogenesis and CD25 expression after TCR activation in cHCV patients.**

A. Increased blastogenesis of CD8<sup>+</sup> T cells at baseline and after TCR activation in cHCV patients (arrow). B. Blasting cells at 24 hours express CD25. C. Kinetics of fold-changes of % CD25 in naive CD8<sup>+</sup> T cells following CD3/CD28 stimulation. D. Representative overlay of histograms of CD25 expression, detected at 24h after TCR stimulation from one HD, one cHBV and one cHCV patient. Plots are gated on naive CD8<sup>+</sup> T cell populations. E. Fold-change in percentage of CD25<sup>+</sup> cells, as compared to unstimulated condition in naive CD8<sup>+</sup> population from HD, cHCV and cHBV patients.



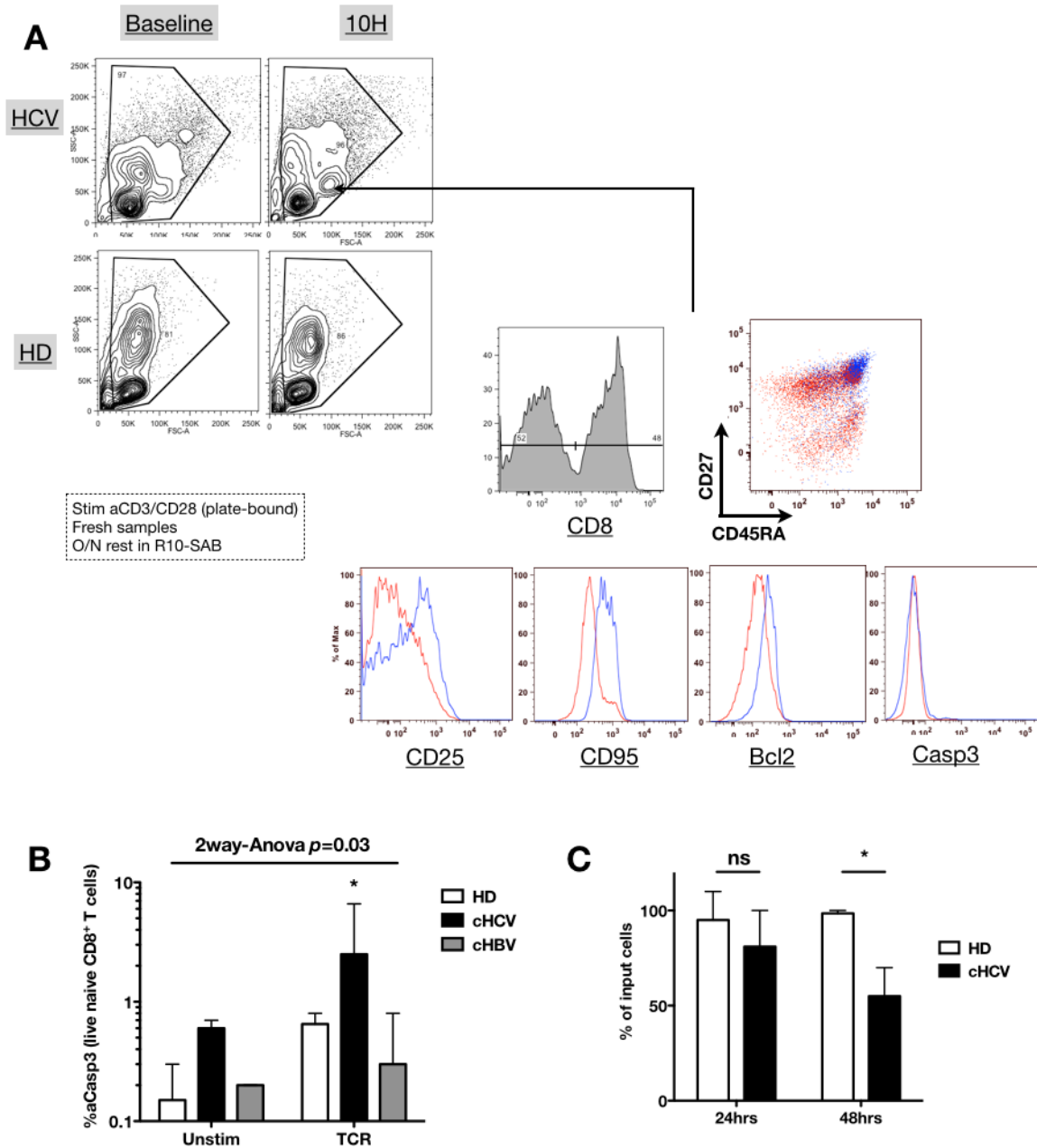


**Figure 42. Increased AICD after TCR activation in cHCV patients.**

A. Increased blastogenesis of CD8<sup>+</sup> T cells at baseline and after TCR activation in cHCV patients (arrow). Phenotype of blasting cells at 10 hours. B. Cumulative representation of % of active (cleaved) caspase-3 (aCasp3) signal in gated live naive CD8 T cells after 24 hours of TCR stimulation as compared to unstimulated condition in 4 HD, 4 cHCV, and 3 HBV patients. C. % of input cells recovered after TCR-activation culture.



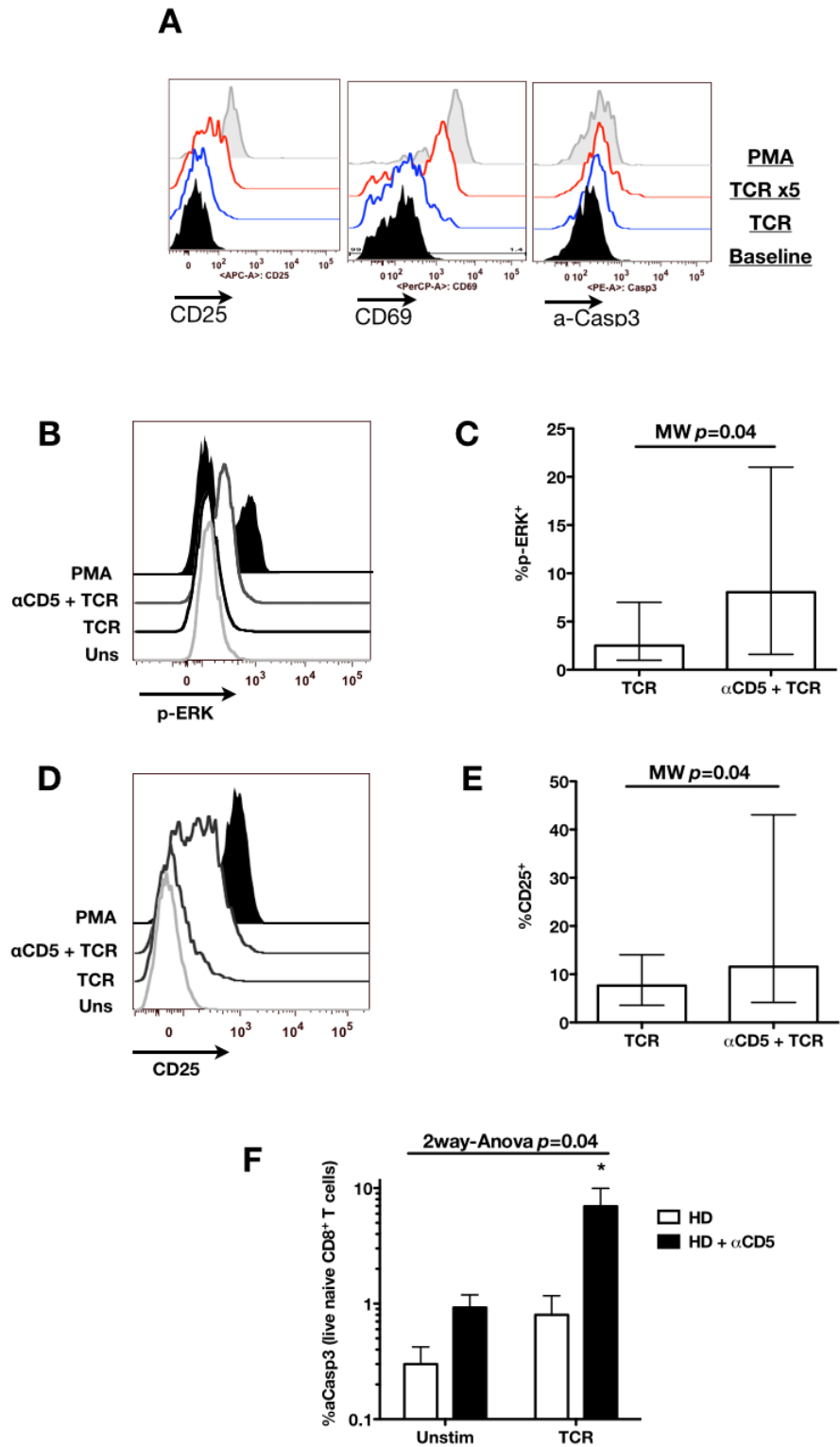


**Figure 43. Anti-CD5 blocking Abs recapitulate the hypersensitivity phenotype.**

A. CD25, CD69 and a-casp3 expression at baseline, after low doses (TCR) or high dose (TCRx5) of CD3/CD28 stimulation, or after incubation with PMA. B. Representative overlay of histograms of p-ERK signal detection in naive CD8<sup>+</sup> T cells in a HD 5 minutes after TCR stimulation with or without one hour of preincubation with anti-CD5 blocking Abs (bCD5). C. Percentages of p-ERK detected in naive CD8<sup>+</sup> T cells in ten HD 5 minutes after TCR stimulation with or without one hour of preincubation with bCD5. D. Representative overlay of histograms of CD25 signal detection in naive CD8<sup>+</sup> T cells in a HD after TCR stimulation with or without one hour preincubation with bCD5. E. Percentages of CD25 cells in naive CD8<sup>+</sup> T cells in HD ( $n = 8$ ), after TCR stimulation with or without one hour preincubation with bCD5 antibodies. F. Representation of % of active (cleaved) caspase-3 (aCasp3) in gated live naive CD8 T cells in HD ( $n = 4$ ) after TCR stimulation as compared to unstimulated condition with or without one hour preincubation with bCD5.



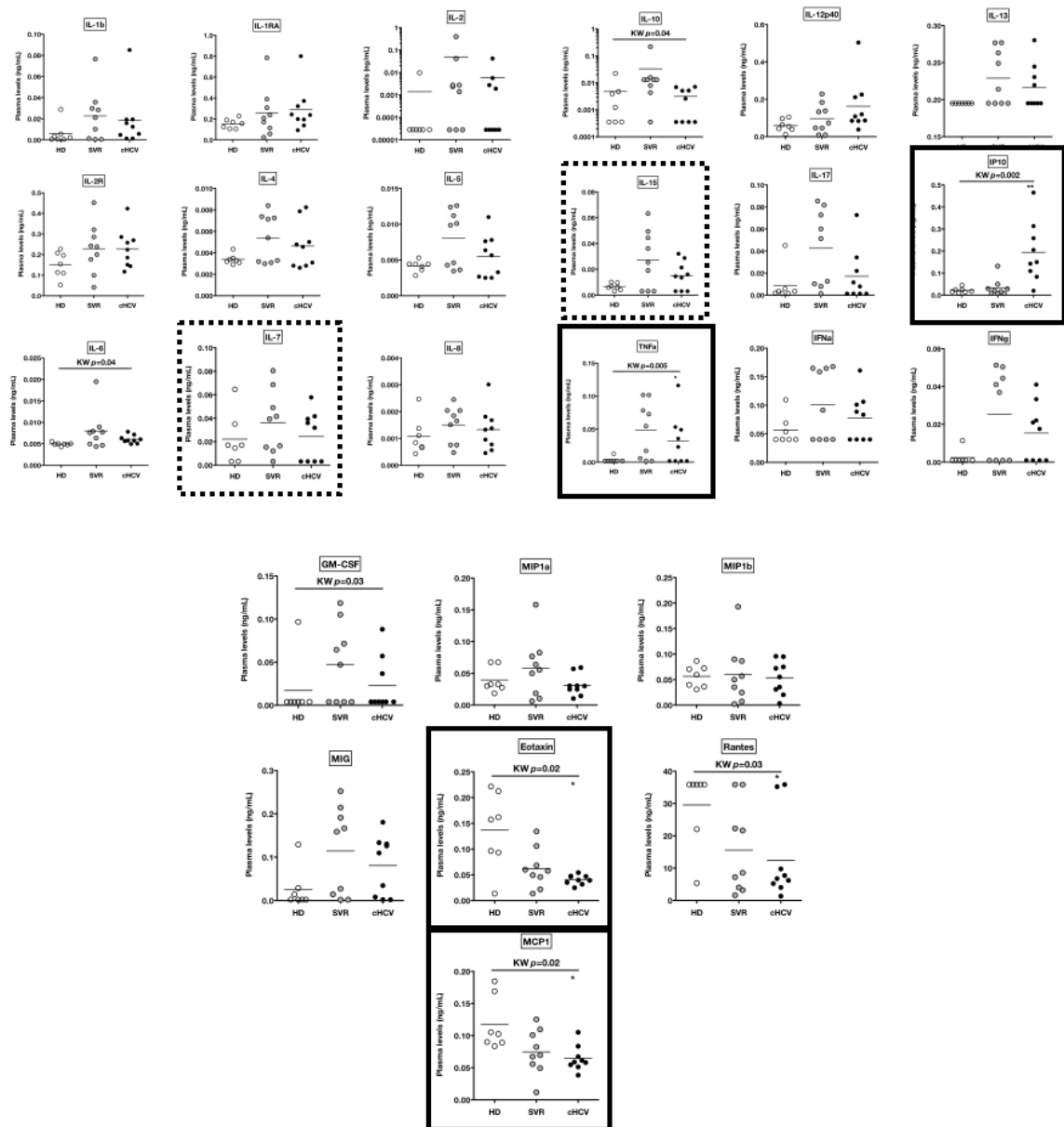


**Figure 44. Cytokines levels detected in plasma of cHCV, and SVR patients, as compared to HD.** Cytokines levels detected in plasma of HD, SVR, and cHCV patients. Squares indicate significant differences as compared to healthy donors.



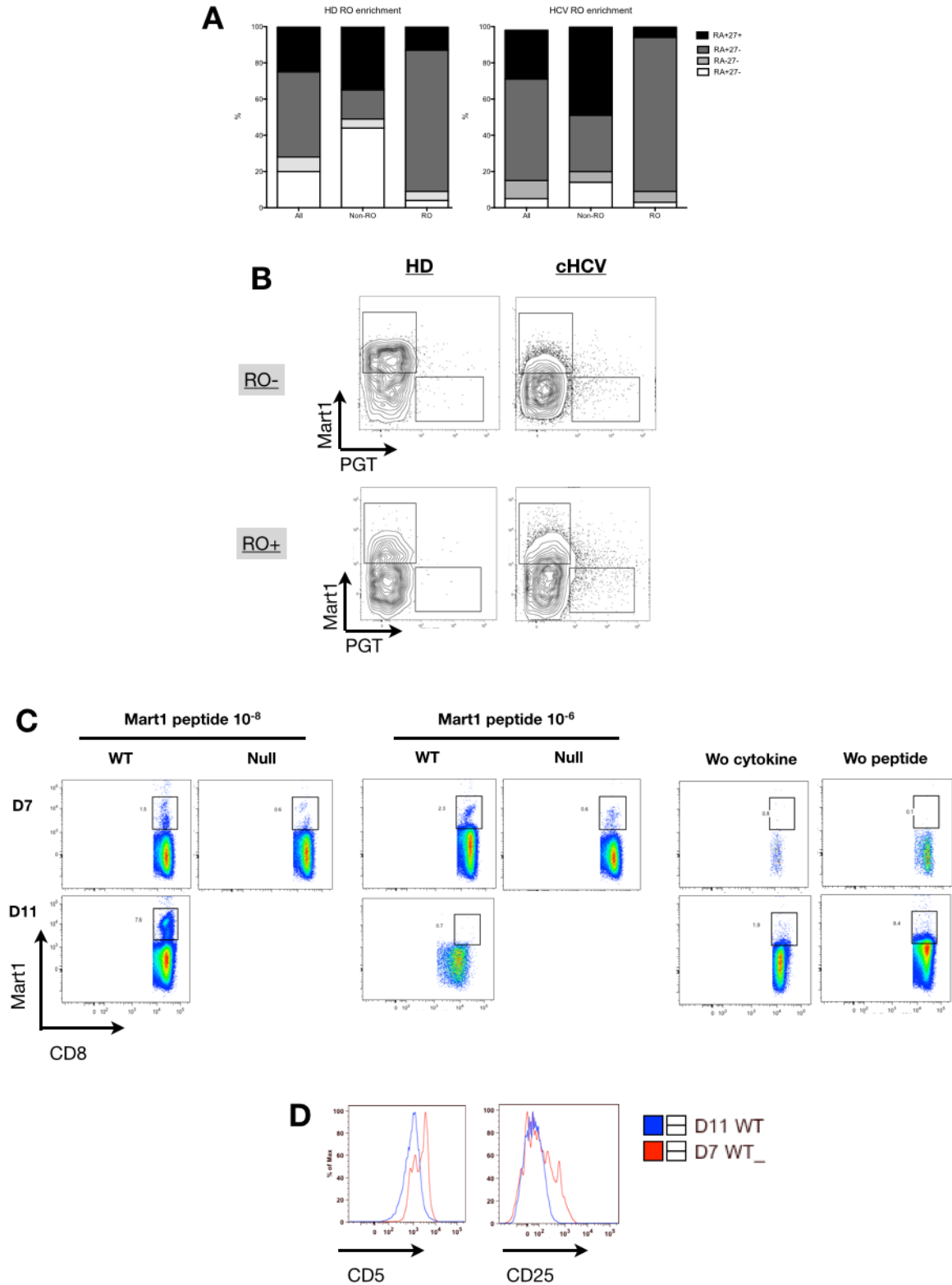


**Figure 45. In vitro priming of Mart1-specific CD8<sup>+</sup> T cells.**

A. Impact of CD45RO-magnetic enrichment on naive/memory T cell subsets on one HD (left) and one cHCV patient (right). B. Expansion of Mart1-specific T cells from RO<sup>-</sup> fraction of HD. C. Detection of Mart1 expanded specific cells after 10 days of in vitro priming assay on enriched CD8<sup>+</sup> T cells from one cHCV patient. Cells were detected by conventional tetramer (WT) of CD8null tetramer (Null). Two doses of Mart1 peptide were tested: low (10<sup>-8</sup>) or high (10<sup>-6</sup>). Cells were analysed at Day 7 or Day 11. Wells without cytokines or without peptide were used as control. D. CD5 and CD25 expression on Mart1-specific cells detected by the WT tetramer at Day 7 and 11.



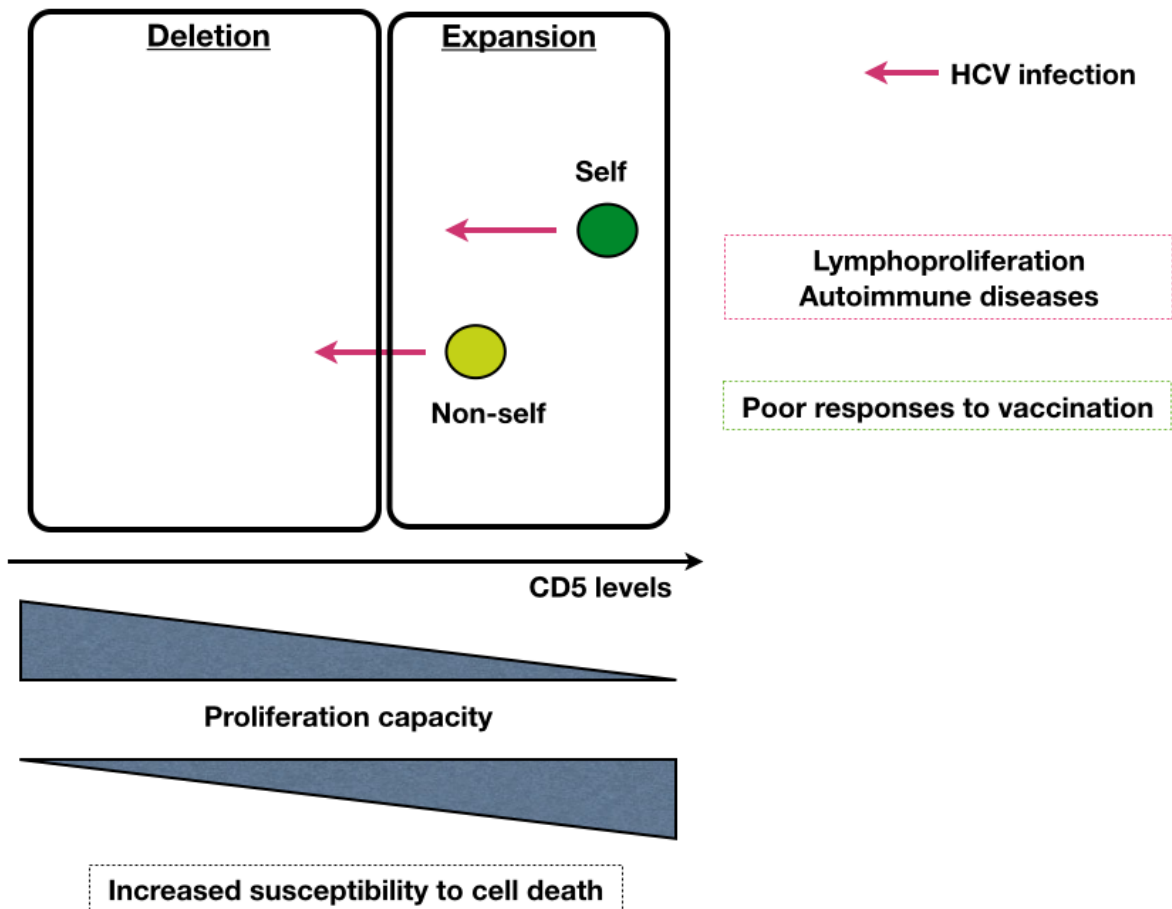


**Figure 46. Proposed models for dysregulation of naive CD8<sup>+</sup> T cells during cHCV chronic infection.**

The activation threshold hypothesis. In healthy donors, before immunization, a given antigen-specific population contains T cells with ranges of CD5 expression (high, dark green; low, light green). In periphery, those cells are maintained by cytokines, and by low affinity pMHC contacts, and some of them may occasionally derive toward a memory-phenotype (violet). After immunization with its cognate peptide, the antigen-specific population expand largely, and express lower CD5 levels – although there is still a mix of high (dark violet) and low (light violet) expression. Some rare cells are not engaged into the response and remain as naive-phenotype into the globally experienced population. In the context of cHCV, most naive CD8<sup>+</sup> T cells express low levels of CD5 at their cell surface. This lead to aspecific expansion and differentiation when encountering low affinity ligands in the periphery. When those cells encounter their antigen during the immunization phase, they will generate low-affinity and low-frequency specific populations.



## **Chapter 4.**

# **Study the impact of Cxcr3 receptor on inexperienced T cells**

---



# I. INTRODUCTION

Our laboratory recently provided the first evidence for dipeptidylpeptidase 4 (DPP4) mediated chemokine antagonism in the context of chronic HCV pathogenesis (Casrouge et al., 2011b). DPP4 (also known as CD26) is a member of the family of X-prolyl dipeptidylpeptidases (DPPs) family, and is capable of enzymatically removing the N-terminal two amino acids of proteins that possess a proline or an alanine in the second position (De Meester et al., 1999). Although several molecules possess the consensus motive for DPP4 recognition (Ou et al., 2013), only few were experimentally tested and defined as DPP4 substrates. More importantly, the biological relevance of DPP4-mediated post-translational modifications of proteins remains poorly studied. Two notable exceptions are the incretin hormones glucagon-like peptide-1 (GLP-1) and glucose-dependent insulintropic polypeptide (GIP); and the chemokine CXCL12. N-terminal truncation of GLP-1 and GIP renders these hormones incapable of inducing insulin secretion, and therefore over 30 million type II diabetes patients are being treated with DPP4 inhibitors. In analogy, processing of the chemokine CXCL12 by DPP4 diminishes the efficiency of hematopoietic cell engraftment and regulates G-CSF and GM-CSF mobilization of CXCR4-expressing hematopoietic stem cells (Christopherson, 2003; Christopherson et al., 2004).

Although CXCL12 remains the only member of the chemokine family for which there is *in vivo* evidence of altered chemotactic activity induced by DPP4, *in vitro* studies revealed that CXCL10 is also a target of this enzyme. DPP4 truncation of CXCL10 generates a dominant negative form of the chemokine, which binds its receptor, CXCR3, but does not induce signaling (Proost et al, Blood 2001). Studies from our lab revealed that high levels of the chemokine CXCL10 correlated with the inability of HCV infected patients to respond to therapy and to achieve viral clearance. Specifically, we detected N-terminal truncation of the chemokine interferon-induced protein 10 (IP-10 or CXCL10) in cHCV patients, which correlated with higher DPP4 plasma activity, reduced trafficking of CXCR3-expressing lymphocytes and poor response to treatment (Casrouge et al., 2011b; Riva et al., 2014). DPP4 truncation of IP-10 generates a dominant negative form of the chemokine, which binds its receptor, CXCR3, but does not induce signaling. As a result, it suggested that DPP4 perturbs lymphocyte trafficking in the context of HCV pathogenesis, accounting for DPP4 activity being a correlate of treatment failure.

These observations inspired my work, and pushed me to explore whether disruption of chemokine gradients may alter inexperienced T cell homing *in vivo*. Specifically, I investigated the impact of steady-state CXCR3-expression on the homeostasis of (i) intrathymic and (ii) peripheral inexperienced CD8<sup>+</sup> T cells *in vivo*. This work was initiated during the last year of my thesis and is a work-in-progress. In this Chapter, I present preliminary results from these studies, with the hope to initiate a discussion and establish a plan for completing my studies on tissue-resident inexperienced T cells.

## I. IN THE THYMUS

CXCR3-expression by intrathymic T cells has been reported to direct T cell egress after full maturation (Annunziato et al., 2001; Romagnani, 2001). In humans, four thymocyte populations express CXCR3: (i) a subset of TCR $\alpha\beta$ <sup>+</sup>CD3<sup>+</sup>CD8<sup>+</sup>SP cells; (ii) a subset of TCR $\alpha\beta$ <sup>+</sup>CD3<sup>+</sup>DP thymocytes; (iii) TCR $\gamma\delta$ <sup>+</sup> and (iv) NKT cells (Drennan et al., 2009). We confirmed this pattern of expression by phenotyping thymocytes extracted from three distinct thymi of human neonates undergoing cardiac surgery (**Figure 47A**). About 5 +/-2% of the CD3<sup>+</sup>CD8SP intrathymic T cells were found to express CXCR3. We similarly studied CXCR3 expression on three thymi from C57BL/6 mice (aged 8 weeks), and observed 1 to 3% of CXCR3<sup>+</sup>CD8SP intrathymic T cells (**Figure 47B**).

To investigate the function of CXCR3 on intrathymic T cells, we evaluated the effect of *cxcr3* gene disruption using CXCR3-knockout (*cxcr3*<sup>-/-</sup>) mice. We observed decreased percentages (M-W *p*=0.007) and lower absolute numbers (M-W *p*=0.007) of CD3<sup>+</sup>CD8<sup>+</sup>SP T cells in the thymus of *cxcr3*<sup>-/-</sup> as compared to control WT mice (**Figure 47C and D**). By contrast, absolute numbers of DN, DP and CD3<sup>+</sup>CD4<sup>+</sup>SP cells were unchanged (data not shown).

When considering additional phenotypic markers, we identified a subset of about 5.5% of CD3<sup>+</sup> thymocytes that included both CD4<sup>+</sup> and CD8<sup>+</sup> cells, and expressed high levels of CD44 and no CD62L (**Figure 47E and F**). This subset was significantly less abundant in *cxcr3*<sup>-/-</sup> mice, and could account for the loss of at least some of the CD8<sup>+</sup>SP thymocytes observed in these mice. In control mice, the CD62L<sup>-</sup>CD44<sup>hi</sup> subset of T cells expressed higher levels of CXCR3 and lower levels of CD3 and TCR $\beta$  than the other thymocytes (**Figure 47G**). As detailed in the introduction, intrathymic T cells contain both T cells in early stages of development, and activated T cells rehoming to this organ. To discrimination between the two, we used RAG2p-GFP mice, where GFP expression is under the promoter of *Rag2* and stain T cells under the process of development (Yu et al., 1999). We observed that CD62L<sup>-</sup>CD44<sup>hi</sup> cells were GFP<sup>neg</sup>, which indicates that they are T cells rehoming to the thymus (**Figure 47H**). We thus hypothesized that they could be intrathymic resident memory T cells (Mackay and Gebhardt, 2013). Accordingly, we found that those cells expressed high levels of CD69 and CD103 (**Figure 47I**).

Together, our data suggest that the expression of CXCR3 is necessary for the rehoming of CD8<sup>+</sup> T lymphocytes into the thymus, where they constitute a subset of CXCR3-expressing resident memory T cells.

## II. IN PERIPHERY

### A. MP cells in the blood of non-immunized *cxc3*<sup>-/-</sup> animals

I next analyzed the number and phenotype of T lymphocytes in the peripheral blood, again comparing WT and *cxc3*<sup>-/-</sup> mice. We observed similar numbers of CD3<sup>+</sup>CD8<sup>+</sup> (**Figure 48A**) and CD3<sup>+</sup>CD4<sup>+</sup> T cells (data not shown) in *cxc3*<sup>-/-</sup> mice as compared to WT controls. However, we found increased proportions (**Figure 48B and C**) and absolute numbers of CD62L<sup>-</sup>CD44<sup>+</sup> memory-phenotype (MP) CD3<sup>+</sup>CD8<sup>+</sup> T cells circulating in the blood of *cxc3*-deficient mice (**Figure 48D**). Of note, similar observations were made in the CD3<sup>+</sup>CD4<sup>+</sup> T cell subset (data not shown). To evaluate the impact of these perturbations on antigen-specific populations, we developed *cxc3*<sup>-/-</sup> OTI transgenic mice. OTI mice contain transgenic inserts for mouse TCR $\alpha$ -V2 and TCR $\beta$ -V5 genes, driving the expression of a transgenic TCR that recognize ovalbumin residues 257-264 in the context of H2-Kb molecules. As *cxc3* is located on the X chromosome, we bred OTI<sup>tg/tg</sup> (Rag-competent) males (*cxc3*<sup>+/-</sup>) with *cxc3*<sup>-/-</sup> females. We utilized in our experiments (i) F1 males (OTI<sup>tg/0</sup>-Rag competent CXCR3<sup>-/0</sup>, later referred to as OTI-CXCR3KO) for analysis, and (ii) F0 animals (later referred to as OTI-WT) as controls. When examining the peripheral blood of OTI-CXCR3KO mice, we found comparable absolute numbers of OTI cells as in OTI-WT animals, but increased proportion of MP cells (**Figure 48E and F**). Similar observations were made in the spleen (data not shown).

Together, our results argue for a dysregulated T cell preimmune repertoire in the context of *Cxcr3*-deficiency, with increased representation of memory-phenotype (MP) cells into Ag-specific inexperienced populations.

### B. Distinct TCR activation pattern

As presented in the Introduction, MP cells in the preimmune repertoire can have distinct threshold for TCR activation as compared to naïve-phenotype cells. To evaluate the threshold of TCR activation of *cxc3*-sufficient and *cxc3*-deficient Ag-specific CD8<sup>+</sup> T cells, we examined expression of surface activation markers in OTI-WT and OTI-CXCR3KO blood cells 24 hours after *in vitro* stimulation with their cognate SIINFEKL peptide. We tested two distinct concentrations of peptide (C1= 1 $\mu$ g/ml, C2= 5ng/ml), and used CD3/CD28-coated beads and PMA-Ionomycin as positive controls for T cell activation. We found OTI-CXCR3KO cells expressing lower levels of CD69 and CD25 after stimulation with different concentrations of the SIINFEKL peptide (**Figure 49A and B**). These lower levels were related to the presence of two distinct patterns of activation in OTI-CXCR3KO populations, rather than to a global decrease (**Figure 49C**). When examining cell phenotype, we identified a population of CD62L<sup>-</sup>CD8<sup>+</sup> T cells (blue) associated with lower levels of CD69-expression as compared to CD62L<sup>+</sup> T cells (red) (**Figure 49D**). These results suggest that the CD62L<sup>-</sup>CD44<sup>+</sup> MP

population (overrepresented in *cxcr3*<sup>-/-</sup> mice) displays a different response to peptide-induced stimulation, and might play distinct immune functions from its naïve counterparts.

These data highlight the impact of the heterogeneity in the preimmune repertoire of OTI-CXCR3KO animals on TCR-induced activation and cell death.

### C. MP OTI cells in the skin of unimmunized WT animals

The results presented so far revealed that CXCR3-deficiency results in an altered phenotype of CD8<sup>+</sup> T cells in blood and spleen of antigen-specific OTI transgenic mice. We therefore became interested to study the phenotype of CD8<sup>+</sup> T cell populations in other lymphoid and non-lymphoid organs of OTI-CXCR3KO and OTI-WT mice. To address this question, we investigated the presence of Ova-specific tetramer-positive T cells in lymph nodes, bone marrow, liver and skin of transgenic mice. Our first analysis revealed an elevated number of transgenic OT1 cells the bone marrow, spleen and liver of OTI-CXCR3KO mice, as compared to WT mice (**Figure 50A, red gate**). Inversely, OT1 cells were less frequent in the skin of *Cxcr3*-deficient animals (**blue gate**). When considering the phenotype of cells harvested from OTI-WT tissues, we observed that circulating OTI cells (*i.e.* cells localizing in the blood and the spleen) were predominantly of naïve-phenotype (NP). In contrast, OTI cells harvested from the skin contained high proportions of memory-phenotype (MP) cells (**Figure 50B, left**). Additionally, these cells expressed high levels of CD103 and CD69 (**Figure 50C**), suggesting that they are resident memory T cells (Clark, 2015). Of note, MP cells were still detectable – although less frequent, in Rag-deficient OTI animals (**Figure 50D**). This suggests that non-exclusive  $\alpha$ -chain TCR rearrangement account for part – but not all – of the OTI skin phenotype. When examining *Cxcr3*-deficient animals, OTI skin cells were rare, and displaying a similar phenotype as compared to the controls (**Figure 50B, right**).

In the above experiments, we compared the distribution and phenotype of OTI transgenic CD8<sup>+</sup> T cells in organs from F0 OTI<sup>tg/tg</sup> *cxcr3*<sup>+/-</sup> (OTI-WT) and F1 OTI<sup>tg/0</sup> *cxcr3*<sup>-/0</sup> (OTI-CXCR3KO) mice. We therefore tested if our results were dependent on the number of OTI transgene copies present in the different genetically modified mice. For this, we enumerated skin OTI cells in *cxcr3*-sufficient transgenic mice harboring different OT1 transgene copies: OTI WT (2 transgene copies); OTI<sup>tg/0</sup> WT (1 transgene copy) and OTI<sup>tg/tg</sup> Rag<sup>-/-</sup> WT (2 transgene copies). We found similar numbers of skin OTI cells in the three *cxcr3*-sufficient OT1 mouse strains, and those numbers were significantly higher than in OTI-CXCR3KO animals (**Figure 50E**). We therefore excluded transgene-related bias as a reason for OT1 accumulation in the skin.

## D. MP OTI cells arise in homeostatic environments

The altered number and phenotype of CD8<sup>+</sup> T cells found in *cxc3*-deficient mice led us to hypothesize that the expression of this chemokine receptor might be important for the steady-state migration and/or retention of CD8<sup>+</sup> T cells into peripheral tissues, such as skin. To evaluate the behavior of OTI-WT and OTI-CXCR3KO cells in a unique homeostatic environment, we created mixed bone marrow chimeras (**Figure 51A**). We reconstituted irradiated WT CD45.1 C57/Bl6 mice with a mix (ratio 1:1) of bone marrow from OTI-Rag<sup>-/-</sup>-GFP<sup>Ub</sup> (OTI-WT:GFP) and from OTI-CXCR3KO (CD45.2). After 2 months, we harvested the thymus, blood, spleen and skin of reconstituted animals for enumeration and phenotypic analysis of OTI cells. In the blood, we observed similar proportions and absolute numbers of OTI-WT and OTI-CXCR3KO specific cells (**Figure 51B and C**), suggesting that *cxc3*-deficient or sufficient bone marrow was equally engrafted upon transfer. However, circulating OTI-CXCR3KO population contained higher proportions of CD62L<sup>-</sup>CD44<sup>+</sup> MP cells as compared to OTI-WT (**Figure 51B and D**). Same phenotype was observed in the spleens of those animals (data not shown). Confirming our previous results, circulating MP cells presented a distinct pattern of activation after activation with their cognate peptide (**Figure 51E**). In the skin, however, we observed similar phenotype and number of reconstituted WT or *cxc3*-deficient OTI cells. These preliminary observations indicate that circulating memory phenotype OTI cells do not arise as a result of possible microenvironment differences, but rather relate to intrinsic T cell properties. Additionally, we interpret the discrepancy between our skin observations in single KO animals and bone marrow chimeras as indicating that T cell depletion observed in OTI-CXCR3KO animals reflects the depletion of non-cognate crossreactive resident tissue-memory cells, rather than a distinct engraftment capacity. While these experiments need to be repeated, one should notice that the OTI WT bone marrow used in these experiments presents at least two differences as compared to the OTI-CXCR3KO bone marrow: they have two copies of the transgene, and they are Rag-deficient. Therefore, we are planning experiments using OTI<sup>tg/o</sup> animals, as source of *cxc3*-sufficient bone marrow.

Our results suggest that the identification of steady-state inexperienced MP CD8<sup>+</sup> T cells into tissues relates to them being tissue resident-memory cells, which localization is dependent on the expression of the chemokine receptor CXCR3 (**Figure 52**). Whether abrogation of CXCR3-mediated migration results in a higher number of Ag-specific MP cells circulating in the blood is unclear.

### III. DISCUSSION

Our work confirms that MP Ag-specific inexperienced T cells do exist in unimmunized animals (Goldrath et al., 2000) and identifies three situations: (i) the skin, where Ag-specific inexperienced T cells do localize at steady-state, resembling resident memory T cells (Ariotti et al., 2014), (ii) the thymus, where  $cxcr3^+CD8^+$  T cells likely correspond to rehoming memory T cells trafficking through CXCR3-mediated signaling (Mackay and Gebhardt, 2013), and (iii) the blood, where high numbers of MP cells circulate in the context of *Cxcr3*-deficiency.

Although preliminary, our results identify T cells residing into tissues as a source of inexperienced T cells. Further experiments will be needed to test whether those cells are deeply into the tissues, or trapped into the vasculature (Anderson et al., 2012). In the skin, CXCL9 and CXCL10 (both being ligands for CXCR3) are quickly and strongly upregulated after stimulation (Villarroel et al., 2014). Increased basal levels of CXCL10 have been implicated in several T-cell mediated skin diseases such as alopecia (McPhee et al., 2012), erythema migrans (Mullegger et al., 2007), as well as contact hypersensitivity (Suga et al., 2013). On the other hand, *cxcr3* deficiency results in reduced control of cutaneous Leishmania infection (Rosas et al., 2005), as well as less severe acute skin GVHD lesions in a murine Ova-specific model of acute skin GVHD (Villarroel et al., 2014). Here, we observed memory-phenotype (MP) inexperienced Ag-specific T cells (i) localizing into this tissue, (ii) depleted in *cxcr3*<sup>-/-</sup> mice, (iii) but not in mixed bone marrow chimeras. Our interpretation is that MP cells correspond to skin resident memory T ( $T_{RM}$ ) cells that have the potential to be crossreactive for specificities of the preimmune repertoire.  $T_{RM}$  cells have been identified in parabiosis and transplant experiments as resting tissue memory  $CD8^+$  T cells with specific non-circulating properties (Shin and Iwasaki, 2013). They are conserved across species (mouse, rat, pigs), and found in multiple tissues such as small intestine, vaginal mucosa, brain, lung, salivary glands, and thymus (Mackay and Gebhardt, 2013; Mueller et al., 2014). Their recruitment into the skin, lungs, and vaginal mucosa, is dependent on cell-surface expression of CXCR3 (Mackay et al., 2013). This has been demonstrated by a depleted  $T_{RM}$  compartment in *cxcr3*<sup>-/-</sup> animals. Their behavior after sublethal irradiation is unknown, and it is not excluded that - as happening for some DCs subsets (Bogunovic et al., 2006) - they could be radioresistant. This could explain why we do lose our skin phenotype in our mixed bone marrow chimeras experiments.  $T_{RM}$  are characterized by high expression levels of  $\alpha E$  integrin (CD103) and CD69 (Mueller et al., 2014), and a specific gene-expression signature (Ariotti et al., 2014). They are fully functional, quickly producing  $IFN\gamma$  upon local peptide stimulation, and triggering a state of tissue-wide pathogen alert (Ariotti et al., 2014). In the thymus,  $T_{RM}$  have recently been identified, and demonstrated as important in local immunity (Mackay and Gebhardt, 2013). Our results suggest that, similar to the skin situation, trafficking and/or retention of those cells into the thymus is dependent on *cxcr3*.

In the blood, we highlighted a dysregulated preimmune repertoire in OTI-CXCR3KO mice, with high proportions of MP cells. High proportions of MP cells have been described into inexperienced OTI-Rag<sup>-/-</sup> populations in mice when those cells were adoptively transferred into sublethally irradiated animals. This effect reflected homeostatic-driven proliferation, and was transient, with a recovery of a naive T cell phenotype within 120 days after the adoptive transfer (Goldrath et al., 2000). In line with this, in our hands, OTI-Rag<sup>-/-</sup> cells harvested from BMC hosts 2 months after the allograft were of naive phenotype. Presence of MP cells into the OTI-CXCR3KO population thus could indicate (i) an inability of those cells to reach target tissues, or (ii) a lack of clearance of cells generated by homeostatic proliferation. Results from our mixed bone marrow chimeras experiments argue in favor of a trafficking issue, with comparable skin engraftment of OTI-WT and OTI-CXCR3KO cells. It is possible that our results reflect a defective clearance of MP inexperienced T cells as a result of *Cxcr3* deficiency. This would be in line with observations of attenuated contraction and resistance to apoptosis of *cxcr3*<sup>-/-</sup> memory OTI CD8<sup>+</sup> T cells in models of acute viral (Ova-expressing vaccinia virus, VV) and bacterial (LM-Ova) infections (Kurachi et al., 2011). Whatever the mechanism, we believe that increased numbers of antigen-specific memory T cells reported in the latter study is a direct consequence of high numbers of MP cells in the preimmune repertoire of OTI-CXCR3KO mice.

Finally, OTI T cells deficient in *Cxcr3* presented a distinct pattern of TCR activation as compared to OTI-WT cells, related to the presence of MP cells. This confirms the influence of preimmune repertoire diversity in early kinetics of activation. In the VV-Ova and LM-Ova models, other groups observed a faster downregulation of CD25 and CD69 markers on OTI-CXCR3KO cells as compared to OTI-WT (Kurachi et al., 2011). Our results of lower CD25 and CD69 after 24 hours of activation could also reflect higher sensitivity to TCR activation, but investigation of additional earlier time points will be required to formally document this effect. For which concerns the impact of preimmune repertoire perturbations on long-term immune responses, we believe that our observations might account for the documented skewing of OTI-CXCR3KO cells towards a high potential for memory precursor effector-cells (MPECs) generation. Further studies will be needed to validate this assumption.

## IV. PROSPECTIVES

Altogether, our interpretation of these preliminary results is that (i) CXCR3-dependent tissue resident memory T cells can be crossreactive for preimmune repertoire specificities, (ii) CXCR3-expression might facilitate the homeostatic clearance of MP inexperienced Ag-specific T cells, and (iii) MP preimmune cells can impact early, mid, and long term aspects of the immune response.

In the next months, we will study the functionality of MP circulating T cells, with (i) PhosFlow at early time points (t=5min), and (ii) precise kinetics of activation and cell death events

during the first 24-48 hours after stimulation with SIINFEKL peptide. These experiments will allow us to test the hypothesis that OTI-CXCR3KO cells have a decreased threshold for TCR activation. Additionally, we will document the sensitivity of *Cxcr3*-deficient cells to TCR-induced cell death.

In parallel, we will evaluate if some of the MP cells circulate in OTI-CXCR3KO mice because they are lacking ability to access their target tissue. We plan to investigate this by comparing gene-expression patterns of FACS-sorted (i) skin MP OTI cells from OTI-WT, (ii) spleen MP OTI cells from OTI-CXCR3KO mice, and (iii) thymus GFP<sup>+</sup>CD3<sup>+</sup>CD8<sup>+</sup> T cells. We will focus on genes previously identified as differentially expressed on tissue resident memory cells (Ariotti et al., 2014). We will compare those subsets to “true memory” cells, *i.e.* OTI cells recovered >40 days after *in vivo* infection with LM-Ova. These experiments will evaluate the distance between those different subsets of T cells, providing important informations on their nature. Our hypothesis is that skin and thymic subsets will be close, and different from both the spleen MP OTI-CXCR3KO, and “true memory” cells.

We also plan to repeat bone marrow chimeras experiments, with grafting OTI<sup>tg/0</sup>-*cxcr3*<sup>+/-</sup>-WT and OTI<sup>tg/0</sup>-*cxcr3*<sup>-/-</sup> (OTI-CXCR3KO) Rag-competent cells into WT and *cxcr3*<sup>-/-</sup> hosts. These experiments will provide additional information towards the hypothesis of skin resident memory T cells crossreacting with the preimmune repertoire.

Finally, we propose to enrich Ova-, LCMV-, and MCMV- specific inexperienced populations from the thymus of WT and *cxcr3*<sup>-/-</sup> RAG-GFP unimmunized animals. Enumerating and phenotyping those cells will provide informations about the residency of inexperienced T cells into the thymus. Same analysis on animals infected by LM-Ova will provide additional information on memory T cells rehoming into this tissue, as well as their potential for crossreactivity.

Ultimately, our work indicates that CXCR3 blockade before immunization could be a useful strategy for shaping the preimmune repertoire towards higher reactivity – therefore improving vaccine efficacy. To test this, we will evaluate the impact of *i.p.* injections of blocking anti-CXCR3 antibodies on the T cell preimmune repertoire of OTI-WT mice, and in early kinetics of the immune response after LM-Ova challenges. Blocking anti-CCR5 antibodies, as well as relevant isotype will be used as controls. These experiments will bring innovative insights into the possibility of artificially shaping the T cell preimmune repertoire, and dictating the magnitude and/or qualitative aspects of the later immune responses.

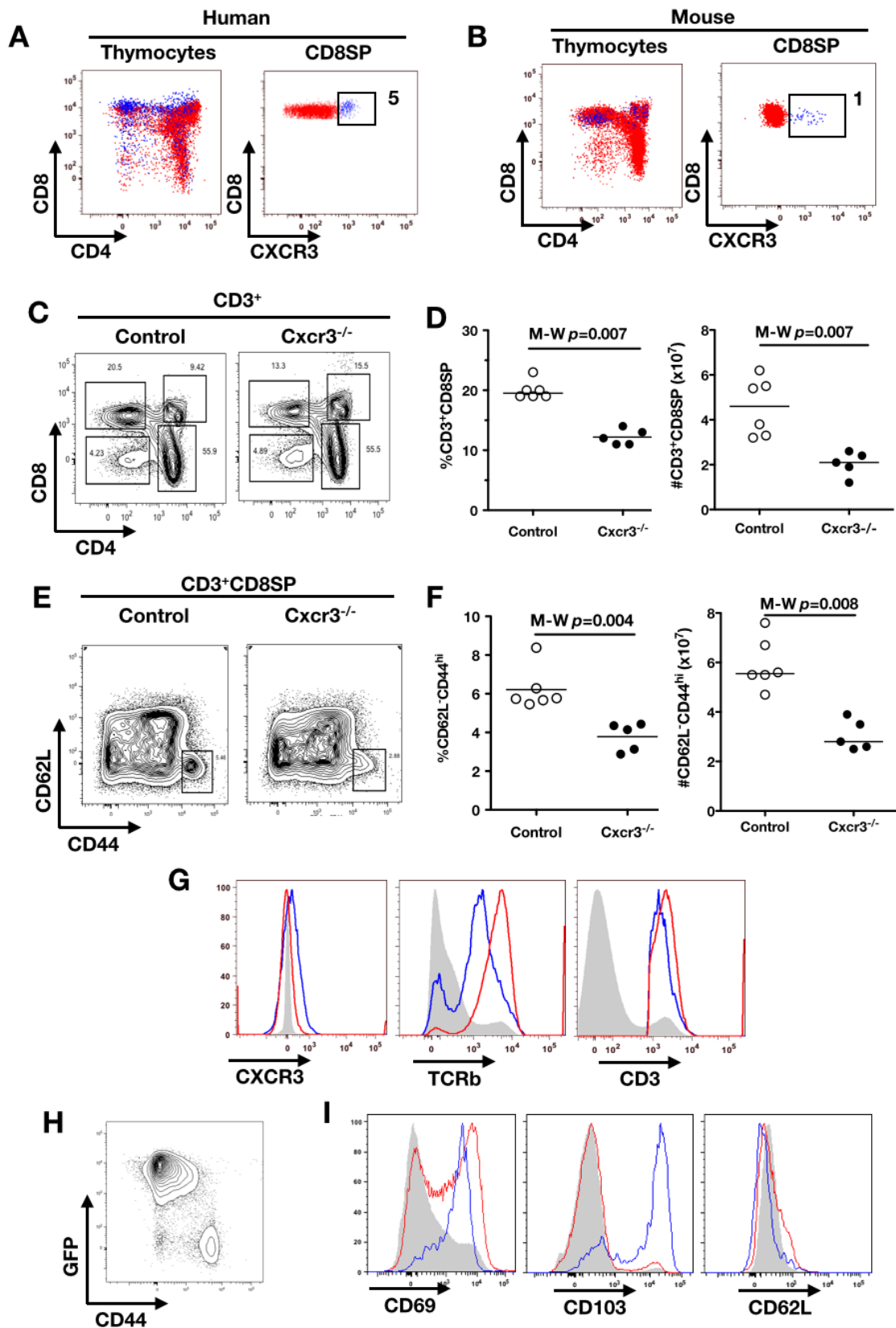


**Figure 47. CXCR3KO mice have lower numbers of CD8SP thymocytes.**

A. Human CXCR3-expressing thymocytes (blue) within all thymocytes (left, red) or CD8SP. B. Mouse CXCR3-expressing thymocytes (blue) within all thymocytes (left, red) or CD8SP. B and C. *Cxcr3*<sup>-/-</sup> mice present lower percentages and absolute numbers of intrathymic CD8SP. E and F. Decreased proportions of CD62L<sup>+</sup>CD44<sup>hi</sup> T CD8SP cells in *Cxcr3*<sup>-/-</sup> animals. G. Phenotype of gated CD62L<sup>+</sup>CD44<sup>hi</sup> (blue) intrathymic T cells as compared to other thymocytes (red) and DN population (grey). H. CD44 expression by GFP<sup>+</sup> and GFP<sup>-</sup> T cell populations in Rag2p-GFP mice. I. Phenotype of CD44<sup>hi</sup>GFP<sup>-</sup> (blue) as compared to developmental thymocytes (red) and DN population (grey).



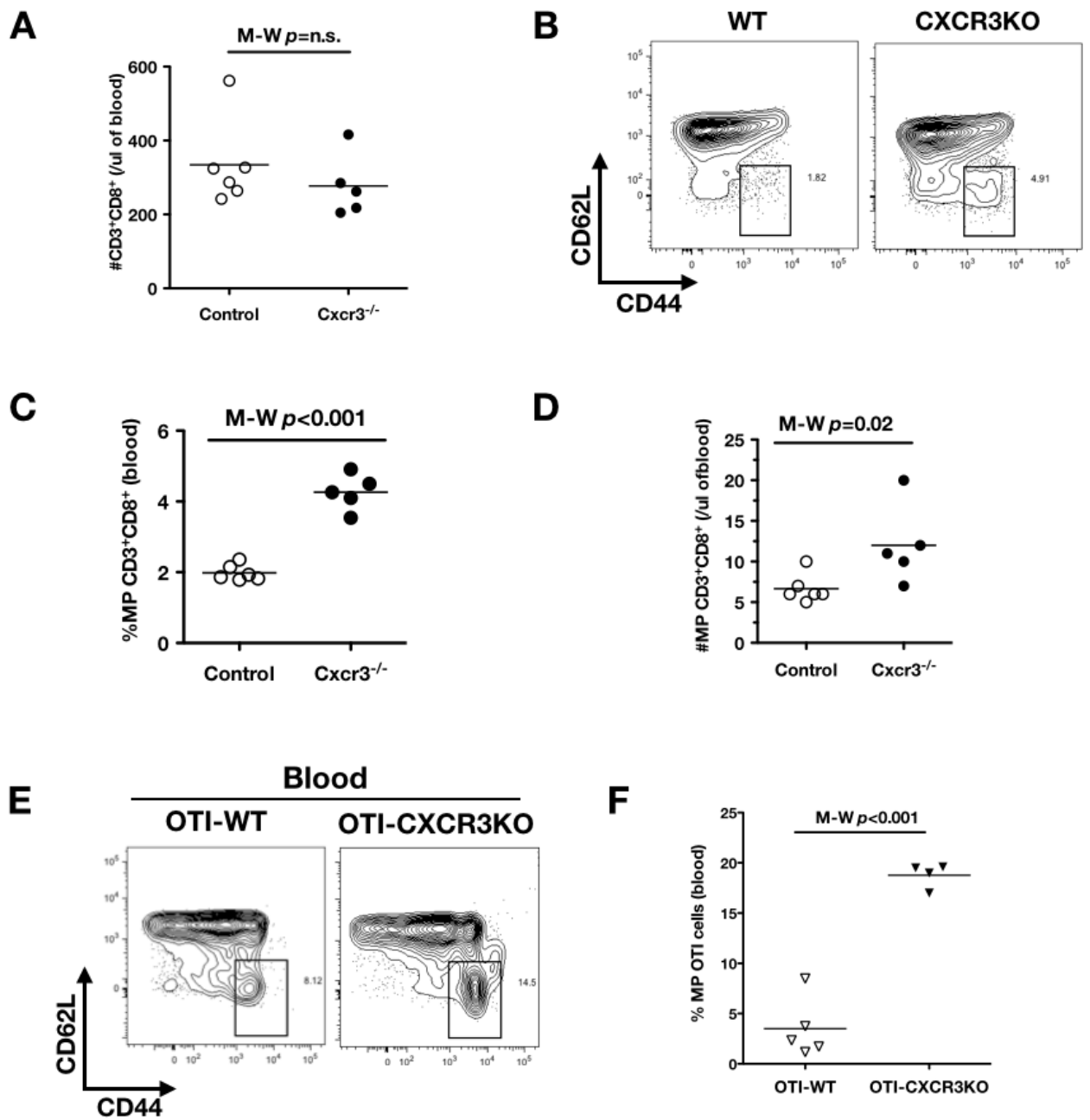


**Figure 48. Cxcr3<sup>-/-</sup> mice present increased numbers of circulating MP CD8<sup>+</sup> T cells.**

A. Normal numbers of CD8<sup>+</sup> T cells into the blood of Cxcr3<sup>-/-</sup> mice. B, C and D. High proportions and absolute numbers of memory-phenotype (MP) CD8<sup>+</sup> T cells in the blood of Cxcr3<sup>-/-</sup> mice. E and F. High proportions of MP CD8<sup>+</sup> T cells in the blood of OTI-CXCR3KO mice.



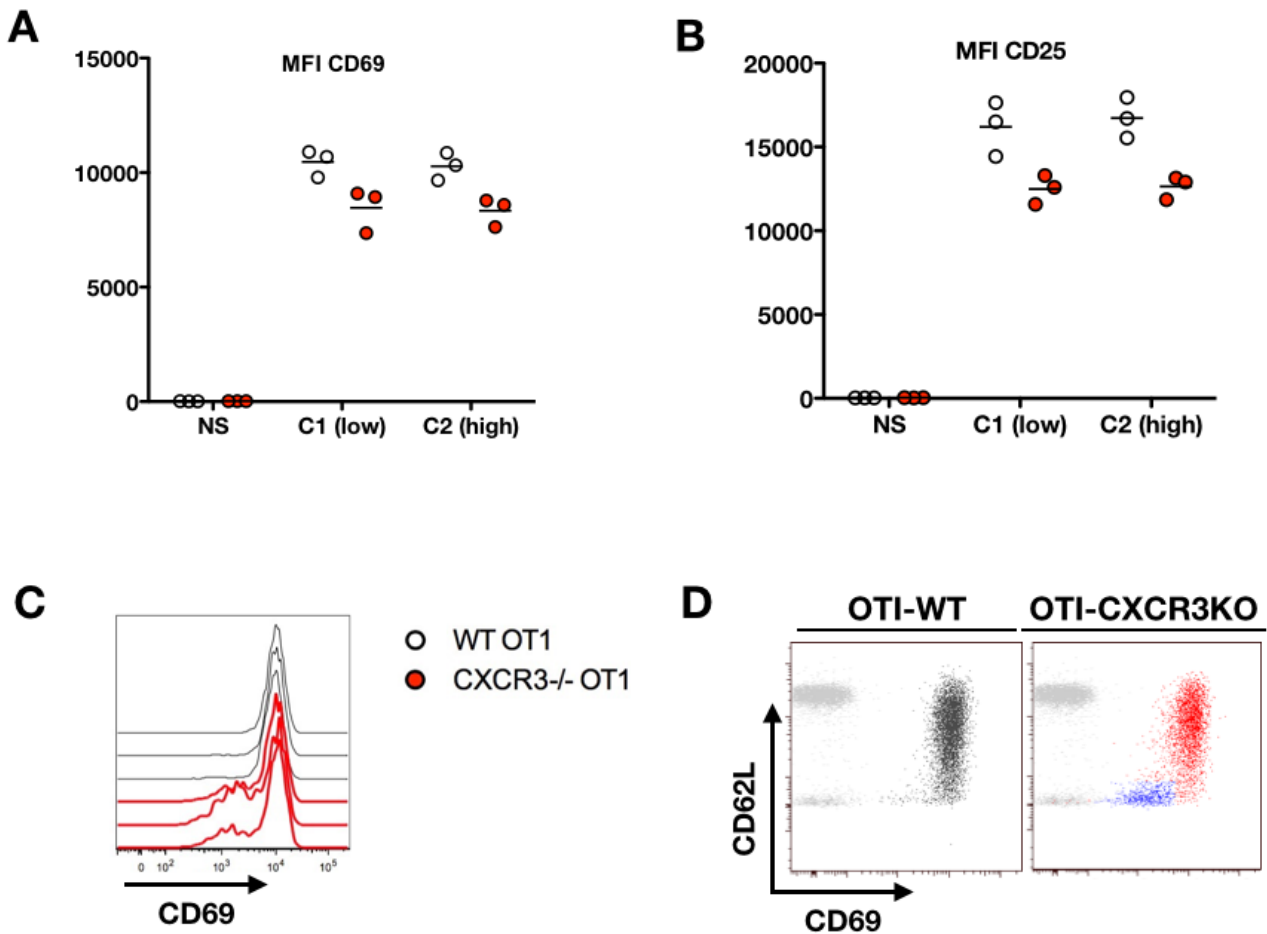


**Figure 49. Activation profile of OTI-CXCR3KO cells after stimulation with the Ova peptide.** A and B. CD69 and CD25 expression on OTI-WT (white) and OTI-CXCR3KO (red) cells after 24h *in vitro* stimulation with SIINFEKL peptide. C. Overlay of CD69 histograms after 24h *in vitro* stimulation with SIINFEKL peptide. D. CD69/CD62L expression of OTI-WT cells (black, left), NP OTI-CXCR3KO (red) and MP OTI-CXCR3KO (blue) after 24h of stimulation with SIINFEKL peptide, as compared to unstimulated OTI-WT cells (grey).



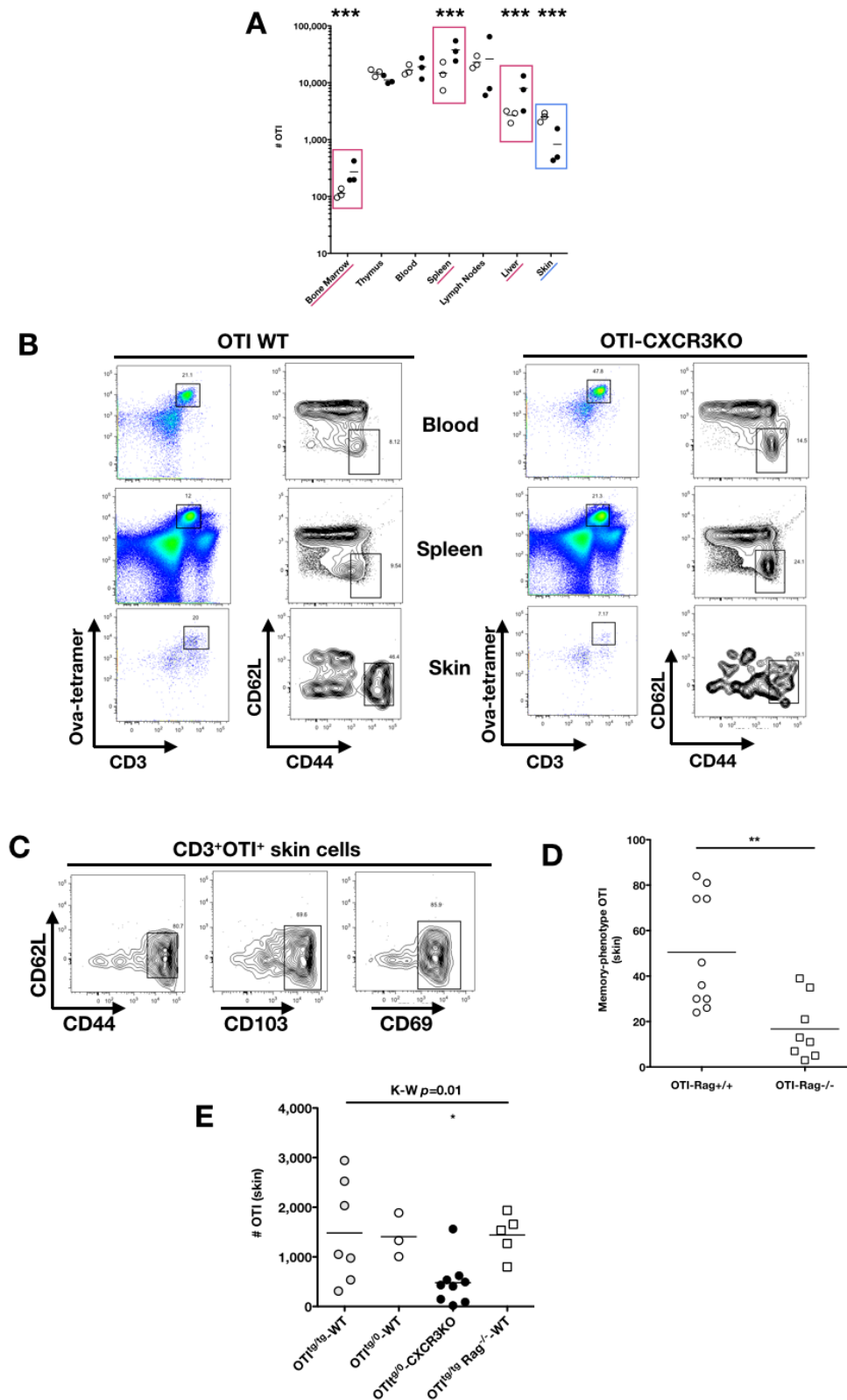


**Figure 50. MP cells are found into the skin of OTI-WT transgenic unimmunized animals.**

A. Absolute numbers of OTI cells detected into tissues of OTI-WT (white) and OTI-CXCR3KO (black) mice. B. Detection and CD62L/CD44 phenotyping of OTI cells in the blood, spleen and skin from OTI-WT (left) and OTI-CXCR3KO (right) animals. C. Expression of CD62L, CD44, CD103, CD69 by skin OTI cells harvested from OTI-WT mice. D. Percentages of MP OTI cells into the skin of OTI-Rag competent (white circle) and OTI-Rag deficient animals (white square). E. Number of OTI cells into the skin of OTI<sup>tg/tg</sup>-WT, OTI<sup>tg/0</sup>-WT, OTI<sup>tg/0</sup>-CXCR3KO, and OTI<sup>tg/tg</sup>-Rag<sup>-/-</sup>-WT mice.



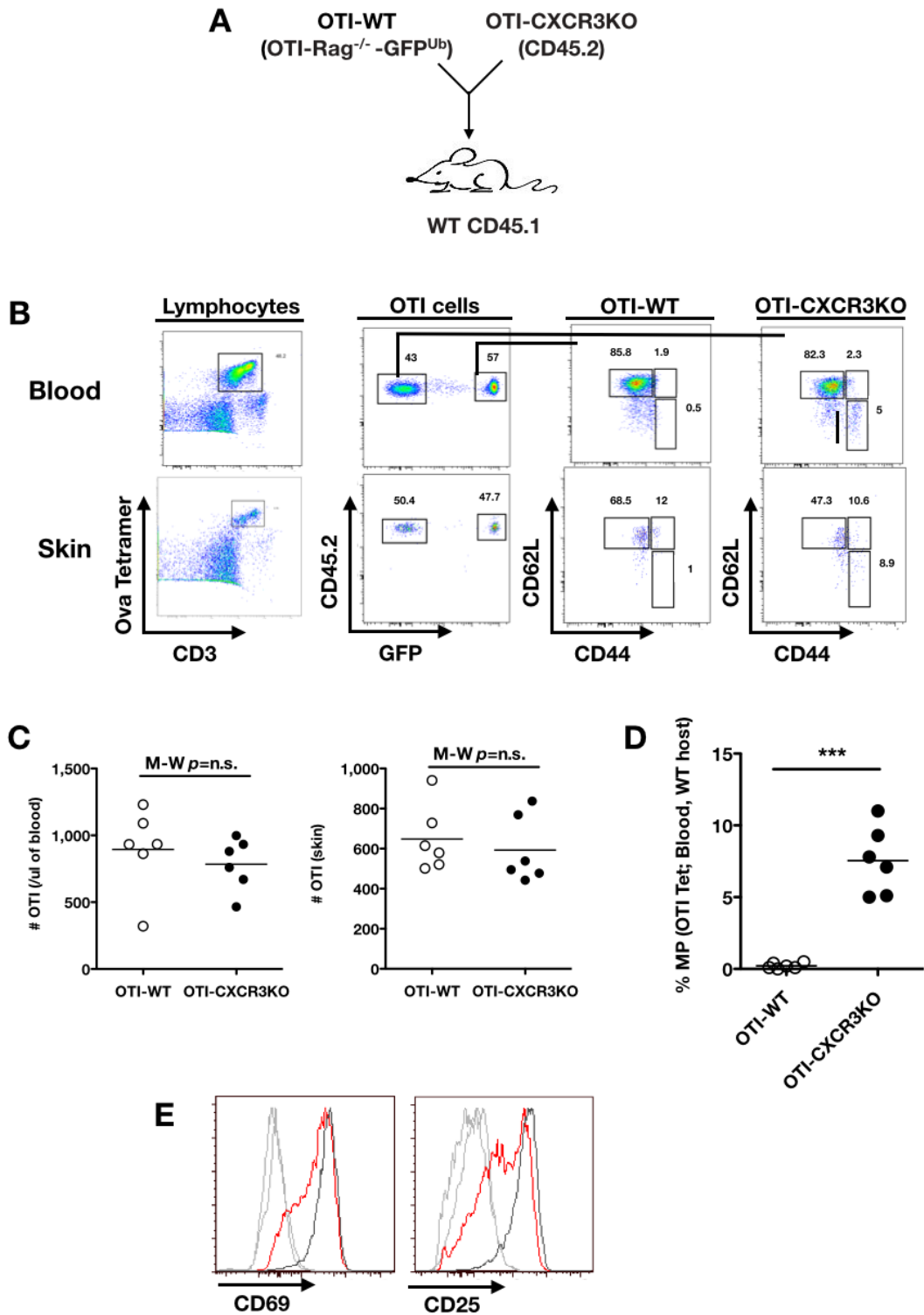


**Figure 51. MP cells are present in OTI-CXCR3KO cells of mixed bone marrow chimeras.**

A. Mixed bone marrow chimeras were generated by reconstituting irradiated WT (CD45.1) animals with a 1:1 mix of OTI<sup>tg</sup>Rag<sup>-/-</sup>-GFP<sup>Ub</sup> (CD45.2) and OTI-CXCR3KO (CD45.2) bone marrows. B. Identification and CD62L/CD44 phenotyping of OTI cells arising from OTI-WT and OTI-CXCR3KO bone marrows in blood and skin of grafted animals. C. Absolute numbers of OTI-WT and OTI-CXCR3KO cells recovered into the blood and skin of grafted animals. D. Percentages of MP cells into OTI-WT and OTI-CXCR3KO cells circulating in the blood of grafted mice. E. Expression of CD69 and CD25 activation markers on OTI-WT (dark grey) and OTI-CXCR3KO (red) cells after 24 hours of *in vitro* stimulation with SIINFEKL peptide, as compared to unstimulated conditions (light grey).



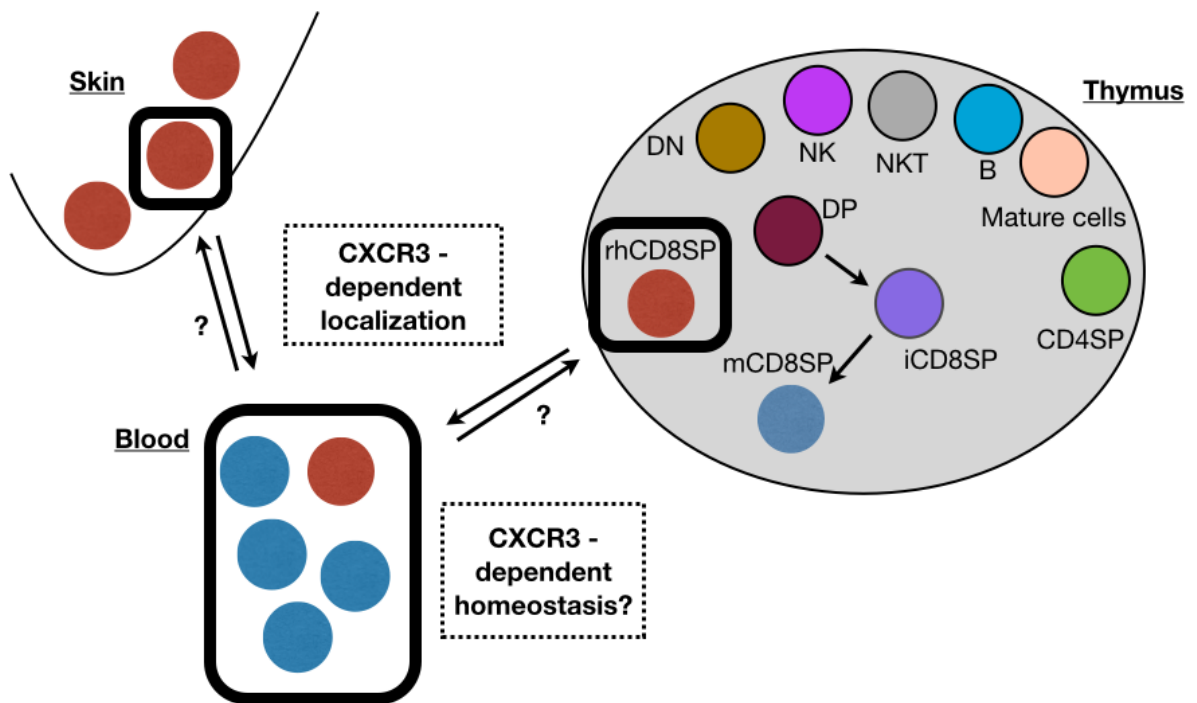


**Figure 52. Proposed model of MP Ag-specific inexperienced T cells migration.**

From our results, we propose that MP might be resident memory T cells that (i) seed into the skin (and maybe the thymus) tissues at steady state in unimmunized animals under the influence of CXCR3/ligands gradients; and (ii) might have the potential to crossreact with unknown specificities of the pre-immune repertoire. Whether high numbers of MP Ag-inexperienced T cells are circulating into the blood of *cxcr3*-deficient animals reflects (i) resident-memory T cells lacking their ability to reach target tissues, and/or (ii) a direct effect of *Cxcr3* is unclear and needs additional investigations.



# **Chapter 5.**

## **General Discussion**

---



## I. IMMUNOPHENOTYPING CHALLENGES

When I joined the lab, my project was to enumerate and characterize Ag-specific naive T cells from the blood of healthy humans. I thus immediately dived into the reading of previous studies on naive and memory T cell compartments – and found myself lucky to work on naive T cells and not memory as the diversity in the latter is quite intimidating. I selected phenotypic markers that I knew will identify naive cells, and developed my work without too much concerns. When we came to HCV studies, and the observation of sometimes large numbers of MP cells into inexperienced populations, I turned pale. When I gate on bulk T cells with naive/memory markers, how do I know the proportion of cells that are MP but part of inexperienced T cells vs. true memory? How can I interpret an increase in memory cells if I don't know which of these subset is concerned? While I was working on HCV and naive T cells, several research papers were published about the new subset of tissue resident memory cells – and again I found myself released not to have to deal with such an issue in humans: at least naive cells are circulating in the blood... When I started studies on mice, and observed MP Ag-specific inexperienced T cells hidden into the organs at steady state, I became very confused. If similar things happen in humans, what is the relevance of my observations in peripheral blood? How much circulating cells are representative of the body capacity? Maybe I am looking at only a very small subset of what can be part of antigen-inexperienced populations, leading to important biases in my interpretations. Now I get extremely cautious when I need to interpret CD45RA/CD27 FACS plots.

I am trained as a medical biologist, and as such had the opportunity to participate to the immunomonitoring of several clinical trials in different hospital sites. Most of the analyses that we were doing on the blood samples of the patients were phenotypic analysis, with different FACS panels to enumerate and characterize subsets of hematopoietic cells. One of them usually referred to naive and memory T cells, with two or three markers coupled to CD3/4/8 antibodies. Others and we were hoping to observe some perturbations of these compartments that might correlate with clinical outcome, and to be able to later utilize those biomarkers to predict vaccine efficacy. Others and we were always disappointed to see no evidence of correlation, although it was clear that CD8<sup>+</sup> T cell differentiation was clue. After my PhD way of the cross, I think the unexpected diversity and migration properties of the preimmune repertoire might be one of the reason of this failure, leading to a lot of confusion in what we thought were clear-cut markers.

So how do we move forward?

First I think we have to be more aware of the limits of immunophenotyping, and more critic (in a positive way) for immunomonitoring studies.

Then, we have to consider immunity in the tissue. Until now, we have largely underestimated its importance, especially in homeostatic conditions. However, as we get more and more evidence that for

many situations blood is not enough informative, then we have to find out a solution, even if that sounds like a big challenge. A.Einstein was saying: « La folie, c'est de faire toujours la même chose et de s'attendre à un résultat différent. ». I think it fits pretty well with my actual vision of immunomonitoring studies, which are technically heavy, time-consuming and costly. Epigenetic imprinting, isolation of rare circulating tissue-cells, optimization of organ dissociations or immunohistochemical protocols, studies on deceased organ donors, or more systematic immunoscope studies might be some tracks to evolve it in a more productive way.

Finally, we also need to admit that we cannot do without tracking Ag-specific T cell populations with tetramers. There have been some fabulous improvements over the past decade, especially as a result of the creativity of Ton Schumacher's group with this technology, but we need to do better, and implement them in routine analysis. This will require significant efforts from the community for large-scale production, generation of appropriate quality controls, and spreading of analysis expertise. This is feasible, as illustrated by the standardization work of the CIMT group with CIP proficiency panels (<http://www.cimt.eu/workgroups/cip/proficiency>), but for practical reasons, this will probably require to have some specific sites dedicated to this expertise. On our side, we propose to adapt the combicolor coding technology to the Sony spectral analyzer that we have in place, and couple it to tetramer enrichment. This will permit to recover a large number of information from very limited amount of sample. And we hope it will also permit to efficiently analyze tissue pieces by diminishing the constraints relating to autofluorescence and background staining. An important last point is that all of these efforts take time, much more than repeating standard analysis on blood of patient's cohorts, and that needs to be sufficiently valorized by the community.

## **II. PREIMMUNE REPERTOIRE AND PERSONALIZED MEDICINE**

Beside the pure phenotypic aspects, our work evidences that the preimmune repertoire of both mice and humans is more complex than anticipated. Not all naive T cells are created equal. Not all Ag-specific inexperienced T cell populations are the same, both in frequency and composition. They do not have a similar inherent ability to be recruited into the subsequent response. And all of this is not fixed, but can vary as a result of environmental modifications. Like « memory T cells » includes different subsets with distinct behavior and functions, « naive T cells » (or inexperienced T cells) now refers to very diverse subpopulations. And this diversity has to be taken into account while interpreting any T cell priming experiment. My belief is that the T cell response to a given antigen is the sum of the behavior of individual subsets that are part of Ag-specific inexperienced populations. And that the composition of the preimmune repertoire is a point of regulation of CD8<sup>+</sup> T cell immune responses. Whether our observations also hold true for CD4<sup>+</sup> T cells is unclear, and will need

additional explorations. Identifying markers for those subsets, and understanding their contribution to the global function will be clue.

One example of the subset we need to better identify is recent thymic emigrants (RTEs). Cord and newborn bloods are expected to contain higher numbers of these cells than later in life, but we miss phenotypic markers for tracking them. We suggest we take advantage of this age-stratified evolution to find biomarkers for identification of this population. From microarrays data that we have on CD8SP neonate thymocytes, we will select 80 genes defining a transcriptomic signature of intrathymic cells that distinguishes them from naive peripheral T cells. We will then collect, and FACS-sort (i) single and (ii) bulk naive T cells from cord and peripheral blood of age-stratified healthy children. On bulk cells, we will evaluate the proportion of sjTRECs in the naive CD8<sup>+</sup> T cell population. On single cells, we will evaluate gene expression levels for the 80 pre-selected genes. Assuming that sjTRECs do identify RTEs – at least in children, we will then be able to know how many of the 100 sorted single cells are RTEs, and to identify them as bearing the more thymus-like profile. By this strategy, we hope to identify tracking markers for RTEs, which would be extremely useful for example in studies on childhood vaccinations.

Similar studies could be proposed for the other aspects of preimmune repertoire diversity. At the end, the dream would be to be able to provide for each patient a cartography of its preimmune repertoire for different antigenic specificities. That would be a basis for personalized medicine where specific immunotherapies could be proposed on a patient-per-patient basis.

### **III. PREIMMUNE REPERTOIRE AND PERSISTENT VIRUSES**

Finally, we believe that our findings of dysregulated preimmune repertoire during HCV chronic infection are not unique to this virus, and could also happen in the context of other persistent infections. Since birth – and even before, we all are in permanent contact with lots of pathogens that infect us, usually driving asymptomatic to mild-severe infections, and later persist for years or life in a resting state in our organism. These hosts that inhabits us constitute the « virome », which includes viruses that infect eukaryotic cells (eukaryotic virome), bacteriophages that infect bacteria (bacterial virome), viruses that infect archaea (archaeal virome), and virus-derived genetic elements in host chromosomes, as well as the mycobiome and other members of the meiofauna such as protists and metazoans (Virgin, 2014). They can be « hidden » into neurons, hematopoietic cells, stem cells, vascular endothelial cells, and likely many additional cell types. Specifically, there are chronic viruses that may be considered commensals, and those viruses are thought to alter disease susceptibility via significant effects on their host, independent of their role as pathogens. Our hypothesis is that these viruses could shape the preimmune repertoire, and explain some of the diversity in immune responses

observed among individuals. One example is the cytomegalovirus, which infects half of a healthy adult population, and has dramatic effects on CD8<sup>+</sup> naive/memory T cell phenotypes.

In the context of a French scientific initiative, financed by the Investissement d'Avenir as part of a Laboratoire d'Excellence (LabEx) research program, the Milieu Intérieur Consortium was developed with the objective to define the determinants of human immune variance. The aim was to define the genetic and environmental factors that contribute to the observed heterogeneity in immune responses. To this purpose, 1000 healthy volunteers, descendants of mainland French persons for at least three generations, split equally by sex (1:1 sex ratio) and stratified across five-decades of life were recruited. For which concern analysis of environmental factors, the study included a large questionnaire with detailed questions addressing sociodemographic factors, personal and familial history of disease, smoking and alcohol habits, sport activities, as well as some nutritional aspects. In term of viral history, we know the serologic status of the donors for viruses that were defined as excluding factors (i.e. IgG anti-HIV1/2, IgG anti-HCV, and anti-HbS antigen to exclude ongoing HBV chronic infection), as well as IgG titers for CMV, HTLV1 and Influenza. We are now planning to extend this analysis to (i) other persistent pathogens such as EBV (IgG EBNA, IgG VCA), HSV1/2, VZV, toxoplasmosis, helicobacter pilori, and (ii) pathogens that are included into vaccines commonly used in the French population (HBV IgG anti-HbS and anti-HbC, Smallpox). The aim is to generate a personalized map of previous stimulations with either pathogens or vaccines, and to get insights into the impact of these events – as well as their sequential order – on phenotypic and functional aspects of the immune system.

# Methods

---



# I. GENERATION OF pMHC CLASS I TETRAMERS THROUGH LIGAND EXCHANGE.

This unit presents a set of linked protocols from Ton Schumacher's laboratory, adapted by Cécile Alanio and Matthew Buckwalter with the help of Fabrice Lemaitre and Philippe Bousso, and later optimized by Vincent Bondet. It can be used to create large collections of recombinant MHC class I molecules loaded with peptides of interest. The collections of peptide-MHC (pMHC) complexes that can be produced by this method are useful for two major purposes. First, the measurement of MHC binding affinity of a set of potential MHC ligands. Second, the production of large collections of MHC tetramers to measure antigen-specific T cell responses by MHC tetramer flow cytometry.

The first basic protocol describes the expression and purification of recombinant MHC class I heavy and light chains. The second basic protocol describes the refolding and biotinylation of MHC class I complexes that are occupied with a conditional ligand. The third protocol describes how such MHC class I complexes that are occupied with conditional ligands can be utilized to produce pMHC complexes of interest in UV-induced peptide exchange reactions. The fourth basic protocol describes an ELISA-based strategy to measure the binding of peptides of interest to 'empty' MHC complexes generated by UV exposure. The fifth basic protocol describes how MHC complexes generated by ligand exchange can be used to produce MHC tetramers for T cell staining. One support protocol is included that describe the measurement of biotinylation efficiency.

The technology that is described in this unit has been developed for the human MHC alleles HLA-A\*0101, -A\*0201, -A\*0301, -A\*1101 and -B\*0702 (Toebe et al., 2006; Rodenko et al., 2006; Bakker et al., 2008) and the mouse alleles H-2Db, Kb and Ld (Toebe et al., 2006; Frickel et al., 2008; Grotenbreg et al., 2008), and it should be possible to extend it to other MHC alleles. HLA molecules that are loaded with UV sensitive peptide are also available through commercial sources (see background information), providing an alternative to some of the protocols described in this Unit.

## ***BASIC PROTOCOL 1***

### **BACTERIAL EXPRESSION AND PURIFICATION OF HLA CLASS I HEAVY CHAINS AND HUMAN $\beta$ 2M (4 DAYS)**

A soluble version of the MHC class I heavy chain containing a COOH-terminal biotinylation sequence (biotag) accepted by the Bir A biotin ligase and h $\beta$ 2m are both produced by expression in E coli and are isolated as inclusion bodies. The procedure detailed below for HLA-A\*0201 is based on that first described by Garboczi et al. (Garboczi et al., 1992) and can be used for different human and mouse MHC class I alleles.

#### ***Materials:***

- Luria-Bertani (LB) medium (6L, RT)
- Carbenicillin (diluted in water, 1 000X stock 50mg/mL at -20°)
- Chloramphenicol (diluted in ethanol, 1 000X stock 34mg/mL at -20°)
- LB plates + antibiotics (Cf= 50  $\mu$ g/mL carbenicillin, 34  $\mu$ g/mL chloramphenicol; 500mL = 16 plaques; 4°)
- Singles Competent Cells (50  $\mu$ l reactions, -80°): E.Coli expression strain BL21 (DE3) pLysS
- SOC medium (4°)
- 1-S-Isopropyl- $\beta$ -(D)-thiogalactopyranoside (IPTG) 1M: 2,38g in 10mL H<sub>2</sub>O (-20°)
- Lysozyme (powder, -20°)
- DL-Dithiothreitol (DTT) 1M: 1,54g in 10mL H<sub>2</sub>O (-20°)
- MgCl<sub>2</sub> 1M (RT)
- Saccharose (powder)
- Triton X-100 (RT)
- EDTA 0,5M (RT)
- Tris-HCl 1M pH8 (60,6g Trizma base in 500mL H<sub>2</sub>O, +HCl until pH8, stored at RT)
- Sodium Azide 10% (RT)
- NaCl 1M (29,22g in 500mL H<sub>2</sub>O, RT)
- Guanidine-HCl 8M (RT)
- Glycerol (RT)
- MilliQ H<sub>2</sub>O (RT)
  
- DNase I 2 mg/mL : 16mg DNase I + 4 mL glycerol (50 %) + 600  $\mu$ l NaCl 1M (75mM) + 3,4mL H<sub>2</sub>O ; stored at -20°C.
- Resuspension buffer: 50 mM Tris-HCl pH8, 25% sucrose, 1 mM EDTA, 0,1% azide, DTT 10mM.  
For 500ml : 25mL Tris-HCl 1M pH8 (50mM) + 125g saccharose (25%) + 1mL EDTA 0,5M (1mM) + 5mL azide 10% (0,1%) + eau QSP 500mL.
- Detergent buffer: 50 mM Tris-HCl pH8, 100mM NaCl, 1 mM EDTA, 0,5% Triton-X-100, 0,1 % azide, DTT 1mM.  
For 500mL : 25mL Tris-HCl 1M pH8 (50mM) + 50mL NaCl 1M (100mM) + 1mL EDTA 0,5M (1mM) + 5mL azide 10% (0,1%) + 2,5mL Triton-X-100 (0,5%) + eau QSP 500mL. Add 50  $\mu$ l/50mL of 1M DTT (1mM) just before use.

- Wash buffer: idem detergent buffer but without Triton.
- 1-10 ng/μl MHC-BSP expression constructs, reconstituted in water or TE buffer (10mM Tris-HCl pH8, 1mM EDTA).

The cDNA sequence encoding amino acid residue 1-100 of human β2m is cloned in pET3a. The cDNA sequence encoding the MHC class I heavy chain without the signal peptide, transmembrane domain and cytoplasmic domain (amino acid residue 1-276 for HLA-A\*0201) is cloned into pMBio5, a derivative of pET3a that encodes an in-frame COOH terminal peptide tag (GSGGSGGSAGGGLNDIFEAKIEW) that serves as a substrate for BirA biotin ligase.

- Incubator + shaker
- Centrifuge
- Spectrophotometer + Plastic cuvettes
- 30mL Corex tubes
- Liquid nitrogen
- Waterbath

**1. (Day 1) MHC class I heavy chains and β2m are expressed separately in the bacterial strain**

BI21 (DE3) pLysS. Transform bacteria according to supplier's protocol (for Novagen Competent Cells, see below) and grow overnight on Luria-Bertani (LB) plates in the presence of 50 μg/ml carbenicillin and 34 μg/mL chloramphenicol.

*Novagen Competent Cells : Transformation Protocol*

- *Remove 2 Single Cell Kits (50ul reaction) from the freezer. Immediately place the tubes on ice, so that all but the cap is immersed in ice. Allow the cells to thaw on ice for 2-5 min. Gently finger-flick (never vortex) the tube 1-2 times.*
- *Add 1 and 2 ul of 1-10ng/ul purified plasmid (diluted in water or in TE buffer : 10mM Tris-HCl, 1mM EDTA, pH8) directly to each of the two aliquots of cells. Stir gently to mix, return the tube to ice, and incubate for 5 min.*
- *Heat the tubes for exactly 30s in a 42°C water bath. Do not shake.*
- *Place the tubes on ice for 2 min.*
- *Add 250ul of RT SOC medium to each tube. Keep the tubes on ice until all have received SOC.*
- *Incubate for 1 hour at 37° while shaking at 250rpm.*
- *Prepare 3 dilutions for each plasmid condition (pure, 1/10, 1/100). Plate on LB medium containing antibiotics for the plasmid-encoded drug resistance (approx. 50uL per plate, 6 plates in total).*
- *Incubate all plates, cover-slide down, overnight at 37°.*

**2. (Day 2) Inoculate 1-2 colonies in 60 ml LB plus antibiotics (60μl carbenicillin at 50mg/ml ; 60μl chloramphenicol at 34mg/ml). Place at 37°, 200rpm, until OD<sub>600nm</sub> is approx. 0.8 (37°C, approx. 4 hrs). Place at 4°C overnight.**

3. (Day 3) After overnight storage of inoculate, dilute 6 x 10mL in 6 x 1 L LB plus antibiotics (1/1000 ; for every 1L : 1ml carbenicillin at 50mg/ml ; 1ml chloramphenicol at 34mg/ml).  
*This protocol describes a 6L expression, which may be scaled up or down accordingly.*
4. Grow bacteria at 37°C to a density of OD<sub>600nm</sub> = 0.6 (this takes 4 to 5 hrs, check regularly, starting after 2 hrs).
5. Add 400 µL of a 1 M IPTG solution in H<sub>2</sub>O (0.4 mM ; can be decreased to 0.05mM depending on each protein !) to each 2L Erlenmeyer containing 1L bacterial culture to induce protein expression (2,4ml for 6L).
6. Grow cells for approximately 4 h at 37°C in an orbital shaker. Then put cells on ice until centrifuge is ready.
7. Harvest the cells by centrifugation at 4°C, 4,000 g for 15 min. Remove all medium.
8. Pool pellets in 6 x 50 mL LB, and spin at 4°C, 4,000 g for 30 min. Remove all medium. Typically 6 L should yields 10-20g of cells.
9. Store cell pellets at -20°C until Day 4 (or for months !).
10. (Day 4) Weigh the cell pellet (the whiter the pellet the better the yield of protein will be).
11. Add 55 ml of Resuspension buffer to approximately 30 g of cells (expected yield from 6 L of bacterial culture) and resuspend well in a plastic beaker.  
*Failure to resuspend well will result in a significantly reduced protein yield.*
12. Add 60 mg lysozyme dissolved in 5 mL Resuspension buffer (V<sub>f</sub> = 50ml, C<sub>f</sub>=1mg/ml).
13. Incubate for 30 min on ice or (preferably) stir in cold room for 30 min.
14. Add 300 µl of 1 M MgCl<sub>2</sub> (5mM) ; 1,5 ml of a 2 mg/mL DNase I (50 µg/mL) ; 600 µl of Triton-X-100 (1%) ; and 600 µl of 1M DTT (10mM).
15. Incubate for 30 min on ice or, preferably, tumble in cold room for 30 min.
16. Sonicate for 2 mins on ice (power 40%, pulses 0,5 sec). Ultra-centrifuge 10 min at 10 000 rpm, 4°C in 4 x 30mL Corex tubes.  
*Make sure your ultra-centrifuge is perfectly equilibrated by weighting the Corex tubes !*
17. Discard the pale orange supernatant. Resuspend in Detergent buffer. First add 2 mL to each tube, vortex or dissociate with a glass stick and transfer to the plastic beacker. Add buffer until 15mL. Add 50 µl/50mL of 1M DTT (1mM) just before use. Sonicate, then ultra-centrifuge 10min at 10 000 rpm, 4° in 1 x 30mL tube.
18. Repeat steps 17 twice or more, until the pellet is white and supernatant translucent.

**19.** Resuspend in 20mL Wash buffer. Add 20 µl/20mL of 1M DTT (1mM). Sonicate.

**20.** Centrifuge at 10,000 rpm, 10min, 4°C. Discard supernatant. Resuspend the pellet in 3,5mL H<sub>2</sub>O, then add 7,5mL 8M guanidine-HCl.

**21.** Spin for 30min at 14,000 rpm. Take supernatant. Measure OD<sub>280nm</sub> (1/100 dilution in 8M guanidine-HCl).

$e$  (280 nm) of HLA A\*0201 (1-276 pMBio) with biotag = 80 750 M-1cm-1.

$e$  (280 nm) of  $\beta$ 2m (1-100) = 19 180 M-1cm-1.

$E$  (280nm) = ((1280 x n Tyr) + (5690 x n Trp) + (120 x n Cys) / MW (Da)

MW  $\beta$ 2m = 13 705 Da ; MW HLA A\*0201 (1-276 pMBio) with biotag = 33 910 Da

$E$   $\beta$ 2m = 1.4 ;  $E$  HLA A\*0201 (1-276 pMBio) with biotag = 2.18

HLA-A\*01:01  $E$  = 2,018

HLA-A\*03:01  $E$  = 2,189

HLA-A\*11:01  $E$  = 2,216

HLA-B\*08:01  $E$  = 2,183

$C(M) = OD / [e (M-1cm-1) \times L (cm)]$ , where L is the length of the cuvette (usually = 1 cm).

$C(mg/mL) = OD / [E \times L (cm)]$ , where L is the length of the cuvette (usually = 1 cm).

**22.** Aliquot per 500 nmoles for A2, and 3 000 nmoles for  $\beta$ 2m (17mg for heavy chains ; 41mg for  $\beta$ 2m) in polypropylene tubes. Keep the tubes on ice while working.

*The use of polypropylene tubes minimizes sticking of peptide or protein to the tube.*

**23.** Snap-freeze aliquots, and store at -80°.

*Inclusion bodies can be stored at -80°C for at least 1 year.*

## BASIC PROTOCOL 2

### REFOLDING, BIOTINYLATION AND PURIFICATION OF MHC CLASS I COMPLEXES WITH CONDITIONAL LIGANDS

The refolding of HLA A\*0201 complexes occupied with conditional ligand is largely based on the procedures established by Garboczi et al. (Garboczi et al., 1992). The conditional ligand used for HLA-A\*0201 is the sequence KILGFVVFJV, in which J indicates the UV sensitive amino acid (See Support protocol 1). Conditional ligands for a series of other MHC class I alleles developed by us and others are listed in Table 1.

HLA A*0101	STAPGJLEY	Bakker et al., 2008
HLA A*0201	KILGFVVFJV	Toebe et al., 2006
HLA A*0301	RIYRJGATR	Bakker et al., 2008
HLA B*0702	AARGJTLAM	Bakker et al., 2008
HLA A*1101	RVFAJSFIK	Bakker et al., 2008
H2-D <sup>b</sup>	ASNENJETM	Toebe et al., 2006
H2-K <sup>b</sup>	FAPGNYJAL	Grotenbreg et al., 2008
H2-L <sup>d</sup>	YPNVNIHJF	Frickel et al., 2008

**Table 1** Conditional ligands described to date. It is likely that most of these ligands can also be utilized for related HLA allele subtypes with the same or a very similar ligand preference (e.g. KILGFVVFJV for HLA A\*0202, A\*0203 etc.), but this has not been tested.

*Molecular weight of the conditional ligand peptides is calculated by adding 89.004 Da to the amino acid at the UV sensitive position. For example, A2 KILGFVFCV MW is 1025.3, so A2 photocleavable peptide molecular weight is 1114.3. But we always assume our 9-mers are MW 1000, so that 10mg/ml corresponds to 10mM, and that works very fine !*

#### Materials:

- Tris-HCl 10mM, pH8 (RT)
- Protease inhibitor cocktail (10X stock : 5 tablets in 50mL H<sub>2</sub>O ; -20° ; stock tablets at 4°)
- EDTA 0,5M (RT)
- Guanidine-HCl 8M (RT)

- L-Arginine (powder)
- Reduced glutathion (powder)
- Oxidized glutathion (powder)
- Phenylmethanesulfonyl fluoride (PMSF 100mM : 0.87g in 50mL isopropanol ; 4°)
- DMSO (RT)
- Photocleavable conditional ligand (powder)
- Biotin ligase : either biotin ligase obtained by E coli expression (B ; see Support protocol 2), either bulk BirA, Avidity, Denver, USA (A) (-80°)
- D-Biotin (B) (5 mM dissolved in 100 mM phosphate buffer, pH 7.5)
- ATP (B) (0.5 M dissolved in 1 M Tris pH 9.5)
- Ligase buffer (10X): 50 mM MgCl<sub>2</sub>, 0.2 M Tris pH 7.5 (B)
- Glycerol (B) (RT)
- MilliQ H<sub>2</sub>O (RT)
  
- Sephadex PD10 columns (PK30).
- Amicon ultrafiltration membrane (Mw cut-off 30 kDa) for pressure filtration.
- Amicon stirred ultrafiltration cells for pressure filtration (Model 8400).
- Nitrogen.
- Amicon Ultra-4 PLTK Ultracel-PL Membrane, 30KDa
- Amicon Ultra-15 PLTK Ultracel-PL Membrane, 30KDa
- HPLC (or FPLC) system with a gel-filtration column, e.g. a HiLoad 16/600 Superdex 200pg. •• PBS pH=7.4 for running buffer
- Centrifuge
- 0.22 µm 500mL Stericups
  
- Dilution buffer (B ; see recipe below ; must be prepared fresh).

Reagent	Amount	Final concentration
1 M Tris-HCl pH 8	50 ml	100 mM Tris-HCl pH 8
L-Arginine	34,8 g	400 mM L-arginine
Reduced glutathione	0,61g	5 mM reduced glutathione
Oxidized glutathione	0,15 g	0.5 mM oxidized glutathione
0.5 M EDTA	2 ml	2 mM EDTA
10X Protease inhibitor cocktail	50 ml	Not applicable
H <sub>2</sub> O (milliQ)	350 ml	Adjust to 500mL final volume

1. (Day 1) Thaw 1x500 nmol MHC Class I heavy chain (3x1 aliquot over 3 days; 3 $\mu$ M final) and 1x3 000 nmol h $\beta$ 2m (1 aliquot; 6 $\mu$ M final). Resuspend each in 1 mL 8M guanidine-HCl.

*To each 500 ml refolding, an aliquot of HLA class I heavy chain corresponding to a 1 $\mu$ M final concentration is added on 3 consecutive days (resulting in an MHC class I heavy chain concentration of 3  $\mu$ M on day 3). Thus, a total of 3 aliquots of 500 nmoles is required to perform a 500 mL refolding.*

*HLA class I heavy chain fractions to be added on Day 2 and 3 should be stored at -20° in 8M guanidine-HCl until use.*

2. Prepare 500mL dilution buffer.

3. Add 0,6mL conditional ligand dissolved in 100 % DMSO (50mM stock ; 60 $\mu$ M final).

4. Set up the 500mL refolding reaction by adding the following components to cold refolding buffer in the critical order indicated below.

a) Add 5mL of 100mM PMSF (1mM final).

*PMSF is very unstable in aqueous solution.*

b) Add slowly the aliquot of 3000 nmoles h $\beta$ 2m (6 $\mu$ M final) to the border of the vortex.

c) Proceed similarly for HLA class I heavy chain (1 aliquot of 500 nmol; 1  $\mu$ M final).

d) Stir slowly O/N at 4° (cold room). Keep dark.

e) (Day 2) Repeat addition of PMSF.

f) Repeat addition of HLA class I heavy chain (1 aliquot of 500 nmol; 1  $\mu$ M final).

g) Stir slowly O/N at 4° (cold room). Keep dark.

h) (Day 3) Repeat addition of PMSF.

i) Repeat addition of HLA class I heavy chain (1 aliquot of 500 nmol; 1  $\mu$ M final).

j) Stir for 48hrs. Keep dark.

*Day 4 : Prepare the concentration step by washing two Amicon ultrafiltration cells with distilled water. Dispose two Amicon ultrafiltration membrane (MW cut-off 30kDa) in two Petri dishes filled with sterile water (glossy part up).*

5. (Day 5) Spin refolding reaction in Falcon 50 at 4500 rpm to sediment aggregates, and filter supernatant on 0.22  $\mu$ m 500mL Stericups.

6. Carefully dispose Amicon ultrafiltration membranes into their support, and prepare the two Amicon ultrafiltration cells. Fill each with 2 x 250mL filtered refolding reaction.

7. Concentrate the refolding reaction to approximately 2 x 10 mL by nitrogen flow concentration (1 bar) over the Amicon ultrafiltration membrane (stir continuously during concentration) in two Amicon stirred ultrafiltration cells.

8. Rinse filter twice with 1 mL of PBS to give about 2 x 12 mL in total. Pool.

9. Wash an Ultra-50 PLTK Ultracel-PL Membrane (Mw cut-off 30 kDa) by placing 3 mL milliQ H<sub>2</sub>O on the filter and spin at 4°C, 4,500 rpm for 2 min. Concentrate the flow through fraction to 1.8mL in the Amicon. Add antiproteases (100ul of the 10X cocktail stock; 20ul of PMSF 100X stocks).

*The desired end volume depends on the HPLC or FPLC system used for subsequent purification.*

10. Purify by gel-filtration HPLC : wash the column with PBS at 1mL/min, then inject refolding reaction using one 2 mL injection on the column with a 2 mL loop (normally max 5mL/run). Collect relevant fractions (approximately 15 mL) and keep the sample on ice.

*Following purification, the sample is generally used immediately for biotinylation. The use of MHC class I complexes stored in glycerol is not recommended as glycerol affects biotinylation efficiency. However, MHC class I complexes occupied by conditional ligand may be stored by snap-freezing in liquid nitrogen without the addition of glycerol.*

11. Wash 6 PD10 columns with 25mL Tris-HCl 10mM pH8. Pass 2,5mL refolding on each column. Discard the flow through. Eluate with 3,5mL of Tris-HCl 10mM pH8.

*You need to exchange PBS to Tris because biotin ligase is inhibited by high concentrations of NaCl and Tris. See also the Avidity website: <http://www.avidity.com/tech-protein.html>.*

12. Wash an Ultra-15 PLTK Ultracel-PL Membrane (Mw cut-off 30 kDa) by placing 3 mL milliQ H<sub>2</sub>O on the filter and spin at 4°C, 4,500 rpm for 2 min. Concentrate the 21ml eluate fraction to 1.2mL in the Amicon (4-5 min).

13. To biotinylate the biotag of the HLA class I heavy chain, you can either use commercially available bulk BirA (A), or either use biotin ligase obtained by E coli expression (Option B).

Option A: Mix 7 volumes of Tris-monomer (1200ul) with 1 volume of Biomix A buffer (171,4), 1 volume Biomix B buffer (171,4), 1 volume Biotin (171,4), and 5µl BirA enzyme (desired final volume < 2ml).

*Option B: Add 1 volume of freshly prepared biotinylation solution to 1 volume of pMHC class I monomer, using 0.03 µM ligase for 1 µM of MHC class I.*

<b>Reagent</b>	<b>Amount</b>
<i>D-biotin (5 mM dissolved in 100 mM phosphate buffer, pH 7.5)</i>	<i>0.04 vol</i>
<i>ATP (0.5 M dissolved in 1 M Tris pH 9.5)</i>	<i>0.04 vol</i>
<i>BirA his-tagged biotin ligase (6.6 μM)</i>	<i>0.01 vol</i>
<i>10x ligase buffer</i>	<i>0.2 vol</i>
<i>EDTA-free protease inhibitor cocktail (25x: 1 tablet in 2 mL H<sub>2</sub>O exchange buffer)</i>	<i>0.08 vol</i>
<i>H<sub>2</sub>O (MilliQ)</i>	<i>0.63 vol</i>

*Prepared fresh and ensure that ATP is dissolved in Tris buffer.*

**14.** Incubate overnight at RT.

**15.** (Day 6) Purify by gel-filtration HPLC (or FPLC) : wash the column with PBS at 1mL/min, then inject refolding reaction using one 2 mL injection on the column with a 2 mL loop (normally max 5mL/run). Collect the biotinylated HLA class I molecules. Keep the sample on ice.

**16.** Wash an Ultra-4 PLTK Ultracel-PL Membrane (Mw cut-off 30 kDa) by placing 4 mL milliQ H<sub>2</sub>O on the filter and centrifugation at 4°C, 4,500 rpm for 2 min. Discard H<sub>2</sub>O, add sample (2 times 4 mL?) and concentrate the sample on the membrane filter to a volume of 3 mL.

**17.** Recover concentrated sample, rinse the filter once with 50 μL PBS, and add to concentrated sample.

**18.** Measure protein concentration at OD<sub>280nm</sub>.

*From a 500 ml refolding, a final amount of around 5mg biotinylated monomer is usually obtained, depending on the refolding efficiency.*

**19.** Aliquot at 1mg/mL (50μg in 50μl final volume) in PBS in polypropylene Starstedt tubes.

*Biotinylated MHC class I molecules (Mw 47 kDa) with a final concentration of approximately 1 mg/mL can be stored at -20°C for up to 1 year, or at -80° and LN for years. Biotinylation reactions performed according to the protocol above should give complete or near-complete biotinylation of the tagged MHC class I heavy chain. It is nevertheless recommended to verify the degree of biotinylation for every batch of MHC class I before further use. See Support protocol 3.*

## **BASIC PROTOCOL 3**

### **UV MEDIATED PEPTIDE EXCHANGE**

UV-mediated cleavage of the conditional ligand is time dependent. With the set-up described below, peptide cleavage is detected after 1 min and is essentially complete after approximately 15 min. A 30 to 60 min incubation time is normally used to ensure optimal exchange of the conditional ligand with the peptide of interest. Protein concentration may influence the rate of UV-mediated cleavage, as both the nitrophenyl moiety and the reaction product absorb long wavelength UV light. In addition, path length may affect the reaction speed. Empty, peptide receptive MHC molecules that are formed upon UV exposure can be rescued by performing the UV-mediated cleavage in the presence of an MHC ligand of interest. In most experiments, a 100 fold molar excess of peptide over MHC is used. UV-induced peptide exchange is routinely performed using 25 µg/mL of UV sensitive MHC class I complexes. However, peptide exchange reactions have been performed with MHC class I concentrations up to 100 µg/mL.

#### **Materials:**

- 96 well plates (polypropylene microplate 96 well V sharp, BD)

*Use polypropylene material to avoid sticking of peptide or protein to the plate.*

- UV-lamp 366 nm CAMAG UV fitted with UV Lamp long-wave UV, 366 nm, 2x8 W

*The use of short wavelength (254 nm) or broad-band UV lamps is detrimental to the MHC complex and should be avoided at all times.*

- Centrifuge with rotor for microtiter plates.

Work on ice to avoid proteases + dark during all the steps.

Work on polypropylene plates to avoid sticking of peptide or protein to the plate.

1. Calculate total volume of monomer you will need to exchange ( $C_i=400\text{nM}$  ;  $C_f = 20\text{nM}$  ; so usually 5ul in 100ul for 1 staining).

*Be aware that only 60-80% of the starting volume will be left at the end due to evaporation.*

2. Prepare appropriate quantity of p\*monomer + 1X PBS mix :

*i.e.  $V_i = C_f (0.1\mu\text{M} = 0.1\text{mg/ml}) \times V_f (\text{that you need}) / C_i$  (look on the aliquot : usually around 1mg/ml)*

*For more detailed protocol, see « 2012-04-01 Protocol 7 colors CA » and related files.*

3. In a 96 well plate, add the following reagents to each well:

- Exchange Peptide (10mM stock in DMSO, 50X, -20° ;  $C_f=200\mu\text{M}$ )

*9-mers peptides can be approximated to have a  $M_w = 1000$ , so 10mM stocks = 10mg/mL. They are reconstituted in 100% DMSO.*

*They are used at 1/50 dilution, so 0.1ul of the stock in each 5ul p\* monomer volume.*

- Then immediately add diluted photocleavable monomer (from step 2) on the top, and pipette up and down 5 times.

*As peptides are in very small volumes, they evaporate, so you should do this procedure 3 peptides at a time (pipette 3 peptides, add monomers, then 3 more peptides, etc...)*

**4.** Place the 96-well plate under a UV lamp (366nm) for 1 hr in the cold room, with a distance between the UV lamp and sample of approximately 5 cm.

*Temperature of the solution may rise to approximately 30 °C, avoid overheating.*

**5.** Spin the plate (with parafilm) at 4500rpm for 15 minutes (4°). Transfer supernatant (keep the plate at an angle to avoid transferring any pellet) to a new polypropylen 96 well plate for downstream applications.

*Be aware that only 60-80% of the starting volume will be left due to evaporation.*

*Resulting MHC complexes may be used to determine exchange efficiency by MHC ELISA (Basic protocol 4), or to produce MHC tetramers for T cell detection (Basic protocol 5).*

## ***BASIC PROTOCOL 4***

### **MEASURING PEPTIDE-MEDIATED MHC STABILIZATION BY HLA ELISA**

This protocol describes an ELISA that measures the concentration of correctly folded HLA class I molecules. This assay can be used to verify the success of routine peptide exchange reactions, i.e. to ensure that the HLA ligand of choice indeed rescued the HLA class I complex, but can also be used for high-throughput screening of potential MHC ligands. Depending on the number of epitopes that is screened, the assay can be performed both in a 96 (described below) or a 384 well format. A 96 well-based assay is also available commercially (see Background information).

The HLA ELISA (described here for HLA-A\*0201) measures the concentration of HLA class I complexes in the range of 0.5 to 10 nM. It is recommended to include a standard MHC titration curve, to ensure that the obtained absorbance values are within the linear range of the assay. UV-irradiation of the UV-sensitive HLA A\*0201-KILGFVFI complex leads to a reduction of the absorbance signal of approximately 70-80% and an estimated reduction in concentration of folded HLA of 85%. This reduction is comparable to the reduction in HLA concentration as detected by gel-filtration chromatography. It is important to note that this assay will generally underestimate the extent of peptide cleavage, which is usually complete (see anticipated results). Inclusion of a high affinity HLA A\*0201 restricted ligand in UV-mediated exchange reactions leads to recovery of 80-100% of the original ELISA signal. Lower rescue is observed using peptides with a moderate to low affinity for HLA A\*0201.

#### **Materials:**

- Nunc immuno plate 96 wells (cat. #: 439454, F96 CERT Maxisorp, Nunc)
- Absorbance plate reader
- Coating solution: 2 µg/mL streptavidin (cat. #: S888, Invitrogen, Molecular probes) in PBS
- Wash buffer: 0.05% Tween 20 (cat. #: P1379, Sigma-Aldrich) in PBS
- Blocking buffer: 2% BSA (cat. #: A-7030, Sigma-Aldrich) in PBS
- Horseradish peroxidase (HRP)-conjugated anti-human β2m antibody

*We have used directly conjugated rabbit anti-human β2m antibody from DakoCytomation (cat. #: P0174), but alternatives may be used.*

- Developing reagent:
  - 10x substrate buffer
  - 50x 2',2'-azino-bis (3-ethylbenzthiazoline-6-sulphonic acid) diammonium salt (ABTS) solution

- 100x H<sub>2</sub>O<sub>2</sub> solution

Stop buffer

*We have used custom-produced developing reagent and stop buffer from Sanquin Reagents. Alternatives are available but have not been tested.*

1. In a 96 well plate, add 100 µL of 2 µg/mL streptavidin in PBS per well.

2. Incubate for 2 hr at 37 °C or overnight at RT. Cover the plate to avoid evaporation and contamination.
3. Wash 4 times with wash buffer, 300 µL per well, discarding the wash buffer after each wash.
4. Add blocking buffer, 300 µL per well.
5. Incubate for 30 min at RT. Cover the plate with a lid.
6. Dilute HLA class I samples to a final concentration of 5nM. Prepare 250 µL of each HLA class I complex to allow analysis in duplicate.
7. Tip out blocking buffer. Add 100 µL per well of diluted HLA class I solutions from experimental samples or of standard HLA class I dilutions to obtain a standard-titration curve.

To generate a standard titration-curve: Add dilutions of a stock of HLA class I in a concentration range of 0.08 to 40 nM. Refolded HLA A\*0201– GILGFVFTL (influenza A Matrix 1(58-66) epitope) may for instance be used as a standard HLA class I complex, but any stable HLA class I complex should suffice. Concentration of this standard HLA class I complex is determined by absorbance at 280 nm.

8. Incubate the plate for 1 h at 37 °C. Cover the plate with a lid.
9. Wash 4 times with wash buffer, 300 µL per well, discarding the wash buffer after each wash. Carefully dry plates by tipping out excess liquid on a tissue.
10. Add HRP conjugated anti-β2m antibody solution (1 µg/mL in blocking buffer), 100 µL per well.
11. Incubate the plate for 1 h at 37 °C. Cover the plate with a lid.
12. Wash 4 times with wash buffer, 300 µL per well.
13. Prepare 10 mL ABTS coloring solution for each 96 well plate by mixing:
  - 8.7 mL H<sub>2</sub>O
  - 1 mL 10x substrate buffer
  - 200 µL 50x ABTS solution
  - 100 µL 100x H<sub>2</sub>O<sub>2</sub> solution (3%)
14. Add 100 µL of ABTS coloring solution per well.
15. Incubate for 10-15 min at RT. Monitor color development by eye.
16. Block the reaction by adding 50 µL of stop buffer per well.

**17.** Measure absorbance at 405 nm in a plate reader.

*A 384-well ELISA may also be used to measure HLA class I stabilization by added ligands. In our hands the assay is somewhat more sensitive in this format (possibly a reflection of a different dynamic range of the plate reader used) and pHLA class I complexes should be diluted to a final concentration of 1.6 nM. All reaction steps are performed using 25 uL/well, blocking and washing steps using 100 uL/well, and stop buffer is added in 12.5 uL/well.*

## **BASIC PROTOCOL 5**

### **TETRAMERIZATION OF MHC CLASS I MOLECULES**

MHC class I complexes may be complexed with fluorophore-labeled streptavidin to form MHC class I tetramers for T cell analysis. Commonly used fluorophores include allophycocyanin and phycoerythrin, and the formation of MHC tetramers with these conjugates is described below. However, streptavidin-coated quantum dots may also be used to prepare MHC tetramers for T cell detection.

We strongly recommend to first determine the efficiency of biotinylation of the UV-sensitive HLA class I batch, as described in Support protocol 3. In case biotinylation is found to be complete or near complete, tetramerization of peptide-MHC class I complexes obtained by UV-induced exchange is performed as described below.

#### **Materials:**

- PE-streptavidin solution 1 mg/mL (cat. #: S866, Molecular Probes) or any fluorochrome-linked streptavidin solution at 1 mg/mL (APC, PE-Cy7, Qdots,...)

*If Streptavidin-Qdots are used, spin the mat 10,000rpm, 2min, 4° before use, and take the top portion.*

- Polypropylene plates with exchanged MHC class I complexes prepared according to Basic protocol 3, containing 100 µg/mL of exchanged pMHC in a given volume/well.

1. Add appropriate amount of streptavidin-fluorochrome into each well of a new polypropylene plate.

*Appropriate amounts are ideally calculated following titration of the streptavidin-fluorochrome on CD8-biotin antibodies. Usually we use these reagents at 1/10 ratio, meaning 1ul in 10ul pMHC volume.*

2. Immediately add exchanged monomer on top, pipette up and down 5 times.

3. Cover the plates with aluminium.

4. Incubate 30mn (or longer is fine).

*It may be better to add the total streptavidin amount in four different time-points (10mn intervals), or in ten different time-points (5mn intervals), instead of only once, but one addition works.*

5. Prepare a 20X D-biotin solution from the 200X stock by adding PBS.
6. The wells might have different volumes. Choose the one with the highest volume, and calculate the amount of 20X D-biotin to add (1ul for 20ul).
7. Cover the plates with aluminium. Incubate 20mn on ice (or longer is fine, usually we do it overnight).

*MHC tetramers can then be used directly for T cell staining or can be stored at  $-20^{\circ}\text{C}$ . In the latter case, BSA and glycerol are added to a final concentration of 0.5 % and 16 %, respectively. Typically, 5  $\mu\text{L}$  of MHC tetramer is used for the staining of approx  $10^6$  cells in 100  $\mu\text{L}$  FACS buffer.*

## **SUPPORT PROTOCOL**

### **DETERMINATION OF BIOTINYLATION EFFICIENCY**

The degree of biotinylation of MHC class I molecules can be determined by incubation of biotinylated MHC class I molecules with streptavidin and subsequent analysis of samples by SDS-Page electrophoresis. In case of full biotinylation, all MHC class I molecules should be bound to streptavidin when an excess of streptavidin is used (more than one streptavidin molecule per four MHC class I molecules), resulting in a shift in retention time of streptavidin and the complete disappearance of the monomeric MHC class I band in the gel (Fig. 3).

#### **Materials:**

- PE-streptavidin solution 1 mg/mL (cat. #: S866, Molecular Probes) or APC-streptavidin solution 1 mg/mL (cat. #: S868, Molecular Probes)
- 10x UV-sensitive MHC monomer (250 µg/mL; ~5 µM)
- PBS
- polypropylene microtubes 1.5 mL with cap (cat. #: 72692, Sarstedt)
- SDS-Page electrophoresis material

1. To determine the optimal ratio of streptavidin conjugate and HLA class I complex, prepare the following 4 samples in a total volume of 100ul in 1.5 mL tubes :

1. UV-sensitive HLA class I monomer (Cf = 5 nM)
2. UV-sensitive HLA class I monomer (Cf = 5 nM) + streptavidin-PE solution 1/100
3. UV-sensitive HLA class I monomer (Cf = 5 nM) + streptavidin-PE solution 2/100
4. UV-sensitive HLA class I monomer (Cf = 5 nM) + streptavidin-PE solution 4/100

2. Analyze each sample on SDS-Page electrophoresis under reducing and non denaturing conditions.

*This analysis will reveal the fraction of HLA class I that is maximally bound by streptavidin and this number can be used to calculate the optimal ratio of HLA class I and streptavidin conjugate, that gives high order tetramers, while leaving little residual monomeric HLA class I present. It is noted that an excess of fluorochrome-streptavidin over HLA class I results in the formation of HLA class I tetramers with a lower valency and the binding of such lower order tetramers to antigen-specific T cells is poor. In addition, a failure to saturate the available biotin-binding sites can lead to spurious background signal in case biotinylated antibodies are used for co-staining.*

#### **Time Considerations**

The time required to produce a batch of refolded MHC class I occupied with UV sensitive ligand (Basic protocol 1 and 2) is fairly significant, but not different from that required to produce a batch of MHC class I occupied with any other peptide ligand. The actual ligand exchange process (Basic protocol 3) is extremely

straightforward, allowing one to produce collections of hundreds of different peptide-MHC complexes in a timespan of hours. The time required for the measurement of MHC class I stabilization by ELISA (Basic protocol 4) is restricted to several hours, and formation of MHC tetramers (Basic protocol 5) can likewise be completed within hours.

## II. TAME PROTOCOL

### Purpose

To achieve a 100-fold enrichment of antigen specific T cells from human peripheral blood. More details about the procedure can be found in (Alanio et al., 2013).

### Materials

- Fresh or Frozen human PBMCs of known haplotype
- PE - labeled tetramers
- Anti-PE microbeads (Miltenyi Biotec)
- Pulldown buffer (PB): PBS 1X (Gibco)+ 5% Human Serum Albumin 20% (PAA Laboratories) + 5% Citrate Dextrose Anticoagulant (ACD; Sigma-Aldrich)
- MS MACS Separation columns, magnets, stands (Miltenyi Biotec)
- FcR Blocking Reagent (Miltenyi Biotec)
- BD Falcon Cell Strainer 70µm (BD Biosciences)
- DUMP channel mix of antibodies (CD14, CD16, CD19, CD56– PacBlue)
- Dapi Nucleic Acid Stain (Invitrogen)
- Cocktail of antibodies for characterization of T cells (For example CD8 Amcyan, CD11a FITC, CD3 PerCP, CD45RA PE-Cy7)

### Protocol

1. Count and aliquot cells into 15ml Falcon tubes.

*Depending on expected precursor frequency, use 10 – 200 million PBMCs (for a typical pulldown of naive cells, 100 million will give you a sensitivity of 10<sup>-7</sup>)*

2. Wash cells once at 1300rpm for 8mins (4°) and resuspend in 80µl pulldown buffer (PB).

3. Add 10µl of FcR Blocking Reagent (Miltenyi) .

4. Vortex and incubate for 15mins at 4° .

5. Add Tetramers at Cf=20nM (10µl per 100µl PB for our preparations)

*If the experiment includes several tetramers in different colors, add all of them at this step, and adjust PB volumes accordingly.*

6. Vortex gently and incubate for 30mins at 4° in the dark.

7. Wash once in 2mL PB, spinning at 1300rpm for 8mins (4°).

8. Resuspend in 400µL PB.

9. Take a 5µL aliquot and place it in 5ml FACS tubes (« Before » fraction).

10. Add 100µL of anti-PE microbeads (Miltenyi).

11. Vortex and incubate for 20mins at 4° in the dark.

12. Wash twice in 2mL PB at 1300rpm for 8mn (4°).

13. During the wash steps, prepare MS columns (one per Falcon15 tube) on a magnet support. Clean each column with 1000µL of PB (throw away the first elution). Prepare Falcon15 tubes for collecting first flow through fraction.

14. Resuspend each sample in 1000µL PB.

15. Load columns with 1mL of cells.

*You need to filter your cells just before loading to the column (BD Falcon Cell Strainer 70 $\mu$ m).*

16. Wait until the sample is completely passed.
17. Add 1mL of PB to the initial Falcon15 tube (Wash step to get every last cell).
18. Load column with this fraction.
19. Wait until the sample is completely passed.
20. Collect first flow through fraction and load it into column a second time.
21. Wait until the sample is completely passed.
22. Add 1mL of PB to the initial Falcon15 tube (Wash step to get every last cell).
23. Wash the column with 1mL of PB.
24. Wait until the sample is completely passed.

*The flow through is your Depleted Fraction.*

25. Remove successively each MS column.
26. Each time, pull each in Falcon15 tubes , add 2mL of PB to the upper fraction of the column, push the piston, and discard the colum.

*You obtain the Enriched Fraction.*

27. Spin Depleted and Enriched samples at 1300rpm for 8mins (4°).
27. Stain them and analyse on FACS machine using standard procedures.

*Set your stopping gate at 2 000 000 events on Single cells (SSC-AlongSSC-Wlow). Acquire the entire sample for Enriched fraction (adding PBS several times).*



# Manuscripts

---



**Cécile Alanio**, F.Lemaitre, H.Law, M.Hasan, Matthew L. Albert. Enumeration of human antigen-specific naive CD8<sup>+</sup> T cells reveals conserved precursor frequencies. **Blood** **2010**; 115 (18):3718-3725.

*This manuscript contains results presented in Chapter 2.*

**Cécile Alanio**, I.Bouvier, H.Jusforgues-Saklani, Matthew L. Albert. Tracking antigen-specific T cells using MHC Class I tetramers. **Methods in Molecular Biology** **2013**; 960:309-26.

*This book chapter complete results presented in Chapter 2.*

**Cécile Alanio**, Sultanik P, Flecken T, Perot B, Gowry M, Duffy D, Lim A, Clave E, van Buuren MM, Schnuriger A, Garbarg-Chenon A, Bousquet L, Mottez E, Schumacher TN, Toubert A, Appay V, Heshmati F, Thimme R, Pol S, Mallet V, Albert ML. Bystander hyperactivation of preimmune CD8<sup>+</sup> T cells in chronic HCV patients can be reversed by viral clearance. **Submitted**.

*This manuscript contains results presented in Chapter 3.*

Philippe Sultanik, Casrouge A, **Alanio C**, Mottez E, Rosa-Hézode I, Hézode C, Renard P, Bousquet L, Uzé G, Pol S, Albert ML, Mallet V. Baseline sensitivity of T cells to alpha-interferon correlates with sustained virological response to alpha-IFN-based triple therapy in chronic hepatitis C virus infection — ANRS 11416. **J Viral Hepatitis** **2014**.

Stéphanie Thomas, Rouilly V, Patin E, **Alanio C**, Dubois A, Delval C, Marquier LG, Fauchoux N, Sayegrih S, Vray M, Duffy D, Quintana-Murci L, Albert ML, for The Milieu Intérieur Consortium. *The Milieu Intérieur* study – a resource for study of human immunologic variance. **Clinical Immunology** **2**



## References

---



- Acierno, P., Newton, D., Brown, E., Maes, L., Baatz, J., and Gattoni-Celli, S. (2003). Cross-reactivity between HLA-A2-restricted Flu-M1:58-66 and HIV p17 Gag:77-85 epitopes in HIV-infected and uninfected individuals. *J Transl Med* *1*, 3.
- Agace, W.W. (2006). Tissue-tropic effector T cells: generation and targeting opportunities. *Nat Rev Immunol* *6*, 682–692.
- Ahmed, M., Lanzer, K.G., Yager, E.J., Adams, P.S., Johnson, L.L., and Blackman, M.A. (2009). Clonal expansions and loss of receptor diversity in the naive CD8 T cell repertoire of aged mice. *J Immunol* *182*, 784–792.
- Ahmed, R., and Rouse, B.T. (2006). Immunological memory. *Immunol Rev* *211*, 5–7.
- Alanio, C., Lemaitre, F., Law, H.K.W., Hasan, M., and Albert, M.L. (2010). Enumeration of human antigen-specific naive CD8<sup>+</sup> T cells reveals conserved precursor frequencies. *Blood* *115*, 3718–3725.
- Alanio, C., Bouvier, I., Jusforgues-Saklani, H., and Albert, M.L. (2013). Tracking antigen-specific CD8<sup>+</sup> T cells using MHC class I multimers. *Methods Mol Biol* *960*, 309–326.
- Albert, M.L., Decalf, J., and Pol, S. (2008). Plasmacytoid dendritic cells move down on the list of suspects: In search of the immune pathogenesis of chronic hepatitis C. *Journal of Hepatology* *49*, 1069–1078.
- Altman, J.D., Moss, P.A., Goulder, P.J., Barouch, D.H., McHeyzer-Williams, M.G., Bell, J.I., McMichael, A.J., and Davis, M.M. (1996). Phenotypic analysis of antigen-specific T lymphocytes. *Science* *274*, 94–96.
- Altman, J.D., and Davis, M.M. (2003). MHC-peptide tetramers to visualize antigen-specific T cells. *Curr Protoc Immunol Chapter 17*, Unit17.3.
- Anderson, K.G., Sung, H., Skon, C.N., Lefrancois, L., Deisinger, A., Vezys, V., and Masopust, D. (2012). Cutting Edge: Intravascular Staining Redefines Lung CD8 T Cell Responses. *The Journal of Immunology* *189*, 2702–2706.
- Andrian, von, U.H., and Mackay, C.R. (2000). T-cell function and migration. Two sides of the same coin. *N Engl J Med* *343*, 1020–1034.
- Annunziato, F. (2006). CXCR3 and E7 integrin identify a subset of CD8<sup>+</sup> mature thymocytes that share phenotypic and functional properties with CD8<sup>+</sup> gut intraepithelial lymphocytes. *Gut* *55*, 961–968.
- Annunziato, F., Romagnani, P., Cosmi, L., Lazzeri, E., and Romagnani, S. (2001). Chemokines and lymphopoiesis in human thymus. *Trends Immunol* *22*, 277–281.
- Appay, V., and Sauce, D. (2014). Naive T cells: the crux of cellular immune aging? *Exp. Gerontol.* *54*, 90–93.
- Appay, V., Dunbar, P.R., Callan, M., Klenerman, P., Gillespie, G.M.A., Papagno, L., Ogg, G.S., King, A., Lechner, F., Spina, C.A., et al. (2002). Memory CD8<sup>+</sup> T cells vary in differentiation phenotype in different persistent virus infections. *Nat Med* *8*, 379–385.
- Ariotti, S., Hogenbirk, M.A., Dijkgraaf, F.E., Visser, L.L., Hoekstra, M.E., Song, J.Y., Jacobs, H., Haanen, J.B., and Schumacher, T.N. (2014). Skin-resident memory CD8<sup>+</sup> T cells trigger a state of tissue-wide pathogen alert. *Science* *346*, 101–105.
- Arman, M., Calvo, J., Trojanowska, M.E., Cockerill, P.N., Santana, M., López-Cabrera, M., Vives, J., and Lozano, F. (2004). Transcriptional regulation of human CD5: important role of Ets transcription factors in CD5 expression in T cells. *J Immunol* *172*, 7519–7529.
- Arstila, T.P., Casrouge, A., Baron, V., Even, J., Kanellopoulos, J., and Kourilsky, P. (1999). A direct estimate of the human alpha T cell receptor diversity. *Science* *286*, 958–961.
- Axtell, R.C., Xu, L., Barnum, S.R., and Raman, C. (2006). CD5-CK2 binding/activation-deficient mice are resistant to experimental autoimmune encephalomyelitis: protection is associated with diminished populations of IL-17-expressing T cells in the central nervous system. *J Immunol* *177*, 8542–8549.

- Badovinac, V., Haring, J., and Harty, J. (2007). Initial T Cell Receptor Transgenic Cell Precursor Frequency Dictates Critical Aspects of the CD8<sup>+</sup> T Cell Response to Infection. *Immunity* *26*, 827–841.
- Bailey, J.R., Laskey, S., Wasilewski, L.N., Munshaw, S., Fanning, L.J., Kenny-Walsh, E., and Ray, S.C. (2012). Constraints on Viral Evolution during Chronic Hepatitis C Virus Infection Arising from a Common-Source Exposure. *J Virol* *86*, 12582–12590.
- Baitsch, L., Baumgaertner, P., Devedre, E., Raghav, S.K., Legat, A., Barba, L., Wieckowski, S., Bouzourene, H., Deplancke, B., Romero, P., et al. (2011). Exhaustion of tumor-specific CD8<sup>+</sup> T cells in metastases from melanoma patients. *J Clin Invest* *121*, 2350–2360.
- Bakker, A.H., Hoppes, R., Linnemann, C., Toebes, M., Rodenko, B., Berkers, C.R., Hadrup, S.R., van Esch, W.J.E., Heemskerk, M.H.M., Ovaa, H., et al. (2008). Conditional MHC class I ligands and peptide exchange technology for the human MHC gene products HLA-A1, -A3, -A11, and -B7. *Proc Natl Acad Sci USA* *105*, 3825–3830.
- Berkley, A.M., Hendricks, D.W., Simmons, K.B., and Fink, P.J. (2013). Recent Thymic Emigrants and Mature Naive T Cells Exhibit Differential DNA Methylation at Key Cytokine Loci. *J Immunol* *190*, 6180–6186.
- Bermppohl, F., Löster, K., Reutter, W., and Baum, O. (1998). Rat dipeptidyl peptidase IV (DPP IV) exhibits endopeptidase activity with specificity for denatured fibrillar collagens. *FEBS Letters* *428*, 152–156.
- Blattman, J.N., Antia, R., Sourdive, D.J.D., Wang, X., Kaech, S.M., Murali-Krishna, K., Altman, J.D., and Ahmed, R. (2002). Estimating the precursor frequency of naive antigen-specific CD8 T cells. *J Exp Med* *195*, 657–664.
- Boehm, T., and Swann, J.B. (2013). Thymus involution and regeneration: two sides of the same coin? *Nat Rev Immunol* 1–8.
- Bogunovic, M., Ginhoux, F., Wagers, A., Loubeau, M., Isola, L.M., Lubrano, L., Najfeld, V., Phelps, R.G., Grosskreutz, C., Scigliano, E., et al. (2006). Identification of a radio-resistant and cycling dermal dendritic cell population in mice and men. *J Exp Med* *203*, 2627–2638.
- Bouneaud, C., Kourilsky, P., and Bousso, P. (2000). Impact of negative selection on the T cell repertoire reactive to a self-peptide: a large fraction of T cell clones escapes clonal deletion. *Immunity* *13*, 829–840.
- Boursalian, T.E., Golob, J., Soper, D.M., Cooper, C.J., and Fink, P.J. (2004). Continued maturation of thymic emigrants in the periphery. *Nature Immunology* *5*, 418–425.
- Bousso, P. (2000). Generation of MHC-peptide tetramers: a new opportunity for dissecting T-cell immune responses. *Microbes Infect* *2*, 425–429.
- Boyman, O., Krieg, C., Homann, D., and Sprent, J. (2012). Homeostatic maintenance of T cells and natural killer cells. *Cell Mol Life Sci* *69*, 1597–1608.
- Braber, den, I., Mugwagwa, T., Vriskoop, N., Westera, L., Mögling, R., de Boer, A.B., Willems, N., Schrijver, E.H.R., Spienburg, G., Gaiser, K., et al. (2012). Maintenance of Peripheral Naive T Cells Is Sustained by Thymus Output in Mice but Not Humans. *Immunity* *36*, 288–297.
- Bretschneider, I., Clemente, M.J., Meisel, C., Guerreiro, M., Streitz, M., Hopfenmüller, W., Maciejewski, J.P., Wlodarski, M.W., and Volk, H.-D. (2013). Discrimination of T-cell subsets and T-cell receptor repertoire distribution. *Immunol Res* *58*, 20–27.
- Brodeur, J.F., Li, S., Damlaj, O., and Dave, V.P. (2009). Expression of fully assembled TCR-CD3 complex on double positive thymocytes: synergistic role for the PRS and ER retention motifs in the intra-cytoplasmic tail of CD3. *Int Immunol* *21*, 1317–1327.
- Buxton, J.A., and Kim, J.H. (2008). Hepatitis A and hepatitis B vaccination responses in persons with chronic hepatitis C infections: A review of the evidence and current recommendations. *Can J Infect Dis Med Microbiol* *19*, 197–202.
- Campion, S.L., Brodie, T.M., Fischer, W., Korber, B.T., Rossetti, A., Goonetilleke, N., McMichael, A.J., and

- Sallusto, F. (2014). Proteome-wide analysis of HIV-specific naive and memory CD4<sup>+</sup> T cells in unexposed blood donors. *J Exp Med* *211*, 1273–1280.
- Casrouge, A., Bisiaux, A., Stephen, L., Schmolz, M., Mapes, J., Pfister, C., Pol, S., Mallet, V., and Albert, M.L. (2011a). Discrimination of agonist and antagonist forms of CXCL10 in biological samples. *Clin Exp Immunol* *167*, 137–148.
- Casrouge, A., Decalf, J., Ahloulay, M., Lababidi, C., Mansour, H., Vallet-Pichard, A., Mallet, V., Mottez, E., Mapes, J., Fontanet, A., et al. (2011b). Evidence for an antagonist form of the chemokine CXCL10 in patients chronically infected with HCV. *J Clin Invest* *121*, 308–317.
- Cheung, K.P., Yang, E., and Goldrath, A.W. (2009). Memory-Like CD8<sup>+</sup> T Cells Generated during Homeostatic Proliferation Defer to Antigen-Experienced Memory Cells. *J Immunol* *183*, 3364–3372.
- Chidgey, A., Boyd, R., and Hugo, P. (2007). The Thymic Niche and Thymopoiesis (Encyclopedia of Life Sciences).
- Chiravuri, M., Lee, H., Mathieu, S.L., and Huber, B.T. (2000). Homodimerization via a leucine zipper motif is required for enzymatic activity of quiescent cell proline dipeptidase. *J Biol Chem* *275*, 26994–26999.
- Christopherson, K.W. (2003). Cell surface peptidase CD26/DPPIV mediates G-CSF mobilization of mouse progenitor cells. *Blood* *101*, 4680–4686.
- Christopherson, K.W., Hangoc, G., Mantel, C.R., and Broxmeyer, H.E. (2004). Modulation of hematopoietic stem cell homing and engraftment by CD26. *Science* *305*, 1000–1003.
- Ciofani, M., and Zúñiga-Pflücker, J.-C. (2006). A survival guide to early T cell development. *Immunol Res* *34*, 117–132.
- Clark, R.A. (2015). Resident memory T cells in human health and disease. *Sci Transl Med* *7*, 269rv1.
- Clave, E., Busson, M., Douay, C., Peffault De Latour, R., Berrou, J., Rabian, C., Carmagnat, M., Rocha, V., Charron, D., Socie, G., et al. (2009). Acute graft-versus-host disease transiently impairs thymic output in young patients after allogeneic hematopoietic stem cell transplantation. *Blood* *113*, 6477–6484.
- Coulie, P.G., Karanikas, V., Lurquin, C., Colau, D., Connerotte, T., Hanagiri, T., Van Pel, A., Lucas, S., Godelaine, D., Lonchay, C., et al. (2002). Cytolytic T-cell responses of cancer patients vaccinated with a MAGE antigen. *Immunol Rev* *188*, 33–42.
- Cukalac, T., Chadderton, J., Zeng, W., Cullen, J.G., Kan, W.T., Doherty, P.C., Jackson, D.C., Turner, S.J., and La Gruta, N.L. (2014). The Influenza Virus-Specific CTL Immunodominance Hierarchy in Mice Is Determined by the Relative Frequency of High-Avidity T Cells. *J Immunol* *192*, 4061–4068.
- Dalloul, A. (2009). CD5: A safeguard against autoimmunity and a shield for cancer cells. *Autoimmunity Reviews* *8*, 349–353.
- Dang, N.H., Torimoto, Y., Deusch, K., Schlossman, S.F., and Morimoto, C. (1990). Comitogenic effect of solid-phase immobilized anti-1F7 on human CD4 T cell activation via CD3 and CD2 pathways. *J Immunol* *144*, 4092–4100.
- Dar, W.A., and Knechtle, S.J. (2007). CXCR3-mediated T-cell chemotaxis involves ZAP-70 and is regulated by signalling through the T-cell receptor. *Immunology* *120*, 467–485.
- Davis, M.M., Altman, J.D., and Newell, E.W. (2011). Interrogating the repertoire: broadening the scope of peptide–MHC multimer analysis. *Nat Rev Immunol* *11*, 551–558.
- De Meester, I., Korom, S., Van Damme, J., and Scharpe, S. (1999). CD26, let it cut or cut it down. *Immunol Today* *20*, 367–375.
- De Rosa, S.C., Herzenberg, L.A., Herzenberg, L.A., and Roederer, M. (2001). 11-color, 13-parameter flow cytometry: identification of human naive T cells by phenotype, function, and T-cell receptor diversity. *Nature Med* *7*, 245–248.

- Deshpande, P., Cavanagh, M.M., Le Saux, S., Singh, K., Weyand, C.M., and Goronzy, J.J. (2013). IL-7- and IL-15-mediated TCR sensitization enables T cell responses to self-antigens. *J Immunol* *190*, 1416–1423.
- Dong, J., Chen, Y., Xu, X., Jin, R., Teng, F., Yan, F., Tang, H., Li, P., Sun, X., Li, Y., et al. (2013). Homeostatic Properties and Phenotypic Maturation of Murine CD4<sup>+</sup> Pre-Thymic Emigrants in the Thymus. *PLoS ONE* *8*, e56378.
- Dorner, M., Horwitz, J.A., Donovan, B.M., Labitt, R.N., Budell, W.C., Friling, T., Vogt, A., Catanese, M.T., Satoh, T., Kawai, T., et al. (2014). Completion of the entire hepatitis C virus life cycle ingenetically humanized mice. *Nature* *501*, 237–241.
- Douek, D.C., McFarland, R.D., Keiser, P.H., Gage, E.A., Massey, J.M., Haynes, B.F., Polis, M.A., Haase, A.T., Feinberg, M.B., Sullivan, J.L., et al. (1998). Changes in thymic function with age and during the treatment of HIV infection. *Nature* *396*, 690–695.
- Drennan, M.B., Franki, A.S., Dewint, P., Van Beneden, K., Seeuws, S., van de Pavert, S.A., Reilly, E.C., Verbruggen, G., Lane, T.E., Mebius, R.E., et al. (2009). Cutting Edge: The Chemokine Receptor CXCR3 Retains Invariant NK T Cells in the Thymus. *J Immunol* *183*, 2213–2216.
- Duffy, D., Rouilly, V., Libri, V., Hasan, M., Beitz, B., David, M., Urrutia, A., Bisiaux, A., LaBrie, S.T., Dubois, A., et al. (2014). Functional Analysis via Standardized Whole-Blood Stimulation Systems Defines the Boundaries of a Healthy Immune Response to Complex Stimuli. *Immunity* *40*, 436–450.
- Durinx, C., Lambeir, A.M., Bosmans, E., Falmagne, J.B., Berghmans, R., Haemers, A., Scharpe, S., and De Meester, I. (2000). Molecular characterization of dipeptidyl peptidase activity in serum: soluble CD26/dipeptidyl peptidase IV is responsible for the release of X-Pro dipeptides. *Eur. J. Biochem.* *267*, 5608–5613.
- Dzhagalov, I., and Phee, H. (2011). How to find your way through the thymus: a practical guide for aspiring T cells. *Cell Mol Life Sci* *69*, 663–682.
- Ehlert, J.E., Addison, C.A., Burdick, M.D., Kunkel, S.L., and Strieter, R.M. (2004). Identification and partial characterization of a variant of human CXCR3 generated by posttranscriptional exon skipping. *J Immunol* *173*, 6234–6240.
- Erlich, H. (2012). HLA DNA typing: past, present, and future. *Tissue Antigens* *80*, 1–11.
- Favre, D., Stoddart, C.A., Emu, B., Hoh, R., Martin, J.N., Hecht, F.M., Deeks, S.G., and McCune, J.M. (2011). HIV disease progression correlates with the generation of dysfunctional naive CD8<sup>low</sup> T cells. *Blood* *117*, 2189–2199.
- Feghali, C.A., and Wright, T.M. (1997). Cytokines in acute and chronic inflammation. *Front Biosci* *2*, d12–d26.
- Feld, J.J., and Hoofnagle, J.H. (2005). Mechanism of action of interferon and ribavirin in treatment of hepatitis C. *Nature* *436*, 967–972.
- Fenutría, R., Martínez, V.G., Simões, I., Postigo, J., Gil, V., Martínez-Florensa, M., Sintes, J., Naves, R., Cashman, K.S., Alberola-Ila, J., et al. (2014). Transgenic Expression of Soluble Human CD5 Enhances Experimentally-Induced Autoimmune and Anti-Tumoral Immune Responses. *PLoS ONE* *9*, e84895.
- Ferrando-Martínez, S., Franco, J.M., Hernández, A., Ordoñez, A., Gutierrez, E., Abad, A., and Leal, M. (2009). Thymopoiesis in elderly human is associated with systemic inflammatory status. *Age* *31*, 87–97.
- Ferrando-Martínez, S., Romero-Sánchez, M.C., Solana, R., Delgado, J., la Rosa, de, R., Muñoz-Fernández, M.Á., Ruiz-Mateos, E., and Leal, M. (2011). Thymic function failure and C-reactive protein levels are independent predictors of all-cause mortality in healthy elderly humans. *Age* *35*, 251–259.
- Ferrando-Martínez, S., Ruiz-Mateos, E., Hernández, A., Gutiérrez, E., Rodríguez-Méndez, M.D.M., Ordoñez, A., and Leal, M. (2010). Age-related deregulation of naive T cell homeostasis in elderly humans. *Age* *33*, 197–207.
- Fink, P.J. (2013). The biology of recent thymic emigrants. *Annu Rev Immunol* *31*, 31–50.

- Fink, P.J., and Hendricks, D.W. (2011). Post-thymic maturation: young T cells assert their individuality. *Nat Rev Immunol* 11, 544–549.
- Fitzmaurice, K., Petrovic, D., Ramamurthy, N., Simmons, R., Merani, S., Gaudieri, S., Sims, S., Dempsey, E., Freitas, E., Lea, S., et al. (2011). Molecular footprints reveal the impact of the protective HLA-A\*03 allele in hepatitis C virus infection. *Gut* 60, 1563–1571.
- Ford, M.L., Koehn, B.H., Wagener, M.E., Jiang, W., Gangappa, S., Pearson, T.C., and Larsen, C.P. (2007). Antigen-specific precursor frequency impacts T cell proliferation, differentiation, and requirement for costimulation. *J Exp Med* 204, 299–309.
- Frank, C., Mohamed, M.K., Strickland, G.T., Lavanchy, D., Arthur, R.R., Magder, L.S., Khoby, El, T., Abdel-Wahab, Y., Aly Ohn, E.S., Anwar, W., et al. (2000). The role of parenteral antischistosomal therapy in the spread of hepatitis C virus in Egypt. *Lancet* 355, 887–891.
- Friedman, R.S., Jacobelli, J., and Krummel, M.F. (2006). Surface-bound chemokines capture and prime T cells for synapse formation. *Nature Immunology* 7, 1101–1108.
- Fuller, M.J., Callendret, B., Zhu, B., Freeman, G.J., Hasselschwert, D.L., Satterfield, W., Sharpe, A.H., Dustin, L.B., Rice, C.M., Grakoui, A., et al. (2013). Immunotherapy of chronic hepatitis C virus infection with antibodies against programmed cell death-1 (PD-1). *Proc Natl Acad Sci USA* 110, 15001–15006.
- Fulton, R.B., Hamilton, S.E., Xing, Y., Best, J.A., Goldrath, A.W., Hogquist, K.A., and Jameson, S.C. (2014). The TCR's sensitivity to self peptide–MHC dictates the ability of naive CD8+ T cells to respond to foreign antigens. *Nature Immunology* 16, 107–117.
- Gale, M., and Foy, E.M. (2005). Evasion of intracellular host defence by hepatitis C virus. *Nature* 436, 939–945.
- Ganusov, V.V., and De Boer, R.J. (2007). Do most lymphocytes in humans really reside in the gut? *Trends Immunol* 28, 514–518.
- Garris, C.S., Blaho, V.A., Hla, T., and Han, M.H. (2014). Sphingosine-1-phosphate receptor 1 signalling in T cells: trafficking and beyond. *Immunology* 142, 347–353.
- Gebhardt, T., Wakim, L.M., Eidsmo, L., Reading, P.C., Heath, W.R., and Carbone, F.R. (2009). Memory T cells in nonlymphoid tissue that provide enhanced local immunity during infection with herpes simplex virus. *Nature Immunology* 10, 524–530.
- Geiger, R., Duhon, T., Lanzavecchia, A., and Sallusto, F. (2009). Human naive and memory CD4+ T cell repertoires specific for naturally processed antigens analyzed using libraries of amplified T cells. *J Exp Med* 206, 1525–1534.
- Godfrey, D.I., Kennedy, J., Suda, T., and Zlotnik, A. (1993). A developmental pathway involving four phenotypically and functionally distinct subsets of CD3-CD4-CD8- triple-negative adult mouse thymocytes defined by CD44 and CD25 expression. *J Immunol* 150, 4244–4252.
- Goldrath, A.W., Bogatzki, L.Y., and Bevan, M.J. (2000). Naive T cells transiently acquire a memory-like phenotype during homeostasis-driven proliferation. *J Exp Med* 192, 557–564.
- Gorrell, M.D., Gysbers, V., and McCaughan, G.W. (2001). CD26: a multifunctional integral membrane and secreted protein of activated lymphocytes. *Scand. J. Immunol.* 54, 249–264.
- Gorrell, M.D. (2005). Dipeptidyl peptidase IV and related enzymes in cell biology and liver disorders. *Clin. Sci.* 108, 277–292.
- Green, D.R., Droin, N., and Pinkoski, M. (2003). Activation-induced cell death in T cells. *Immunol Rev* 193, 70–81.
- Greenberg, P.D., and Ihl, M.W.O. (2014). Antigen-specific activation and cytokine-facilitated expansion of naive, human CD8. *Nat Protoc* 9, 950–966.
- Griffith, J.W., Sokol, C.L., and Luster, A.D. (2014). Chemokines and Chemokine Receptors: Positioning Cells

for Host Defense and Immunity. *Annu Rev Immunol* 32, 659–702.

Groom, J.R., and Luster, A.D. (2011). CXCR3 in T cell function. *Experimental Cell Research* 317, 620–631.

Groom, J.R., Richmond, J., Murooka, T.T., Sorensen, E.W., Sung, J.H., Bankert, K., Andrian, Von, U.H., Moon, J.J., Mempel, T.R., and Luster, A.D. (2012). CXCR3 Chemokine Receptor-Ligand Interactions in the Lymph Node Optimize CD4+ T Helper 1 Cell Differentiation. *Immunity* 37, 1091–1103.

Grossman, Z., and Paul, W.E. (2015). Dynamic tuning of lymphocytes: physiological basis, mechanisms, and function. *Annu Rev Immunol* 33, 677–713.

Haanen, J.B., Wolkers, M.C., Kruisbeek, A.M., and Schumacher, T.N. (1999). Selective expansion of cross-reactive CD8(+) memory T cells by viral variants. *J Exp Med* 190, 1319–1328.

Hadeiba, H., Lahl, K., Edalati, A., Oderup, C., Habtezion, A., Pachynski, R., Nguyen, L., Ghodsi, A., Adler, S., and Butcher, E.C. (2012). Plasmacytoid Dendritic Cells Transport Peripheral Antigens to the Thymus to Promote Central Tolerance. *Immunity* 36, 438–450.

Hadrup, S.R., Bakker, A.H., Shu, C.J., Andersen, R.S., van Veluw, J., Hombrink, P., Castermans, E., Thor Straten, P., Blank, C., Haanen, J.B., et al. (2009a). Parallel detection of antigen-specific T-cell responses by multidimensional encoding of MHC multimers. *Nat Meth* 6, 520–526.

Hadrup, S.R., Toebe, M., Rodenko, B., Bakker, A.H., Egan, D.A., Ovaa, H., and Schumacher, T.N.M. (2009b). High-throughput T-cell epitope discovery through MHC peptide exchange. *Methods Mol Biol* 524, 383–405.

Hajarizadeh, B., Grebely, J., and Dore, G.J. (2013). Epidemiology and natural history of HCV infection. *Nat Rev Gastroenterol Hepatol* 10, 553–562.

Hale, J.S., and Fink, P.J. (2008). Back to the thymus: peripheral T cells come home. *Immunol Cell Biol* 87, 58–64.

Halkias, J., Melichar, H.J., Taylor, K.T., Ross, J.O., Yen, B., Cooper, S.B., Winoto, A., and Robey, E.A. (2013). Opposing chemokine gradients control human thymocyte migration in situ. *J Clin Invest* 123, 2131–2142.

Halliday, J., Klenerman, P., and Barnes, E. (2011). Vaccination for hepatitis C virus: closing in on an evasive target. *Expert Rev Vaccines* 10, 659–672.

Haluszczak, C., Akue, A.D., Hamilton, S.E., Johnson, L.D.S., Pujanauski, L., Teodorovic, L., Jameson, S.C., and Kedl, R.M. (2009). The antigen-specific CD8+ T cell repertoire in unimmunized mice includes memory phenotype cells bearing markers of homeostatic expansion. *J Exp Med* 206, 435–448.

Hamann, D., Baars, P.A., Rep, M.H., Hooibrink, B., Kerkhof-Garde, S.R., Klein, M.R., and van Lier, R.A. (1997). Phenotypic and functional separation of memory and effector human CD8+ T cells. *J Exp Med* 186, 1407–1418.

Hamilton, S.E., and Jameson, S.C. (2012). CD8 T cell quiescence revisited. *Trends Immunol* 33, 224–230.

Hasan, M., Beitz, B., Rouilly, V., Libri, V., Urrutia, A., Duffy, D., Cassard, L., Di Santo, J.P., Mottez, E., Quintana-Murci, L., et al. (2015). Semi-automated and standardized cytometric procedures for multi-panel and multi-parametric whole blood immunophenotyping. *Clin Immunol* 157, 261–276.

Hawiger, D., Masilamani, R.F., Bettelli, E., Kuchroo, V.K., and Nussenzweig, M.C. (2004). Immunological unresponsiveness characterized by increased expression of CD5 on peripheral T cells induced by dendritic cells in vivo. *Immunity* 20, 695–705.

Hazenbergh, M.D., Hamann, D., Schuitemaker, H., and Miedema, F. (2000a). T cell depletion in HIV-1 infection: how CD4+ T cells go out of stock. *Nature Immunology* 1, 285–289.

Hazenbergh, M.D., Otto, S.A., Cohen Stuart, J.W., Verschuren, M.C., Borleffs, J.C., Boucher, C.A., Coutinho, R.A., Lange, J.M., Rinke de Wit, T.F., Tsegaye, A., et al. (2000b). Increased cell division but not thymic dysfunction rapidly affects the T-cell receptor excision circle content of the naive T cell population in HIV-1 infection. *Nat Med* 6, 1036–1042.

- Hazenberg, M.D., Borghans, J.A.M., De Boer, R.J., and Miedema, F. (2003). Thymic output: a bad TREC record. *Nature Immunology* 4, 97–99.
- Ho, J.E., and Hsue, P.Y. (2009). Cardiovascular manifestations of HIV infection. *Heart* 95, 1193–1202.
- Hofmann, M., Oschowitz, A., Kurzhals, S.R., Krüger, C.C., and Pircher, H. (2013). Thymus-resident memory CD8 +T cells mediate local immunity. *Eur. J. Immunol.* 43, 2295–2304.
- Jameson, S.C., and Fulton, R.B. (2011). Not all naive CD8 T cells are created equal. *Immunol Cell Biol* 89, 576–577.
- Jameson, S.C., Lee, Y.J., and Hogquist, K.A. (2015). Innate Memory T cells (*Advances in Immunology*).
- Jenkins, M.K., and Moon, J.J. (2012). The Role of Naive T Cell Precursor Frequency and Recruitment in Dictating Immune Response Magnitude. *J Immunol* 188, 4135–4140.
- Jenkins, M.K., Chu, H.H., Mclachlan, J.B., and Moon, J.J. (2010). On the Composition of the Preimmune Repertoire of T Cells Specific for Peptide–Major Histocompatibility Complex Ligands. *Annu Rev Immunol* 28, 275–294.
- Jiang, X., Clark, R.A., Liu, L., Wagers, A.J., Fuhlbrigge, R.C., and Kupper, T.S. (2012a). Skin infection generates non-migratory memory CD8+ TRM cells providing global skin immunity. *Nature* 483, 227–231.
- Jiang, Z., Jhunjhunwala, S., Liu, J., Haverty, P.M., Kennemer, M.I., Guan, Y., Lee, W., Carnevali, P., Stinson, J., Johnson, S., et al. (2012b). The effects of hepatitis B virus integration into the genomes of hepatocellular carcinoma patients. *Genome Res.* 22, 593–601.
- Jones, J.L., Thompson, S.A.J., Loh, P., Davies, J.L., Tuohy, O.C., Curry, A.J., Azzopardi, L., Hill-Cawthorne, G., Fahey, M.T., Compston, A., et al. (2013). Human autoimmunity after lymphocyte depletion is caused by homeostatic T-cell proliferation. *Proc Natl Acad Sci USA* 110, 20200–20205.
- Kan-Mitchell, J., Bajcz, M., Schaubert, K.L., Price, D.A., Brenchley, J.M., Asher, T.E., Douek, D.C., Ng, H.L., Yang, O.O., Rinaldo, C.R., et al. (2006). Degeneracy and repertoire of the human HIV-1 Gag p17(77-85) CTL response. *J Immunol* 176, 6690–6701.
- Kanodia, S., Wieder, E., Lu, S., Talpaz, M., Alatrash, G., Clise-Dwyer, K., and Molldrem, J.J. (2010). PR1-specific T cells are associated with unmaintained cytogenetic remission of chronic myelogenous leukemia after interferon withdrawal. *PLoS ONE* 5, e11770.
- Kedzierska, K., Day, E.B., Pi, J., Heard, S.B., Doherty, P.C., Turner, S.J., and Perlman, S. (2006). Quantification of repertoire diversity of influenza-specific epitopes with predominant public or private TCR usage. *J Immunol* 177, 6705–6712.
- Kennedy, P.T.F., Urbani, S., Moses, R.A., Amadei, B., Fiscaro, P., Lloyd, J., Maini, M.K., Dusheiko, G., Ferrari, C., and Bertoletti, A. (2006). The influence of T cell cross-reactivity on HCV-peptide specific human T cell response. *Hepatology* 43, 602–611.
- Kerdiles, Y.M., Beisner, D.R., Tinoco, R., Dejean, A.S., Castrillon, D.H., DePinho, R.A., and Hedrick, S.M. (2009). Foxo1 links homing and survival of naive T cells by regulating L-selectin, CCR7 and interleukin 7 receptor. *Nature Immunology* 10, 176–184.
- Kern, F., Gratama, J.W., Manca, F., Roederer, M., Appay, V., Van Lier, R.A.W., Sallusto, F., and Roederer, M. (2008). Phenotype and function of human T lymphocyte subsets: Consensus and issues. *Cytometry* 73A, 975–983.
- Kew, M.C. (2012). Hepatocellular carcinoma in developing countries: Prevention, diagnosis and treatment. *World J Hepatol* 4, 99–104.
- Khan, I.A., MacLean, J.A., Lee, F.S., Casciotti, L., DeHaan, E., Schwartzman, J.D., and Luster, A.D. (2000). IP-10 is critical for effector T cell trafficking and host survival in *Toxoplasma gondii* infection. *Immunity* 12, 483–494.

- Kim, P.S., and Ahmed, R. (2010). Features of responding T cells in cancer and chronic infection. *Curr Opin Immunol* 22, 223–230.
- King, C., Ilic, A., Koelsch, K., and Sarvetnick, N. (2004). Homeostatic expansion of T cells during immune insufficiency generates autoimmunity. *Cell* 117, 265–277.
- Klein, L., Kyewski, B., Allen, P.M., and Hogquist, K.A. (2014). Positive and negative selection of the T cell repertoire: what thymocytes see (and don't see). *Nat Rev Immunol* 14, 377–391.
- Klenerman, P., and Thimme, R. (2012). T cell responses in hepatitis C: the good, the bad and the unconventional. *Gut* 61, 1226–1234.
- Klenerman, P., Cerundolo, V., and Dunbar, P.R. (2002). Tracking T cells with tetramers: new tales from new tools. *Nature Publishing Group* 2, 263–272.
- Ko, H.M., Hernandez-Prera, J.C., Zhu, H., Dikman, S.H., Sidhu, H.K., Ward, S.C., and Thung, S.N. (2012). Morphologic Features of Extrahepatic Manifestations of Hepatitis C Virus Infection. *Clin Dev Immunol* 2012, 1–9.
- Kondo, Y., and Shimosegawa, T. (2013). Direct effects of hepatitis C virus on the lymphoid cells. *World J Gastroenterol*. 19, 7889–7895.
- Kotturi, M.F., Scott, I., Wolfe, T., Peters, B., Sidney, J., Cheroutre, H., Herrath, Von, M.G., Buchmeier, M.J., Grey, H., and Sette, A. (2008). Naive precursor frequencies and MHC binding rather than the degree of epitope diversity shape CD8+ T cell immunodominance. *J Immunol* 181, 2124–2133.
- Krishnamurty, A.T., and Pepper, M. (2014). Inflammatory interference of memory formation. *Trends Immunol* 35, 355–357.
- Kurachi, M., Kurachi, J., Suenaga, F., Tsukui, T., Abe, J., Ueha, S., Tomura, M., Sugihara, K., Takamura, S., Kakimi, K., et al. (2011). Chemokine receptor CXCR3 facilitates CD8+ T cell differentiation into short-lived effector cells leading to memory degeneration. *J Exp Med* 208, 1605–1620.
- Kurioka, A., Ussher, J.E., Cosgrove, C., Clough, C., Fergusson, J.R., Smith, K., Kang, Y.H., Walker, L.J., Hansen, T.H., Willberg, C.B., et al. (2014). MAIT cells are licensed through granzyme exchange to kill bacterially sensitized targets. *Mucosal Immunology* 8, 429–440.
- Kurkschiev, P.D., Raziorrouh, B., Schraut, W., Backmund, M., Wachtler, M., Wendtner, C.M., Bengsch, B., Thimme, R., Denk, G., Zachoval, R., et al. (2014). Dysfunctional CD8+ T cells in hepatitis B and C are characterized by a lack of antigen-specific T-bet induction. *J Exp Med* 208, 167.
- Kwok, W.W., Tan, V., Gillette, L., Littell, C.T., Soltis, M.A., LaFond, R.B., Yang, J., James, E.A., and DeLong, J.H. (2012). Frequency of Epitope-Specific Naive CD4+ T Cells Correlates with Immunodominance in the Human Memory Repertoire. *J Immunol* 188, 2537–2544.
- Kyewski, B., and Klein, L. (2006). A central role for central tolerance. *Annu Rev Immunol* 24, 571–606.
- La Gruta, N.L., Rothwell, W.T., Cukalac, T., Swan, N.G., Valkenburg, S.A., Kedzierska, K., Thomas, P.G., Doherty, P.C., and Turner, S.J. (2010). Primary CTL response magnitude in mice is determined by the extent of naive T cell recruitment and subsequent clonal expansion. *J Clin Invest* 120, 1885–1894.
- Larrubia, J.R., Benito-Martínez, S., Miquel, J., Calvino, M., Sanz-de-Villalobos, E., González-Praetorius, A., Albertos, S., García-Garzón, S., Lokhande, M., and Parra-Cid, T. (2011). Bim-mediated apoptosis and PD-1/PD-L1 pathway impair reactivity of PD1+/CD127- HCV-specific CD8+ cells targeting the virus in chronic hepatitis C virus infection. *Cellular Immunology* 269, 104–114.
- Le Saout, C., Mennechet, S., Taylor, N., and Hernandez, J. (2008). Memory-like CD8+ and CD4+ T cells cooperate to break peripheral tolerance under lymphopenic conditions. *Proc Natl Acad Sci USA* 105, 19414–19419.
- Lee, J.-Y., Hamilton, S.E., Akue, A.D., Hogquist, K.A., and Jameson, S.C. (2013). Virtual memory CD8 T cells display unique functional properties. *Proc Natl Acad Sci USA* 110, 13498–13503.

- Lee, M.-H., Yang, H.-I., Lu, S.-N., Jen, C.-L., You, S.-L., Wang, L.-Y., Wang, C.-H., Chen, W.J., Chen, C.-J., R.E.V.E.A.L.-HCV Study Group (2012). Chronic hepatitis C virus infection increases mortality from hepatic and extrahepatic diseases: a community-based long-term prospective study. *J Infect Dis* 206, 469–477.
- Legoux, F., Debeaupuis, E., Echasserieau, K., La Salle, De, H., Saulquin, X., and Bonneville, M. (2010). Impact of TCR Reactivity and HLA Phenotype on Naive CD8 T Cell Frequency in Humans. *J Immunol* 184, 6731–6738.
- Li, G., Yu, M., Lee, W.-W., Tsang, M., Krishnan, E., Weyand, C.M., and Goronzy, J.J. (2012). Decline in miR-181a expression with age impairs T cell receptor sensitivity by increasing DUSP6 activity. *Nat Med* 18, 1518–1524.
- Ling, K.-W., van Hamburg, J.P., de Bruijn, M.J.W., Kurek, D., Dingjan, G.M., and Hendriks, R.W. (2007). GATA3 controls the expression of CD5 and the T cell receptor during CD4 T cell lineage development. *Eur. J. Immunol.* 37, 1043–1052.
- Lo, W.-L., Solomon, B.D., Donermeyer, D.L., Hsieh, C.-S., and Allen, P.M. (2014). T cell immunodominance is dictated by the positively selecting self-peptide. *Elife* 3, e01457.
- Longman, R.S., Talal, A.H., Jacobson, I.M., Rice, C.M., and Albert, M.L. (2005). Normal functional capacity in circulating myeloid and plasmacytoid dendritic cells in patients with chronic hepatitis C. *J Infect Dis* 192, 497–503.
- Luxembourg, A.T., Borrow, P., Teyton, L., Brunmark, A.B., Peterson, P.A., and Jackson, M.R. (1998). Biomagnetic isolation of antigen-specific CD8+ T cells usable in immunotherapy. *Nat Biotechnol* 16, 281–285.
- Mackay, L.K., and Gebhardt, T. (2013). Tissue-resident memory T cells: local guards of the thymus. *Eur. J. Immunol.* 43, 2259–2262.
- Mackay, L.K., Rahimpour, A., Ma, J.Z., Collins, N., Stock, A.T., Hafon, M.-L., Vega-Ramos, J., Lauzurica, P., Mueller, S.N., Stefanovic, T., et al. (2013). The developmental pathway for CD103. *Nature Immunology* 14, 1294–1301.
- Maini, M.K., Boni, C., Lee, C.K., Larrubia, J.R., Reignat, S., Ogg, G.S., King, A.S., Herberg, J., Gilson, R., Alisa, A., et al. (2000). The role of virus-specific CD8(+) cells in liver damage and viral control during persistent hepatitis B virus infection. *J Exp Med* 191, 1269–1280.
- Maki, A., Kono, H., Gupta, M., Asakawa, M., Suzuki, T., Matsuda, M., Fujii, H., and Rusyn, I. (2006). Predictive Power of Biomarkers of Oxidative Stress and Inflammation in Patients with Hepatitis C Virus-Associated Hepatocellular Carcinoma. *Ann Surg Oncol* 14, 1182–1190.
- Malherbe, L., Hausl, C., Teyton, L., and McHeyzer-Williams, M.G. (2004). Clonal selection of helper T cells is determined by an affinity threshold with no further skewing of TCR binding properties. *Immunity* 21, 669–679.
- Martin, C.E., and Surh, C.D. (2014). Self-gratification yields not-so-naive T cells. *Nature Immunology* 15, 217–219.
- Marzo, A.L., Klonowski, K.D., Bon, A.L., Borrow, P., Tough, D.F., and Lefrançois, L. (2005). Initial T cell frequency dictates memory CD8+ T cell lineage commitment. *Nature Immunology* 6, 793–799.
- Mason, D. (1998). A very high level of crossreactivity is an essential feature of the T-cell receptor. *Immunol Today* 19, 395–404.
- Matsutani, T., Ohmori, T., Ogata, M., Soga, H., Kasahara, S., Yoshioka, T., Suzuki, R., and Itoh, T. (2007). Comparison of CDR3 length among thymocyte subpopulations: Impacts of MHC and BV segment on the CDR3 shortening. *Molecular Immunology* 44, 2378–2387.
- McFarland, R.D., Douek, D.C., Koup, R.A., and Picker, L.J. (2000). Identification of a human recent thymic emigrant phenotype. *Proc Natl Acad Sci USA* 97, 4215–4220.
- McHeyzer-Williams, M.G., and Davis, M.M. (1995). Antigen-specific development of primary and memory T cells in vivo. *Science* 268, 106–111.

- McPhee, C.G., Duncan, F.J., Silva, K.A., King, L.E., HogenEsch, H., Roopenian, D.C., Everts, H.B., and Sundberg, J.P. (2012). Increased Expression of Cxcr3 and Its Ligands, Cxcl9 and Cxcl10, during the Development of Alopecia Areata in the Mouse. *J Invest Dermatol* 132, 1736–1738.
- Mencin, A., Kluwe, J., and Schwabe, R.F. (2009). Toll-like receptors as targets in chronic liver diseases. *Gut* 58, 704–720.
- Missale, G., Pilli, M., Zerbini, A., Penna, A., Ravanetti, L., Barili, V., Orlandini, A., Molinari, A., Fasano, M., Santantonio, T., et al. (2012). Lack of full CD8 functional restoration after antiviral treatment for acute and chronic hepatitis C virus infection. *Gut* 61, 1076–1084.
- Mizukoshi, E., Nakamoto, Y., Arai, K., Yamashita, T., Sakai, A., Sakai, Y., Kagaya, T., Yamashita, T., Honda, M., and Kaneko, S. (2011). Comparative analysis of various tumor-associated antigen-specific t-cell responses in patients with hepatocellular carcinoma. *Hepatology* 53, 1206–1216.
- Moelants, E.A., Mortier, A., Van Damme, J., and Proost, P. (2013). In vivo regulation of chemokine activity by post-translational modification. *Immunol Cell Biol* 91, 402–407.
- Mohd Hanafiah, K., Groeger, J., Flaxman, A.D., and Wiersma, S.T. (2013). Global epidemiology of hepatitis C virus infection: New estimates of age-specific antibody to HCV seroprevalence. *Hepatology* 57, 1333–1342.
- Moon, J., Chu, H., Pepper, M., Mcorley, S., Jameson, S., Kedl, R., and Jenkins, M. (2007). Naive CD4+ T Cell Frequency Varies for Different Epitopes and Predicts Repertoire Diversity and Response Magnitude. *Immunity* 27, 203–213.
- Moon, J.J., Chu, H.H., Hataye, J., Pagán, A.J., Pepper, M., Mclachlan, J.B., Zell, T., and Jenkins, M.K. (2009). Tracking epitope-specific T cells. *Nat Protoc* 4, 565–581.
- Moorman, J.P., Zhang, C.L., Ni, L., Ma, C.J., Zhang, Y., Wu, X.Y., Thayer, P., Islam, T.M., Borthwick, T., and Yao, Z.Q. (2011). Impaired hepatitis B vaccine responses during chronic hepatitis C infection: Involvement of the PD-1 pathway in regulating CD4+ T cell responses. *Vaccine* 29, 3169–3176.
- Mueller, S.N., Gebhardt, T., Carbone, F.R., and Heath, W.R. (2013). Memory T Cell Subsets, Migration Patterns, and Tissue Residence. *Annu Rev Immunol* 31, 137–161.
- Mueller, S.N., Zaid, A., and Carbone, F.R. (2014). Tissue-resident T cells: dynamic players in skin immunity. *Front. Immun.* 5, 332.
- Mulleger, R.R., Means, T.K., Shin, J.J., Lee, M., Jones, K.L., Glickstein, L.J., Luster, A.D., and Steere, A.C. (2007). Chemokine Signatures in the Skin Disorders of Lyme Borreliosis in Europe: Predominance of CXCL9 and CXCL10 in Erythema Migrans and Acrodermatitis and CXCL13 in Lymphocytoma. *Infect Immun* 75, 4621–4628.
- Neller, M.A., Ladell, K., McLaren, J.E., Matthews, K.K., Gostick, E., Pentier, J.M., Dolton, G., Schauenburg, A.J., Koning, D., Costa, A.I.C.F., et al. (2015). Naive CD8 T-cell precursors display structured TCR repertoires and composite antigen-driven selection dynamics. *Immunol Cell Biol* 1–9.
- Nelson, R.W., Beisang, D., Tubo, N.J., Dileepan, T., Wiesner, D.L., Nielsen, K., Wüthrich, M., Klein, B.S., Kotov, D.I., Spanier, J.A., et al. (2015). T cell receptor cross-reactivity between similar foreign and self peptides influences naive cell population size and autoimmunity. *Immunity* 42, 95–107.
- Neveu, B. (2006). Impact of CD8-MHC class I interaction in detection and sorting efficiencies of antigen-specific T cells using MHC class I/peptide multimers: contribution of pMHC valency. *Int Immunol* 18, 1139–1145.
- Neveu, B., Debeaupuis, E., Echasserieau, K., Le Moullac-Vaidye, B., Gassin, M., Jegou, L., Decalf, J., Albert, M., Ferry, N., Gournay, J., et al. (2008). Selection of high-avidity CD8 T cells correlates with control of hepatitis C virus infection. *Hepatology* 48, 713–722.
- Newton, P., O’Boyle, G., Jenkins, Y., Ali, S., and Kirby, J.A. (2009). Molecular Immunology. *Molecular Immunology* 47, 485–492.

- Nunez, O. (2004). Increased intrahepatic cyclooxygenase 2, matrix metalloproteinase 2, and matrix metalloproteinase 9 expression is associated with progressive liver disease in chronic hepatitis C virus infection: role of viral core and NS5A proteins. *Gut* 53, 1665–1672.
- Obar, J., Khanna, K., and Lefrancois, L. (2008). Endogenous Naive CD8+ T Cell Precursor Frequency Regulates Primary and Memory Responses to Infection. *Immunity* 28, 859–869.
- Okada, T., Ngo, V.N., Ekland, E.H., Förster, R., Lipp, M., Littman, D.R., and Cyster, J.G. (2002). Chemokine Requirements for B Cell Entry to Lymph Nodes and Peyer's Patches. *J Exp Med* 196, 65–75.
- Oliveira, C.P.M.S., Kappel, C.R., Siqueira, E.R., Lima, V.M.R., Stefano, J.T., Michalczuk, M.T., Marini, S.S., Barbeiro, H.V., Soriano, F.G., Carrilho, F.J., et al. (2013). Effects of Hepatitis C virus on cardiovascular risk in infected patients: a comparative study. *International Journal of Cardiology* 164, 221–226.
- Oo, Y.H., Shetty, S., and Adams, D.H. (2010). The Role of Chemokines in the Recruitment of Lymphocytes to the Liver. *Dig Dis* 28, 31–44.
- Ou, X., O'Leary, H.A., and Broxmeyer, H.E. (2013). Implications of DPP4 modification of proteins that regulate stem/progenitor and more mature cell types. *Blood* 122, 161–169.
- Park, H., Serti, E., Eke, O., Muchmore, B., Prokunina-Olsson, L., Capone, S., Folgari, A., and Rehermann, B. (2012). IL-29 is the dominant type III interferon produced by hepatocytes during acute hepatitis C virus infection. *Hepatology* 56, 2060–2070.
- Park, S.-H., and Rehermann, B. (2014). Immune Responses to HCV and Other Hepatitis Viruses. *Immunity* 40, 13–24.
- Penin, F.O., Dubuisson, J., Rey, F.A., Moradpour, D., and Pawlotsky, J.-M. (2004). Structural biology of hepatitis C virus. *Hepatology* 39, 5–19.
- Petrilli, V., Dostert, C., Muruve, D., and Tschopp, J. (2007). The inflammasome: a danger sensing complex triggering innate immunity. *Curr Opin Immunol* 19, 615–622.
- Pittet, M.J., Valmori, D., Dunbar, P.R., Speiser, D.E., Liénard, D., Lejeune, F., Fleischhauer, K., Cerundolo, V., Cerottini, J.C., and Romero, P. (1999). High frequencies of naive Melan-A/MART-1-specific CD8(+) T cells in a large proportion of human histocompatibility leukocyte antigen (HLA)-A2 individuals. *J Exp Med* 190, 705–715.
- Pol, S., Corouge, M., and Sogni, P. (2013). Oral antiviral therapies for chronic hepatitis C infection. *Ther Adv Infect Dis* 1, 107–116.
- Poltorak, M., Arndt, B., Kowtharapu, B.S., Reddycherla, A.V., Witte, V., Lindquist, J.A., Schraven, B., and Simeoni, L. (2013). TCR activation kinetics and feedback regulation in primary human T cells. *Cell Commun Signal* 11, 4.
- Qi, Q., Liu, Y., Cheng, Y., Glanville, J., Zhang, D., Lee, J.Y., Olshen, R.A., Weyand, C.M., Boyd, S.D., and Goronzy, J.J. (2014). Diversity and clonal selection in the human T-cell repertoire. *Proc Natl Acad Sci USA* 111, 13139–13144.
- Raman, C. (2002). CD5, an important regulator of lymphocyte selection and immune tolerance. *Immunol Res* 26, 255–263.
- Raué, H.-P., Beadling, C., Haun, J., and Slifka, M.K. (2013). Cytokine-Mediated Programmed Proliferation of Virus-Specific CD8+ Memory T Cells. *Immunity* 38, 131–139.
- Rehermann, B. (2013). Pathogenesis of chronic viral hepatitis: differential roles of T cells and NK cells. *Nat Med* 19, 859–868.
- Rehermann, B., and Nascimbeni, M. (2005). Immunology of hepatitis B virus and hepatitis C virus infection. *Nat Rev Immunol* 5, 215–229.
- Richer, M.J., Nolz, J.C., and Harty, J.T. (2013). Pathogen-Specific Inflammatory Milieux Tune the Antigen

Sensitivity of CD8<sup>+</sup> T Cells by Enhancing T Cell Receptor Signaling. *Immunity* 38, 140–152.

Riva, A., Laird, M., Casrouge, A., Ambrozaitis, A., Williams, R., Naoumov, N.V., Albert, M.L., and Chokshi, S. (2014). Truncated CXCL10 is associated with failure to achieve spontaneous clearance of acute hepatitis C infection. *Hepatology* 60, 487–496.

Rocha, B., and Tanchot, C. (2004). CD8 T cell memory. *Semin Immunol* 16, 305–314.

Roederer, M., Bigos, M., Nozaki, T., Stovel, R.T., Parks, D.R., and Herzenberg, L.A. (2004). Heterogeneous calcium flux in peripheral T cell subsets revealed by five-color flow cytometry using log-ratio circuitry. *Cytometry* 21, 187–196.

Romagnani, P. (2001). Interferon-inducible protein 10, monokine induced by interferon gamma, and interferon-inducible T-cell alpha chemoattractant are produced by thymic epithelial cells and attract T-cell receptor (TCR) alphabeta+CD8<sup>+</sup> single-positive T cells, TCRgammadelta+ T cells, and natural killer-type cells in human thymus. *Blood* 97, 601–607.

Romero, P., Valmori, D., Pittet, M.J., Zippelius, A., Rimoldi, D., Lévy, F., Dutoit, V., Ayyoub, M., Rubio-Godoy, V., Michielin, O., et al. (2002). Antigenicity and immunogenicity of Melan-A/MART-1 derived peptides as targets for tumor reactive CTL in human melanoma. *Immunol Rev* 188, 81–96.

Rosas, L.E., Barbi, J., Lu, B., Fujiwara, Y., Gerard, C., Sanders, V.M., and Satoskar, A.R. (2005). CXCR3<sup>-/-</sup> mice mount an efficient Th1 response but fail to control *Leishmania major* infection. *Eur. J. Immunol.* 35, 515–523.

Rot, A., and Andrian, Von, U.H. (2004). Chemokines in innate and adaptive host defense: basic chemokines grammar for immune cells. *Annu Rev Immunol* 22, 891–928.

Ruckwardt, T.J., Malloy, A.M.W., Gostick, E., Price, D.A., Dash, P., McClaren, J.L., Thomas, P.G., and Graham, B.S. (2011). Neonatal CD8 T-cell Hierarchy Is Distinct from Adults and Is Influenced by Intrinsic T cell Properties in Respiratory Syncytial Virus Infected Mice. *PLoS Pathog* 7, e1002377.

Rudd, B.D., Venturi, V., Li, G., Samadder, P., Ertelt, J.M., Way, S.S., Davenport, M.P., and Nikolich-Zugich, J. (2011). Nonrandom attrition of the naive CD8<sup>+</sup> T-cell pool with aging governed by T-cell receptor: pMHC interactions. *Proc Natl Acad Sci USA* 108, 13694–13699.

Sallusto, F., Geginat, J., and Lanzavecchia, A. (2004). Central Memory and Effector Memory T Cell Subsets: Function, Generation, and Maintenance. *Annu Rev Immunol* 22, 745–763.

Sarhan, M.A., Pham, T.N.Q., Chen, A.Y., and Michalak, T.I. (2012). Hepatitis C Virus Infection of Human T Lymphocytes Is Mediated by CD5. *J Virol* 86, 3723–3735.

Sarris, M., Masson, J.-B., Maurin, D., Van der Aa, L.M., Boudinot, P., Lortat-Jacob, H., and Herbomel, P. (2012). Inflammatory Chemokines Direct and Restrict Leukocyte Migration within Live Tissues as Glycan-Bound Gradients. *Current Biology* 22, 2375–2382.

Sato, S., Li, K., Kameyama, T., Hayashi, T., Ishida, Y., Murakami, S., Watanabe, T., Iijima, S., Sakurai, Y., Watashi, K., et al. (2015). The RNA Sensor RIG-I Dually Functions as an Innate Sensor and Direct Antiviral Factor for Hepatitis B Virus. *Immunity* 42, 123–132.

Sattentau, Q. (2008). Avoiding the void: cell-to-cell spread of human viruses. *Nat Rev Micro* 6, 815–826.

Sauce, D., Larsen, M., Fastenackels, S., Roux, A., Gorochov, G., Katlama, C., Sidi, D., Sibony-Prat, J., and Appay, V. (2012). Lymphopenia-driven homeostatic regulation of naive T cells in elderly and thymectomized young adults. *J Immunol* 189, 5541–5548.

Schluns, K.S., and Lefrançois, L. (2003). Cytokine control of memory T-cell development and survival. *Nat Rev Immunol* 3, 269–279.

Schmidt, J., Blum, H.E., and Thimme, R. (2013). T-cell responses in hepatitis B and C virus infection: similarities and differences. *Emerging Microbes & Infections* 2, e15.

- Schmidt, J., Neumann-Haefelin, C., Altay, T., Gostick, E., Price, D.A., Lohmann, V., Blum, H.E., and Thimme, R. (2011). Immunodominance of HLA-A2-Restricted Hepatitis C Virus-Specific CD8+ T Cell Responses Is Linked to Naive-Precursor Frequency. *J Virol* 85, 5232–5236.
- Scimone, M.L. (2004). CXCL12 Mediates CCR7-independent Homing of Central Memory Cells, But Not Naive T Cells, in Peripheral Lymph Nodes. *J Exp Med* 199, 1113–1120.
- Shen, T., Zheng, J., Xu, C., Liu, J., Zhang, W., Lu, F., and Zhuang, H. (2010). PD-1 expression on peripheral CD8+ TEM/TEMRA subsets closely correlated with HCV viral load in chronic hepatitis C patients. *Virology* 407, 310.
- Shimizu, Y., Hishiki, T., Ujino, S., Sugiyama, K., Funami, K., and Shimotohno, K. (2011). Lipoprotein component associated with hepatitis C virus is essential for virus infectivity. *Current Opinion in Virology* 1, 19–26.
- Shin, H., and Iwasaki, A. (2013). Tissue-resident memory T cells. *Immunol Rev* 255, 165–181.
- Shoukry, N.H., Grakoui, A., Houghton, M., Chien, D.Y., Ghayeb, J., Reimann, K.A., and Walker, C.M. (2003). Memory CD8+ T cells are required for protection from persistent hepatitis C virus infection. *J Exp Med* 197, 1645–1655.
- Sigmundsdottir, H., Pan, J., Debes, G.F., Alt, C., Habtezion, A., Soler, D., and Butcher, E.C. (2007). DCs metabolize sunlight-induced vitamin D3 to “program” T cell attraction to the epidermal chemokine CCL27. *Nature Immunology* 8, 285–293.
- Simmonds, P., Bukh, J., Combet, C., Deléage, G., Enomoto, N., Feinstone, S., Halfon, P., Inchauspé, G., Kuiken, C., Maertens, G., et al. (2005). Consensus proposals for a unified system of nomenclature of hepatitis C virus genotypes. *Hepatology* 42, 962–973.
- Singh, K., Deshpande, P., Pryshchep, S., Colmegna, I., Liarski, V., Weyand, C.M., and Goronzy, J.J. (2009). ERK-Dependent T Cell Receptor Threshold Calibration in Rheumatoid Arthritis. *J Immunol* 183, 8258–8267.
- Skon, C.N., Lee, J.-Y., Anderson, K.G., Masopust, D., Hogquist, K.A., and Jameson, S.C. (2013). Transcriptional downregulation of S1pr1 is required for the establishment of resident memory CD8. *Nature Immunology* 14, 1285–1293.
- Smit, M.J. (2003). CXCR3-mediated chemotaxis of human T cells is regulated by a Gi- and phospholipase C-dependent pathway and not via activation of MEK/p44/p42 MAPK nor Akt/PI-3 kinase. *Blood* 102, 1959–1965.
- Smith, K., Seddon, B., Purbhoo, M.A., Zamoyska, R., Fisher, A.G., and Merkenschlager, M. (2001). Sensory adaptation in naive peripheral CD4 T cells. *J Exp Med* 194, 1253–1261.
- Soldevila, G., Raman, C., and Lozano, F. (2011). The immunomodulatory properties of the CD5 lymphocyte receptor in health and disease. *Curr Opin Immunol* 23, 310–318.
- Sprent, J., and Surh, C.D. (2011). Normal T cell homeostasis: the conversion of naive cells into memory-phenotype cells. *Nature Immunology* 12, 478–484.
- Stamou, P., de Jersey, J., Carmignac, D., Mamalaki, C., Kioussis, D., and Stockinger, B. (2003). Chronic exposure to low levels of antigen in the periphery causes reversible functional impairment correlating with changes in CD5 levels in monoclonal CD8 T cells. *J Immunol* 171, 1278–1284.
- Starr, T.K., Jameson, S.C., and Hogquist, K.A. (2003). Positive and negative selection of T cells. *Annu Rev Immunol* 21, 139–176.
- Staton, T.L., Habtezion, A., Winslow, M.M., Sato, T., Love, P.E., and Butcher, E.C. (2006). CD8+ recent thymic emigrants home to and efficiently repopulate the small intestine epithelium. *Nature Immunology* 7, 482–488.
- Stelekati, E., and Wherry, E.J. (2012). Chronic Bystander Infections and Immunity to Unrelated Antigens. *Cell Host & Microbe* 12, 458–469.

- Stelekati, E., Shin, H., Doering, T.A., Dolfi, D.V., Ziegler, C.G., Beiting, D.P., Dawson, L., Liboon, J., Wolski, D., Ali, M.-A.A., et al. (2014). Bystander Chronic Infection Negatively Impacts Development of CD8. *Immunity* *40*, 801–813.
- Stemberger, C., Neuenhahn, M., Gebhardt, F.E., Schiemann, M., Buchholz, V.R., and Busch, D.H. (2009). Stem cell-like plasticity of naïve and distinct memory CD8(+) T cell subsets. *Semin Immunol* *21*, 62–68.
- Su, L.F., and Davis, M.M. (2013). Antiviral memory phenotype T cells in unexposed adults. *Immunol Rev* *255*, 95–109.
- Su, L.F., Kidd, B.A., Han, A., Kotzin, J.J., and Davis, M.M. (2013). Virus-specific CD4(+) memory-phenotype T cells are abundant in unexposed adults. *Immunity* *38*, 373–383.
- Suga, H., Sugaya, M., Miyagaki, T., Ohmatsu, H., Okochi, H., and Sato, S. (2013). CXCR3 Deficiency Prolongs Th1-Type Contact Hypersensitivity. *J Immunol* *190*, 6059–6070.
- Sung, J.H., Zhang, H., Moseman, E.A., Alvarez, D., Iannaccone, M., Henrickson, S.E., la Torre, de, J.C., Groom, J.R., Luster, A.D., and Andrian, Von, U.H. (2012). Chemokine Guidance of Central Memory T Cells Is Critical for Antiviral Recall Responses in Lymph Nodes. *Cell* *150*, 1249–1263.
- Tabbekh, M., Franciszkiewicz, K., Haouas, H., Lecluse, Y., Benihoud, K., Raman, C., and Mami-Chouaib, F. (2011). Rescue of Tumor-Infiltrating Lymphocytes from Activation-Induced Cell Death Enhances the Antitumor CTL Response in CD5-Deficient Mice. *J Immunol* *187*, 102–109.
- Tabbekh, M., Mokrani-Hammani, M., Bismuth, G., and Mami-Chouaib, F. (2013). T-cell modulatory properties of CD5 and its role in antitumor immune responses. *Oncoimmunology* *2*, e22841.
- Takada, K., and Jameson, S.C. (2009). Naive T cell homeostasis: from awareness of space to a sense of place. *Nat Rev Immunol* *9*, 823–832.
- Tan, A.C.L., La Gruta, N.L., Zeng, W., and Jackson, D.C. (2011). Precursor Frequency and Competition Dictate the HLA-A2-Restricted CD8+ T Cell Responses to Influenza A Infection and Vaccination in HLA-A2.1 Transgenic Mice. *J Immunol* *187*, 1895–1902.
- Tarakhovskiy, A., Kanner, S.B., Hombach, J., Ledbetter, J.A., Muller, W., Killeen, N., and Rajewsky, K. (1995). A role for CD5 in TCR-mediated signal transduction and thymocyte selection. *Science* *269*, 535–537.
- Taswell, C. (1981). Limiting dilution assays for the determination of immunocompetent cell frequencies. I. Data analysis. *J Immunol* *126*, 1614–1619.
- Thelen, M., and Stein, J.V. (2008). How chemokines invite leukocytes to dance. *Nature Immunology* *9*, 953–959.
- Thimme, R., Bukh, J., Spangenberg, H.C., Wieland, S., Pemberton, J., Steiger, C., Govindarajan, S., Purcell, R.H., and Chisari, F.V. (2002). Viral and immunological determinants of hepatitis C virus clearance, persistence, and disease. *Proc Natl Acad Sci USA* *99*, 15661–15668.
- Thomas, S., Rouilly, V., Patin, E., Alanio, C., Dubois, A., Delval, C., Marquier, L.-G., Fauchoux, N., Sayegrih, S., Vray, M., et al. (2015). The Milieu Intérieur study - An integrative approach for study of human immunological variance. *Clin Immunol* *157*, 277–293.
- Thome, J.J.C., Yudanin, N., Ohmura, Y., Kubota, M., Grinshpun, B., Sathaliyawala, T., Kato, T., Lerner, H., Shen, Y., and Farber, D.L. (2014). Spatial Map of Human T Cell Compartmentalization and Maintenance over Decades of Life. *Cell* *159*, 814–828.
- Toebe, M., Coccoris, M., Bins, A., Rodenko, B., Gomez, R., Nieuwkoop, N.J., Van De Kastele, W., Rimmelzwaan, G.F., Haanen, J.B.A.G., Ova, H., et al. (2006). Design and use of conditional MHC class I ligands. *Nat Med* *12*, 246–251.
- Tough, D.F., and Sprent, J. (1994). Turnover of naive- and memory-phenotype T cells. *J Exp Med* *179*, 1127–1135.

- Tubo, N.J., and Jenkins, M.K. (2014). TCR signal quantity and quality in CD4. *Trends Immunol* 35, 591–596.
- Tung, J.W., Kunnavatana, S.S., Herzenberg, L.A., and Herzenberg, L.A. (2001). The regulation of CD5 expression in murine T cells. *BMC Mol. Biol.* 2, 5.
- van Buuren, M.M., Dijkgraaf, F.E., Linnemann, C., Toebes, M., Chang, C.X.L., Mok, J.Y., Nguyen, M., van Esch, W.J.E., Kvistborg, P., Grotenbreg, G.M., et al. (2014). HLA Micropolymorphisms Strongly Affect Peptide-MHC Multimer-Based Monitoring of Antigen-Specific CD8<sup>+</sup> T Cell Responses. *J Immunol* 192, 641–648.
- van der Meer, A.J., Wedemeyer, H., Feld, J.J., Hansen, B.E., Manns, M.P., Zeuzem, S., and Janssen, H.L.A. (2014). Is there sufficient evidence to recommend antiviral therapy in hepatitis C? *Journal of Hepatology* 60, 191–196.
- Villarroel, V.A., Okiyama, N., Tsuji, G., Linton, J.T., and Katz, S.I. (2014). CXCR3-Mediated Skin Homing of Autoreactive CD8 T Cells Is a Key Determinant in Murine Graft-Versus-Host Disease. *J Investig Dermatol* 134, 1552–1560.
- Virgin, H.W. (2014). The Virome in Mammalian Physiology and Disease. *Cell* 157, 142–150.
- Walker, L.J., Kang, Y.H., Smith, M.O., Tharmalingham, H., Ramamurthy, N., Fleming, V.M., Sahgal, N., Leslie, A., Oo, Y., Geremia, A., et al. (2012). Human MAIT and CD8<sup>+</sup> cells develop from a pool of type-17 precommitted CD8<sup>+</sup> T cells. *Blood* 119, 422–433.
- Wei, S.H., Parker, I., Miller, M.J., and Cahalan, M.D. (2003). A stochastic view of lymphocyte motility and trafficking within the lymph node. *Immunol Rev* 195, 136–159.
- Welsh, R.M., Che, J.W., Brehm, M.A., and Selin, L.K. (2010). Heterologous immunity between viruses. *Immunol Rev* 235, 244–266.
- Wiese, M., Fischer, J., Löbermann, M., Göbel, U., Grüngreiff, K., Güthoff, W., Kullig, U., Richter, F., Schiefke, I., Tenckhoff, H., et al. (2013). Evaluation of liver disease progression in the German hepatitis C virus (1b)-contaminated anti-D cohort at 35 years after infection. *Hepatology* 59, 49–57.
- Wilson, E.B., and Brooks, D.G. (2013). Inflammation Makes T Cells Sensitive. *Immunity* 38, 5–7.
- Wilson, M.J., Ruhland, A.R., Pryor, J.L., Ercole, C., Sinha, A.A., Hensleigh, H., Kaye, K.W., Dawkins, H.J., Wasserman, N.F., Reddy, P., et al. (2005). Prostate specific origin of dipeptidylpeptidase IV (CD-26) in human seminal plasma. *J. Urol.* 160, 1905–1909.
- Wu, L., and Shortman, K. (2005). Heterogeneity of thymic dendritic cells. *Semin Immunol* 17, 304–312.
- Yonkers, N.L., Sieg, S., Rodriguez, B., and Anthony, D.D. (2011). Reduced Naive CD4 T Cell Numbers and Impaired Induction of CD27 in Response to T Cell Receptor Stimulation Reflect a State of Immune Activation in Chronic Hepatitis C Virus Infection. *J Infect Dis* 203, 635–645.
- Younes, S.-A., Punkosdy, G., Caucheteux, S., Chen, T., Grossman, Z., and Paul, W.E. (2011). Memory Phenotype CD4 T Cells Undergoing Rapid, Nonburst-Like, Cytokine-Driven Proliferation Can Be Distinguished from Antigen-Experienced Memory Cells. *Plos Biol* 9, e1001171.
- Yu, W., Misulovin, Z., Suh, H., Hardy, R.R., Jankovic, M., Yannoutsos, N., and Nussenzweig, M.C. (1999). Coordinate regulation of RAG1 and RAG2 by cell type-specific DNA elements 5' of RAG2. *Science* 285, 1080–1084.
- Zachariah, M.A., and Cyster, J.G. (2010). Neural Crest-Derived Pericytes Promote Egress of Mature Thymocytes at the Corticomedullary Junction. *Science* 328, 1129–1135.
- Zampino, R., Marrone, A., Restivo, L., Guerrero, B., Sellitto, A., Rinaldi, L., Romano, C., and Adinolfi, L.E. (2013). Chronic HCV infection and inflammation: Clinical impact on hepatic and extra-hepatic manifestations. *World J Hepatol* 5, 528–540.
- Zhang, X., Hou, J., and Lu, M. (2013). Regulation of hepatitis B virus replication by epigenetic mechanisms and

microRNAs. *Front Genet* 4, 202.

Ziegler, A., Müller, C.A., Böckmann, R.A., and Uchanska-Ziegler, B. (2009). Low-affinity peptides and T-cell selection. *Trends Immunol* 30, 53–60.

Zignego, A.L., and Bréchet, C. (2001). Extrahepatic manifestations of HCV infection: facts and controversies. *Journal of Hepatology* 31, 369–376.

Zippelius, A., Pittet, M.J., Batard, P., Rufer, N., de Smedt, M., Guillaume, P., Ellefsen, K., Valmori, D., Liénard, D., Plum, J., et al. (2002). Thymic selection generates a large T cell pool recognizing a self-peptide in humans. *J Exp Med* 195, 485–494.